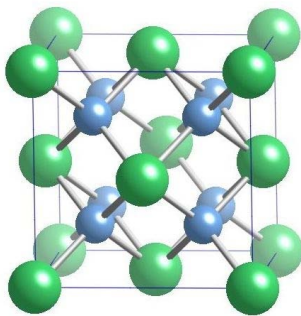


# Distributed Energy Program FY06 Annual Reports

---



**OAK RIDGE NATIONAL LABORATORY**

MANAGED BY UT-BATTELLE FOR THE DEPARTMENT OF ENERGY



# Contents

## **ADVANCED RECIPROCATING ENGINES**

### CHARACTERIZATION AND DEVELOPMENT OF SPARK PLUG

MATERIALS AND COMPONENTS .....	3
ADAPTIVE CONTROL STRATEGIES FOR CLEAN EFFICIENT COMBUSTION.....	9
LEAN NO <sub>x</sub> TRAP AFTERTREATMENT FOR LEAN NATURAL GAS ENGINES .....	15

## **MATERIALS**

ADVANCED ALLOYS FOR HIGH-TEMPERATURE RECUPERATORS .....	27
RECUPERATOR TESTING AND EVALUATION.....	45
MICROSTRUCTURAL CHARACTERIZATION OF CFCCS AND PROTECTIVE COATINGS .....	51
OXIDATION/CORROSION CHARACTERIZATION OF MICROTURBINE MATERIALS.....	55
RELIABILITY EVALUATION OF MICROTURBINE COMPONENTS .....	59
ENVIRONMENTAL PROTECTION SYSTEMS FOR CERAMICS IN MICROTURBINES AND INDUSTRIAL GAS TURBINE APPLICATIONS—PART B: SLURRY COATINGS .....	65
NDE TECHNOLOGY DEVELOPMENT FOR MICROTURBINES .....	71
ADVANCED MATERIALS FOR RECIPROCATING ENGINE COMPONENTS .....	77
CHARACTERIZATION AND DEVELOPMENT OF SPARK PLUG MATERIALS AND COMPONENTS .....	83

## **THERMALLY ACTIVATED TECHNOLOGIES**

TAT LAB PERFORMANCE AND ANALYSIS .....	91
INDUSTRY PARTNERSHIP.....	97
ORGANIC RANKINE CYCLE .....	101
THERMAL ENERGY PERFORMANCE EVALUATION.....	103
MICRO-CHANNEL HEAT EXCHANGER DEVELOPMENT.....	113
WOVEN GRAPHITE FIBER HEAT EXCHANGER.....	115
CFD MODELING ANALYSIS .....	117
ROTATING HEAT EXCHANGER .....	121

## **COOLING, HEATING AND POWER**

INTEGRATED ENERGY SYSTEMS (AKA COOLING, HEATING, AND POWER OR CHP SYSTEMS) .....	125
DISTRIBUTED ENERGY SYSTEMS APPLICATIONS INTEGRATION .....	141
COOLING, HEATING AND POWER .....	149
ANCILLARY SERVICES OFFERED BY DISTRIBUTED ENERGY (DE) SYSTEMS .....	167

**DE BENEFITS**

DE CROSSCUTTING, SYSTEMS INTEGRATION, AND ANALYSIS ..... 177







## 1.2 Characterization and Development of Spark Plug Materials and Components

*H. T. Lin\* (primary contact), M. P. Brady\*, M.D. Kass\*\*, and J.B. Tassitano\*\**

*\*Materials Science and Technology Division*

*\*\*Engineering Science & Technology Division*

*Oak Ridge National Laboratory, Oak Ridge, TN 37831-6068*

*Phone: (865) 576-8857; Fax: (865) 574-6098; E-mail: [linh@ornl.gov](mailto:linh@ornl.gov)*

*DOE Technology Program Manager: Ron Fiskum*

*Phone: (202) 586-9154; Fax: (202) 586-7114; E-mail: [Ronald.Fiskum@ee.doe.gov](mailto:Ronald.Fiskum@ee.doe.gov)*

*ORNL Technical Advisors: Tim Theiss and David Stinton*

*Phone: (865) 946-1348; Fax: (865) 946-1248; E-mail: [theisstj@ornl.gov](mailto:theisstj@ornl.gov)*

*Phone: (865) 574-4556; Fax: (865) 241-0411; E-mail: [stintondp@ornl.gov](mailto:stintondp@ornl.gov)*

---

### Objective

- Provide insight into the wear mechanisms of natural gas spark plug electrodes as a function of field exposure time and engine conditions.
- Increase the wear resistance of spark plug electrode materials to at least 1 year (or a 2X improvement) in advanced natural gas reciprocating engines designed to meet aggressive emission and efficiency goals.

### Approach

- Characterize engine tested spark plugs to identify key erosion mechanisms and limitations of existing materials.
- Develop, engine test, and optimize new electrode materials for improved erosion resistance based on findings from the characterization effort.

### Accomplishments

- Completed evaluation and characterization of a range of commercially available and developmental spark plug electrode alloys subjected to an accelerated testing protocol in a laboratory gasoline engine in collaboration with Federal Mogul. The alloys represented a wide range of oxidation resistance and thermophysical properties. A key finding was a stronger than anticipated correlation between alloy thermal conductivity and wear, which in many cases overwhelmed improvements in oxidation resistance.
- Completed two sets of natural gas engine tests at ORNL using a Caterpillar G3406 industrial natural gas engine. The first set of plugs was manufactured from model ferritic, austenitic, and Ni-base microstructures optimized for Cr<sub>2</sub>O<sub>3</sub> scale formation. A key finding was the apparent superior resistance to environment-driven cracking of Fe-base alloys, compared to more typically used Ni-base electrode alloys. A second set of spark plugs was manufactured from conventionally available electrode and precious metal insert pad alloys, selected for improved compatibility. Engine testing was completed and post-test analysis is underway.

### Future Directions

- Complete post-test characterization of latest engine tested spark plugs, and conduct additional engine testing for a final iteration of spark plugs manufactured from commercially available electrode alloys and precious metal insert materials.



- Complete initial development of novel, alternative spark plug electrode materials and deliver to collaborators for spark plug manufacture and engine testing.
- Complete transfer of technology via open literature publication relaying understanding gained over the course of this

### **Introduction**

Natural gas (NG) reciprocating engine manufacturers have identified ignition systems as one of the key technologies to achieve cost/performance/emission characteristic goals for lean and stoichiometric engines. Spark plug erosion and subsequent failure have been identified as a major issue in long-term durability of natural gas ignition system. Current spark plug lifetimes are on the order of only ~2-6 months, which results in loss of performance and necessitates frequent, costly downtime maintenance for the plug replacement. Desired spark plug lifetimes for NG engine end users are on the order of at least 1 year (or a 2-fold increase in the spark plug life). It has been recognized that as cylinder pressures, compression ratios, and ignition voltages are increased, and conditions further move towards leaner burning combustion, spark plug reliability and lifetime performance will become even more critical and could limit further advances in engine development. The goal of this effort is to identify the mechanisms of electrode wear and to design new electrode materials to improve the lifetime and reliability of NG spark plugs to meet the lifetime goal.

### **Approach**

Microstructural and spectroscopic analysis of end-of life J-type spark plugs from field-operated NG engines led to the identification of wear phenomena driven by oxidation and cracking of the electrode material during engine operation. The spark plugs typically consisted of a Ni-base electrode alloy with Pt-4W or Ir insert pads at the sparking surface. Extensive cracking and oxidation at the Ni-alloy/insert pad weld interface were observed, as were grain boundary attack and cracking of the insert pads themselves, particularly Pt-4W. The susceptibility of the Pt-W grain boundaries was traced to internal oxidation of W at these locations, followed by volatilization of the W-oxide that was formed. These findings were unexpected, as wear of spark plug electrodes is typically primarily associated

with loss of material due to sputtering, melting, ablation, and particle erosion phenomena during sparking. Efforts in FY2006 focused on engine testing of a range of model and commercially available electrode alloys and precious metal/platinum group inserts selected to systematically explore the effects of a range of thermal, mechanical, and chemical materials parameters on wear behavior. A conventional J-type spark plug arrangement was selected to allow relative comparison of materials effects, and comparison with fielded-tested commercial J-type plugs previously characterized. These spark plugs were manufactured via collaboration with Federal Mogul (FM). Two types of engine testing were pursued: an accelerated test criteria at FM using a laboratory-modified gasoline engine, and a Caterpillar G3406 industrial natural gas engine test bed at ORNL.

### **Results**

The accelerated laboratory gasoline engine tests at FM indicated a stronger than expected effect of alloy thermal conductivity on the rate of electrode wear. This was exacerbated by the use of solid center electrodes of the candidate alloys at this exploratory stage, rather than the Cu-cored approach used to improve thermal conductivity in commercial plugs, such that some plugs/electrode alloys likely ran significantly hotter than others. Note that Cu coring at the exploratory stage adds significant manufacturing complexity. These findings did reveal that the addition of elements such as Cr and Al to improve oxidation resistance could also significantly degrade thermal conductivity as well as moderately depress melting point, such that the benefits gained by improved oxidation resistance could be fully negated. In some instances, the highly alloyed, oxidation-resistant materials behaved far worse than less oxidation-resistant compositions. It should be noted that the aforementioned spark plug electrodes did not incorporate precious metal/Pt group insert pads. However, the insights gained can be applied to plugs with insert pads, particularly regarding the observed

oxidation/cracking behavior at the electrode alloy/insert pad interface in field-tested plugs.

Spark plug electrodes based on model  $\text{Cr}_2\text{O}_3$ -forming alloys with ferritic, austenitic, and Ni-base microstructures were run in a short-term NG engine test at ORNL for comparison with conventionally used 95% Ni base and Ni-15Cr base electrode alloys. These plugs were run for 67h to gain insight into the behavior of electrode alloys without precious metal/platinum group insert pads, for comparison with the accelerated laboratory gasoline engine tests at FM, and as baseline information for subsequent NG tests using alloys with insert pads. Representative microstructures of the solid center electrode alloys are shown in Figs. 1-3. A complex heterogeneous oxide surface was formed on the conventional 95% Ni base electrode alloy (Fig. 1), with regions of Ni-Mn-Ti-Si-Ca-P-O and Ni-Mn-Cr-O phases. Similar complex surface oxides containing base alloy additions, as well as P, S, etc species were observed on the surfaces of all electrodes examined. Cracking of the surface oxide was evident in the surface of the 95% Ni alloy, and confirmed in the cross-section. Even more extensive cracking was observed on the model Ni-base alloy, Ni-25Cr-0.4Si-0.15La wt.% alloy, whose composition was selected to optimize oxidation resistance (Fig. 2). However, cracking was not observed in an optimized Fe(Ni) base austenitic alloy, Fe-25Cr-20Ni-0.4Si-0.15La wt.% (Fig. 3), nor the corresponding model Fe-base ferritic alloy, Fe-25Cr-0.4Si-0.15La wt.% (microstructure not shown). These results suggest that Ni-base alloys are more susceptible to oxidation-cracking attack than Fe-base alloys. Although such alloys without precious metal insert pads are not candidate NG electrodes, such oxidation-cracking attack was observed in field-tested spark plugs at the Ni-base electrode alloy/insert pad interface. Reduction in these phenomena may lead to improved NG plug life via improved durability of the electrode alloy/insert pad interface.

Attempts were also made to assess the extent of gap growth for the NG tested model and conventional electrode alloys. However, the

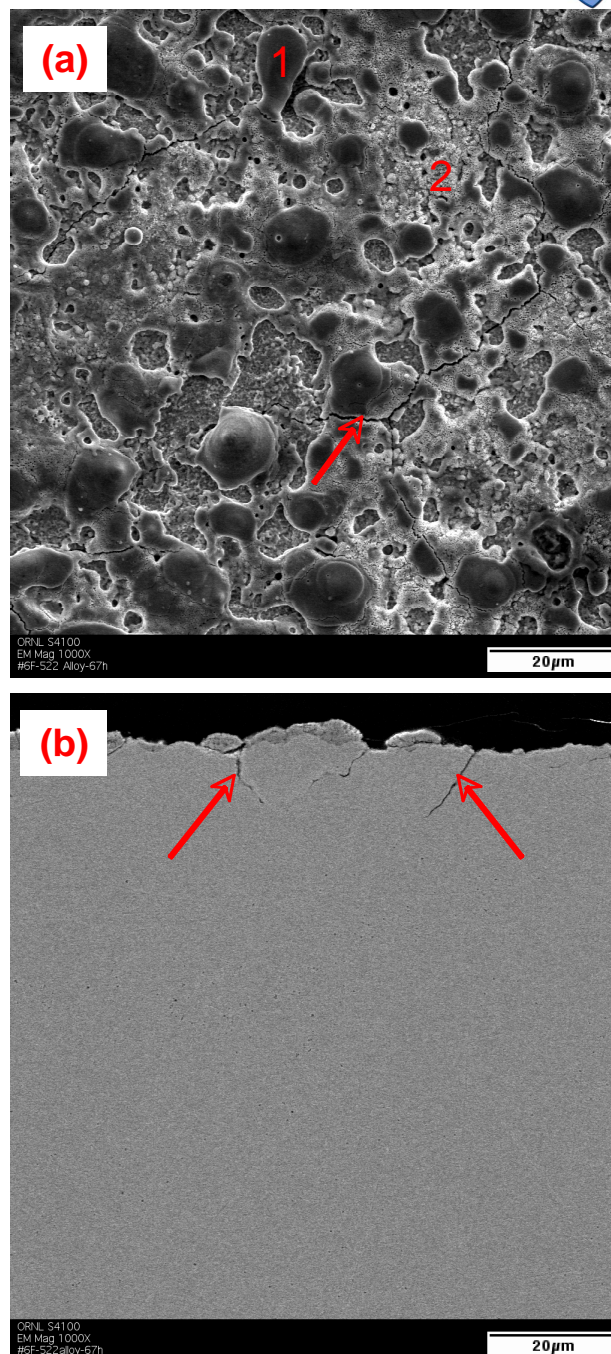


**Figure 1.** SEM micrographs of surface and polished cross section of conventional 95% Ni base electrode alloy after 67h test in Caterpillar G3406 nature gas engine. 1 and 2 denote the Ni-Mn-Ti-Si-Ca-P-O and Ni-Mn-Cr-O phases, respectively. The arrows indicate the crack formation after engine testing.

measurements suggest possible movement of the center electrode during the test, such that reliable gap growth values could not be obtained. Qualitatively, the gap growth of these electrode

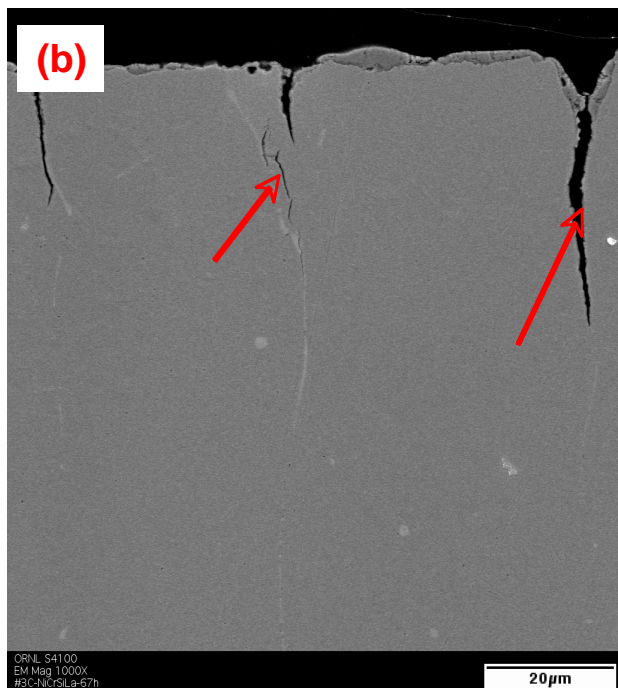
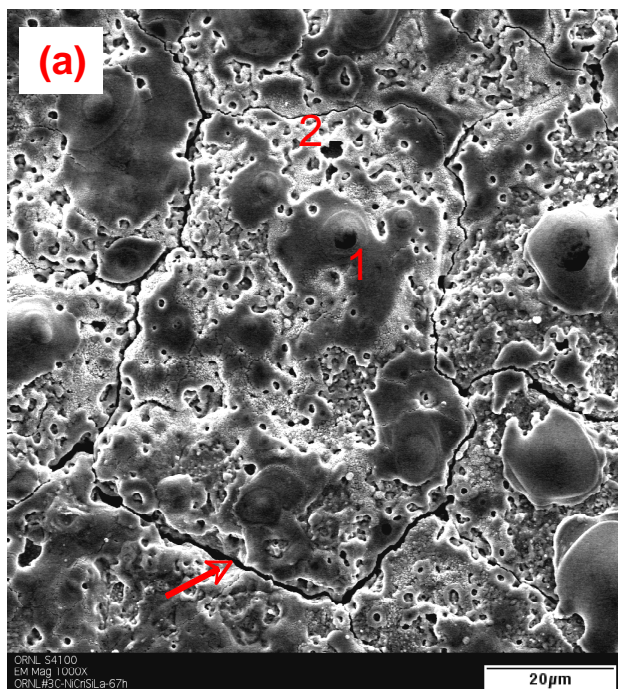


**Figure 2.** SEM micrographs of surface and polished cross section of model Ni-base alloy (Ni-25Cr-0.4Si-0.15La wt.%) alloy after 67h test in Caterpillar G3406 nature gas engine. 1 and 2 denote the Ni-Cr-Si-Ca-P-C-O and Ni-Cr-O phases, respectively. The arrows indicate the crack formation after engine testing.

alloys, with no precious metal/Pt group insert pads (estimated to be on the order of 10-50 microns), exceeded by at least a factor of two the

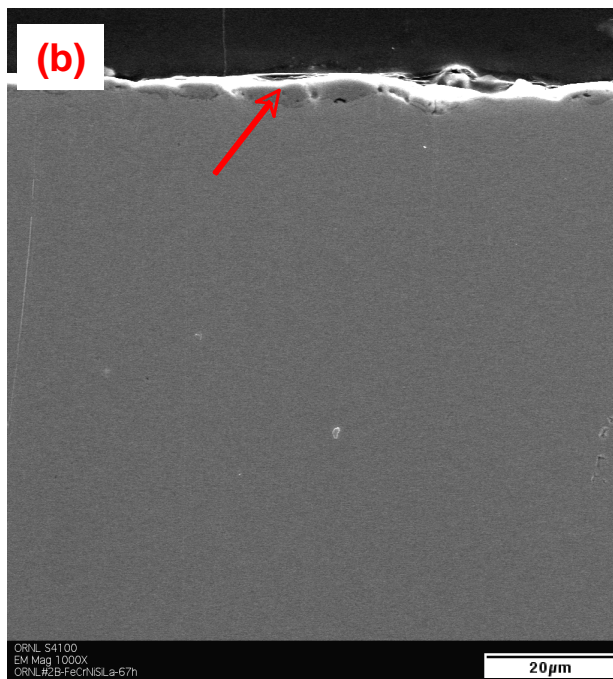
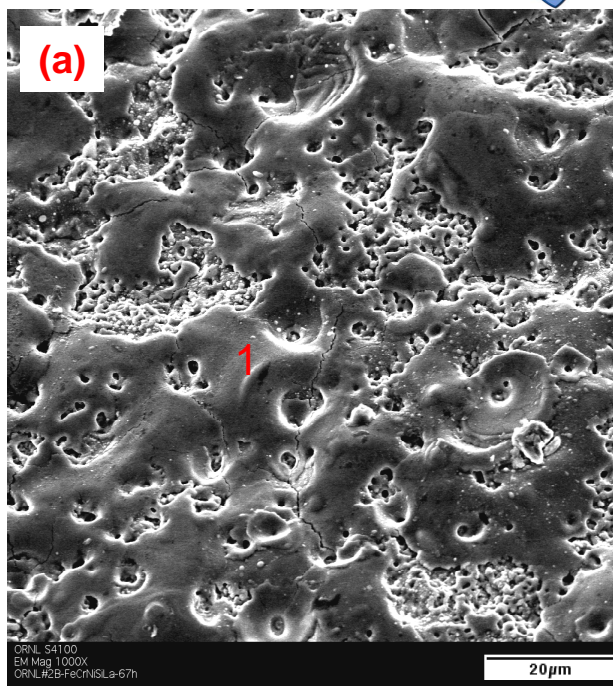


**Figure 3.** SEM micrographs of surface and polished cross section of optimized Fe(Ni) base austenitic alloy (Fe-25Cr-20Ni-0.4Si-0.15La wt.%) alloy after 67h test in Caterpillar G3406 nature gas engine. 1 denotes the Ni-Fe-Ni-Cr-Si-C-O phase. Arrow indicates the Fe-Ni-Cr-O oxide scale formed.

potential material loss due solely to oxidation scaling processes, i.e. sputtering, melting,



ablation, and particle erosion phenomena likely were the main sources of materials loss/gap growth for these alloys.

Based on these findings, and previous studies of field-tested conventional spark plugs, a series of plugs incorporating Pt group metal insert pads and Ni and Fe electrode alloys selected to improve materials compatibility between electrode alloy/insert pad and oxidation resistance was manufactured in collaboration with FM. These materials were selected from commercially available alloys. The electrode alloy was Ni-15Cr base for the improved oxidation resistance relative to the conventionally use 95% Ni base alloys, with a range of Ir and Ir-Pt insert pads. One set of spark plugs also used a commercially available, Fe-Cr base ferritic electrode alloy, due to the increased resistance to cracking observed for Fe-base materials, and the relatively high thermal conductivity of ferritic alloys. Conventionally used Pt-4W and Pt-10Ni insert pad alloys were specifically excluded due to previously observed oxidation-cracking driven materials loss from the selective oxidation of the W/Ni components in the Pt-alloy. The first set of test plugs accumulated approximately 250h of NG operation. Preliminary microstructural analysis revealed loss of the insert pad alloy in many cases, and evidence of significant interdiffusion and attack at the electrode alloy/insert pad interface. It is not yet clear whether this rather poor behavior was due to materials limitations in the engine environment or manufacturing issues with these prototype plugs. Detailed electronic microscopy analysis on both as-received and 250h-tested plugs to elucidate the observed degradations is in progress.

## **Future Works**

Additional NG engine testing and characterization of the spark plugs manufactured from commercially available electrode alloys and precious metal/Pt group inserts, selected for improved compatibility and oxidation-cracking resistance, will be completed. Efforts have also been devoted to identification and optimization of new alternative electrode alloys and insert pad materials for improved wear (a patent disclosure submitted in 2005). Some of these materials are currently in engine testing at FM and will be characterized and assessed in FY 2007. Additional alloys based on these findings will be optimized early in FY 2007 and delivered to FM and other collaborators for spark plug manufacture and engine testing. For example, discussions are ongoing with Woodward about collaborating on this spark plug work, but with a different emphasis than our collaborations with FM. During FY 2007, technology transfer efforts will include an open literature publication relaying understanding gained over the course of this program.





## 1.3 Adaptive Control Strategies for Clean Efficient Combustion

*K. Dean Edwards, Robert M. Wagner*

*Fuels, Engines, and Emissions Research Center*

*Engineering Science and Technology Division*

*Oak Ridge National Laboratory*

*(865) 946-1239; Fax (865) 946-1248; Email: edwardskd@ornl.gov, wagnerm@ornl.gov*

*DOE Technology Development Manager: Ron Fiskum*

*(202) 586-9154; Fax (202) 586-7114; Email: ronald.fiskum@ee.doe.gov*

*ORNL Technical Monitor: Tim Theiss*

*(865) 946-1348; Fax (865) 946-1354; Email: theisstj@ornl.gov*

---

### Objective

- Extend effective combustion lean limit by employing adaptive control.
- Demonstrate technique for estimating the potential benefits of adaptive control.
- Determine ARES representative engine platform for transitioning control technology.
- Evaluate suitability of adaptive control for spark assisted HCCI combustion (leveraged activity with OFCVT).

### Approach

- Develop physics based computer model for simulating combustion and cyclic dispersion in large NG engines.
- Evaluate potential benefits of adaptive control using engine model.
- Identify and acquire ARES representative single-cylinder engine.
- Characterize cyclic dispersion associated with transitioning between conventional SI and HCCI operation.

### Accomplishments

- Developed model based on commercially available and industry accepted software for simulating cyclic dispersion in NG engines.
- Demonstrated ability of computer model to simulate complex cyclic dispersion and predict effect on emissions and efficiency.
- Determined and ordered large single-cylinder engine based on Waukesha Advanced Power Generation (APG) ARES engine. Engine is scheduled for delivery in December 2006.
- Characterized cyclic dispersion associated with spark assisted HCCI combustion and determined behavior is short-time predictable and consequently amenable to control.
- Developed and validated analytical model of single cylinder Waukesha APG engine for use with the single cylinder engine.

### Future Direction (funding dependent)

- Apply benefit estimation technique to ARES size NG engine.
- Transition and evaluate advanced control system on single-cylinder NG engines.
- Transition adaptive control strategies to ARES-sized NG engine.
- Investigate spark assisted HCCI combustion on ARES sized engine platform.



## Introduction

Dilute operation of internal combustion engines through lean fueling and/or high levels of EGR may be employed to increase fuel efficiency, reduce NO<sub>x</sub> emissions, and promote enhanced combustion modes such as HCCI. However, the maximum level of dilution is limited by the development of combustion instabilities that produce unacceptable levels of cycle-to-cycle variability characterized by simple or complex patterns of alternating cycles of good and poor combustion quality and increased emissions of unburned fuel (during partial burns and misfires) and NO<sub>x</sub> (produced during the succeeding enhanced-combustion events). Nonlinear feedback associated with the residual and recirculated exhaust gases exchanged between successive cycles produces small changes in the in-cylinder initial conditions. Lean operation tends to increase the sensitivity of ignition and flame propagation to these variations in initial conditions leading to the development of combustion instabilities with EGR levels as low as 5-10%. At stoichiometric conditions, the combustion process is less sensitive; however, adding high levels of EGR can produce significant fluctuations in initial conditions and lead to the development of similar instabilities.

We have previously shown that application of adaptive feedback control can reduce the severity of the cycle-to-cycle variation allowing the practical operating range of an engine to be extended [1,2]. The adaptive feedback controller observes several hundred cycles of uncontrolled behavior at a given operating condition to develop a relationship between the heat release of the current cycle and that of the following cycle. With knowledge of this relationship, the controller is capable of monitoring the heat release of the current cycle and using that information to predict the behavior of the following cycle. A control perturbation proportional to the difference between the predicted behavior and a desired target point is then applied to the following cycle to steer the system toward the desired behavior. Such control is proactive to prevent expected deviations in behavior rather than reactive to correct for deviations which have already occurred. Control perturbations may be applied to

a variety of system parameters including fueling, ignition timing, and valve timing. Recent work also indicates these techniques may be applicable to HCCI combustion systems [3-5].

In preparation for applying adaptive feedback control to lean burn or high EGR ARES-sized NG engines, we have developed a technique to estimate the expected benefit of adaptive control on a particular engine platform to address requests by industry partners. The foundation of the technique is a hybrid spark ignition (SI) engine model which combines commercially available and industry-accepted engine modeling software (WAVE from Ricardo, Inc.) with an advanced, two-zone combustion model [6]. Detailed engine geometry information and data collected during lean or high-EGR, stoichiometric operation is used to calibrate the hybrid model to accurately simulate the behavior of the specific engine. Specifically, the model is capable of accurately predicting the development and effects of combustion instabilities that occur in highly dilute combustion. Application of adaptive control to the model through a Matlab/Simulink interface allows direct estimation of the gains in fuel efficiency and emissions reduction achievable with adaptive control.

## Development of the single-cylinder version of the Waukesha APG1000

ORNL has contracted with Digital Engines, LLC, to fabricate a single cylinder engine with components from the Waukesha APG 1000 (their new ARES-class engine). The engine has been designed to maximize the amount of flexibility and can be adapted for significantly larger engine piston configurations. Single cylinder engines are an optimum platform for combustion studies and are outstanding tools to develop control algorithms. The engine is planned for installation in a new laboratory at the National Transportation Research Center that will be configured into a new engine test cell. The extent of actual installation will depend on funding projections but our goal is to install the engine for possible use in this or other projects. Fig. 1 shows the engine nearing completion.



**Figure 1.** DE-SCE-1 Single Cylinder Engine for ORNL

### **Model development for single-cylinder engine**

In cooperation with Waukesha, we have developed and validated a model for the single-cylinder version of the Waukesha APG1000 ARES-class engine using WAVE engine modeling software from Ricardo, Inc. (see Figure 2). We used proprietary engine specifications and operational data supplied by Waukesha to build and validate the model. The WAVE model is a low-order model which simulates the entire engine platform including the gas exchange and combustion processes as well as the mechanical components and engine friction. WAVE has built-in emissions models for NO<sub>x</sub>, CO, hydrocarbons, and PM and models for various aftertreatment devices including LNTs which can be added to the modeled system. A Simulink interface allows

real-time application of our adaptive control algorithms directly to the WAVE model which can significantly improve development time.

Once the single-cylinder engine is delivered by Digital Engines and installed and operational at ORNL, the model will be refined and recalibrated to reflect the performance of the installed engine. The model should provide an invaluable tool for developing experimental test plans, interpreting and explaining experimental observations, and rapidly developing and testing control strategies. The combination of the physical engine and the engine model should prove to be a tremendous asset to research activities on the engine and provides an excellent resource for potential collaborative research efforts between ORNL and Waukesha.

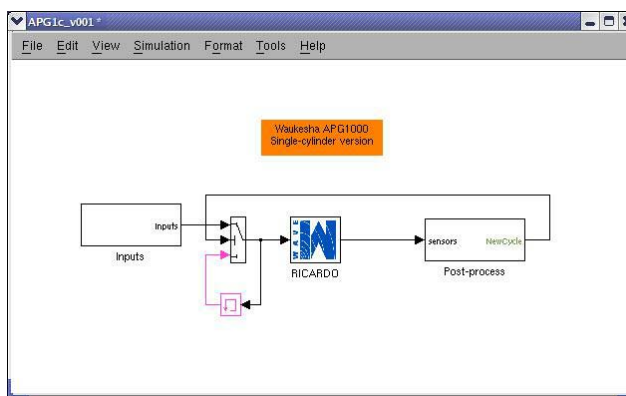
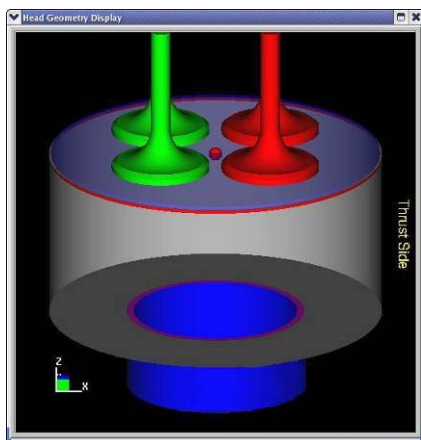
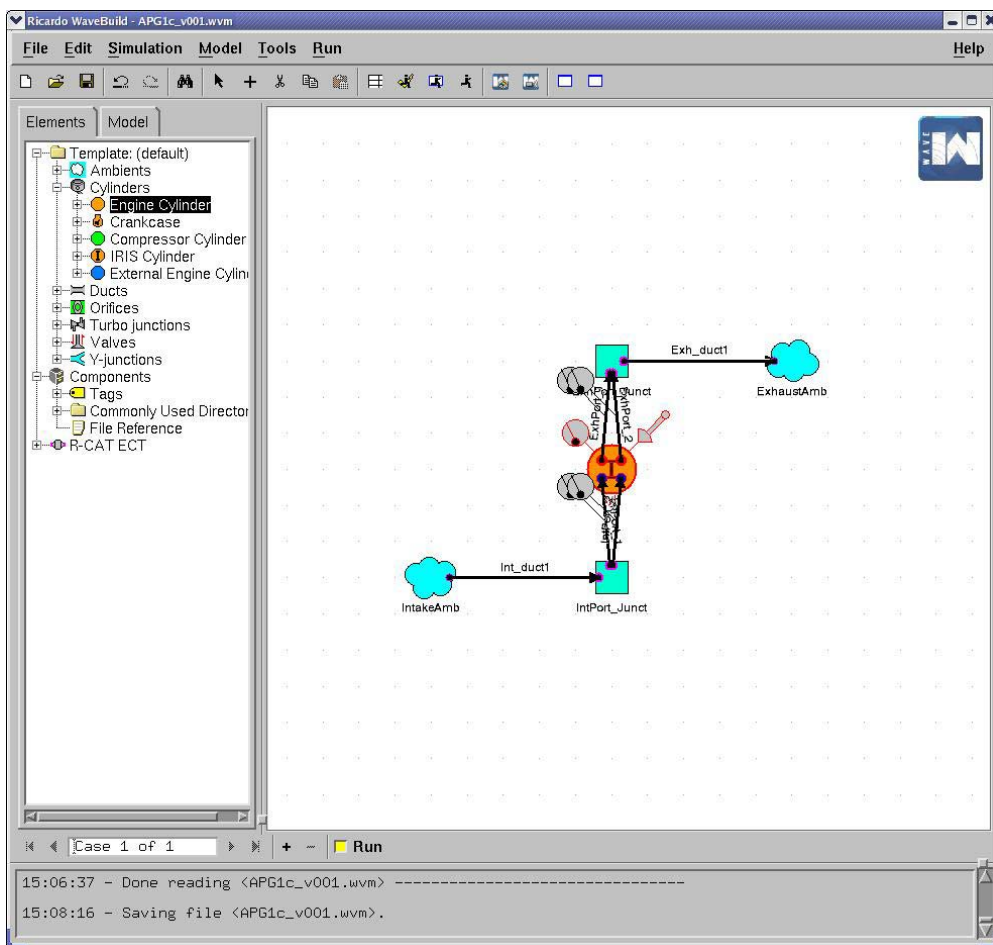


**Figure 2.** The WAVE model of the single-cylinder version of the Waukesha APG1000 has been completed and validated using proprietary data supplied by Waukesha. The model will provide an invaluable asset to the future use of the engine.



## Conclusions

## Future

## Acronyms

APG	Advanced Power Generation
ARES	Advanced Reciprocating Engine Systems
CFR	Cooperative Fuel Research
COV	Coefficient of Variation
EGR	Exhaust Gas Recirculation
HCCI	Homogeneous Charge Compression Ignition
IMEP	Indicated Mean Effective Pressure
NG	Natural Gas
NOx	Oxides of Nitrogen
ORNL	Oak Ridge National Laboratory
SI	Spark Ignition
UHC	Unburned Hydrocarbon emissions

## Publications/Presentations

1. R. M. Wagner, C. S. Daw, K. D. Edwards, J. B. Green, Jr. (2006) "Hybrid SI-HCCI Combustion Modes for Low Emissions in Stationary Power Applications." 3<sup>rd</sup> Annual

## References

1. K. D. Edwards, R. M. Wagner, C. S. Daw (2004) "Adaptive control to limit cyclic dispersion in a lean spark-ignition combustion model during fueling transients." SAE 2004-01-0895.
2. K. D. Edwards, R. M. Wagner, C. S. Daw (2004) "Application of adaptive control to reduce cyclic dispersion near the lean limit in a small-scale, natural gas engine." ASME ICEF2004-855.
3. R. M. Wagner, K. D. Edwards, C. S. Daw, J. B. Green, and B. G. Bunting (2006) "On the Nature of Cyclic Dispersion in Spark Assisted HCCI Combustion." SAE 2006-01-0418.
4. C. S. Daw, R. M. Wagner, K. D. Edwards, J. B. Green, Jr. (2007) "Understanding the Transition Between Conventional Spark-ignited Combustion and HCCI in a Gasoline Engine." 31<sup>st</sup> International Symposium on Combustion, 6-11 August 2006, Heidelberg, Germany.
5. K. D. Edwards, C. S. Daw, R. M. Wagner, J. B. Green, Jr. (2006) "Cyclic Variability During the Transition Between Spark-ignited Combustion and HCCI." *Proceedings of the 2006 Technical Meeting of the Central States Section of The Combustion Institute.* 21-23 May 2006, Cleveland, OH, USA.
6. K. D. Edwards, R. M. Wagner, V. K. Chakravarthy, C. S. Daw, and J. B. Green, Jr. (2005) "A Hybrid 2-Zone/WAVE Engine Combustion Model for Simulating Combustion Instabilities During Dilute Operation." SAE 2005-01-3801.





## 1.6 Lean NO<sub>x</sub> Trap Aftertreatment for Lean Natural Gas Engines

Jim Parks

*Fuels, Engines, and Emissions Research Center*

*Engineering, Science and Technology Division*

*Oak Ridge National Laboratory*

(865) 946-1283, E-mail: [parksjeii@ornl.gov](mailto:parksjeii@ornl.gov)

*DOE Technology Development Manager: Ron Fiskum*

(202) 586-9154; fax: (202) 586-7114; e-mail: [ronald.fiskum@ee.doe.gov](mailto:ronald.fiskum@ee.doe.gov)

*ORNL Technical Monitor: Tim Theiss*

(865) 946-1348; fax: (865) 946-1248; e-mail: [theisstj@ornl.gov](mailto:theisstj@ornl.gov)

---

### Objective

- Study the feasibility of using lean NO<sub>x</sub> trap catalyst technology to reduce the NO<sub>x</sub> emissions of lean burn natural gas engines.
- Determine if natural gas can be used as the reductant for regeneration of lean NO<sub>x</sub> trap catalysts.
- Address key technical barriers to implementing a lean NO<sub>x</sub> trap system, such as catalyst durability, sulfur poisoning, cost, etc.

### Approach

- Study a lean NO<sub>x</sub> trap catalyst system installed on a lean natural gas engine (Cummins C8.3-G+) on a dynamometer test platform.
- Evaluate catalyst performance and study process chemistry with analytical tools unique to ORNL.
  - The test platform contained a full array of emission analyzers and other standard engine and exhaust sensors.
- The lean NO<sub>x</sub> trap catalyst system consists of:
  - a chamber for housing the catalysts
  - exhaust valves to divert exhaust flow from the catalysts during regeneration
  - natural gas fuel injectors for introducing reductant during catalyst regeneration
  - exhaust oxygen sensors to monitor the air-to-fuel ratio during catalyst regeneration
  - a computer control and data acquisition system (LabView based)
- In addition to the lean NO<sub>x</sub> trap catalysts, oxidation and reformer catalysts were used upstream of the lean NO<sub>x</sub> trap catalysts to enable utilization of the methane in natural gas for regeneration of the lean NO<sub>x</sub> trap.

### Accomplishments

- Determined the effect of sulfur (a known catalyst poison) on the oxidation and reformer catalysts in the lean NO<sub>x</sub> trap catalyst system.
  - Accelerated sulfur aging studies of oxidation and reformer catalysts in exhaust from a Cummins C8.3G natural gas engine were conducted; bottled SO<sub>2</sub> was used to control sulfur loading. A full characterization of the oxidation and reforming chemical reactions was conducted for various operational parameters to determine the effect from sulfur exposure.
    - Since the ability of the oxidation and reformer catalysts to convert the methane in natural gas into a useful reductant for NO<sub>x</sub> reduction is critically necessary to the lean NO<sub>x</sub> trap system, the focus of FY06 was on the durability of the oxidation and reformer catalyst components of the system.
    - Results showed that typical sulfur levels in natural gas would not significantly degrade performance by the oxidation and reformer catalysts due to the lean-rich



cycling operation of the catalysts which enabled sulfur to be continually removed from the catalysts during the rich mode of operation.

### Future Direction

- Investigate catalyst washing procedures as a technique for controlling sulfur effects on the lean NOx trap catalyst. Such techniques may be capable of extending durability (cost benefit) in commercial systems.
- Interest has been expressed in advancing the technology from a laboratory setting to a field study or demonstration site. We plan to evaluate opportunities for field studies and design and plan for a field study if funding permits.

### Introduction

Achieving the ARES goals expands the deployment of clean and efficient reciprocating engines for distributed energy production and, thereby, increases the nation's energy security. The project described in this document is focused on these goals; specifically, the goals of the project are to enable <0.1 g/bhp-hr NOx emissions from lean (high efficiency) natural gas engines.

Stoichiometric engines utilize three-way catalysts to simultaneously control carbon monoxide (CO), hydrocarbons, and NOx in exhaust; however, in lean exhaust, excess oxygen in the exhaust allows oxidation of CO and hydrocarbons without reduction of NOx when three-way catalysts are used. Traditionally, selective catalytic reduction (SCR) catalysis with an ammonia reductant has been used to control NOx in lean exhaust conditions; the ammonia is typically supplied from a urea solution which is injected into the exhaust upstream of the SCR catalyst. While urea-based SCR is a commercially available NOx reduction technology, the requirement for urea storage is a deterrent in some applications, and upcoming regulations may contain NOx emission levels that are difficult to obtain cost effectively with urea-based SCR.

The focus of the study presented here is the application of lean NOx trap catalysis to NOx reduction in lean natural gas engine applications. In lean NOx trap catalysis, NOx is stored on the catalyst under lean exhaust conditions; then, under rich exhaust conditions the NOx is released and reduced to harmless nitrogen (N<sub>2</sub>). The technology is also known as "NOx adsorber" catalysis, "NOx storage and reduction" catalysis,

etc. In FY04, a lean NOx trap catalyst was installed and studied on a dynamometer-based engine platform. The natural gas supplying the engine was used as the source of catalyst reductant. NOx emissions less than 0.1 g/bhp-hr (~0.3 lb/MW-hr) were demonstrated downstream of the lean NOx trap catalyst.<sup>1</sup> This level of NOx meets the ARES program target of 0.1 g/bhp-hr NOx. Fuel penalties for the catalyst system were 1-5% and were dependent on the actual engine conditions used during evaluation. These fuel penalties are low enough to maintain the fuel efficiency benefits of the lean burn engine.

During FY04 studies, the catalyst was evaluated under a variety of conditions, and emission measurements were made upstream and downstream of the catalyst to characterize the catalyst performance and process chemistry. Important technical issues and challenges were identified. Efficient utilization of the natural gas, which is primarily methane, is one the significant challenges in this application since methane is difficult to react catalytically. Another key technical issue is the temperature range of lean exhaust from natural gas reciprocating engines since the NOx storage capacity of the lean NOx trap catalyst varies with temperature.

In FY05, studies focused primarily on addressing the technical challenge of utilizing natural gas for regeneration of a lean NOx trap catalyst on a lean burn natural gas reciprocating engine. Lean NOx trap catalysts are not typically efficient at regenerating with a methane reductant, which is the primary component of natural gas; so, methane is typically partially oxidized and/or reformed into hydrogen (H<sub>2</sub>) and/or carbon monoxide (CO)



which are much more effective at regenerating the lean NO<sub>x</sub> trap. Efficient conversion of methane into H<sub>2</sub> and CO reductants is important to minimize fuel penalties associated with the NO<sub>x</sub> reduction process and minimize methane emissions associated with introducing the natural gas into the exhaust stream for catalyst regeneration. The utilization of natural gas across oxidation, reformer, and lean NO<sub>x</sub> trap catalysts is analyzed by measuring methane, CO, and H<sub>2</sub>, etc. upstream and downstream of the catalysts. The results showed that the reformer catalyst greatly assists the generation of H<sub>2</sub> for lean NO<sub>x</sub> trap regeneration. The study gave an improved understanding of the chemistry occurring in the catalytic exhaust system and a cost model for the oxidation and reformer catalyst sizing in the system.

In FY06, the project began focusing on durability issues of the lean NO<sub>x</sub> trap system since the results to date have shown the lean NO<sub>x</sub> trap technology to be suitable for lean natural gas engine applications on a performance basis. The durability study primarily focused on the effects of sulfur on the oxidation and reforming catalyst performance. Sulfur is a known catalyst poison and can potentially degrade the performance of these catalysts over time; thus, studies were conducted under various sulfur exposure scenarios to determine if the oxidation and reformer catalysts could maintain their critical function of producing CO and H<sub>2</sub> reductants from methane for lean NO<sub>x</sub> trap regeneration. Results showed that typical sulfur levels in natural gas would not significantly degrade performance by the oxidation and reformer catalysts due to the lean-rich cycling operation of the catalysts which enabled sulfur to be continually removed from the catalysts during the rich mode of operation.

In this report, the lean NO<sub>x</sub> trap system and experimental engine platform are presented. Then, the details and results of the FY06 study on the sulfur effects on the partial oxidation and reformer catalysts are presented. The technical details have been reported in the ASME publication listed in the "FY2006 Presentations/Publications" section which is heavily referenced for this report.

## Lean NO<sub>x</sub> Trap System and engine Platform

The experiments in this study have been performed on an in-line 6-cylinder 8.3-liter natural gas engine (Cummins CG-280) with a peak torque of 1153 Nm (850 ft-lb) at 1400 rpm and a peak power of 209 kW (280 hp) at 2400 rpm. The engine load and speed were controlled by a 600-hp dynamometer system (General Electric Model 42G61). All experiments were performed at 1800 rpm and steady-state conditions to simulate genset speeds. Intake air conditions were controlled to approximately 23.9°C (75°F) with a relative humidity of 55%.

The catalyst system mounted to the engine exhaust consisted of a two-chamber system with two exhaust brake valves (US Gear) controlling the flow to both chambers (see **Figures 1 and 2**). One chamber simply consisted of an empty pipe and will be referred to as the "bypass leg". The second chamber contained the oxidation, reformer, and lean NO<sub>x</sub> trap catalysts and will be referred to as the "catalyst chamber" or "leg". Downstream of the bypass and catalyst legs, the exhaust from the two legs combined again to exit the system.

The volumes of catalysts in the catalyst chamber were 7 liters, 7 liters, and 14 liters for the oxidation, reformer, and lean NO<sub>x</sub> trap catalysts respectively. The order from upstream to downstream of the catalysts in the catalyst chamber was oxidation, reformer, and then lean NO<sub>x</sub> trap catalysts. All catalysts were supplied by EmeraChem LLC.

Exhaust was sampled for analysis by emissions analyzers at several locations in the exhaust including positions between catalyst monoliths as described in **Figure 2**. Exhaust samples were made at various points in the system as indicated by the abbreviations "Sys In", "Oxi Cat In", "Oxi Cat Out", "Ref Cat Out", "LNT Out", and "Sys Out".

The combination of standard emission analyzers, FTIR gas cell analysis, and a novel tool developed by ORNL for H<sub>2</sub> analysis known as "SpaciMS" enabled the measurement of the major species of interest for methane partial oxidation and reforming processes. **Figure 3** shows a schematic



**Figure 1.** Picture of the lean NOx trap catalyst system installed on the ORNL engine-dynamometer platform.

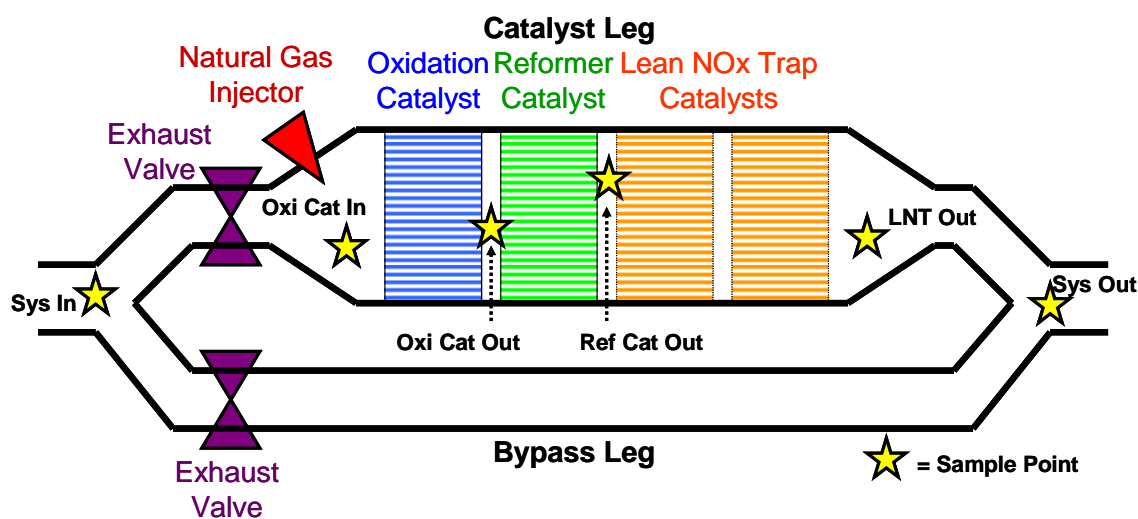


**Figure 2.** Lean NOx trap catalyst system.

of the exhaust analysis system with reference to the analyzers employed and the gas species measured.

### Sulfur Exposure Experiment

In the FY06 study presented here, the oxidation and reformer catalysts were exposed to sulfur to determine the effects of sulfur on the durability of the catalysts. Sulfur exposure was performed by adding sulfur in the form of sulfur dioxide ( $\text{SO}_2$ ) into the exhaust system; a bottled gas tank of 1%  $\text{SO}_2$  in  $\text{N}_2$  was the  $\text{SO}_2$  source. The  $\text{SO}_2$  was added downstream of the engine turbo and downstream of an air-to-liquid heat exchanger in the exhaust system. The  $\text{SO}_2$  added to the system

passed through a curved section of exhaust prior to entering the catalyst system; this allowed mixing of the  $\text{SO}_2$  to occur prior to catalyst exposure. Measurement of the  $\text{SO}_2$  in the exhaust was performed by sampling a small (~1-2 liter/min) amount of exhaust just prior to the catalyst system. The concentration of  $\text{SO}_2$  was measured in chilled exhaust with an  $\text{SO}_2$  analyzer (Ametek Model 922). During the sulfur exposure experiments, the lean NOx trap catalysts were removed from the system; this study focused on the sulfur effects on the oxidation and reformer catalysts.

During the experiments, the engine load and speed were kept constant at 180 hp (~75% load at 1800 rpm) and 1800 rpm, respectively. The

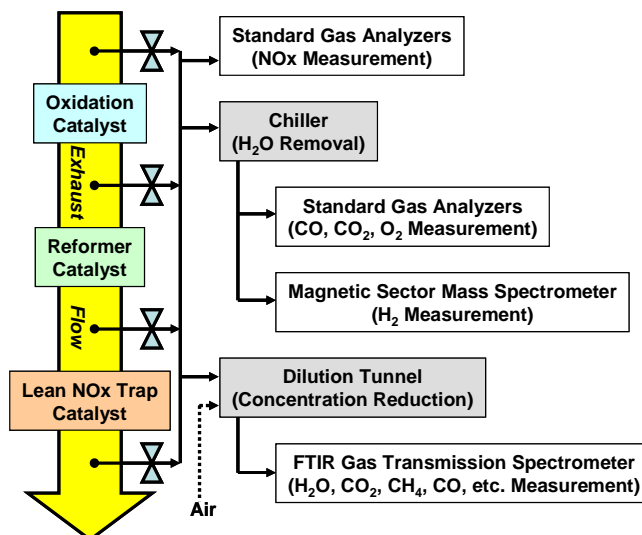


**Figure 3.** Schematic of exhaust gas analysis system.

catalysts were cycled in a lean-rich manner typical of operation for a lean NO<sub>x</sub> trap system. The cycle parameters were held constant throughout the experiment; the cycle was composed of 45 seconds of lean operation (main exhaust flow through catalyst leg) and 15 seconds regeneration that included transition of the exhaust control valves (main exhaust flow through bypass leg with catalyst leg becoming rich for LNT regeneration). Thus, each cycle lasted 1 minute total. The space velocity of the exhaust for the oxidation and reformer catalysts varied during the lean-rich cycle. During lean operation with full exhaust flow the space velocity was 102,000/hr for each catalyst, but during the lower flow rich operation, the space velocity was 7,000/hr for each catalyst. The rich mode exhaust flow was determined by measuring O<sub>2</sub> dilution during addition of a known flow rate of N<sub>2</sub> to the exhaust. During the 15 second regeneration period, fuel was injected into the catalyst chamber upstream of the oxidation catalyst for 10 seconds; the remaining time allowed the fuel to be purged from the catalyst chamber prior to the influx of lean exhaust. A small flow of exhaust from the engine passed through the catalyst chamber during regeneration which carried the injected fuel through the catalysts. Flow of fuel through the injectors was controlled to attain a target excess air ratio ( $\lambda$ ) of 0.75 during the regeneration period;  $\lambda$  was monitored with UEGO sensors in the system. In

general, the catalysts were cycled before, during, and after SO<sub>2</sub> exposure; however, some periods of lean only operation were purposely practiced to determine if lean vs. rich operation allows recovery of lost performance due to SO<sub>2</sub> exposure.

The flow of SO<sub>2</sub> was controlled to attain different levels of additional SO<sub>2</sub> exposure: concentrations of 3, 15, and 40 ppm SO<sub>2</sub> entering the catalyst system. Here the term “additional SO<sub>2</sub> exposure” points out that a small level (<1 ppm) of SO<sub>2</sub> is already in the exhaust due to sulfur in the fuel and oil. It is important to note that the levels of SO<sub>2</sub> artificially imposed in this study are much greater than typical levels of SO<sub>2</sub> experienced in natural gas engine applications. The higher SO<sub>2</sub> levels were used to accelerate any effects from sulfur so that those effects could be measured practically in a controlled experiment. The exposure times varied but were less than 1 hour. Originally, longer exposure times were planned, but it was observed that reactions to SO<sub>2</sub> exposure were rapid with performance quickly approaching steady-state conditions. Thus, experiments focused on characterizing the reaction of the catalysts to the SO<sub>2</sub> exposure until steady-state conditions occurred. Then, after SO<sub>2</sub> exposure was complete, the performance of the catalysts was again monitored to determine if recovery from the negative effects of SO<sub>2</sub> exposure would occur.



Catalyst temperatures were controlled with the upstream air-to-liquid heat exchanger and were generally stable during the experiments. Typically, the average oxidation and reformer catalyst temperatures were between 520 and 525°C. Note that during the catalyst cycle, the catalyst temperature fluctuated due to exotherms produced as fuel was oxidized over the catalyst in the transition from lean to rich conditions. A typical range of temperatures experienced by the catalysts during a cycle was typically 514-536°C for the oxidation catalyst and 518-533°C for the reformer catalyst; here the oxidation temperature range is greater since more fuel is oxidized over the oxidation catalyst. For the 40-ppm SO<sub>2</sub> exposure, a second catalyst temperature range was used with average oxidation and reformer catalyst temperatures of 460 to 465°C; in this case, typical ranges of temperature were 455-473°C and 458-470°C for the oxidation and reformer catalysts, respectively.

#### **FY06 Results**

Reactions of the oxidation and reformer catalyst performance to a typical SO<sub>2</sub> exposure experiment are shown in **Figure 4** which shows data from 15-ppm SO<sub>2</sub> exposure. Peak CO and H<sub>2</sub> downstream of the oxidation and reformer catalysts are plotted vs. time in minutes which is also equivalent to the number of cycles (since each cycle lasted one minute); the peak concentrations of the reductant species are shown in this graph. The phases of the exposure include a pre-SO<sub>2</sub> phase, the 15-ppm SO<sub>2</sub> exposure, a lean period, and a recovery period with lean-rich cycling but no SO<sub>2</sub> added. During all phases, the engine load and speed were kept constant at 75% and 1800 rpm, respectively. During the pre-SO<sub>2</sub> phase, the catalysts were cycled with the parameters detailed above; the parameters are typical of normal cycling during lean NOx trap system operation. At time=20 minutes, the flow of SO<sub>2</sub> at a 15-ppm concentration began, and immediately, the oxidation and reforming processes lost efficiency due to the SO<sub>2</sub> exposure. After approximately 10 cycles/minutes, the performance had decreased to a steady-state level and did not change with additional SO<sub>2</sub> exposure time. At this point (time=70 minutes), the SO<sub>2</sub> exposure was stopped,

and the catalyst was left in a lean (oxygen rich) state to determine if SO<sub>2</sub> chemisorbed on the catalyst would desorb under lean conditions with exhaust flowing over the catalysts. Then, after 30 minutes, lean-rich cycling was restarted without SO<sub>2</sub> addition; this phase is called “recovery” since performance does recover here. No recovery of lost performance due to SO<sub>2</sub> exposure was observed after the 30 minute lean period based on the performance at the initiation of the lean-rich cycling at time=100 minutes. However, during the lean-rich cycling of the recovery phase, reductant concentration rose, and performance did recover. All of the initial performance was recovered within the experimental accuracy of the experiment. The fact that the recovery occurred during lean-rich cycling but not during lean operation suggests that SO<sub>2</sub> is being desorbed from the catalysts during rich operation (most likely in the form of H<sub>2</sub>S). Note that the Ref Cat Out H<sub>2</sub> data suggests that performance after recovery was actually higher than the pre-SO<sub>2</sub> level; however, the lower initial results were most likely due to an incomplete recovery from the previous experiment conducted with 40-ppm SO<sub>2</sub> exposure on the previous day (recovery from 40-ppm exposure is apparently slower as discussed below).

Data from exposure to 3 ppm SO<sub>2</sub> (shown in **Figure 5**) followed a similar pattern to the 15-ppm data. Again, CO and H<sub>2</sub> downstream of the oxidation and reformer catalysts are shown as a function of time. During SO<sub>2</sub> exposure, performance degraded to a steady-state level. No significant recovery in performance was observed in the following lean period, but once lean-rich cycling was commenced without SO<sub>2</sub> addition, recovery in performance was observed. Thus, the same general pattern was observed for both the 15-ppm and 3-ppm SO<sub>2</sub> data: performance degradation to a steady-state level during SO<sub>2</sub> exposure followed by performance recovery during lean-rich cycling without SO<sub>2</sub> addition. The differences in the data from 15-ppm and 3-ppm SO<sub>2</sub> exposure were the rate of change in performance and the level of steady-state performance attained. In general, the degradation rate was slower and the recovery rate was faster

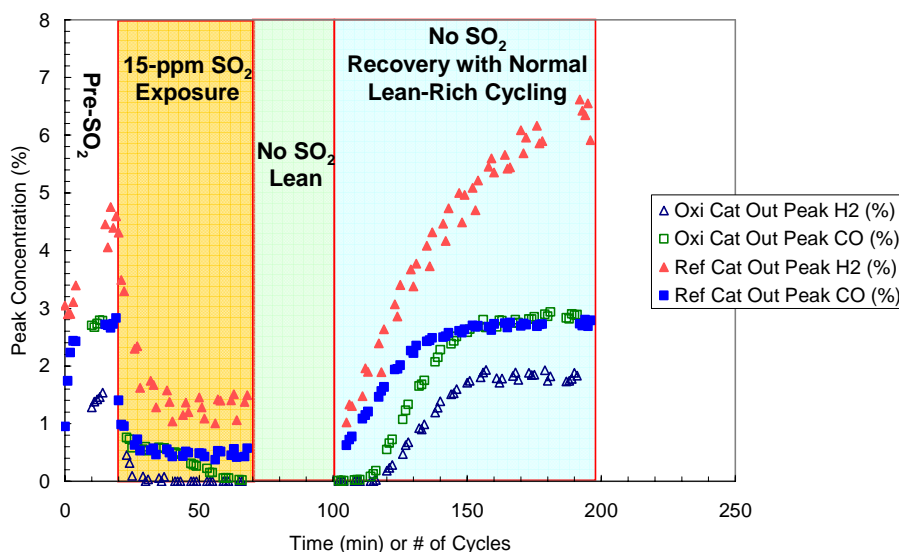


**Figure 4.** CO and H<sub>2</sub> as a function of time and cycles before, during, and after exposure to 15 ppm SO<sub>2</sub>.

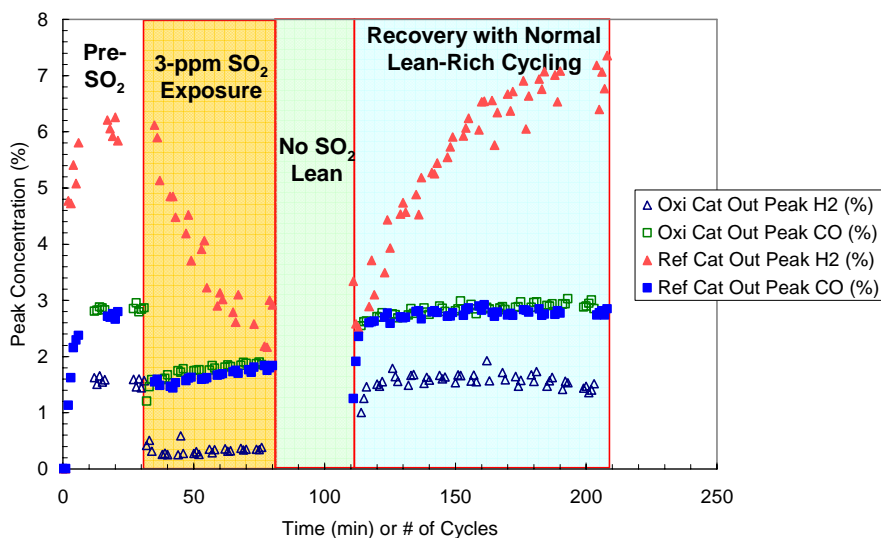


**Figure 5.** CO and H<sub>2</sub> as a function of time and cycles before, during, and after exposure to 3 ppm SO<sub>2</sub>.

for the lower (3-ppm) SO<sub>2</sub> exposure. In addition, the steady-state level of performance attained after exposure was generally higher (greater reductant concentration) for lower level SO<sub>2</sub> exposure. Thus, the qualitative nature of the SO<sub>2</sub> poisoning is similar for different SO<sub>2</sub> concentrations, but the quantitative results for rates of change and performance levels differed.

Another interesting finding from the 3-ppm SO<sub>2</sub> data shown in **Figure 5** relates to the comparative degradation and recovery rates among sample position and reductant type. The decrease in CO and H<sub>2</sub> downstream of the oxidation catalyst was very rapid. For the reformer catalyst, CO decreased rapidly, but H<sub>2</sub> degradation occurred at a relatively slower rate. Likewise, during recovery, H<sub>2</sub> at the reformer catalyst out position again occurred at the



slowest rate. The cause of the slower reaction of the reformer catalyst out H<sub>2</sub> data is confounded by the fact that the reforming chemistry must follow the oxidation reaction. The rate of recovery of performance is an even stronger function of SO<sub>2</sub> concentration during SO<sub>2</sub> exposure when comparing results for 3-ppm, 15-ppm, and 40-ppm SO<sub>2</sub> (**Figure 6**). The effect does not appear to be linear as the 40-ppm SO<sub>2</sub> concentration data takes much longer to recover from the SO<sub>2</sub> exposure.

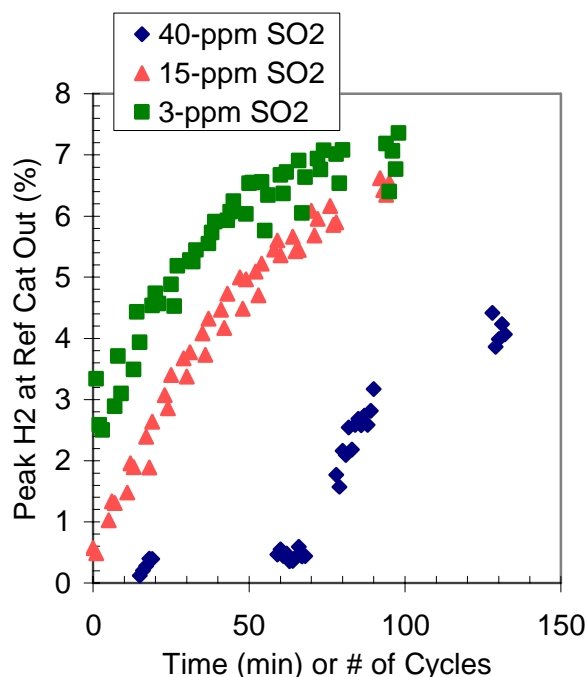


**Figure 6.** Recovery of H<sub>2</sub> downstream of the reformer catalyst after exposure to SO<sub>2</sub>.

A comparison of data from all levels of SO<sub>2</sub> (3 ppm, 15 ppm, and 40 ppm) is shown in **Figure 7** for the 520°C catalyst temperature. The results show that recovery occurs for all concentrations of SO<sub>2</sub> used during exposure. There is slightly less H<sub>2</sub> for the 40-ppm SO<sub>2</sub> reformer catalyst out case (**Figure 7.d**); however, the performance was still increasing at the end of the data collection. The 40-ppm SO<sub>2</sub> case did not show any significantly interesting effects in comparison to the 3-ppm and 15-ppm cases. Degradation was essentially complete for the 40-ppm case, but recovery did occur.

**Figure 8** shows a comparison of data from 40 ppm SO<sub>2</sub> exposure for two catalyst temperatures: 460°C and 520°C. Here again, the results show that complete recovery does occur after lean-rich cycling in the recovery phase regardless of the catalyst temperature. The oxidation and reforming processes have different efficiencies for the two different temperatures, but both temperatures show recovery of performance occurring. Degradation for the lower temperature case where the partial oxidation is less efficient even for the cases without SO<sub>2</sub> was significant enough to result in no reductant production downstream of the reformer catalyst.

### Discussion: Implications of the Results

The results for different SO<sub>2</sub> concentrations consistently showed that degradation of oxidation and reforming processes occurs with SO<sub>2</sub> exposure, but full recovery also occurs during normal lean-rich cycling once SO<sub>2</sub> exposure is stopped. It is worth repeating that the SO<sub>2</sub> concentrations used in these studies were orders of magnitude higher than SO<sub>2</sub> concentrations commonly found in natural gas engine exhaust. Sulfur levels in natural gas fuel are typically less than 10 ppm, and since fuel and air are mixed in the combustion process, SO<sub>2</sub> levels in exhaust are typically <1 ppm (including contributions from sulfur in combusted oil). At these low levels of SO<sub>2</sub>, degradation from sulfur poisoning is unlikely to be significant as long as the catalysts are cycled in a lean-rich fashion since the rich operation causes any accumulated sulfur poisons to be released.

For applications where higher levels (>1 ppm) of sulfur are present in the natural gas (for example, gas compression engines at an oil field), the effect of sulfur will be dependent on the magnitude of SO<sub>2</sub> in the exhaust with increasing SO<sub>2</sub> content causing a decrease in catalytic performance. Brief exposure to high SO<sub>2</sub> concentrations can be tolerated since the lean-rich cycling is continually removing sulfur from the catalysts as well. Actual performance

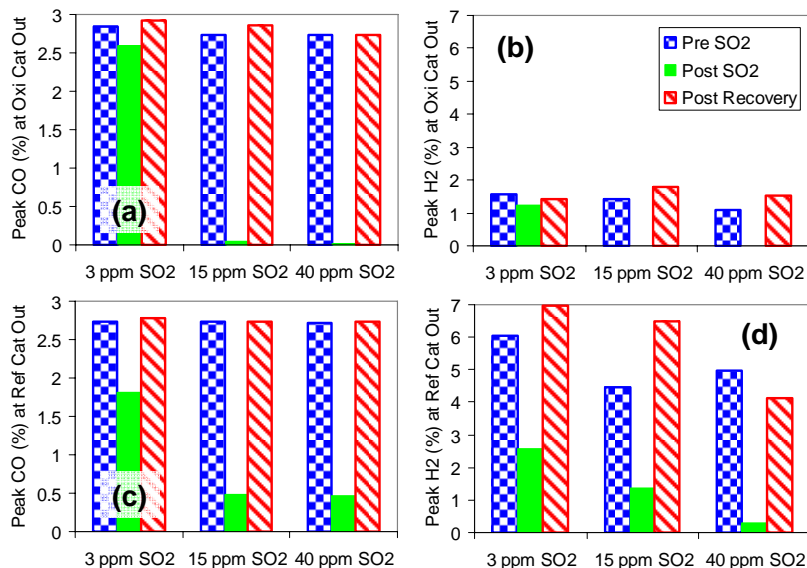


**Figure 7.** Comparison of pre-SO<sub>2</sub>, post-SO<sub>2</sub>, and post-recovery reductant concentrations for 3-ppm, 15-ppm, and 40-ppm SO<sub>2</sub> exposure experiments; peak reductant concentrations shown for (a) oxidation catalyst out CO, (b) oxidation catalyst out H<sub>2</sub>, (c) reformer catalyst out CO, and (d) reformer catalyst out H<sub>2</sub>.

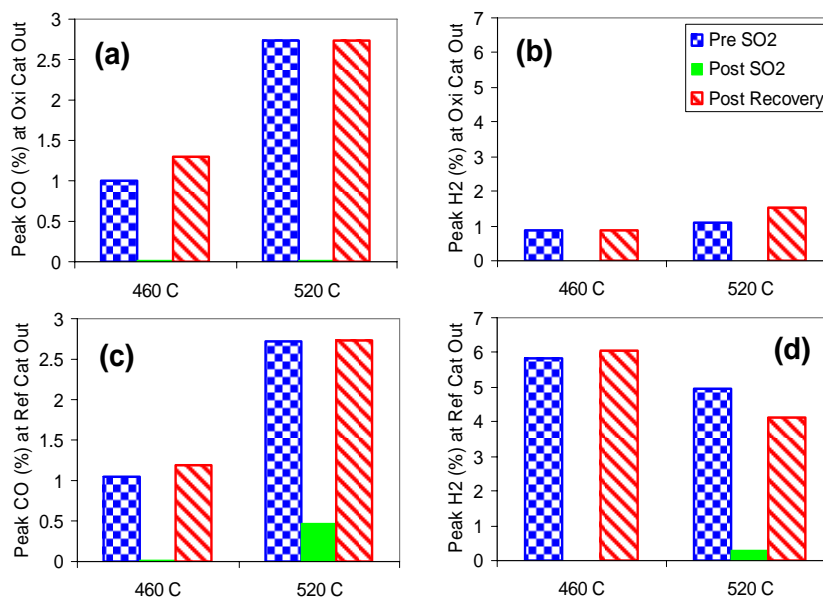


**Figure 8.** Comparison of pre-SO<sub>2</sub>, post-SO<sub>2</sub>, and post-recovery reductant concentrations for 460°C and 520°C catalyst temperatures for 40-ppm SO<sub>2</sub> exposure; peak reductant concentrations shown for (a) oxidation catalyst out CO, (b) oxidation catalyst out H<sub>2</sub>, (c) reformer catalyst out CO, and (d) reformer catalyst out H<sub>2</sub>.

will be determined by the steady-state equilibrium established by the quantity of SO<sub>2</sub> in the exhaust and the rate at which the SO<sub>2</sub> is removed from the catalysts by the periodic rich operation. In cases where oxidation and

reformer catalyst performance is not sufficient, partial oxidation of methane by operating a reciprocating engine rich is a possible replacement technique; however, at SO<sub>2</sub> levels where the oxidation and reformer catalysts do



not perform well, the lean NO<sub>x</sub> trap catalyst is likely to suffer even greater performance loss.

In the lean NO<sub>x</sub> trap application where the oxidation and reformer catalysts are cycled between lean and rich conditions, the sulfur exposure effect is primarily dependent on the concentration of sulfur exposure as opposed to the total mass of sulfur exposure. In contrast, typical reformer catalyst applications, where the catalyst is operated continuously under rich conditions, experience degradation primarily proportional to the total mass of sulfur exposure (regardless of sulfur concentration). The lean-rich cycle changes the rich-only model by enabling oxidation of chemisorbed sulfur species (H<sub>2</sub>S, COS, etc.) over the catalyst during lean operation and reduction and release of chemisorbed sulfur species (SO<sub>2</sub>) during lean operation. The kinetics of these oxidation and reduction reactions dictates the amount of sulfur removal from the catalyst and becomes a factor in the overall sulfur accumulation rate under lean-rich cycling. Thus, the accumulated mass of sulfur exposure is still a primary factor but is primarily determined by the rate of sulfur accumulation (concentration dependent) and the rate of sulfur release (kinetic dependent).

### Conclusions

Studies related to the durability of a lean NO<sub>x</sub> trap catalyst system were conducted on a lean natural gas reciprocating engine platform. Experiments focused on the effect of sulfur on the oxidation and reformer catalysts of the lean NO<sub>x</sub> trap system. The catalysts were exposed to SO<sub>2</sub> at different concentrations, and the ability of the catalysts to produce CO and H<sub>2</sub> reductants through partial oxidation of methane and reforming processes was characterized.

Upon exposure to SO<sub>2</sub>, a rapid loss in reductant production occurred; however, once SO<sub>2</sub> exposure was stopped, performance recovered to initial levels under normal lean-rich cycling conditions. The recovery occurs during rich operation since no recovery was observed after lean operation. Similar effects were observed for different levels of SO<sub>2</sub> during exposure, but the magnitude of the effects varied. Performance during SO<sub>2</sub> exposure decreased to a

steady-state level of performance; higher levels of steady-state performance were associated with lower levels of SO<sub>2</sub> concentration during exposure.

The results indicate that sulfur will not significantly affect the critical oxidation and reforming processes for most applications where low levels (<1 ppm) of sulfur occur and the catalysts are cycled in a lean-rich manner typically associated with lean NO<sub>x</sub> trap catalysts. For higher levels of sulfur that may be experienced in some applications, performance of the oxidation and reformer catalysts may be hampered with the magnitude of the effect proportional to the level of sulfur in the exhaust, but the effect should not be permanent with performance recovering once sulfur levels decrease. These results specifically address the oxidation and reformer catalyst portions of the lean NO<sub>x</sub> trap system; the effect of sulfur on lean NO<sub>x</sub> trap catalyst durability is severe and will need to be addressed in future work.

### Acknowledgments

Oak Ridge National Laboratory (ORNL) would like to acknowledge EmeraChem LLC for supply of the catalysts. This work is a part of the U. S. Department of Energy (DOE) Advanced Reciprocating Engine System (ARES) Program within the Office of Distributed Energy Resources. The ARES program, under the leadership of Ron Fiskum, is in cooperation with representatives from Caterpillar, Cummins, and Waukesha. Senthil Ponnusamy performed work under a subcontract with Oak Ridge Associated Universities. ORNL is managed by UT-Battelle LLC for the US Department of Energy under subcontract DE-AC05-00OR22725.

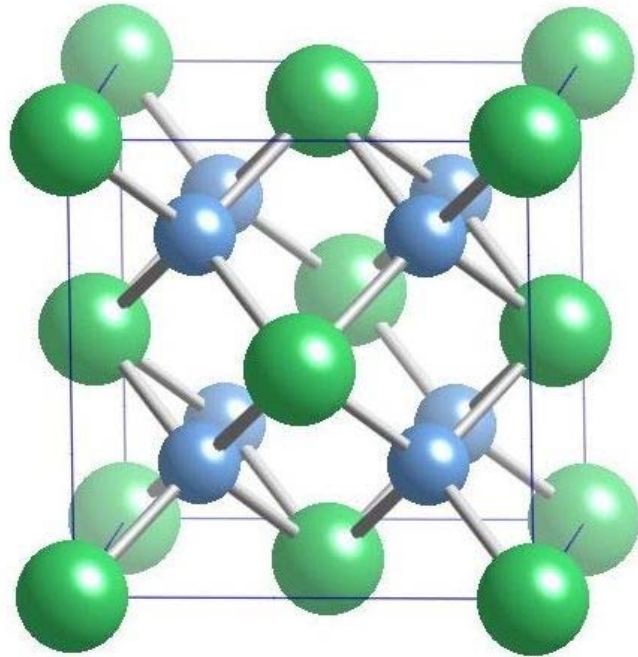
### FY2006 Presentations/Publications

- Jim Parks and Senthil Ponnusamy, "Lean NO<sub>x</sub> Trap Catalysis: NO<sub>x</sub> Reduction for Lean Natural Gas Engine Applications", *3rd Annual Advanced Stationary Reciprocating Engines Meeting*, Argonne, IL, June 28-30, 2006.
- James E. Parks II and Senthil Ponnusamy, "The Effect of Sulfur on Methane Partial



Oxidation and Reforming Processes for  
Lean NO<sub>x</sub> Trap Catalysis”, *Proceedings of  
ASME Internal Combustion Division: 2006*

*Fall Technical Conference ICEF2006-1535  
(2006).*



**Materials**



## 2.1.1 Advanced Alloys for High-Temperature Recuperators

*P.J. Maziasz*

*Metals and Ceramics Division*

*Oak Ridge National Laboratory*

*P.O. Box 2008, MS-6115*

*Oak Ridge, TN 37831-6115*

*(865) 574-5082; fax: (865) 754-7659; e-mail: [maziaszpj@ornl.gov](mailto:maziaszpj@ornl.gov)*

*DOE Technology Development Manager: Debbie Haught*

*(202) 586-2211; fax: (202) 586-7114; e-mail: [debbie.haught@ee.doe.gov](mailto:debbie.haught@ee.doe.gov)*

*ORNL Technical Advisor: Dave Stinton*

*(865) 574-4556; fax: (865) 576-5413; e-mail: [stintondp@ornl.gov](mailto:stintondp@ornl.gov)*

---

### Objectives

- Determine creep- and oxidation-resistance of cost-effective commercial high-temperature recuperator alloys.
- Test commercial sheets and foils of AL20-25+*Nb* alloy with modified processing to optimize creep-resistance (Phases I and II) at ORNL.
- Characterize recuperator aircells made from advanced stainless alloys (HR120 and AL20-25+*Nb*).

### Approach

- Build the unique data base of creep- and oxidation-resistance data of commercial sheets/foils of advanced heat/corrosion resistant alloys for improved performance and reliability at 700-750°C.
- ORNL established a joint program with Allegheny-Ludlum to produce and deliver commercialization of AL20-25+*Nb* alloy to recuperator OEMs.
- ORNL concluded creep-rupture tests and microcharacterization of the same Phase I and II foils/sheets of AL20-25+*Nb* alloy to verify product performance and compare with other advanced alloys.

### Accomplishments

- ORNL testing of Phase II sheets/foils of AL20-25+*Nb* alloy show that modified processing of sheet increased the uniform grain size to almost double creep-rupture life at 750°C compared to Phase I. Creep resistance exceeds HR120 and HR230, and comes close to that of alloy 625.

### Future Directions

- Complete microcharacterization of creep-tested foils/sheets of AL20-25+*Nb* and HR120 alloys, and alloy 625 to better understand performance differences and provide better lifetime predictions for advanced recuperator applications.



## Introduction

Previous reviews and papers adequately define the critical role that recuperators play in advanced microturbines, the growing evidence of the inadequacy of 347 steel, and the need for the most cost-effective alloys capable of reliable performance at 650-700°C and above [1-6]. Use of opportunity or alternate fuels (gaseous or liquid) instead of clean natural gas and cyclic operation will further challenge the recuperator.

Several years ago, ATI Allegheny-Ludlum and Solar Turbines introduced the new AL20-25+Nb stainless alloy as one of the upgrade options for the primary-surface (PS) recuperator for the new Mercury 50 low-emission industrial gas turbine engine [7-9]. Oxidation testing in 7-10% water vapor at 700-760°C by Rakowski et al [7,9] has shown good, long-term resistance of AL20-25+Nb stainless alloy to the moisture enhanced oxidation that plagues 347 stainless steels above 650°C. Similarly, good long-term resistance to moisture enhanced oxidation has been shown by Pint et al [4,10] in 10% water vapor at 650-800°C for foils of HR120 and NF709 (also Fe-20Cr-25Ni alloy) alloys, far better than 347 steel. All investigators show outstanding resistance of the Ni-based superalloy 625 to moisture-enhanced oxidation. Lara-Curzio further demonstrates significant shorter-term advantages of foils of HR120 alloy compared to 347 steel for both moisture-enhanced oxidation and creep in accelerated testing in the ORNL Recuperator Test Facility, which also includes the dynamic effects of high-velocity gas during oxidation [6].

In 2004, ORNL and ATI Allegheny-Ludlum began a collaborative project to extend previous work by producing a wide range of commercial quantities of AL20-25+Nb stainless alloy foils and sheets needed to manufacture air cells for both brazed plate and fin (BPF) and PS recuperators for the new, larger 200-250 kW advanced microturbine engines. AL20-25+Nb alloy is another in a group of austenitic stainless alloys based on the Fe-20Cr-25Ni composition, including NF709 from Nippon Steel Corp., and 12R72HV from Sandvik, developed to have more creep

strength than 347 or 17-14CuMo stainless steels for fossil boiler tubing applications [11-14]. While alloy 625 has outstanding oxidation resistance and strength for advanced recuperator applications, its initial cost is still relatively high compared to 347 steel [3,15]. It also tends to have lower rupture ductility, particularly close to 700°C, which can also cause concern for cyclic microturbine operation. HR120 alloy has outstanding oxidation resistance, but it is not as strong as alloy 625 and costs only slightly less [15]. AL20-25+Nb alloy has the potential to cost significantly less than alloy 625, and have the most cost-effective combination of oxidation and creep-resistance improvement relative to 347 steel. Therefore, this joint ORNL and ATI Allegheny-Ludlum project was designed to a) measure the properties and microstructure of the commercial sheets and foils used for both kinds of recuperator aircells, and b) modify commercial processing parameters to control the microstructure for improved creep-resistance. The basis for foil/sheet processing changes producing controlled increases in grain size as well as dramatic refinements in NbC precipitate dispersions was established by previous ORNL/ATI Allegheny-Ludlum work that produced AL347HP<sup>TM</sup> [15,16]. This annual report summarizes progress made on this project during FY2006.

## Approach

The collaborative project began with a 5000 lb coil (42 inch width) of hot-band from the original heat of AL20-25+Nb, and the alloy composition is given in Table 1. Compositions of heats of 347 steel and alloy 625 supplied as foils and sheets by ATI Allegheny-Ludlum to compliment this study are also listed in Table 1. Compositions of all other alloys test at ORNL and used to make further comparisons are similar to or the same as those reported previously [15].

This collaborative project was divided into two phases. Phase I was the main commercial foil and sheet effort, producing over 1000 lb of finished foils, and 800 lb of finished sheets, with standard processing similar to previous work on



**Table 1 – Alloy Compositions (wt.%)**

<u>Alloy</u>	<u>Cr</u>	<u>Ni</u>	<u>Nb</u>	<u>N</u>	<u>C</u>	<u>Mo</u>	<u>Mn</u>	<u>Other</u>
347	18	9.4	.63	.036	.04	.25	1.5	bal. Fe
AL20-25+Nb	20	26	.38	.1	.09	1.51		bal. Fe
HR120	25	35	0.7	.2	.05	2	1	bal. Fe
625	21	bal.	3.4	-	.025	8.3	.03	4.4Fe, 0.2Ti, 0.2Al
HR230	22	bal.	-	-	.1	2	-	3 Fe, 14W, 5Co, 0.3Al

the AL20-25+Nb alloy [7,9]. Phase II of this project produced a much smaller quantity, and only selected thicknesses of foils or sheets, but involved important changes in the processing parameters specifically designed to modify the grain size and solutionizing of NbC for improved creep resistance.

Phase I of this project at ATI Allegheny-Ludlum processed about 5000 lb of original hot-band into over 1000 lb of foils (0.004, 0.005 and 0.008 inch thickness), and 800 lb of sheets (0.010 and 0.015 inch thicknesses) with standard processing conditions. Portions of the 0.010 and 0.015 inch thick sheets were slit into final finished coils, while other portions were used as intermediate stock for further reductions to foils. The 0.004 and 0.005 inch foils were processed directly from 0.010 inch sheet, and the 0.008 inch foil was processed directly from the 0.015 inch sheet. The Phase I foil/sheet products were slit and shipped to Ingersoll Rand Energy Systems (IRES) in 2004/2005, to produce the various different pieces required for making brazed plate-and-fin (BPF) air cells for recuperators for their new 250 kW PowerWorks microturbine.

Phase II of this effort modified the processing of 0.010 inch sheet, and a portion of that was further reduced (with modified processing at this step too) to make several hundred pounds of 0.0032 inch finished foil, which was slit and shipped to Capstone Turbines (CT) for manufacturing trials for welded primary-surface (PS) air-cells for recuperator application in support of their 200 kW microturbine. The remainders of the Phase II effort retained some of the 0.010 inch thick sheet for creep properties studies, and reduced a portion into 0.005 inch thick foil, with further processing modification for enhanced creep resistance.

Panels of all the various Phase I and Phase II sheets and foils of AL20-25+Nb were shipped to ORNL for more detailed creep-rupture and lab-scale oxidation testing, as well as detailed microstructural analysis. Some of these foils have been used to make probes for testing in the ORNL Recuperator Testing Facility, and tests are in-progress now. ORNL wire-EDMed out special sheet creep specimens from each foil or sheet panel, with the specimen gage length parallel to the rolling direction of the material. Tabs were also cut from sheets and foils, and tack-welded to the shoulders for support in the grips. Creep-rupture testing was performed in dead-load machines, with furnaces opened to air. Extensometers are used to measure strain, with computer controlled digital data acquisition. Generally only one specimen per alloy/condition was creep-tested due to limitations in available equipment. However, in some cases, duplicate creep tests were run or are planned.

Microstructural analysis included standard optical metallographic techniques to reveal grain size for transverse cross-sections parallel to the rolling direction of all the as-processed foils and sheets. Some of the creep-ruptured specimens were also examined in transverse cross-section by optical metallography and scanning electron microscopy (SEM). High resolution SEM was performed on some of the creep-ruptured metallographic specimens (polished and unetched) or on electropolished transmission electron microscopy (TEM) discs EDMed from the gage portion of the creep specimen, away from the fracture area. Phase identification was done on a JEOL 6500F microscope, with a field emission gun (FEG) and capability for both secondary electron and back-scattered electron imaging (SE and BSE, respectively). BSE imaging was done at 5 kV for



enhanced contrast, while x-ray energy dispersive spectroscopy (XEDS) was done at 15 kV for microcompositional analysis of individual precipitate particles.

## Results

### Creep-Rupture Testing

Figures 1 and 2 contain updates of the ongoing long-term creep-rupture testing of results presented last year [5], at 750°C/100 MPa and 704°C/152 MPa, respectively. Alloy 625 commercial sheet (0.015 inches thick) shows excellent creep-resistance at both 704 and 750°C, with only about 2% strain and no rupture after over 13,000 h at 750°C. Sheet of the Fe-based oxide dispersion-strengthened (ODS) Plansee alloy, PM2000, by contrast shows minimal creep (< 0.2%) after about 12,000 h at a higher stress; however, PM2000 is much more expensive and more difficult to fabricate for these recuperator applications. Figures 1 and 2 show new data for alloy 625 foils (0.004 inches thick) at both 704 and 750°C, and clearly show that they have much less creep-resistance than sheets, suggesting an effect of fine grain size reducing creep-rupture resistance, as is found in many other heat-resistant alloys [15]. Measurements show that the grain size of the alloy 625 foil is much finer than sheet (8.7 compared to 39  $\mu$ m). However, at 750°C, the foil of alloy 625 is still much more creep-resistant than foil of another Ni-based superalloy, HR230. Figure 2 also shows that at 704°C, AL20-25+Nb (Phase I) alloy foil has similar creep-resistance but over twice the rupture ductility compared to the HR120 (Fe-25Cr-35Ni, Nb, Mo, C, N) stainless alloy.

Results of all ORNL creep-rupture testing done at 650-750°C to date on foils (0.003 to 0.005 inches thick) of AL20-25+Nb alloy and other heat-resistant alloys considered or used for recuperator applications are compared in Figure 3, using the Larson-Miller Parameter, calculated using rupture time and test temperature. For foils, all of these more heat-resistant alloys, including AL347HP (formerly, T347CR [15]), have significantly more creep-resistance than standard 347 steel. Unfortunately, processing to control grain size and intragranular NbC dispersions in 347 steel for improved creep-rupture resistance does nothing to

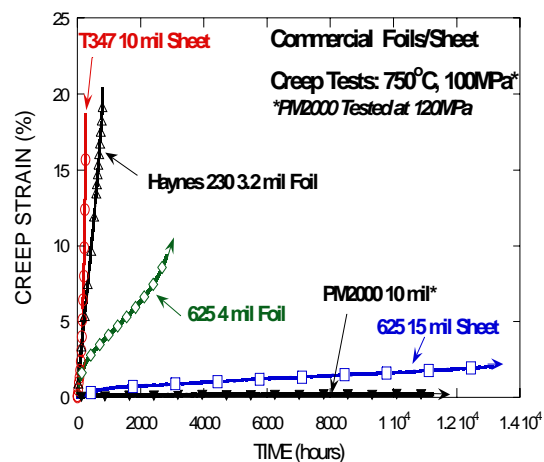


**Figure 1.** Creep-rupture strain versus time data for various commercial heat-resistant alloy sheets and foils tested at 750°C and 100 MPa (except for the PM2000 ODS alloy, tested at 120 MPa) in air. Both alloy 625 and the PM2000 (ODS ferritic alloy) are still in-test.

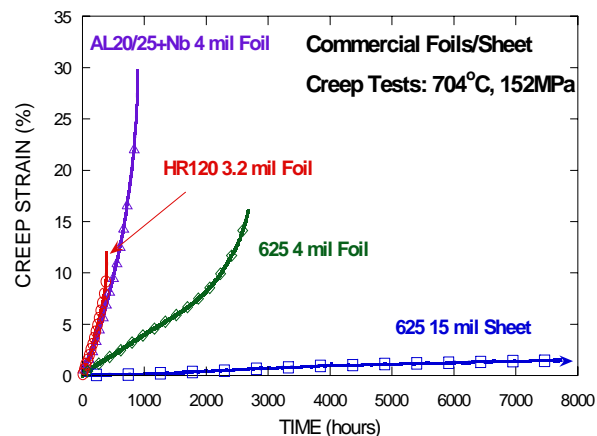


**Figure 2.** Creep data on commercial sheets and foils tested at 704°C and 152 MPa in air. The sheet of alloy 625 has shown little creep at these conditions so far, and is still in-test.

change its inadequate resistance to moisture-enhanced oxidation [10], which is a function of the alloy composition, particularly Cr and Ni contents. AL20-25+Nb, HR120, HR230 and 625 alloys are

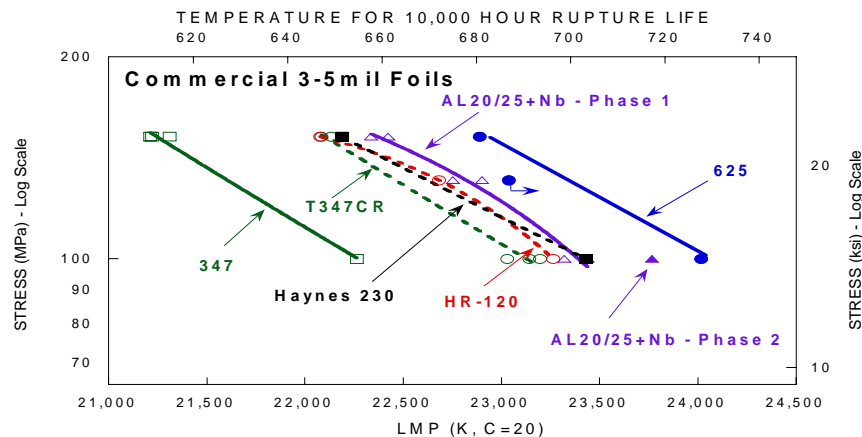


**Figure 3.** A plot of creep-rupture stress versus Larson-Miller Parameter (LMP) for the various foils of commercial heat-resistant stainless steels, stainless alloys and Ni-based superalloys tested at 650-750°C in air at ORNL.

all inherently more resistant to moisture-enhance oxidation due to both higher Cr and Ni contents.

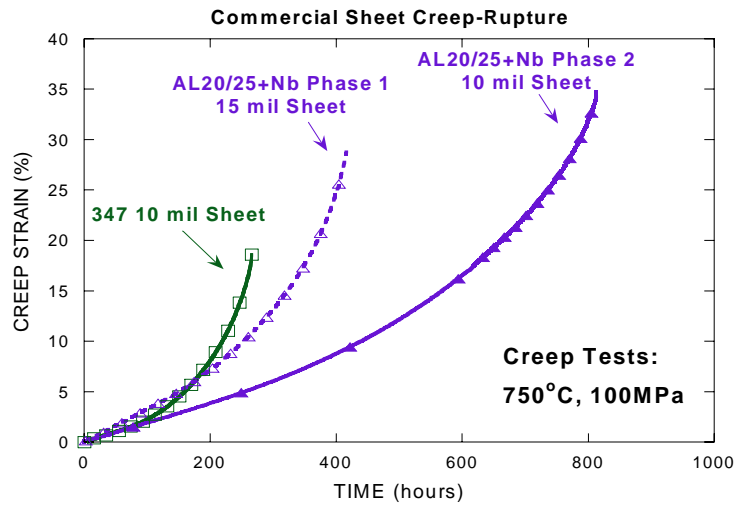
The creep-rupture strength of AL20-25+Nb (Phase I) foils is slightly higher than HR230 and HR120 alloy foils. Since HR230 is almost twice the cost of HR120, HR120 and AL20-25+Nb are more cost-effective for the same level of creep-resistance. Testing has just begun on foils of AL20-25+Nb (Phase II) alloy, but the initial results show significantly more creep resistance than comparable Phase I material, and that creep-resistance now comes closer to the behavior of alloy 625 than any of the other alloys.

Figure 4 shows a more detailed comparison of individual creep strain curves at 750°C/100 MPa for AL20-25+Nb alloy sheets with Phase I and Phase II processing, while Figure 5 shows a similar comparison for foils. Sheets of 347 steel typically have more creep resistance than thin foils, with 200-250 h compared to 50 h or less for standard processing [15]. AL20-25+Nb (Phase I) sheet has similar creep resistance to 347 steel (similar creep rate), but has a longer rupture life by virtue of having more creep ductility before rupture (Fig. 4). By comparison, AL20-25+Nb (Phase II) has about double the rupture life due to a much lower creep rate and slightly better rupture ductility. Clearly a small change in processing has

a significant effect on creep-resistance for this alloy. Figure 5 indicates a far more dramatic effect of processing changes on AL20-25+Nb, despite difference in foil thickness. With Phase I processing, 0.004 – 0.005 inch thick foils of AL20-25+Nb alloy have more creep resistance than 347 steel, but have slightly higher creep rates than HR120, and slightly longer rupture lives due to almost 3 times the rupture ductility. The 0.0032 inch thick foil of AL20-25+Nb (Phase II) shows over 3 time the creep-rupture life of HR120, due to dramatically prolonged secondary creep regime at the minimum creep rate combined with double the rupture ductility. Clearly the effect of changing the processing parameters has an even more dramatic effect on foils of AL20-25+Nb alloy than it does on thicker sheets. Similar creep-rupture testing of 0.005 inch thick foil of Phase II material is currently in progress to verify this behavior.

### Microstructural Analysis of Creep-Tested Foils

Microstructural analyses of as-processed grain size structures of Phase I and Phase II sheets (0.010 inches thick) of AL20-25+Nb are shown in Figure 6. Both the metallographic images and the grain size distribution histograms show that Phase II processing increases the uniform grain size by coalescence of most of the patches of finer grains that are present in the Phase I microstructure.



**Figure 4.** Comparison of creep-strain versus time plots for creep-rupture testing of 10-15 mil sheets of standard 347 stainless steel, and of AL20-25+Nb stainless alloy at 750°C and 100 MPa in air. Differences in processing parameters produced coarser uniform grain size in the Phase II material compared to the Phase I material.

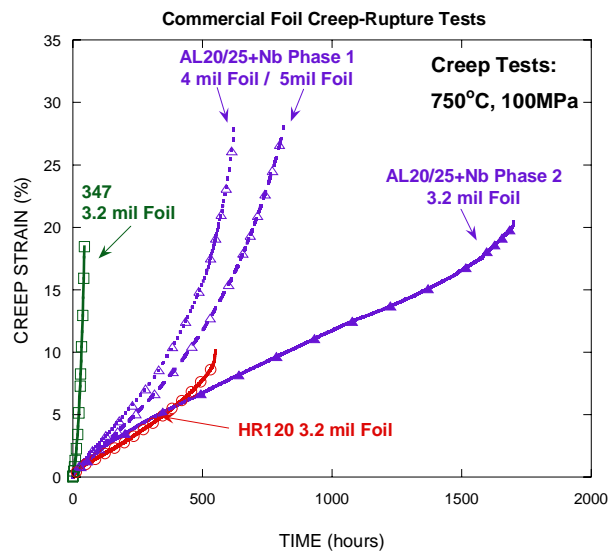


**Figure 5.** Comparison of creep-strain versus time plots for creep-rupture testing of 3-5 mil foils of standard 347 stainless steel, and of HR120 and AL20-25+Nb stainless alloys at 750°C and 100 MPa in air. Differences in processing parameters of the AL20-25+Nb alloy produced a coarser uniform grain size in the Phase II material compared to the Phase I material.

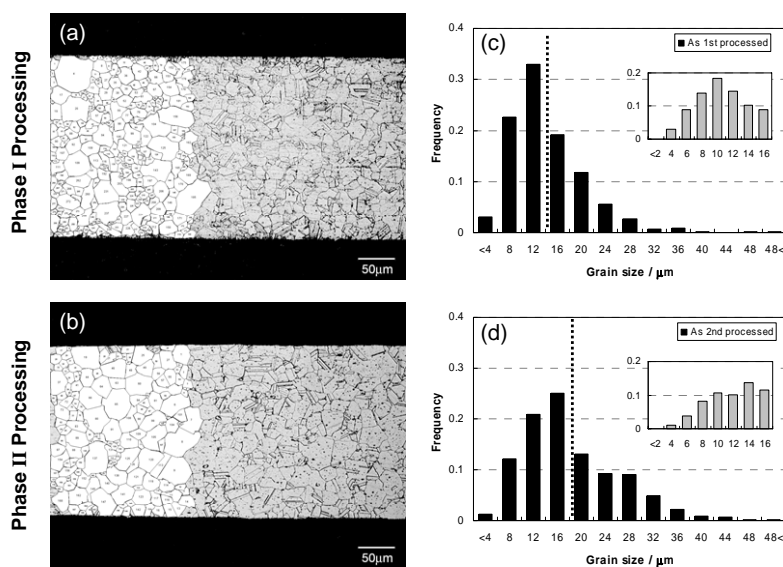


**Figure 6.** Optical metallographic microstructures of cross-section specimens of AL20-25+Nb sheets (0.010 inches or 0.254 mm thick) from (a) Phase I processing, and (b) Phase II processing. Superimposed on the left hand portions of (a) and (b) are redrawn schematic diagrams of the actual grain structure that were used for quantitative grain size distribution analysis. Histograms of the grain size distribution obtained from analysis of those images are plotted in (c) Phase I and (d) Phase II. Dotted lines on these histograms indicate the average grain size, and the smaller inset histograms are analysis of the smallest grains using finer grain-size steps.

Average grain size numbers are presented in Table 2 for all the AL20-25+Nb alloy foils and sheets for both Phase I and Phase II materials. The change in average grain size is more dramatic for the 0.010 in thick sheet specimens than the 0.005 inch thick foils, but that is likely due to the sheets containing larger regions of very fine grains (grains <10-12  $\mu\text{m}$ ), which are removed by the higher temperature processing. For reference, a grain size of about 12  $\mu\text{m}$  corresponds to an ASTM grain size of 9.5, whereas a grain size of 4  $\mu\text{m}$  corresponds to an ASMT grain size of 12.5. By comparison to several of the other heat-resistant alloy foils, the 625 foil has a grain size similar to AL20-25+Nb alloy, whereas the HR120 foil has a much coarser grain size, close to 28  $\mu\text{m}$  (ASTM grain size of about 7).

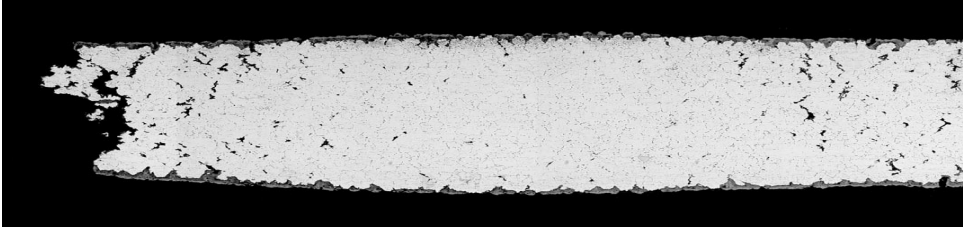
**Table 2. Quantitative Grain Size Data for AL20-25+Nb Alloy**

Thickness	Average grain size / $\mu\text{m}$	
	Phase 1	Phase 2
15 mil (381 $\mu\text{m}$ )	11.4	-
10 mil (254 $\mu\text{m}$ )	12.8	18.2
8 mil (203 $\mu\text{m}$ )	11.4	-
5 mil (127 $\mu\text{m}$ )	11.2	12.5
4 mil (102 $\mu\text{m}$ )	12.5	-
3.2 mil (81.3 $\mu\text{m}$ )	-	13.2

Comparison of the microstructures of gage cross-sections from AL20-25+Nb alloy sheets of Phase I and Phase II materials after creep-rupture at 750°C/100 MPa are shown in Figure 7 (these are taken from the creep-tested specimens shown in Fig. 4). The cavities or porosity seen in both

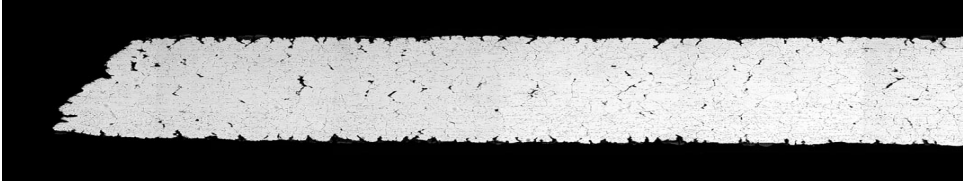


AL20-25+Nb, 15mil, Phase 1, crept at 750°C/100MPa (OM, 200x)



100μm

AL20-25+Nb, 10mil, Phase 2, crept at 750°C/100MPa (OM, 200x)



100μm

**Figure 7.** Optical metallographic micrographs showing the transverse cross-sections sheet specimens of sheets of AL20-25+Nb after creep-rupture testing at 750°C and 100 MPa in air. The top sheet specimen is 15 mil Phase I alloy, which ruptured after about 400 h, while the bottom sheet is 10 mil Phase II alloy, which ruptured after over 800 h. The creep-rupture curves corresponding to these specimens are shown in Figure 4.

samples are the creep damage caused by creep-voids forming at grain boundaries and triple points, and linking up to separate the grain boundaries and weaken the material and cause final fracture. Clearly the Phase I materials has many more such internal cracks, with thinning of the areas with more cracks because they are now weaker. By contrast, the Phase II material, which is thinner sheet and has also been exposed to those same creep conditions and lasted twice as long, has less of such creep damage, and that damage is more confined to the center of the specimen. While TEM analysis has not been done yet, this does suggest that the processing differences have at least retarded the mechanisms causing creep damage, and possibly have changed them. More detailed microstructural analysis is needed.

Finally, preliminary higher magnification analysis of grain boundaries and precipitation in the gage sections of AL20-25+Nb (Phase II) and HR120 foils tested at 750°C/100 MPa are shown in Figure 8. While both alloys show mixtures of Si-Mo-Cr-Ni  $M_6C$  and Cr-rich  $M_{23}C_6$  particles along

the grain boundaries and in the matrix, there are some obvious differences. The HR120 has a finer dispersion of mainly  $M_{23}C_6$  and some  $M_6C$  particles along the grain boundaries, while the AL20-25+Nb has coarser  $M_{23}C_6$  and  $M_6C$ , with a larger relative fraction of the latter. The AL20-25+Nb alloy also shows the unexpected presence of fine laths of AlN engulfed in many of the Cr-rich carbides. This may reflect Al contamination of this particular large, development heat, but should not be typical of other commercial production heats where such contamination effects can be eliminated.

### **Preliminary Feedback on Recuperator Manufacturing**

Ingersoll-Rand Energy Systems (IRES) has provided some preliminary, qualitative feedback on the use of the new AL20-25+Nb (Phase I) alloy foils and sheets for manufacturing tests prior to making BPF air-cells. While PS air cells tend to be made from the same foils of the same alloy, BPF air cells can introduce the more heat/corrosion resistant alloys for only those parts that see the

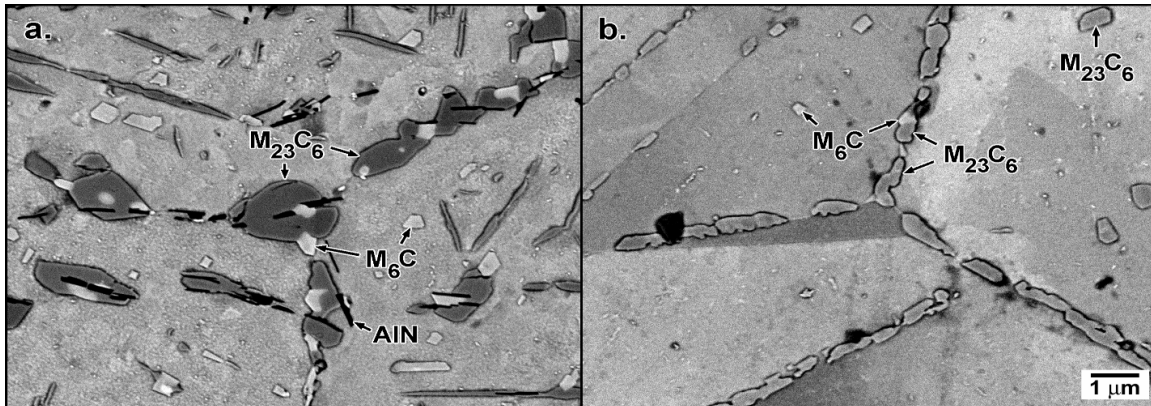


**Figure 8.** Scanning electron microscopy back-scattered (SEM/BS) images of typical grain boundary regions showing the differences in precipitate phases developed during creep-rupture testing at 750°C and 100 MPa in 3.2 mil foils of a) AL20-25+Nb stainless alloy, Phase II processing, with rupture after about 1,700 h, and b) HR120, with rupture after about 530 h. Both alloys contain mixtures of Cr-rich  $M_{23}C_6$  and Mo-, Si- and Ni-rich  $M_6C$  phase along the grain boundaries and within the grains, and both pictures are at the same magnification. Creep curves corresponding to both of these specimens are shown in Fig. 5.

highest temperatures, resulting in a mixed-alloy air cell. To date, IRES indicates the new alloy has good folding, forming, welding and brazing characteristics, similar to 347 steel. More test results will be shared as they become available.

## Conclusions

A collaborative project by ORNL and ATI Allegheny-Ludlum in Phase I has produced a wide range of commercial foils and sheets of the new AL20-25+Nb alloy for recuperator air-cell manufacturing with upgraded performance relative to 347 stainless steel. These foils and sheets show better creep resistance than 347 steel at 700-750°C, and Phase I foils meet or exceed the creep-rupture strength of HR120 and HR230. Phase II processing increased the average grain size and eliminated the smallest grains to boost the creep-resistance significantly. Phase II foils come closer to the strength of alloy 625. Creep-testing of the Phase I materials will be completed, and that of the Phase II material will be expanded. Microstructural analysis of creep-tested specimens of AL20-25+Nb will continue and expand, and include selected comparisons to other heat-resistant alloys.

Both HR120 and AL20-25+Nb alloys are expected to provide microturbine recuperators with all of the fabrication benefits of 347 steel (easy folding,

welding and brazing), and still provide performance and durability improvements, even with higher recuperator temperatures, cyclic operation or alternative, more corrosive opportunity fuels (flare gas, land-fill gas, biofuels, etc.).

## References

1. McDonald, C.F., 2003, "Recuperator Considerations for Future Higher Efficiency Microturbines," *Applied Thermal Engineering*, **23**, pp. 1463-1487.
2. Treece, B., Vessa, P., and McKeirnan, R., 2002, "Microturbine Recuperator Manufacturing and Operating Experience," ASME paper GT-2002-30404, Am. Soc. Mech. Engin., New York, NY.
3. Kesseli, J., Wolf, T., Nash, J., and Freedman, S., 2003, "Micro, Industrial, and Advanced Gas Turbines Employing Recuperators," ASME paper GT2003-38938, Am. Soc. Mech. Engin., New York, NY.
4. Pint, B.A., and More, K.L., 2004, "Stainless Steels with Improved Oxidation Resistance for Recuperators," ASME paper GT2004-53627, Am. Soc. Mech. Engin., New York, NY.
5. Maziasz, P.J., Shingledecker, J.P., Pint, B.A., Evans, N.D., Yamamoto, Y., More, K.L., and Lara-Curzio, E., 2005, "Overview of Creep



- Strength and Oxidation of Heat-Resistant Alloy Sheets and Foils for Compact Heat-Exchangers,” ASME paper GT2005-68927, Am. Soc. Mech. Engin., New York, NY.
6. Lara-Curzio, E., Trejo, R., More, K.L., Maziasz, P.J., and Pint, B.A., 2005, “Evaluation and Characterization of Iron- and Nickel-Based Alloys for Microturbine Recuperators,” ASME paper GT2005-68630, Am. Soc. Mech. Engin., New York, NY.
  7. Rakowski, J.M., Stinner, C.P., Lipschutz, M., and Montague, J.P., 2004, “The Use and Performance of Oxidation and Creep-Resistant Stainless Steels in an Exhaust Gas Primary Surface Recuperator Application,” ASME paper GT2004-53917, Am. Soc. Mech. Engin., New York, NY.
  8. Stambler, I., “Mercury 50 Rated at 4600 kW and 38.5% Efficiency With 5 ppm NO<sub>x</sub>,” 2004, Gas Turbine World (Feb.-Mar.), pp. 12-16.
  9. Rakowski, J.M., Stinner, C.P., Bergstrom, D.S., Lipschutz, M., and Montague, J.P., 2005, “Performance of Oxidation and Creep Resistant Alloys for Primary Surface Recuperators for the Mercury 50 Gas Turbine,” ASME paper GT2005-68313, Am. Soc. Mech. Engin., New York, NY.
  10. Pint, B.A., 2005 “The Effect of Water Vapor on Cr Depletion in Advanced Recuperator Alloys,” ASME paper GT2005-68495, Am. Soc. Mech. Engin., New York, NY.
  11. Staubli, M., et al., “Materials for Advanced Steam Power Plants: The European COST522 Action,” in Parsons 2003: Engineering Issues in Turbine Machinery, Power Plants and Renewables, The Institute of Materials, Minerals and Mining, Maney Publishing, London, U K, pp. 305-324.
  12. Kikuchi, M., Sakakibara, M., Otoguro, Y., Mimura, H., Araki, S., and Fujita, T., 1987, “An Austenitic Heat Resisting Steel Tube Developed For Advanced Fossil-Fired Steam Plants,” in High Temperature Alloys, Their Exploitable Potential, Elsevier Science Publishing Co., New York, NY, pp. 267-276.
  13. Takahashi, T., et al., 1988, “Development of High-Strength 20Cr-25Ni (NF709) Steel for USC Boiler Tubes,” Nippon Steel Technical Report No. 38 (July 1988), Nippon Steel Corp., Tokyo, Japan.
  14. Quality and Properties of NF709 Austenitic Stainless Steel for Boiler Tubing Applications, 1996, Nippon Steel Corp., Revision 1.1, Tokyo, Japan.
  15. Maziasz, P.J., Swindeman, R.W., Shingledecker, J.P., More, K.L., Pint, B.A., Lara-Curzio, E., and Evans, N.D., 2003, “Improving High Temperature Performance of Austenitic Stainless Steels for Advanced Microturbine Recuperators,” in Parsons 2003: Engineering Issues in Turbine Machinery, Power Plants and Renewables, The Institute of Materials, Minerals and Mining, Maney Publishing, London, UK, pp. 1057-1073.
  16. Stinner, C., “Processing to Improve Creep and Stress Rupture Properties of Alloy T347 Foil,” 2003, Allegheny Ludlum Technical Center internal report, Brackenridge, PA, available upon request.

#### **FY2006 Awards/Patents**

None

#### **FY2006 Publications/Presentations**

- 1 P.J. Maziasz, B.A. Pint, J.P. Shingledecker, N.D. Evans, Y. Yamamoto, K.L. More and E. Lara-Curzio, “Advanced Alloys for Compact, High-Efficiency, High-Temperature Heat Exchangers,” accepted for publication in the *International Journal of Hydrogen Energy*, in 2006.
- 2 P.J. Maziasz, J.P. Shingledecker, B.A. Pint, N.D. Evans, Y. Yamamoto, K.L. More and E. Lara-Curzio, “Overview of Creep Strength and Oxidation of Heat-Resistant Alloy Sheets and Foils for Compact Heat-Exchangers,” to be published in *ASME Journal of Turbomachinery* in October, 2006.
- 3 N.D. Evans, Y. Yamamoto, P.J. Maziasz and J.P. Shingledecker, “Age Induced Gamma Prime Coarsening and Hardness Behavior in Pyromet 31V” in *Microscopy and Microanalysis* **12**(Supp 2) (2006) 1044-1045.



- 4 P.J. Maziasz, J.P. Shingledecker, N.D. Evans, Y. Yamamoto, K.L. More, R. Trejo, E. Lara-Curzio, and C.P. Stinner, “Creep Strength and Microstructure of AL20-25+Nb Alloy Sheets and Foils for Advanced Microturbine Recuperators,” ASME paper GT2006-90195, Proc. ASME Turbo Expo 2006 (9-11 May 2006, Barcelona, Spain), Am. Soc. Mech. Engin., New York, NY (2006).
- 6 P.J. Maziasz, “Advanced Alloys for Compact, High-Efficiency, High-Temperature Heat Exchangers,” presented at the TMS 2006 Symposium on Materials in Clean Power Systems, 12-16 March, 2006 in San Antonio, TX. (invited presentation)
- 7 J.P. Shingledecker, “Research on High-Temperature Engineering Alloys at Oak Ridge National Laboratory,” invited lecture give at North Carolina State University on January 27, 2006. (invited lecture)

### **Presentations:**

- 5 P.J. Maziasz, J.P. Shingledecker, N.D. Evans, Y. Yamamoto, K.L. More, R. Trejo, E. Lara-Curzio, and C.P. Stinner, “Creep Strength and Microstructure of AL20-25+Nb Alloy Sheets and Foils for Advanced Microturbine Recuperators,” (GT2006-90195), talk presented at ASME Turbo Expo 2006, 9-11 May 2006, Barcelona, Spain.

### **Acronyms**

- AL – Allegheny-Ludlum
- ORNL – Oak Ridge National Laboratory
- OEM – original equipment manufacturer
- CT – Capstone Turbines, Inc.
- IRES – Ingersoll-Rand Energy Systems
- ASM – ASM International
- LMP – Larson-Miller Parameter
- SS – stainless steel





## 2.1.4 Recuperator Testing and Evaluation

Jane Y. Howe<sup>1</sup>, James R. Keiser<sup>1</sup>, Rosa M. Trejo<sup>1</sup>, Edgar Lara-Curzio<sup>1</sup>, John M. Storey<sup>2</sup>, and James B. Tassitano<sup>2</sup>, Michael Howell<sup>1</sup>, and Gorti Sarma<sup>3</sup>

<sup>1</sup>Materials Science and Technology Division,

<sup>2</sup>Engineering Science and Technology Division,

<sup>3</sup>Computer Science and Mathematics Division,

Oak Ridge National Laboratory, Oak Ridge, TN 37831

Phone: (865) 241-9745, E-mail: howej@ornl.gov

---

### Objectives

The project is to develop a unique facility at ORNL to evaluate the exhaust emission and assess the degradation of structural materials of turbines, reciprocating engines, and microturbines when conventional and nontraditional fuels are used.

- Measure the temperature and gas species at selected locations inside the turbine
- Evaluate materials degradation by placing coupons inside the turbine
- Measure the SO<sub>x</sub>, NO<sub>x</sub>, CO/CO<sub>2</sub>, water vapor, etc in the exhaust
- Evaluate the degradation of candidate turbine/microturbine structural materials by exposing samples in an exhaust gas stream that is maintained at the desired test temperature and doped with toxic species or components that make the gas stream characteristic of the exhaust when nontraditional fuels are burned.

### Approach

- ORNL Fuel-Flexible Turbine Environment Test (FFTET) Rig is an upgrade of the Microturbine Recuperator Test Facility (MRTF), which is aging after four years of operation under vigorous conditions. In collaboration with Capstone Turbines, Inc., a new 65 kW microturbine was custom-built to have five sample ports with a removable aft dome.
- Using one of the sample ports, gas sampling tubes and thermal couples were installed to monitor the gas emission.
- From the removable dome, a slip stream of the exhaust gas was diverted to a tubular chamber for testing more sample coupons in a controlled environment. Additional gaseous species can be added to the chamber to create an environment that simulates exhaust of nontraditional (alternative) fuels.

### Accomplishments

- Installed a new awning to protect the entire test facility.
- The custom-built C65 engine was installed, and in service for materials test.
- Gas sampling unit was installed and working well.
- Conceptual design of the environment chamber is finished.

### Future Direction

- Finishing the construction of the environment chamber and test the controllability of the setup.
- Evaluation of four types of materials using the test rig.
- Monitoring the exhaust emission using the gas analyzers.



## Introduction

The objective of the project is to develop a unique rig at ORNL to evaluate the exhaust emission and assess the degradation of structural materials of turbines and microturbines when conventional and nontraditional fuels are used.

Conventionally, microturbines burn natural gas to generate electricity. With the recent increase in natural gas prices and the developing interest in using “green”/renewable fuels, many operators are considering the use of “opportunity fuels” to run turbines. Opportunity fuel is a loose term used to describe fuels generated from landfill, waste treatment, biomass, or other sources. These gases have many impurities which can accelerate degradation of turbine components and result in emission of undesired species into the atmosphere. Although there is considerable interest expressed in use of these “opportunity fuels”, relatively little is known about the nature of the impurities, the potential effects of these impurities on the degradation of microturbine/turbine components, and the composition and properties of the exhaust gas.

Turbines operate more efficiently at higher temperatures. This puts a high demand on the durability of the components and parts. The ORNL Fuel-Flexible Turbine Environment Test (FFTET) Rig is designed to perform the following tasks for a given type of fuel:

- Measure the temperature and gas species at various locations inside the turbine
- Evaluate materials degradation by placing coupons inside the turbine
- Measure the SO<sub>x</sub>, NO<sub>x</sub>, CO/CO<sub>2</sub>, etc in the exhaust
- Evaluate the degradation of candidate turbine/microturbine structural materials by exposing samples in an exhaust gas stream that is heated to the desired test temperature and spiked with toxic species or components that may accelerate corrosion

The FFTET Rig is specially designed and will consist of three modules.

1. Microturbine specially modified for materials testing

2. Gas sampling and analysis unit
3. Test module for exposure of samples in a controlled temperature stream of spiked exhaust gas

## Approach

In collaboration with Capstone Turbine Inc. in 2001, ORNL acquired a modified 60kw microturbine to construct the microturbine recuperator test facility (MRTF). By 2005, after running the microturbine at temperatures 165°C higher than the stock models for eight thousand of hour, the microturbine was near the end of its service life [1]. Instead of simply replacing with a new engine, the Fuel-Flexible Turbine Environment Test (FFTET) Rig was constructed with added capabilities of gas sampling and a fully controlled environment chamber.

## Results

### *The Custom Built 65kw Microturbine*

The modified 65kw microturbine has a removable aft dome and five sample ports (Fig. 1). Four out of the five ports will be used for materials evaluation at static or cycling condition. The top port is reserved for gas sampling.

### **The Gas Sampling Unit**

The gas sampling unit can monitor the NO/NO<sub>x</sub>, CO/CO<sub>2</sub>/O<sub>2</sub>, and hydrocarbon species. The exhaust gas is extracted from a gas sampling port, and then fed into three California Analytical Instruments (Orange, CA) analyzers (Fig. 2). The Model 600CLD analyzer measures NO and NO<sub>x</sub> up to 3000 ppm. The model 600HFID measures total hydrocarbons (HC) or methane only, up to 3% by volume. The model 600NDIR analyzer is set to measure CO to 10,000ppm, CO<sub>2</sub> to 20% by volume, and O<sub>2</sub> to 25% by volume. The NO<sub>x</sub> and HC analyzers make their measurements on hot wet exhaust, while the gas must be cooled and dried before entering the NDIR. The gas lines are wrapped in heating tapes and can be maintained at 190°C. All of the units have both analog and digital outputs, can be accessed from a network, and have fully adjustable ranges. A portable unit can be brought in from NTRC intermittently if



**Figure 1.** Modified 65 kw microturbine with removable aft dome, five sample ports, and equipped with gas analyzers.



**Figure 2.** Gas sampling unit which can carry out gas analysis at the exhaust side.

other species and particulates need to be monitored.

### **Environment Chamber**

A slip stream of exhaust gas will be diverted out of the microturbine from the aft removable dome. Computer simulation study was undertaken to assess how much exhaust can be pulled out without compromise the performance of the microturbine. The modeling was carried out using the commercial software FLUENT. A model for

the exhaust gas volume in the diffuser section of the microturbine was generated, in order to model the flow between the turbine exit and the recuperator inlet. Based on the assumption of a uniform velocity of 8.125 m/s at the recuperator inlet, the velocity at the turbine exit was assumed to be 117.3 m/s. Pressure outlet boundary conditions were imposed at the outlet sections, with zero static pressure. The walls were assumed to have no heat flux, so that the temperature of the exhaust gas was assumed to remain essentially constant. While the initial modeling work was



carried out without the presence of fuel injection nozzles, these were subsequently added to the model. After modeling the baseline case with no tube attached to the dome section, several cases were considered with the tube, by varying the location and angle of a 2" inner diameter (ID) tube used to divert a portion of the exhaust gas. Figure 3 shows the model with the tube located at the 3 o'clock position at an angle of 45°. For each case, the fraction of flow rate through the tube was computed, and the results are summarized in Table 1. Based upon the simulation results, it is determined that the ID of the chamber is 2" at 3 o'clock position and a 45° angle (Fig.4a). Haynes HR120 alloy of 1/8" thick is the material of selection. A gate valve will be installed between the aft dome and the environment chamber. The team is still working on the details of the design, specifically the means to inject toxic species and maintain the temperature control. There will be four sample ports and holders for the chamber. The sample holder can have a 1/2" strip welded onto the upper portion and hold six pieces of coupons at the lower portion (Fig. 4b and c).

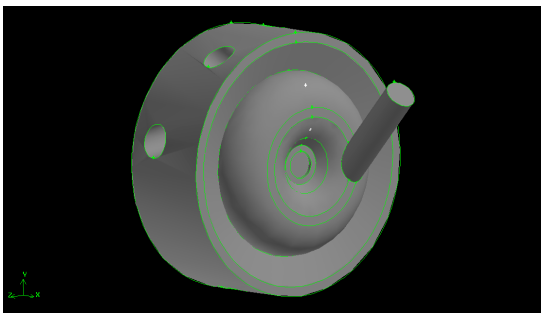


**Figure 3.** Model for the microturbine exhaust diffuser section with a 2" ID tube located at the 3 o'clock position at an angle of 45°.

### Conclusions

Based upon the success of the MRTF, the Fuel-Flexible Turbine Environment Test Rig was designed, and the major part of the construction is completed: 1) the custom-built C65 engine was installed, and in service for materials test; 2) Gas sampling unit was installed and working well; 3) a new awning to protect the entire test facility was added; and 4) the conceptual design of the environment chamber is finished.

**Table 1. Summary of results for different locations and angles for the tube.**

Case	Position [o'clock]	Angle	Tube [in.]	% Outflow
2_2	12	45°	2	7.7
2_2a	12	45°	1	2.1
2_3	6	45°	2	3.3
2_4	3	45°	2	6.5
2_4a	3	30°	2	6.4
2_4b	3	60°	2	7.1
2_5	4:30	45°	2	2.8

### References

1. Lara-Curzio E., Maziasz, P. J., Pint B. A., "Test Facility for Screening and Evaluating Candidate Materials for Advanced Microturbine Recuperators," ASME Technical Paper GT 2002- 30581, 2002.

### Presentation

1. R. Trejo, J. Y. Howe, J. Keiser, E. Lara-Curzio, K. L. More, and J. Storey, "Test Facility to Assess the Effect of Alternative and Opportunity Fuels on the Durability of Microturbine Materials and Components", Women in Science Poster Session, ORNL, May the 4<sup>th</sup>, 2006.

### Acronyms

FFTET-Fuel-Flexible Turbine Environment Test Rig

ORNL-Oak Ridge National Laboratory

MRTF-Microturbine Recuperator Test Facility

HC-hydrocarbon

ID- Inner diameter

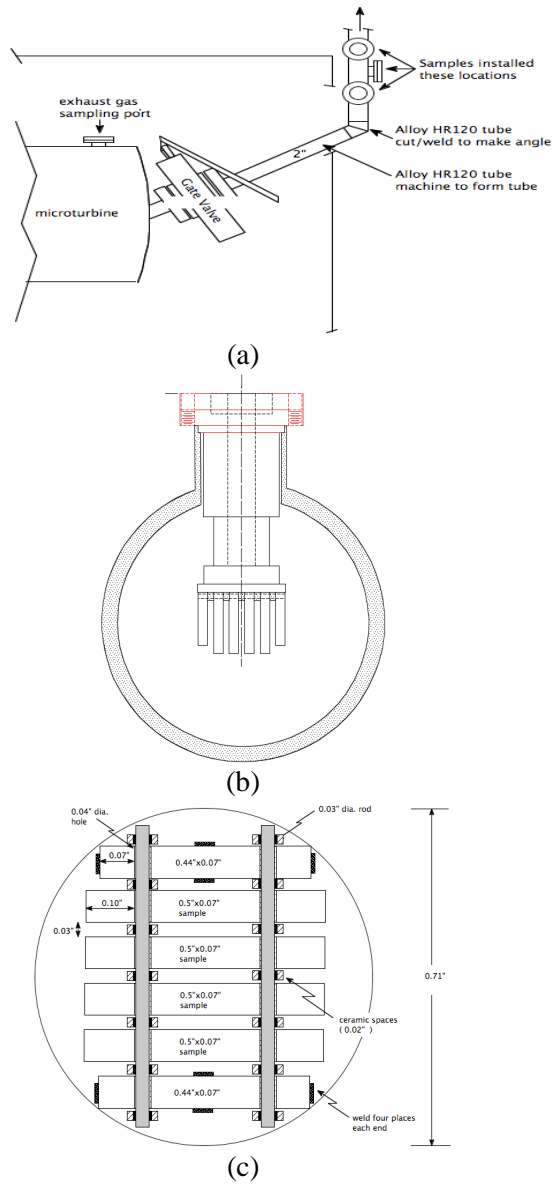


**Figure 4.** (a) The environment chamber layout, (b) drawing sample holder with respect to the chamber, and (c) draw coupon layout on the sample holder.





## 2.2.2 Microstructural Characterization of CFCCs and Protective Coatings

*K.L. More and P.F. Tortorelli*  
*Metals and Ceramics Division*  
*Oak Ridge National Laboratory*  
*Oak Ridge, TN 37831-6064*  
*(865) 574-7788; morekl1@ornl.gov*

*DOE Technology Development Manager: Debbie Haught*  
*(202) 586-2211; (202) 586-7114 (fax); e-mail: debbie.haught@ee.doe.gov*  
*ORNL Technical Advisor: R.A. Lowden*  
*(865) 576-2769; (865) 574-6918 (fax); lowdenra@ornl.gov*

---

### Objectives

- Characterization of CFCC/EBC materials and CFCC combustor liners after exposure to simulated (ORNL's Keiser Rig) and actual (Solar Turbines engine test) combustion environments.
- Exposures of candidate environmental barrier coatings (EBCs) to very high water-vapor pressures (in Keiser Rig) to determine thermal stability, volatility-resistance, and protective capability (permeation-resistance).
- Work with CFCC and EBC suppliers/manufacturers to evaluate new/improved ceramic fibers, protective coatings, and composite materials.

### Approach

- Conduct short- and long-term Keiser Rig exposures of candidate CFCC and EBC compositions at high H<sub>2</sub>O pressures (1.5-18 atm) to evaluate the coating's H<sub>2</sub>O permeation-resistance, volatility-resistance, and thermal stability at temperatures greater than 1200°C
- Work with Solar Turbines to evaluate long-term engine-tested combustor liners for microstructural and mechanical stability in combustion environments.

### Accomplishments

- Completed study of the microstructural and mechanical stability of a Nextel 720 continuous-fiber reinforced alumina matrix composite (A/N720 CMC) after exposure to different H<sub>2</sub>O pressure and 3 temperatures, 1135°C, 1200°C, and 1250°C, for 3000h.
- Continued collaborations with Ceramtec, St. Gobain, and UTRC to expose experimental EBC compositions (>30) in ORNL's Keiser Rig at very high H<sub>2</sub>O pressures for times up to 2000h.
- Completed microstructural characterization of 3 new EBC compositions developed for CFCC combustor liners by UTRC after exposure in ORNL's Keiser Rig for 500 and 1000h.

### Future Directions

- Continue important collaboration with Solar Turbines to evaluate a complete set of field-exposed combustor liners after ~25,000 h engine exposure. The two liners will include (1) an outer oxide/oxide (A/N720 CMC with FGI) liner and (2) a GE pre-preg EBC/CFCC inner liner, both of which are currently running in Centaur 50S engine at ChevronTexaco (Bakersfield, CA) test site. The liners should be removed from engine in November-December, 2007.
- Conduct extensive study of volatilization results from ORNL Keiser Rig such that volatilization mechanisms are understood and candidate EBC compositions are screened for volatilization and ranked/compared.
- Continue collaborations with external EBC producers/processors to evaluate new/improved EBC compositions at normal (1.5 atm) and elevated (18 atm) H<sub>2</sub>O pressures in ORNL Keiser Rigs.



## Introduction

Continuous fiber-reinforced ceramic matrix composites (CFCCs) have been developed to replace several metal components in stationary gas turbine engines. One such application is the uncooled CFCC combustor liner, the use of which can significantly decrease CO and NO<sub>x</sub> emissions at increased combustor wall temperatures (~1200°C and higher).[1] Two engine tests were initially conducted on a Solar Turbines Centaur 50S engine fitted with SiC/SiC CFCC combustor liners, however, as a result of the accelerated attack of SiC-based materials (especially CFCCs) in environments containing H<sub>2</sub>O, such as found in combustion gases, excessive surface recession of the CFCC was observed.[2] In order to increase the life-times of the CFCC components, EBCs will be used on the CFCC liner gas-path surfaces. In recent years, SiC/SiC liners with a BSAS-based EBC ran for ~15,000 h in a single engine test.[3]

In order to attain significantly longer lifetimes (>30,000 h) in combustion environments, alternative materials for the currently-used, commercially-available SiC/SiC+BSAS system are being evaluated for the combustor liner application for use in both gas turbine and microturbine engines. A promising option is the oxide/oxide ceramic matrix composite (CMC), based on continuous Nextel 720 (alumina+mullite) fibers in a porous alumina matrix (designated commercially as A/N720 CMC). This CFCC material has demonstrated little loss in mechanical performance when exposed to water-vapor at temperatures up to 1200°C for 1000h.[4] However, microstructural instabilities of Nextel 720 fibers used in alumina- or aluminosilicate-matrix CMCs have been reported following thermal aging at temperatures >1200°C.[5] During the past 3 years, a 76cm X 18cm A/N720 CMC outer combustor liner (with a friable gradient insulator (FGI) coating) has been running for >25,000 h in a Solar Turbines engine test (at the ChevronTexaco test site in Bakersfield, CA). The inner liner, which has also been running for the entire 25,000 h test duration, has been a GE-manufactured “pre-preg” SiC/SiC MI liner with a BSAS-based EBC. Thus, 2 CMC combustor liner have been engine-exposed for >25,000 h.

## Approach

During FY2006, additional specimens of the A/N720 CMC and bulk FGI, similar to the materials currently running in the Solar Turbines engine test, were exposed to 2 separate exposure tests: (1) a simulated combustion environment (10% H<sub>2</sub>O) in ORNL’s Keiser Rig to evaluate the CMC’s microstructural and mechanical degradation as a function of temperature (1135°C, 1200°C, and 1250°C) and exposure time (up to 3000h) and (2) very high H<sub>2</sub>O pressures (~18 atm) and 1250°C for 2000 h. These results will be compared with microstructural and mechanical data from characterization of the A/N720 CMC outer combustor liner after it is removed from engine service in November-December time frame in FY2006.

## Results

The removal of the set of combustor liners being engine-tested during FY2006 was delayed by Solar Turbines in order to accumulate a total of 25,000 h engine test hours, the longest for a set of ceramic composite combustor liners, exceeding the field-exposure time for a set of BSAS+SiC/SiC liners by >10,000 h. This is a significant achievement, but delayed progress on the ORNL work. Thus, instead of microstructurally and mechanically characterizing a set of CMC liners after 20,000 h exposure in FY2006, our work will continue into FY2007. These two engine-exposed liners, an oxide/oxide+FGI outer liner and a GE pre-preg MI SiC/SiC + BSAS EBC inner liner, will be fully evaluated at ORNL following removal of the liners from the engine in late-November or early-December, FY2007. Much of the progress made in FY2006 was therefore focused on completing and collecting all the necessary Keiser Rig exposure data for the individual materials comprising the 2 liners for direct comparison with liners once they are removed from the test. This same type of comparison was conducted on all previous Solar engine tested combustor liners and was very informative.

A comparison of the weight losses experienced by the individual components comprising the oxide/oxide outer liner (currently running in the



Solar Turbines engine test) after exposure for 2000 h at 18 atm H<sub>2</sub>O and 1250°C is shown in Figure 1. Note that the two FGI materials being compared are FGI original (similar to the FGI currently on outer liner) and FGI cast (improved version of FGI original). Both of the FGI materials exhibited a significant initial weight loss at the start of the Keiser Rig exposure, which then leveled off after 500 h. After the initial weight losses (~15% for FGI original and nearly 8% for FGI cast) the weight loss rate for the FGI cast was slower than that exhibited by the FGI original, indicative of greater microstructural stability for the cast material. It will be interesting to evaluate the FGI on the outer liner after >25,000 h field exposure since Solar Turbines has reported some significant changes to the FGI on the liner as observed by borescope inspections. The A/N 720 CMC clearly had the lowest overall rate of weight loss, but this loss is actually quite significant when compared directly to BSAS-based EBC compositions. Additional exposure data collected on the A/N 720 CMC materials at different temperatures has been reported previously (2005 Annual Report) and some missing data has been accumulated during this fiscal year to complete this study.

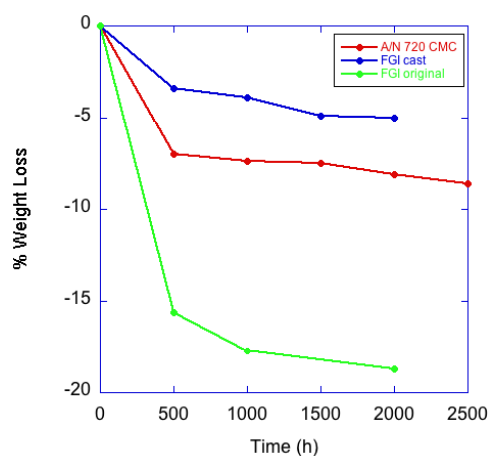


**Figure 1.** % weight loss vs. time for high H<sub>2</sub>O pressure exposure comparing individual oxide/oxide outer liner components (A/N720 CMC and FGI).

## Conclusions

An oxide/oxide composite material, A/N720 CMC, was exposed to high temperatures and pressures similar those in advanced gas turbine combustor environments, as well as to accelerate

volatility testing, in ORNL's Keiser Rig. Results have shown minimal effect of long-term (3000h) exposures at 1135°C on the composite microstructure and strength. However, more severe degradation of the Nextel 720 fibers was observed following exposure of the A/N720 CMC at 1200°C and 1250°C. This included significant grain growth of both alumina and mullite grains within the fibers and an order of magnitude greater degree of fiber surface roughness (from <0.05 μm to ~0.5 μm). The observed fiber degradation, however, did not result in an obvious loss in the tensile strength of the composite after exposure at 1200°C (at the 90% confidence level) but did result in an ~25% drop in UTS following exposure at 1250°C. After exposures for 2000 h at 1250°C and H<sub>2</sub>O pressure of 18 atm, significant weight losses were observed for the FGI materials and the A/N720 CMC.

## References

1. N. Miriyala, J.F. Simpson, V.J. Parthasarathy, and W.D. Brentnall, "The Evaluation of CFCC Liners After Field-Engine Testing in a Gas Turbine," ASME Paper 99-GT-392 (1999).
2. N. Miriyala and J.R. Price, "The Evaluation of CFCC Liners After Field Testing in a Gas Turbine - II," ASME Paper 2000-GT-648 (2000).
3. K.L. More, P.F. Tortorelli, L.R. Walker, J.B. Kimmel, N. Miriyala, J.R. Price, H.E. Eaton, E.Y. Sun, and G.D. Linsey, "Evaluating EBCs on Ceramic Matrix Composites After Engine and Laboratory Exposures," ASME Paper GT-2002-30630 (2002).
4. L.P. Zawada, J. Staehler, and S. Steel, "Consequence of Intermittent Exposure to Moisture and Salt Fog on the High-Temperature Fatigue Durability of Several CMCs," *Journal of the American Ceramic Society*, **86**[8] pp. 1282-91 (2003).
5. M.G. Holmquist and F.F. Lange, "Processing and Properties of a Porous Oxide Matrix Composite Reinforced with Continuous Oxide Fibers," *Journal of The American Ceramic Society* **86**[10] pp. 1733-40 (2003)
6. A. Szveda, S. Butner, J. Ruffoni, C. Bacalski, J. Layne, J. Morrison, G. Merrill, M. van Roode, A. Fahme, D. Leroux, and N. Miriyala, "Development and Evaluation of Hybrid



Oxide/Oxide CMC Combustor Liners,”  
ASME Paper #GT2005-68496 (2005).

### **Awards/Patents**

None

### **Publications/Presentations**

1. *Invited Presentation:* K.L. More, P.F. Tortorelli, T.M. Brummett, “Evaluating the Stability of Candidate EBCs in High Water-Vapor Pressure Environments,” PAC RIM 2005, September 14, 2005, Maui, HI.

### **Acronyms**

A/N 720 (ATK-COI Ceramics/Nextel 720)

CFCC – continuous fiber-reinforced ceramic composite

CMC – ceramic matrix composite

EBC – environmental barrier coating

ORNL – Oak Ridge National Laboratory

UTRC – United Technologies Research Center

BSAS – barium strontium alumino-silicate

FY – fiscal year

FGI – friable graded insulator



## 2.2.4 Oxidation/Corrosion Characterization of Microturbine Materials

*K.L. More and P.F. Tortorelli*

*Metals and Ceramics Division*

*Oak Ridge National Laboratory*

*Oak Ridge, TN 37831-6064*

*(865) 574-7788; email: [morekl1@ornl.gov](mailto:morekl1@ornl.gov)*

*DOE Technology Development Manager: Debbie Haught*

*(202) 586-2211; (202) 586-7114 (fax); e-mail: [debbie.haught@ee.doe.gov](mailto:debbie.haught@ee.doe.gov)*

*ORNL Technical Advisor: R.A. Lowden*

*(865) 576-2769; (865) 574-6918; email: [lowdenra@ornl.gov](mailto:lowdenra@ornl.gov)*

---

### Objectives

- Exposures of candidate ceramic materials to high water-vapor pressures (in Keiser Rigs) to simulate high-temperature, high-pressure environmental effects associated with microturbines. Work with EBC producers to understand degradation behavior and optimize EBC compositions.
- Evaluate the reliability of candidate environmental barrier coatings (EBCs) in terms of volatility-resistance (very high H<sub>2</sub>O pressures ~18 atm) and permeability (elevated H<sub>2</sub>O pressures ~1.5 atm).

### Approach

- Conduct short- and long-term Keiser Rig exposures of candidate EBCs at elevated temperatures (1200°C and 1250°C) and H<sub>2</sub>O pressures (1.5 and 18 atm) to evaluate stability.
- Perform extensive post-exposure microstructural analyses to elucidate oxidation (degradation) mechanisms and kinetics at elevated H<sub>2</sub>O pressures.
- Provide performance data to individual material's manufacturer for process optimization.

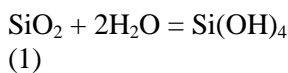
### Accomplishments

- Calculations and experimental results from exposures of selected oxides and Si-based materials definitively demonstrated that very high H<sub>2</sub>O pressures (~18 atm) could offset low gas velocities in the Keiser Rigs so as to differentiate volatilization resistance among various candidate EBCs and provide an accelerated exposure test to rank EBCs.
- Completed collaboration with Ceramtec and Saint Gobain to expose and rank candidate EBC compositions for Si<sub>3</sub>N<sub>4</sub>. Hot-pressed coupons of rare-earth oxides have also been exposed to very high water-vapor conditions.



## Introduction

It is well documented that the high-temperature corrosion resistance of Si-based ceramics is particularly sensitive to water vapor in the environment in terms of accelerated oxidation and/or mass loss by volatilization.[1-7] This degradation mode has been shown to be of specific relevance for SiC and Si<sub>3</sub>N<sub>4</sub>, where SiO<sub>2</sub> forms by (accelerated) oxidation and then readily reacts with environmental H<sub>2</sub>O to form volatile species.[2,5,6] Of the various volatilization reactions, the one forming Si(OH)<sub>4</sub>,



has been shown to be predominant in combustion environments.[4] Consequently, there remains concern about the use of these materials as hot-section components in gas turbine and microturbine engines because, to achieve the highest energy efficiencies and lowest emission levels, the required temperatures and water-vapor pressures in the combustion zones will be such that rapid degradation of Si-based ceramics will occur. Therefore, to take advantage of the high-temperature mechanical properties of these materials for turbine engine applications, environmental barrier coatings (EBCs) [8] will be required on the gas-path surfaces. The application of a BSAS-based EBC to SiC/SiC composite combustor liners in a Solar Turbines natural-gas turbine engine significantly increased the life of the SiC/SiC composite material. However, the long-term phase stability and oxidation/volatilization resistance of current state-of-the-art EBCs (including BSAS and SAS) are not sufficient to achieve desired engine lifetimes at temperatures 1200°C.[9] Therefore, the development and future implementation of improved EBCs for use in high water-vapor-containing environments will be critical for consideration of Si-based ceramic and composite materials for long-term use as hot-section components in gas turbines or microturbines.

In order to be effective for extended periods in combustion environments, an EBC must not only be substantially more volatilization resistant than the Si-based ceramic it is protecting, but also

provide a permeation barrier so that oxidizing species do not readily react with the substrate and compromise properties (prevent accelerated oxidation in the presence of water vapor). In addition, the EBC must be thermally stable and relatively non-reactive with its substrate for long times at the expected use temperature (1100°C-1350°C). Efforts to develop coatings to meet these demanding characteristics have been ongoing for a number of years. A high-temperature, high-pressure exposure facility combined with detailed post-exposure microstructural analysis, has been used for first-stage evaluation of various candidate EBCs at prototypic H<sub>2</sub>O pressures (0.3-2.0 atm) and temperatures.[10] Such an approach has been effective in screening potential EBCs in terms of permeation resistance and phase and interfacial stabilities, but not volatilization tendencies because, under normal operating conditions of low gas-flow velocities in the Keiser Rigs (3-20 cm/min.), the mass flux of volatile species was too low to be measured.

## Approach

During FY05, an extremely high H<sub>2</sub>O pressure (18 atm) and elevated temperature (1250°C) were utilized to experimentally validate that (1) very high water vapor-pressure can be used to compensate for slow-flow gas velocities and induce volatility in the Keiser Rig and (2) measure relative volatilization rates of candidate EBCs. Proof-of-principal specimens showed that these tests were indeed valid for screening candidate stand-alone (no substrate) EBC compositions. Thus, during FY2006, very high H<sub>2</sub>O pressure exposures in ORNL's Keiser Rigs were used to "rank" many different EBC compositions being developed for Si<sub>3</sub>N<sub>4</sub> and CFCCs. These tests were especially important to rank various formulations provided by a single vendor (for example, proprietary compositions provided by St. Gobain and Ceramtec). In this way, these companies could use the Keiser Rig exposures to limit their focus only on the most promising EBC compositions. In addition, more standard EBC compositions being considered could be compared in terms of volatilization-resistance in the presence of H<sub>2</sub>O.



## Results

Bulk stand-alone proprietary EBC compositions produced by Saint Gobain Ceramics and Ceramtec have been exposed at 1250°C and 18 atm H<sub>2</sub>O in ORNL's Keiser Rigs for 2000 h. These exposures were conducted to find the EBCs from each company's process that exhibited the least volatilization, not to directly compare composition and stability between the 2 companies. For this evaluation, each sample was exposed for 500 h, removed from Keiser Rig and carefully weighed, then placed back in the same position in the furnace. The results for 4 different EBCs provided by Saint Gobain (and compared with ceramic standards) are shown in Figure 1. The weight changes observed for these 4 samples were minimal (especially compared with weight losses observed for CVD SiC or quartz standards), and clearly EBC composition #4 exhibited the most weight loss indicating less stability (more volatility) for this particular EBC composition in combustion gases. In a similar way, a series of 6 proprietary stand-alone EBCs were provided by Ceramtec for exposure under similar accelerated Keiser Rig conditions. These results are shown in Figure 2 and the data clearly show that one of these compositions, #6, was superior in terms of stability to water-vapor than the other 5 Ceramtec compositions. Ceramtec #6 exhibited the least weight change after 2000 h, thereby showing the best likelihood for stability in combustion environments (high H<sub>2</sub>O).

While the compositions of these particular EBCs can not be divulged, it is evident from the exposures of the EBCs to very high water-vapor pressures that differences in stability between different compositions can be determined from the weight loss data and used to "rank" EBCs in terms of their stability in elevated H<sub>2</sub>O pressure environments (such as combustion).

## Conclusions

A high-temperature furnace with a water-vapor pressure of 18 atm was used to examine whether very high-gas pressures can compensate for the low-gas velocities so as to conduct first-stage screening of EBC compositions for volatility resistance. Bulk EBC compositions and standards of SiO<sub>2</sub> and CVD SiC were exposed at 1250°C in

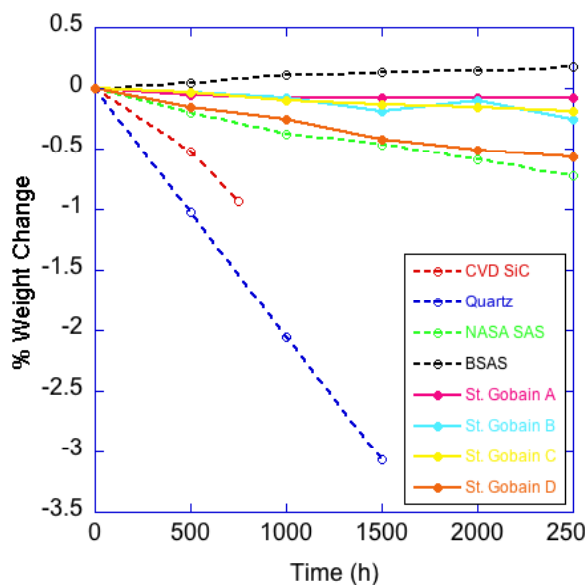


**Figure 1.** Weight change vs. time date for very high H<sub>2</sub>O-pressure exposures comparing candidate EBCs provided by Saint Gobain Ceramics with standards CVD SiC and quartz.

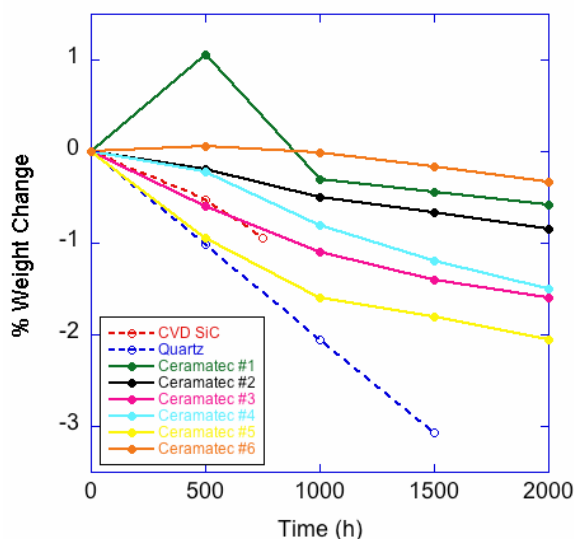


**Figure 2.** Weight change vs. time date for very high H<sub>2</sub>O-pressure exposures comparing candidate EBCs provided by Ceramtec with standards CVD SiC and quartz.

90% H<sub>2</sub>O-10% air at a total system pressure of 20 atm. The gravimetric results showed clear differentiation in volatilization resistance between different EBC compositions from different manufacturers.



## References

1. N.S. Jacobson, "Corrosion of Silicon-Based Ceramics in Combustion Environments," *J. Am. Ceram. Soc.*, **76**[1] (1993).
2. E.J. Opila and R.E. Hann, "Paralinear Oxidation of CVD SiC in Water Vapor," *J. Am. Ceram. Soc.*, **80**[1] (1997).
3. E.J. Opila, "Variation of the Oxidation Rate of Silicon Carbide with Water-Vapor Pressure," *J. Amer. Ceram. Soc.*, **82**[3] (1999).
4. E.J. Opila, J.L. Smialek, R.C. Robinson, D.S. Fox, and N.S. Jacobson, "SiC Recession Caused by SiO<sub>2</sub> Scale Volatility Under Combustion Conditions," *J. Am. Ceram. Soc.*, **82**[7] (1999).
5. R.C. Robinso and J.L. Smialek, "SiC Recession Caused by SiO<sub>2</sub> Scale Volatility Under Combustion Conditions: I, Experimental Results and Empirical Model," *J. Am. Ceram. Soc.*, **82**[7] (1999).
6. K.L. More, P.F. Tortorelli, M.K. Ferber, and J.R. Keiser, "Observations of Accelerated SiC Recession by Oxidation at High Water-Vapor Pressures," *J. Am. Ceram. Soc.*, **83**[1] (2000).
7. P.F. Tortorelli and K.L. More, "Effects of High H<sub>2</sub>O Pressure on Oxidation of Silicon Carbide at 1200°C," *J. Am. Ceram. Soc.*, **86**[8] (2003).
8. H.E. Eaton, G.D. Linsey, K.L. More, J.B. Kimmel, J.R. Price, and N. Miriyala, "EBC Protection of SiC/SiC Composites in a Gas Turbine," ASME Paper #2000-GT-631.
9. K.L. More, P.F. Tortorelli, L.R. Walker, J.B. Kimmel, N. Miriyala, H.E. Eaton, E.Y. Sun, and G.D. Linsey, "Evaluating EBCs on Ceramic Matrix Composites After Engine and Laboratory Exposures," ASME Paper #GT-2002-30630.
10. K.L. More, P.F. Tortorelli, and L.R. Walker, "Verification of an EBC's Protective Capability by First Stage Evaluation in a High-Temperature, High-Pressure Furnace," ASME Paper #GT-2003-38923.
11. K.L. More, P.F. Tortorelli, T. Bhatia, and G.D. Linsey, "Evaluating the Stability of BSAS-Based EBCs in High Water-Vapor Pressure Environments," ASME Paper #GT2004-53863.

## Awards/Patents

None

## Publications/Presentations

1. Invited presentation: K.L. More, P.F. Tortorelli, and T.M. Brummet, "Evaluating the Stability of Candidate EBCs in High Water-Vapor Pressure Environments," PAC RIM 2005, September 14, 2005, Maui, HI.

## Acronyms

EBC – environmental barrier coating

ORNL – Oak Ridge National Laboratory

DOE – Department of Energy

CVD – chemical vapor deposition



## 2.2.7. Reliability Evaluation of Microturbine Components

H. T. Lin

Materials Science and Technology Division

Oak Ridge National Laboratory, Oak Ridge, TN 37831-6068

Phone: (865) 576-8857; Fax: (865) 475-6098; E-mail: [linh@ornl.gov](mailto:linh@ornl.gov)

DOE Technology Program Manager: Debbie Haught

Phone: (202) 586-2211; Fax: (202) 586-7114; E-mail: [Debbie.Haught@EE.DOE.GOV](mailto:Debbie.Haught@EE.DOE.GOV)

ORNL Technical Advisor: David Stinton

Phone: (865) 574-4556; Fax: (865) 241-0411; E-mail: [stintondp@ornl.gov](mailto:stintondp@ornl.gov)

---

Contractor: Oak Ridge National Laboratory, Oak Ridge, Tennessee

Prime Contract Number: DE-AC05-00OR22725

---

### Objective

- Facilitate the successful implementation of ceramic components in advanced microturbines to increase efficiency and reduce NO<sub>x</sub> emission.
- Provide a critical insight into how the microturbine environment influences the microstructure and chemistry, and thus the mechanical reliability of materials.

### Approach

- Evaluate and document the mechanical properties of very small specimens machined from complex-shaped ceramic components for verification of probabilistic component design and life prediction.
- Characterize the evolution and changes in microstructure and chemistry of silicon nitride grains and secondary phase after exposure to engine environments.

### Accomplishments

- Characterization of thermal properties and phase content of ZrO<sub>2</sub>-based thermal barrier coating (TBC) after 40,000h engine field test was completed. Results provide important understanding on the long-term stability of microstructure and chemistry of TBC subjected to engine environments.
- Evaluation of FGI oxide-oxide CMC under high-temperature steam jet at temperatures up to 1288°C was successfully accomplished. Results for the first time provide key inputs to the end users on the long-term microstructure stability (and thus heat protection) under the simulated gas turbine environments.
- Generation of high-temperature creep database of Ni-based superalloys has been completed. The database was provided to gas turbine companies for fuel injector life prediction task.

### Future Directions

- Characterization of cyclic fatigue behavior of SiC-SiC CMCs with environment barrier coating under high-temperature steam environment.
- Characterization of mechanical reliability and chemical stability of solder joints in power electronic packaging components under controlled environments.

### Introduction

The mechanical properties and reliability of complex-shaped ceramic and ceramic composite components play a key role in determining the

long-term performance of advanced turbines and microturbines. Processing steps in fabrication and/or chemical compositions employed sometimes need to be modified in order to



achieve consistent mechanical properties of components. In addition, thin airfoils are often used with as-processed surfaces, which can exhibit microstructures and chemistries that are different from those in the bulk material and test coupons. These differences influence the long-term mechanical reliability and chemical stability of the materials. At present, there is a critical need to generate a database for complex-shaped ceramic components designed and manufactured for advanced microturbines. The mechanical properties of very small specimens machined from ceramic components (e.g. blades, nozzles, vanes, and rotors) in the as-processed condition and after engine testing will be evaluated under various controlled environments. This work will allow microturbine companies to verify mechanical properties of components and apply the generated database in advanced probabilistic component design and lifetime prediction methodologies. The work also provides a critical insight into how the microturbine environments influence the microstructure and chemistry, thus mechanical performance of materials.

### Approach

The thermal properties of ZrO<sub>2</sub>-based thermal barrier coatings (TBCs) have been measured using laser flash diffusivity technique (ASTM 1462) at temperatures ranging from 20° to 1500°C in controlled environments. Also, the differential scanning calorimeter (DSC) was employed to obtain specific heat of the TBCs as a function of temperature in order to calculate thermal conductivity. The laser flash system at ORNL is the Anter FL5000, which has the capability for measuring the thermal diffusivity up to 2500°C. ORNL has an extensive thermal diffusivity and thermal conductivity database. The data were collected in the past 10 years from hundreds of TBCs acquired from many research institutes and companies. Results have shown the trend of the “band” distribution of thermal properties. Thus, data collected from any developmental TBCs could be compared with the existing database. The thermal conductivity database obtained will provide important understanding on the long-term

microstructure stability as functions of test condition and material composition. The stability of tetragonal phase present in the TBCs will be evaluated using the Raman spectroscopy. The extent of tetragonal to monoclinic phase transformation in of ZrO<sub>2</sub>-based TBCs provides important information for further composition optimization to inhibit the diffusion process for transformation and densification process under the application environment. In addition, the piezospectroscopy technique will be used to map out the stress distribution in both TBC and thermally grown oxide layer. The stress distribution profile will allow end users to nondestructively monitor the damage accumulation progressively developed in the TBC systems.

High-temperature steam jet facility was setup in house to evaluate the long-term microstructure and chemistry stability of ceramics, composites, and environmental barrier coating systems, as shown in Fig. 1. The distill water was pre-heated to ~ 250°C using a heating tap and injected onto the specimen surface via a water pump system. The localized steam speed was estimated to be approximately 30 m/sec. The system is housed in a tensile creep system. Thus, studies on the creep behavior of ceramics and composites under a combined stress and steam condition could be also carried out to simulate the combustion environments.

### Results

#### *Characterization of thermal barrier coating and FGI coating*

Results of thermal conductivity measurements of TBC after 40,000h engine field tests are shown in Fig. 2. Thermal barrier coating samples were extracted from hot as well as cold section of inside and outside liner for thermal property measurement. Results showed that 40k hours tested specimens, in general, exhibited higher thermal conductivity values than those reported for the as-received specimens, indicative of change in material microstructure. Also, the thermal property values are consistent with the temperature history experienced in the location from which those corresponding samples were

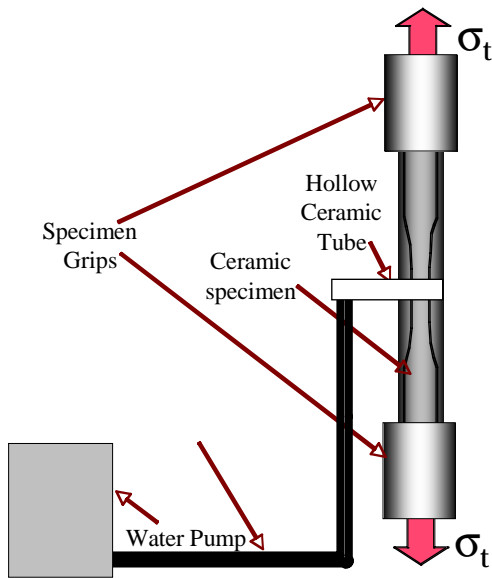


**Figure 1.** High-temperature steam jet facility setup at Ceramic Science and Technology Group, Oak Ridge National Laboratory.

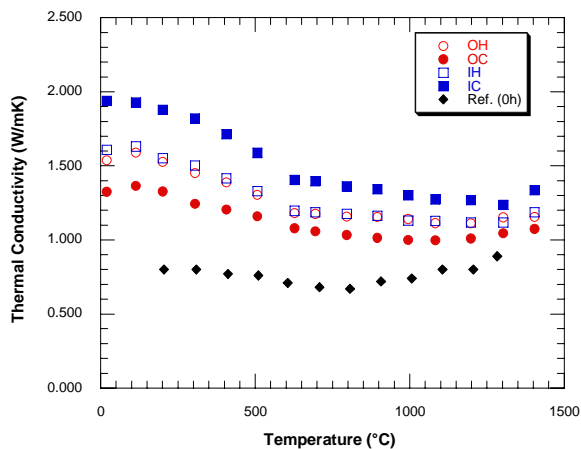


**Figure 2.** Thermal conductivity versus temperature curves for TBC samples extracted from inner and outer combustor line after 40k hours engine testing.

extracted. The subsequent phase identification of phase(s) via Raman spectroscopy showed that samples from inside liner exhibited more phase transformation (from tetragonal to monoclinic) than those from outside liner region, consistent with the thermal property results as well as temperature profile in the liners, as shown in Fig. 3. Results of both thermal property and monoclinic phase content indicated that there was a progressive diffusion processes that resulted in densification of microstructure and

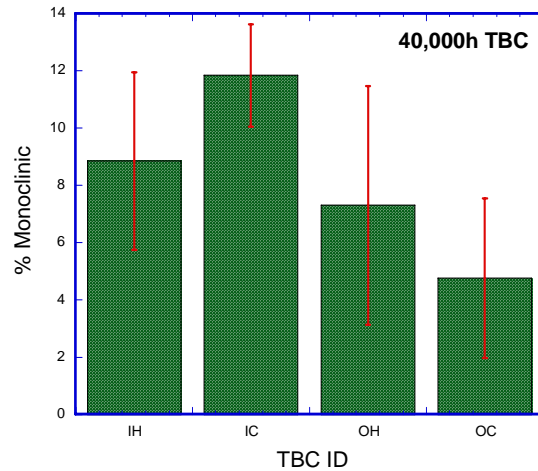


**Figure 3.** The content of monoclinic phase present in 40k hours tested TBC samples identified by Raman spectroscopy.

phase transformation. Further refinement in chemical composition is needed to improve long-term stability of microstructure and thus heat protection functionality.

Figure 4 shows the SEM micrographs of FGI oxide-oxide CMC, acquired from Siemens, after 500h exposure to steam jet environment at 1204°C. Note the SEM micrographs of the as-received material are also included for comparison. Observations showed that there was minor material recession, mainly Al-containing SiO<sub>2</sub> present at the triple grain junctions and two-grain interfaces, observed near the top surface region of FGI as evident by the porous microstructure after testing. Also, there was little change in mullite grains after steam jet test, suggesting good microstructure stability under the test conditions employed in the present study. Moreover, no fiber and matrix degradation observed at the interface of FGI and oxide CMC substrate, indicating excellent heat protection of FGI. On the other hand, similar porous FGI layer due to recession of silicate phase was also observed in FGI layer after 500h steam jet exposure at 1288°C (Fig. 5). SEM results showed that material recession occurred, especially in the mullite grains evident by porous nano grain morphology, became apparent in 1288°C specimens (Fig. 5). The SiO<sub>2</sub> element in mullite reacted with water vapor

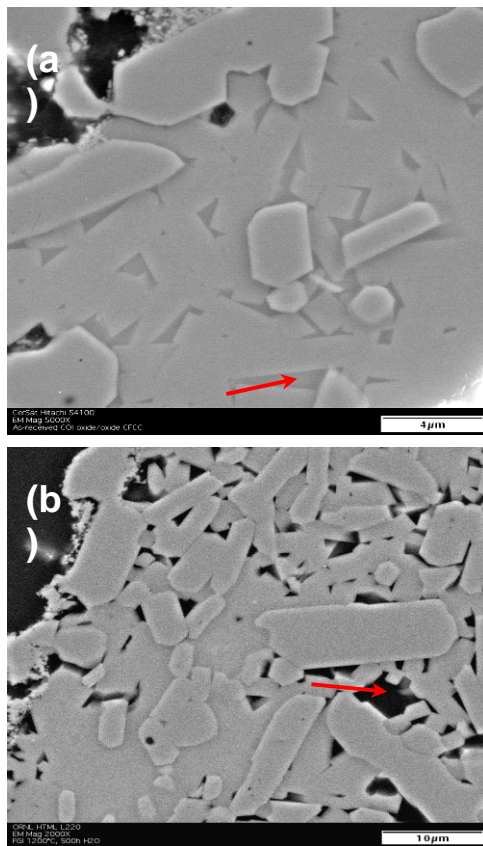


**Figure 4.** Comparison of SEM micrographs of FGI in as-received (top) and after 500h steam jet exposure at 1204°C (bottom).

and formed  $\text{Si}(\text{OH})_4$  gas species, which was swept away by the steam jet gas flow resulting only alumina element present after testing. Nonetheless, no material degradation was observed in the oxide CMC substrate after 1288°C exposure, suggestive of excellent protective functionality of FGI under the present test conditions and time period. It would be important to carry out much longer exposure (e.g., up to 10,000h) and at higher exposure temperatures (up to 1500°C) to determine the upper application limit of FGI layer.

### Mechanical Database Generation

High-temperature creep tests were carried out to generate database for a commercially available Co-based alloy, i.e., Haynes 188, under the test conditions relevant to the application conditions of fuel injector in gas turbine engines. Results showed that data generated from the present

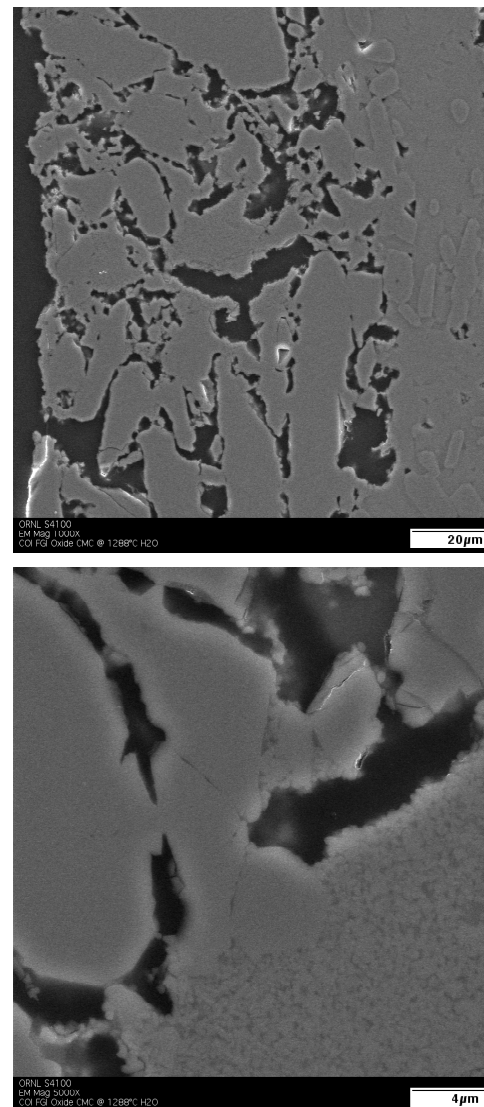


**Figure 5.** SEM micrographs of FGI after 500h steam jet exposure at 1288°C (bottom). Recession of mullite grains occurred as evident by the nano grains feature.

study is quite comparable to those available from the literature, as shown in Fig. 6.

In addition, dynamic fatigue tests were also carried out at 1204°C in air to evaluate the NT154 silicon nitride after proprietary heat treatment process. The purpose of heat treatment was to fully crystallize the remaining amorphous phases present after the densification process. Mechanical results showed that the NT154 after post heat treatment (designated as

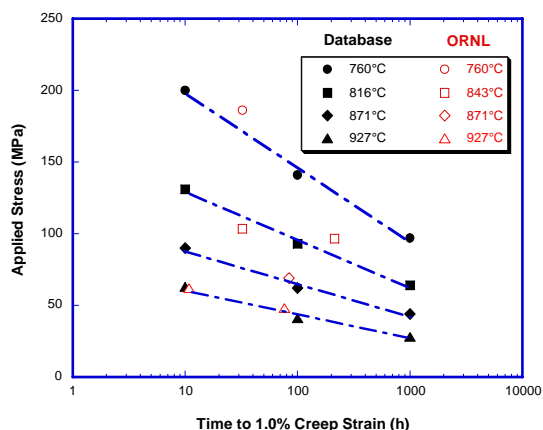


**Figure 6.** Applied stress versus time to reach 1.0% creep strain curves of Haynes 188 alloy.

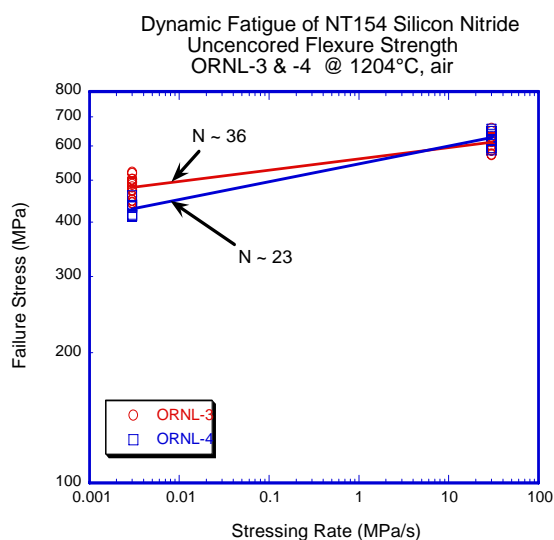


**Figure 7.** Failure stress versus stressing rate curves for NT154 silicon nitride after proprietary heat treatment and tested at 1204°C.

ORNL-4) exhibited low fatigue exponent of ~ 23, similar to that obtained for a standard NT154 without the heat treatment (designated as ORNL-3), as shown in Fig. 7. The low fatigue exponent obtained indicated the heat-treated NT154 still exhibited low resistance to slow crack growth process. Thus, an alternative heat treatment needs to be devised to eliminate the amorphous and thus to improve the long-term high-temperature mechanical performance and reliability.

## Summary

Characterizations of thermal property and phase identification for  $ZrO_2$ -based TBC samples after 40k of hours engine field test showed that a progressive diffusion process still occurred at relative low combustion temperatures, resulting in densification and phase transformation of samples. The measured results are consistent with the temperature profiles experienced in the combustor liner. In addition, SEM analysis showed that there was minor material recession of FGI layer in oxide-oxide CMC and no damage in microstructure of oxide CMC substrate after 500h exposure to the steam jet at 1204°C. Tensile creep date of Haynes 188 was consistent with those reported previously in the literature. An alternative heat treatment process needs to be devised to fully crystallize the amorphous to improve the high-temperature SCG resistance.

## References

1. M. K. Ferber and H. T. Lin, "Mechanical Characterization of Monolithic Ceramics for Gas Turbine Applications," *Key Engineering Materials* Vol. 287 (2005), pp. 368-380

## Honors / Awards / Patents

1. H. T. Lin, Fellow of ASM International, Class of 2006.

## Publications / Presentations

1. H. T. Lin, M. K. Ferber, P. F. Becher, J. R. Price, M. van Roode, J. B. Kimmel, and O.D. Jimenez, "Characterization of First Stage Silicon Nitride Components After Exposure to an Industrial Gas Turbine," *J. Am. Ceram. Soc.* 89 [1] 258-265 (2006).
2. H.-D. Kim, Y.-J. Park, B.-D. Han, M.-W. Park, W.-T. Bae, Y.-W. Kim, H.-T. Lin, and P. F. Becher, "Fabrication of Dense Bulk Nano- $Si_3N_4$  Ceramics without Secondary Phase," *Scripta Materialia* 54 (2006) 615-61.
3. Shunkichi Ueno, D. Doni Jayaseelan, Tatsuki Ohji, and H.- T. Lin, "Recession mechanism of  $Lu_2Si_2O_7$  phase in high speed steam jet environment at high temperatures,"



- Ceramics International*, 32[7], 775-778 (2006)..
4. Shunkichi Ueno, D. Doni Jayaseelan, Tatsuki Ohji, and H.- T. Lin, "Designing lutetium silicate environmental barrier coatings for silicon nitride and its recession behavior in steam jets," *J. Ceramic Processing Research*, 7[1], 20-23 (2006).
  5. S. Ueno, D. D. Jayaseelan, H. Kita, T. Ohji, and H. T. Lin, "Comparison of Water Vapor Corrosion Behavior of  $\text{Ln}_2\text{Si}_2\text{O}_7$  (Ln= Yb, Lu) and  $\text{ASiO}_4$  (A= Ti, Zr, and Hf)," *Key Engineering Materials*, Vol. 317-318, pp. 557-560 (2006).
  6. A. A. Wereszczak, H. T. Lin, G. A. Gilde, "The Effect of Grain Growth on Hardness in Hot-Pressed Silicon Carbides," *J. Mater. Sci.* (2006) 41:4996-5000.
  7. M.P. Brady, P.F. Tortorelli, K.L. More, E.A Payzant, B.L. Armstrong, H.T. Lin, M.J. Lance, F. Huang, and M.L Weaver, "Coating and Near Surface Modification Design Strategies for Protective and Functional Surfaces," *Journal of Materials and Corrosion*, 748-755, 56, No. 11 (2005).
  8. K. P. Plucknett and H. T. Lin, "Sintering Silicon Nitride Ceramics in Air," *J. Am. Ceram. Soc.* 88 [12] 3538-3541 (2005).

#### **Presentations:**

1. H.-T. Lin, Invited Paper, "Re-establishment of Mechanical Performance and Database of NT154 Silicon Nitride," presented at ECI Conference on Novel and Emerging Ceramics and Composites, Kona Coast, Hawaii, June 25-30, 2006.
2. H.-T. Lin, M. K. Ferber, S. B. Waters, and T. P. Kirkland, "Characterization of Mechanical Performance of NT154 Silicon Nitride Microturbine Rotor," presented at the 30th International Conference & Exposition on Advanced Ceramics and Composites, Cocoa Beach, FL, January 22-27, 2006.



## 2.2.9 Environmental Protection Systems for Ceramics in Microturbines and Industrial Gas Turbine Applications—Part B: Slurry Coatings

*Beth L. Armstrong*

*Materials Science & Technology Division*

*Oak Ridge National Laboratory*

*Oak Ridge, TN 37831-6063*

*(865) 241-5862; fax: (865) 574-6918; e-mail: armstrongbl@ornl.gov*

*DOE Technology Development Manager: Debbie Haught*

*(202) 586-2211; fax: (202) 586-7114; e-mail: debbie.haught@ee.doe.gov*

*ORNL Technical Advisor: Dave Stinton*

*(865) 574-5069; fax: (865) 576-4963; e-mail: stintond@ornl.gov*

### **Objectives**

- Develop a low-cost, slurry-based process to apply protective coatings for silicon-based ceramic materials for use in microturbine and/or industrial gas turbine applications.
- Coordinate efforts with other relevant projects to identify the ideal coating material for steam and high-velocity resistance.

### **Approach**

- Study and implement mechanisms of colloidal chemistry for coating systems in aqueous environments.
- Evaluate the protective capacity of coated substrates in test environments.
- Work with industrial collaborators to evaluate the feasibility of the approach and candidate materials.

### **Accomplishments**

- Continued the demonstration of dip coating as a viable approach for a variety of industrial material systems.
- Continued strong collaborations with several industrial parties to ensure that the needs for environmental barrier coating systems (EBCs) are being addressed.

### **Future Direction**

- Continue with industrial parties to optimize and implement coating theory and technology.



## Introduction

Monolithic silicon nitride ceramics and silicon carbide-silicon carbide ceramic matrix composites are currently the ceramic materials being used in combustion engine environments and are under consideration as hot-section structural materials for microturbines as well as other advanced combustion systems. Under oxidizing conditions, these materials typically form a surface oxidation (silicate) layer. In a combustion environment, this silicate layer can undergo rapid degradation due to effects of high temperature, high pressure, and the presence of water vapor. This degradation can severely limit the useful life of the ceramic in this environment. Thus, the development of an environmental protection system for the ceramic has become an essential goal for enabling the long-term utilization of these materials in advanced combustion engine applications. Similar to thermal barrier coatings for nickel-based super alloys that utilize a specialized oxide surface layer and a metallic bond coat, successful environmental protection systems for ceramics and ceramic composites will likely utilize multiple layers and complex combinations of materials. Most recent efforts have focused on the selection and deposition of the oxide surface layer, and due to numerous factors, the majority of the candidates have been from the alumino-silicate family of oxide ceramics. Stable rare-earth silicate deposits have been found on component surfaces after recent engine and rig tests, indicating there may be other stable oxide compositions that have not been fully investigated.

## Approach

Thin coatings of selected compositions were deposited on silicon nitride test coupons using an aqueous-based slurry process technique. When feasible, the coated specimens were exposed to simulated high-pressure combustion environments, and the materials that demonstrated good potential were investigated further.

Efforts were focused on the continued development and refinement of a slurry-based processing method to deposit thin dense coatings of selected compositions on various silicon nitride

substrates. Thin coatings of candidate materials were deposited on test coupons using an aqueous-based colloidal approach. Work focused on refinement of flow behavior as a result of rheology modifiers to improve wetting, adhesion and minimization of drip defects. The specimens were then exposed to simulated water vapor, combustion environments to determine their viability.

## Results

### *Slurry Coatings Development*

Last year, work continued on the optimization of mullite (MULCR®, Baikowski International Corporation, Charlotte, NC) and celsian phase, barium-strontium alumino-silicate (BSAS, H.C. Starck GmbH, Germany) slurry coatings. A single layer system consisting of mullite, a two-layer mullite system, and a two-layer system consisting of mullite and BSAS as the bottom and top coat, respectively, was utilized to protect SiC and SiC-SiC composite substrates. These systems were identified since the protective nature of these coating materials as-deposited by plasma spray and CVD processes has been established in high temperature steam environments, and thus can be used for baseline comparison.<sup>1</sup>

### *Single Layer (Mullite) System*

A single layer of mullite was deposited on SiC, SN282 Si<sub>3</sub>N<sub>4</sub>, and NT154 Si<sub>3</sub>N<sub>4</sub> substrates by inserting them into 25 vol% mullite suspension containing 4 vol% Rhoplex HA8 latex and 10 mg Additive A/ml solution, drying in ambient conditions, and sintering at 1400°C for 2 h. SEM micrographs of the cross sections are shown in Figure 1.

Relatively uniform coatings were observed on all of the substrates with some thinning near the corners. Reaction between the coating material and the substrate occurred for all systems, but it was most obvious for the two silicon nitride

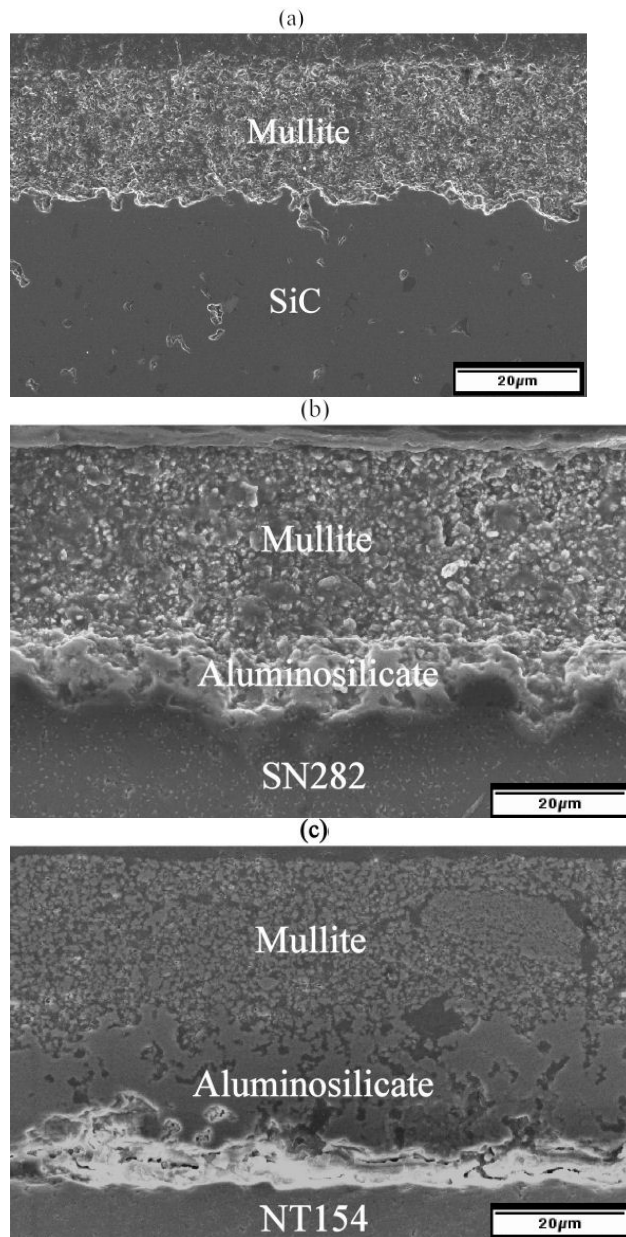


**Figure 1.** A single layer of mullite was deposited on (a) SiC, (b) SN282, and (c) NT154 substrates by inserting them into 25 vol% mullite suspension containing 4 vol% Rhoplex HA8 latex and 10 mg Additive A/ml solution, drying in ambient conditions, and sintering at 1400°C for 2 h.

systems. An alumino-silicate layer, with a gradient in the  $\text{Al}_2\text{O}_3:\text{SiO}_2$  ratio emerged at the interface. A good bond was observed between the mullite layer and the SiC and SN282 substrates; however, degradation of the mullite-NT154 interface was observed. It is unclear if the poor

bonding is a result of processing or simply an artifact of SEM sample preparation. The mullite coatings on SiC and SN282 substrates had similar density, but the density of the coating on NT154 was significantly lower. EDS analysis does not reveal any obvious chemical differences between the mullite layers to explain this discrepancy. The thickness is greater for the mullite layer on NT154, i.e., 43 μm as opposed to 23 μm and 30 μm for the layers on SiC and SN282, respectively. The greater thickness is not surprising since the sintered density is low, i.e., less consolidation occurs during sintering.

### Two-layer (Mullite-Mullite) System

In order to carry out exposure testing of mullite coatings on SiC test bars, a two-layer system was developed to ensure that there was coverage at the corners and edges. The coatings were uniform and had no obvious knit line to distinguish between the first and second layer (see Fig. 2). The combined thickness of the two mullite layers was ~100 μm. The coated test bars were exposed to steam at 1200°C for 500 h. SEM micrographs of the polished cross-sections before and after exposure to high temperature steam are shown in Fig. 2. Before exposure testing, an approximately 6 μm alumino-silicate reaction layer was noted at the mullite-SiC interface. This reaction layer improves the adherence of the coating to the substrate. However, after exposure testing, a silica layer of equivalent thickness was observed at the interface. Oxygen was able to diffuse through the mullite coating and react with the alumino-silicate layer. The mullite coating was not dense enough to fully protect the substrate in high temperature water vapor. Thus, additional measures to improve the density of the coatings were necessary and were the focus of the efforts in FY06.

Four-point bend testing was carried out to measure the flexural strength of uncoated SiC test bars before exposure, mullite-coated SiC test bars before exposure, and mullite-coated SiC test bars after exposure to steam at 1200°C for 500 h. The results indicated little variation in the flexural strength between uncoated and coated SiC test bars. The SEM analysis indicated that failure of the pre-exposed mullite-coated SiC test bars originated from defects in the SiC - not from the

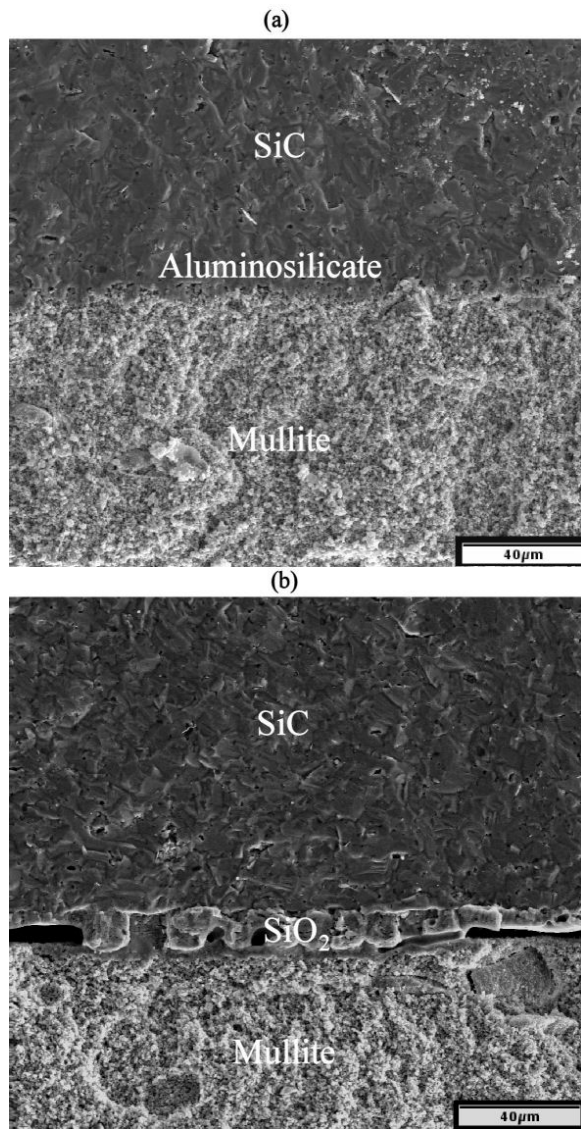


**Figure 2.** Two mullite layers on SiC deposited from 25 vol% mullite suspension (pH 10) containing 4 vol% Rhoplex HA8 latex and 10 mg Additive A/ml solution. The layers were applied, dried in ambient conditions, and sintered separately at 1400°C for 2 h. Images (a) and (b) show the polished cross section of a test bar before and after exposure to steam at 1200°C for 500 h.

coating. Furthermore, exposure to high temperature steam did not result in significant strength degradation despite the formation of silica at the interface.

### *Two-Layer (Mullite-BSAS) System*

In FY2005, the dip-coating process was also applied to a conventional, two-layer environmental barrier coating (EBC) with a mullite bottom layer and a BSAS top coat. The coating system was applied to monolithic SiC and SiC-SiC ceramic matrix composites.

Cross sections of an as-sintered, mullite-BSAS coated monolith and SiC/SiC composite are shown in Fig. 3. The layers were uniform with approximate thicknesses of 65-80  $\mu\text{m}$  for mullite and 85-100  $\mu\text{m}$  for BSAS. The coatings appear to be adherent, with a good interface between the substrate or the silicon bond coat in the case of the SiC/SiC composite and the mullite layer, as well as between the mullite and BSAS layer. The use of varying additives as rheological modifiers did not have marked impact on the quality of the coatings after sintering. This demonstrates the flexibility of colloidal processing techniques - that the rheology necessary to form uniform dip-coatings can be achieved by varying processing strategies.

The coated SiC-SiC composites were exposed to steam at 1315°C for 500 h. Fig. 4 shows that a high SiO<sub>2</sub> aluminosilicate layer formed. This silica scale/reaction layer is a result of the interaction with the silicon bond coat on the surface of the SiC/SiC composite and the mullite layer. The thickness of the SiO<sub>2</sub> scale (~10  $\mu\text{m}$ ) was comparable to that observed at the mullite-SiC interface of plasma-sprayed EBC's; which is an encouraging result given the fact that significant porosity is present in the mullite and BSAS layers. The coating separated at the SiO<sub>2</sub>/mullite interface, although it is not clear if this occurred as a result of steam exposure or metallographic preparation. Mullite and BSAS mixing occurred at the interface between the bottom and top coat. Furthermore, the density of the BSAS layer increased near the mullite/BSAS interface, although some larger pores were also observed within the dense region. These pores correspond to the size and shape of a barium-rich

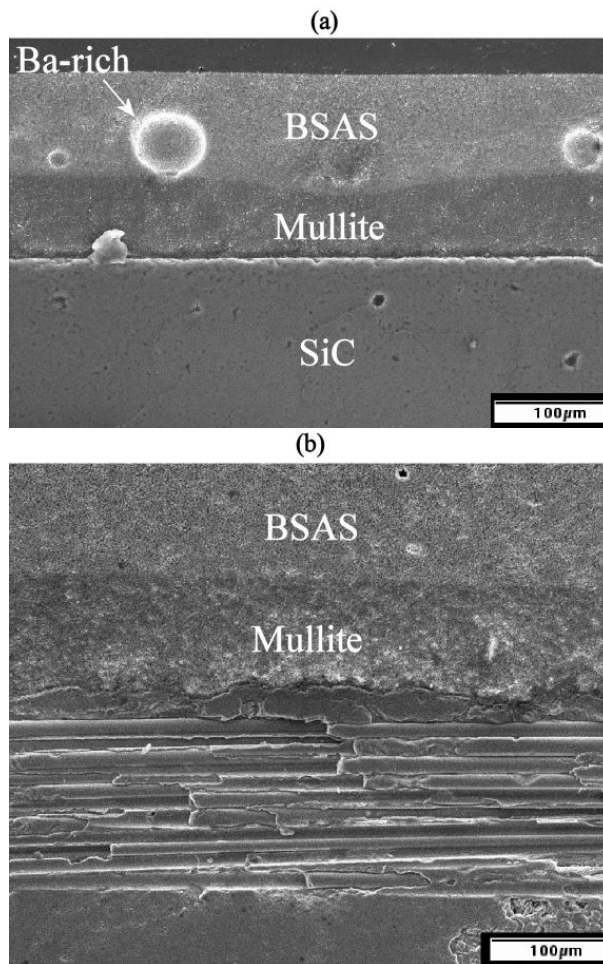


**Figure 3.** Sintered mullite-BSAS coatings on (a) monolithic SiC and (b) a SiC-SiC composite.

secondary phase that was observed in the unexposed coatings (see Fig. 3a). Because this secondary phase is not always observed in as-processed BSAS layers, it was proposed that this stems from chemical inhomogeneity of the starting powder or from processing conditions. Consequently, determination of the cause of the secondary phase as it affects adhesion and durability was investigated in FY06.

As a result of the data summarized previously, refinement of the process as it affects porosity, secondary phase formation, adhesion, and durability of the coatings in simulated and real test environments was the focus of FY06. This work was conducted using “real” industrial systems as collaborations with several industrial partners. Due to the proprietary nature of these systems and

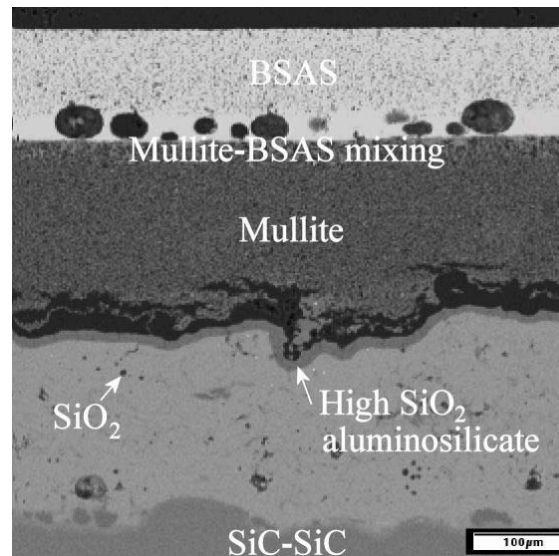


**Figure 4.** Mullite/BSAS coated SiC-SiC composite after exposure to steam at 1315°C for 500 h

the approaches that were taken to meet the individual needs of the industrial partners, the details of the work will not be discussed here.

The research focused on the elimination of the contamination found in the secondary additives/rheological modifiers and/or in the solvent (water). It was found that in silicate-based coating systems, such as mullite or BSAS, small amounts (ppb) of salts such as calcium or potassium created the formation of a stable gel structure in the as-dipped coating. This gel resulted in the formation of a porous network that was not eliminated during the standard sintering process. Only minimal increases in density were seen with iterations of sintering temperatures, times and environments. If the contamination was eliminated with the substitution of “cleaner” additives or solvents, then a dense coating was realized. The key to successful coatings was in the purity of the additive and solvent systems. To illustrate the effect solvent contamination has on the resulting coating microstructure, two micrographs in Figures 5a and 5b show a coating made with contamination-free solvent (deionized water) and a coating made with  $\text{Ca}^{2+}$  contaminated deionized water. Each coating was made with the same lot of powder, substrate, solids loadings, additive concentration, and sintering conditions.



Figure 5a is dense relative to Figure 5b, and Figure 5b illustrates the porous, gel-like structure discussed previously.

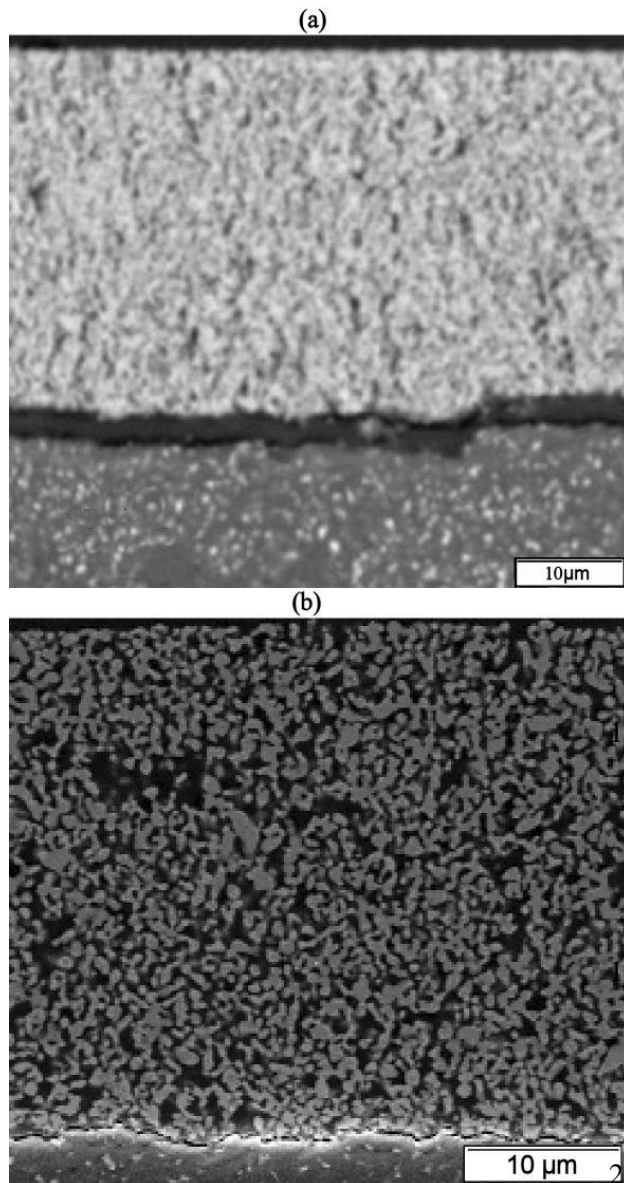


**Figure 5.** Coated SN282 silicon nitrides (a) made with contamination free water and (b)  $\text{Ca}^{2+}$  contaminated water.

A wide variety of alternative additives were tested during the course of FY06 to evaluate the effect of contamination on coating microstructures. Even though the additive chemistry was changed, rheological behavior could still be modified to

produce flowable and driplless coatings; however, the microstructures were dependent upon contaminants present in the additive. The ability to substitute additives to meet purity demands still indicated the robustness of the processing approach. Longevity of the improved or cleaner additive systems evaluated in FY06 still needs to be addressed in FY07.

### Conclusions

Coatings were formed on SiC and  $\text{Si}_3\text{N}_4$ -based substrates by a low-cost, dip coating method that utilizes ceramic slurries of tailored rheological behavior. The coatings were dried in ambient conditions and heat-treated to promote densification. These coatings were exposed to high temperature steam environments to determine if they are protective. Results indicate that slurry coatings made with contaminated additives and/or solvents are not as dense as coatings made with contamination-free starting materials. Purity control is critical to the successful implementation of slurry-based EBC coating systems.

### References

Lee, K., D. Fox, J. Eldridge, D. Zhu, R. Robinson, N. Bansal, and R. Miller, 2003, "Upper Temperature Limit of Environmental Barrier Coatings Based on Mullite and BSAS," *J. Am. Ceram. Soc.*, **86** [8], pp. 1299-1306.

### FY2006 Publications/Presentations

Beth Armstrong, Glen Kirby, and Kevin Cooley, "A Colloidal Approach to Slurry Coating Environmental Protection Systems," presented at the 30th International Conference on Advanced Ceramics and Composites on January 26, 2006 in Cocoa Beach, FL.

Glen Kirby, Beth Armstrong, and Kevin Cooley, "Colloidal Stability of Aqueous Mullite and Barium-Strontium Alumino-silicate Suspensions," in press.



## 2.2.11. NDE TECHNOLOGY DEVELOPMENT FOR MICROTURBINES

*J. G. Sun and W. A. Ellingson  
Argonne National Laboratory  
9700 South Cass Avenue  
Argonne, IL 60439  
630-252-5169, E-Mail: sun@anl.gov*

*DOE Technology Development Manager: Debbie Haught  
(202) 586-2211; fax: (202) 586-7114; e-mail: debbie.haught@hq.doe.gov  
ORNL Technical Advisor: D. P. Stinton  
(865) 754-4556; fax: (865) 241-0411; e-mail: stintondp@ornl.gov*

---

### Objectives

- Develop low-cost, high-speed nondestructive evaluation (NDE) technologies for low-cost monolithic ceramics for hot section components of microturbines and industrial gas turbines.
- Develop reliable NDE methods to evaluate conditions of environmental barrier coatings (EBCs) for monolithic ceramics and continuous fiber ceramic composites (CFCCs).

### Approach

- Work directly with industrial suppliers of monolithic ceramics and EBCs to establish defect types of primary concern and develop appropriate NDE methods for them.
- Work with end users of advanced materials, namely the gas turbine industry, to identify barriers related to implementing the technologies.

### Accomplishments

- Demonstrated high-speed, high-resolution X-ray CT reconstruction using a 300-node JAZZ computer cluster at ANL for full-volume inspection of small ceramic turbine rotors.
- Completed initial assessment of using optical coherence tomography (OCT) method to measure thickness of EBC/TBC coatings on test samples and turbine components.
- Established initial correlation of laser scatter NDE data with thermal cycling damage in TBCs; the correlation may be used to predict coating failure.
- Developed advanced thermal imaging methods to assess EBC damage (cracking and debonding) in CFCC/EBC combustor liners after field engine tests.
- Invented a new thermal imaging method to simultaneously determine multiple parameters for EBCs/TBCs, including coating thickness, thermal conductivity, and optical absorption.

### Future Direction

- Complete development of high-speed reconstruction and automated feature detection software for 3D X-ray CT image data sets.
- Quantify the assessment of EBC damage and pre-spall conditions from engine components by optical and thermal imaging methods.
- Transfer NDE technologies to industry.



## Introduction

The use of advanced ceramic materials in microturbines and industrial gas turbines enables higher operating temperatures and thus greater efficiency. These materials include low-cost monolithic ceramics for hot-section components and environmental barrier coatings (EBCs) for monolithic ceramics and continuous fiber ceramic composites (CFCCs). Given the increased reliance on ceramic components and coatings, it is necessary to have a method for nondestructive evaluating the condition of these components to avoid costly, sometime catastrophic failures. Critical defects that must be detected include internal voids and cracks in monolithic ceramic components; surface and near subsurface features such as cracks and creep damage in monolithics; and spallation, impact damage and overall degradation of EBCs. Several nondestructive evaluation technologies are being investigated for inspection of monolithic ceramic components and EBCs on both monolithic ceramic and CFCC substrates. Because most ceramics are optically translucent, optical methods – such as elastic optical scattering, developed by Argonne National Laboratory (ANL), and optical coherence tomography (OCT) – are useful tools for investigating the surface and near-surface condition of monolithic components and EBCs. Infrared thermal imaging is also used to assess EBC conditions. For detection of internal cracks and voids, 3D X-ray computed tomography (CT) is used. This technology can be automated by using automated feature recognition software.

## Approach

The approach is to develop a knowledge base for NDEs using laboratory test samples and then applying to components, and work directly with material suppliers, end users, and other researchers to maximize total knowledge. This effort has two aspects: develop NDE technologies for (1) monolithic ceramics, and (2) EBCs on monolithic and composite ceramics.

The NDE technology for inspecting ceramic hot-section parts (such as rotors and shrouds) for microturbines is 3D X-ray CT method based on large-area volumetric X-ray imaging with high

spatial resolution. Our goal is to have complete image display within 15 minutes. To achieve this, we continue to develop software, including high-speed 3D-image reconstruction codes and automated feature recognition. The approach being followed for high-speed image reconstruction includes utilization of fast massively-parallelized-architecture computers for handling data sets.

In NDE technology development for EBCs applied on monolithic or composite ceramics, ANL has examined three NDE methods: (a) one-sided flash thermal imaging, (b) laser backscatter, and (c) OCT. As new coatings and processes are developed, they will be examined by these NDE technologies. This evaluation process will continue in order to build the necessary knowledge base to allow quantification of the NDE methods, as well as provide information to suggest future advances in the technology.

## Results

### *High-Resolution X-Ray CT*

For some time the issue with high-speed 3D image reconstruction from the X-ray CT systems was the slow reconstruction times. In cooperation with ANL management, access was provided to the high-speed, 300-node computer cluster called JAZZ. Using this computer, our reconstruction times have been reduced by over an order of magnitude. Small turbine rotors, e.g. 12-15 cm tip to tail, can be reconstructed in their entire volumes in less than 120 minutes. This can be faster if the spatial resolution is reduced. Work continued on automating the edge detection for the images from the 3D x-ray computed tomographic imaging set up.

### **Optical Coherence Tomography**

Optical coherence tomography has recently begun to be investigated as a tool for evaluating the condition of EBCs/TBCs [1]. This scanning tomographic technique is based on a Michelson interferometer. An advantage of this system is the 3D spatial resolution in the image that is produced. Thus, data can be obtained from a cross-sectional plane perpendicular or parallel to the surface of the sample. The average OCT system can scan an object to a resolution of 5–15  $\mu\text{m}$ .

Figure 1 shows an OCT cross-sectional scan image for a slurry-dipped EBC deposited on a glass substrate. In this case the EBC was applied with an estimated thickness of 40  $\mu\text{m}$ . The OCT scan image reveals two strong reflections. The first broader reflection is from the EBC itself, and the second is from the back surface of the glass substrate. The broad EBC reflections can be used to measure the coating thickness. The EBC thickness was estimated to be approximately 42  $\mu\text{m}$ , which is very close to the applied coating thickness. It is important to note that the OCT image and measurements were obtained without destroying the sample, whereas traditional micrographic measurement requires cutting the sample to obtain the cross section. The limits of use for the OCT are the fact that the material must be optically translucent at the wavelength of the diode laser, and the optical scattering within the material must not be so severe that the signal is lost. At present, OCT technology utilizing superluminescent light-emitting diodes with  $>1$   $\mu\text{m}$  wavelength is limited to penetration depths of  $<300$   $\mu\text{m}$  in EBCs/TBCs. The scattering nature of EBCs/TBCs, combined with the OCT requirement for a high signal-to-noise ratio, is the current obstacle.

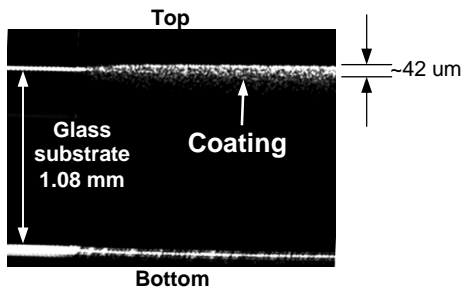


**Figure 1.** Thickness measurement for slurry-dipped EBC from OCT scan image.

Figure 2 shows the result from applying OCT to an actual turbine blade with an EB-PVD TBC. Because of the highly scattering nature of the microstructures of the APS coatings, the use of OCT has been limited to EB-PVD coatings.

### Optical Scattering

The optical scattering technique relies on polarized laser light to probe the subsurface of an

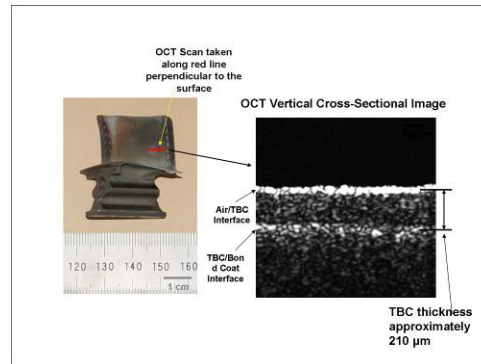


**Figure 2.** OCT measurement of TBC thickness on pressure side of EB-PVD coated turbine blade.

optically translucent material. The technique has been used to investigate thermal barrier coatings, specifically for health monitoring during isothermal heat-treatment testing. The physical properties of ceramic materials are such that when a polarized laser beam is incident on the air/ceramic interface, a portion of the transmitted light will change polarization state, but the reflected light will not. This property allows light scattered from subsurface defects and features to be measured by the cross-polarized optical detector while filtering out all other reflections. The experimental system utilizes a scanning process to generate gray-scale images [2].

The optical scatter method has been applied to two sets of 25-mm diameter button samples consisting of a superalloy substrate, MCrAlY bond coat, and YSZ TBC. The TBC on one set was applied by the EB-PVD method and was approximately 350- $\mu\text{m}$  thick, while the TBC for the second set was applied using APS and was approximately 500- $\mu\text{m}$  thick. The samples were subjected to thermal cycling until failure, and laser backscatter data were acquired at various intervals during the thermal cycling. A thermal cycle consisted of 50 min at 2075°F and 10 min cooling, with a ramp-up time to the temperature of about 8 min.

For the EB-PVD TBCs, typical laser backscatter images are shown in Fig. 3. The average detected power from the backscatter light is plotted as a function of the number of thermal cycles in Fig. 4. The data indicate a significant increase in the total

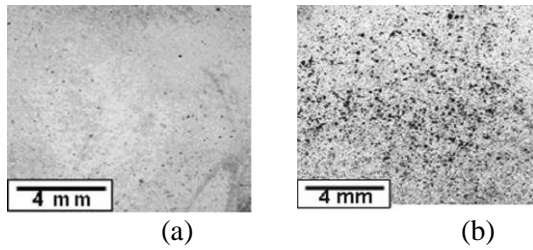


**Figure 3.** Laser backscatter images for EB-PVD TBCs after exposure to (a) 48 and (b) 191 thermal cycles.

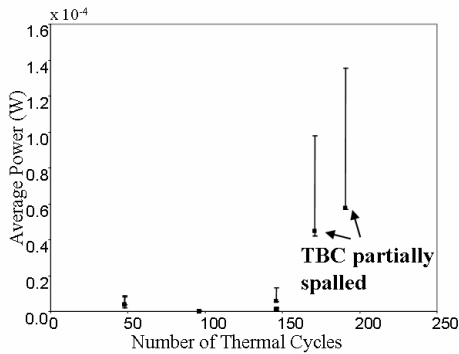


**Figure 4.** Detected light power as function of thermal-cycling number for EB-PVD TBCs.

backscattered light power as the TBC approaches failure.

For the 500- $\mu$ m-thick APS TBCs, the average power is plotted as a function of the number of thermal cycles in Fig. 5. A similar increase in detected power is again observed as the sample approaches failure.

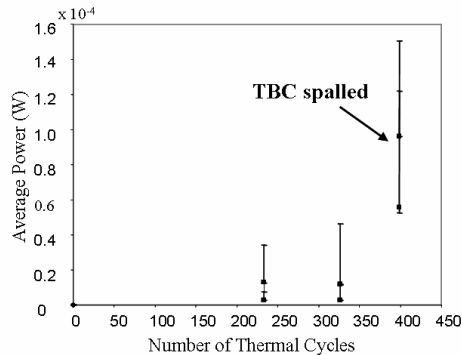


**Figure 5.** Detected light power as function of thermal-cycling number for APS TBCs.

### Infrared Thermal Imaging

A more common approach to detect delaminations of EBCs has been to use focal-plane array infrared cameras that have high frame capture rates. Photographic flash lamps are commonly used to apply an instantaneous heating on the EBC surface, and the decay of the surface temperature is monitored by the infrared camera to determine any damage or pre-spall of the EBC layer.

Extensive studies were conducted for multi-layer EBCs applied on SiC/SiC CFCC liners that were tested in field engines for >15,000 hours. Analyses of EBC microstructure showed that a layer of silica is formed and extensive cracking occurs at the silica peaks within the EBC [3]. The cracking was hypothesized to be the cause of the EBC spallation. Thermal imaging was carried out to detect EBC cracking and debonding in a cut section of an outer liner (Fig. 6a). Figures 6b and 6c show one-sided thermal imaging data, the logarithmic temperature-decay slope  $d(\ln T)/d(\ln t)$  images, where  $T$  is surface temperature and  $t$  is time, at 0.05 and 0.4 s after the thermal flash. In the early-time image, Fig. 6b, all regions with EBC cracking and debonding display lower temperature-decay slopes (darker grayscale) whereas normal EBC regions have relatively higher slopes. In the later-time image, Fig. 6c, regions with EBC cracking now exhibit higher temperature-decay slopes (brighter grayscale), and regions with EBC debonding still display a lower slope than the normal regions. Therefore, the temperature-decay slope can be used to monitor the EBC damage.

In FY2006, a new thermal imaging method was developed for analyzing multi-layer EBC/TBC materials. It can simultaneously determine the distributions of several EBC/TBC parameters, including thickness, thermal conductivity, and optical absorption. For an as-processed TBC specimen with 4 sections at nominal thicknesses 0.33, 0.62, 0.95, and 1.20 mm, shown in Fig. 7, predicted distributions (images) of TBC thickness, conductivity, and absorption coefficient are shown in Fig. 8. It is seen that the predicted thermal conductivity and absorption coefficient of the TBC specimen are generally uniform, while the TBC thickness is uniform in each of the 4 sections.

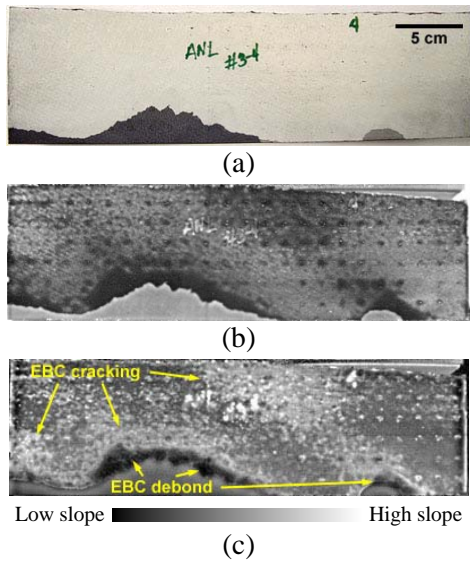


**Figure 6.** (a) A section of a CFCC/EBC outer liner after 15,144-h field test, and temperature-decay slope images at (b) 0.05 s and (c) 0.4 s after one-sided thermal flash.



**Figure 7.** Photograph of a TBC specimen with 4 sections of thicknesses.

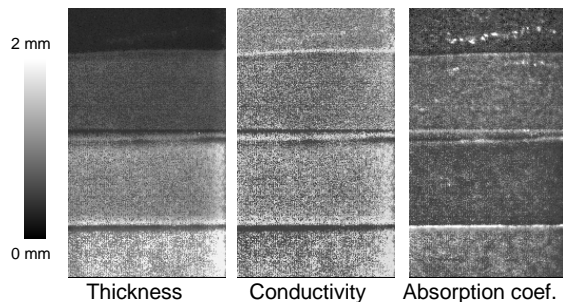


**Figure 8.** Predicted distributions (images) of TBC thickness, conductivity, and absorption coefficient.

## Conclusions

Advances for NDE technology development were achieved in FY2006. High-speed, high-resolution X-ray CT reconstruction for ceramic rotors using a 300-node JAZZ computer cluster at ANL was demonstrated. Several optical NDE methods are under development to assess the condition or “health” of EBCs/TBCs. It was identified that the OCT method can determine coating thickness, while the laser scatter method may predict coating failure. Advanced thermal imaging methods were also developed and used to assess EBC damage and to measure coating thickness and thermal conductivity.

## References

1. R. J. Visser, L. Gast, W. A. Ellingson, and A. Feuerstein, “Health Monitoring and Life Prediction of Thermal Barrier Coatings using a Laser-based Method,” ASME paper GT2005-68252 (2005).
2. J. G. Sun, W. A. Ellingson, J. S. Steckenrider, and S. Ahuja, “Application of Optical Scattering Methods to Detect Damage in Ceramics,” in *Machining of Ceramics and Composites, Part IV: Chapter 19*, Eds. S. Jahanmir, M. Ramulu, and P. Koshy, Marcel Dekker, New York, pp. 669-699, 1999.
3. Kimmel, J., Price, J., More, K., Tortorelli, P., Sun, E., and Linsey, G., “The Evaluation of CFCC Liners after Field Testing in a Gas Turbine - IV,” ASME Paper GT-2003-38920, presented at ASME Turbo Expo 2003, Power for Land, Sea, and Air, Atlanta, Georgia, June 11-19, 2003.

## Awards/Patents

1. J. G. Sun, “Device and Nondestructive Method to Determine Subsurface Micro-Structure in Dense Materials,” US Patent No. 7,042,556, May 9, 2006.
2. J. G. Sun, “Method for Analyzing Multi-Layer Materials from One-Sided Pulsed Thermal Imaging,” ANL Invention Report ANL-IN-05-121, Dec. 2005, US Patent filed in June 2006.
3. J. G. Sun, “An Optical Filter for Flash Lamps in Pulsed Thermal Imaging,” ANL Invention Report ANL-IN-05-125, Dec. 2005, US Patent filed in June 2006.



4. J. G. Sun, "Method for Thermal Tomography of Thermal Effusivity from Pulsed Thermal Imaging," ANL Invention Report ANL-IN-06-017, Mar. 2006, US patent filed in Sep. 2006.

### **Publications/Presentations**

1. W. A. Ellingson, R. J. Visher, R. S. Lipanovich, and C. M. Deemer, "Optical NDT Techniques for Ceramic Thermal Barrier Coatings," *Materials Evaluation*, Vol. 64, No. 1, pp. 45-51, 2006.
2. J. G. Sun, C. M. Deemer, W. A. Ellingson, and J. Wheeler, "NDT Technologies for Ceramic Matrix Composites: Oxide and Nonoxide," *Materials Evaluation*, Vol. 64, No. 1, pp. 52-60, 2006.
3. W. A. Ellingson, C. M. Deemer, J. G. Sun, and E. R. Koehl, "NDE Technology for Ceramic Composites," ASME/IGTI paper GT2006-91349, presented to the ASME Turbo-Expo 2006, Barcelona, Spain.
4. J. G. Sun, J. Benz, W. A. Ellingson, J. B. Kimmel, and J. R. Price, "Nondestructive Evaluation of Environmental Barrier Coatings in CFCC Combustor Liners" presented at the American Ceramic Society's 30th International Conference & Exposition on Advanced Ceramics & Composites, Cocoa Beach, FL, Jan. 22-27, 2006.
5. W. A. Ellingson, R. J. Visher, S. Hopson, R. Lipanovich, and C. Deemer, "Optical Nondestructive Evaluation Techniques for Environmental Barrier Techniques for Environmental Barrier Coating," presented to Environmental Barrier Coatings Workshop, November 15-16, 2005, Nashville, TN.



## 2.3.1 Advanced Materials for Reciprocating Engine Components

*P.J. Maziasz*

*Materials Science and Technology Division*

*Oak Ridge National Laboratory*

*P.O. Box 2008, MS-6115*

*Oak Ridge, TN 37831-6115*

*(865) 574-5082; fax: (865) 754-7659; e-mail: [maziaszpj@ornl.gov](mailto:maziaszpj@ornl.gov)*

*DOE Technology Development Manager: Debbie Haught*

*(202) 586-2211; fax: (202) 586-7114; e-mail: [debbie.haught@ee.doe.gov](mailto:debbie.haught@ee.doe.gov)*

*ORNL Technical Advisor: Dave Stinton*

*(865) 574-4556; fax: (865) 576-5413; e-mail: [stintondp@ornl.gov](mailto:stintondp@ornl.gov)*

---

### Objectives

- Determine the temperature and performance limitations for reciprocating engine exhaust valves and identify alloy/processing/coating options for improved valve durability.

### Approach

- ORNL/TRW/Waukesha collaborative project will test and evaluate alloys and coatings most appropriate to producing new flex-valve design with improved temperature capability and long-term reliability.
- ORNL and TRW will use characterization and testing to define the best alloy/coating combinations, to enable commercial production of trial upgrade valves which can then be engine-tested by Waukesha.

### Accomplishments

- TRW and ORNL identified commercial alloy alternatives to Pyromet 31V and identified commercial coating processes for enhanced oxidation resistance at 800°C and above.
- TRW obtained commercial coatings on various alloy discs for microcharacterization and for oxidation screening at 800°C in 10% water vapor at ORNL. Initial results up to 500h indicated several coatings are clearly better than the others and impart significant resistance to moisture-enhanced oxidation relative to bare Ni-based superalloy metal.
- Completed DE FY2006 CPS/Control Milestones: Section 2 – Materials, Milestone 3 – Complete mechanical testing, aging and evaluation of exhaust valve alloys, in collaboration with TRW to determine temperature limitations (August 31, 2006)

### Future Directions

- Continue testing and characterization of the new TRW commercial alloy/coating combinations at 800°C in 10% water vapor, to down-select coating best for engine-testing of coated exhaust valves.



## Introduction

The objective of this new focused collaborative project with ORNL, TRW and Waukesha Engines, Dresser (WED) is to continue the critical work identified earlier for improving exhaust valve reliability. A new feature of the 2006 work was ORNL and TRW obtaining commercial coatings on discs of the Ni-based superalloys use to make exhaust valves, and testing these at ORNL for their effectiveness in resisting moisture-enhanced oxidation. These new coated valves should have upgraded performance, reliability and resistance to early oxidation attack/failure. ORNL began oxidation/corrosion and mechanical testing in 2006, and concluded the microstructural characterization of aged Pyromet 31V specimens from last year. This new work is an essential step in enabling TRW to confidently perform commercial-scale coating of exhaust valves, which can then be delivered to Waukesha for engine-testing and verification of upgraded performance.

## Approach

Collaborative work between ORNL and Waukesha Engine Dresser, Inc. (WED) expanded in FY2004 to include both intake and exhaust valves, and their seats, and then in FY2005, focused more specifically on the Ni-based superalloy (Pyromet 31V) exhaust valves. In FY2006, ORNL completed detailed microanalysis of a series of Pyromet 31V alloy control specimens aged at 700-800°C for 100, 1000, and 3000h, which showed relative  $\gamma'$ (Ni<sub>3</sub>Al) stability at 700-750°C, but then rapid coarsening at 800°C. Comparison of the aged specimens to the series of engine-exposed valves and to failed valve with premature failure suggested that accelerated oxidation attack due to moisture-accelerated oxidation rather than over-temperature was the root cause of failure. ORNL and TRW identified commercial coatings rather than alloy compositional modifications as the best approach to enhance such failure resistance, and are getting both specimens for lab-testing and some valves for engine-testing coated. At the end of FY2006, oxidation testing of both coated and uncoated specimens of Pyromet 31V and 751 alloys began at 800°C and 10% water vapor. Microcharacterization of coated and uncoated

discs to evaluate the nature and quality of the coatings also began. Aging of coated and uncoated specimens in air at 750-850°C also began at the end of FY2006, to assess the coating stability, and the effects of the coatings on the base-metal behavior. These are critical, necessary steps in providing TRW the input it needs to make commercial trials of coated exhaust valves suitable for engine-testing by WED next year.

## Technical Process

In this study, the temperature-dependent coarsening rate of  $\gamma'$  precipitates was characterized in Pyromet 31V (Ni-22Cr-15Fe, with Ti and Al additions for  $\gamma'$  dispersion strengthening). This superalloy is presently used in the tulip region of some ARES exhaust valves. Alloy samples were heat treated in argon-filled quartz ampoules for 100 h, 1000 h, and 3000 h at 700, 750, and 800°C. Prior to annealing, specimens were either solutionized (4 h at 1093°C, oil quench; designated "SA") or solutionized and heat treated (4 h at 1093°C, oil quench; 4 h at 857°C, air cool; 4 h at 732°C, air cool; designated "SA+HT"). The SA+HT specimens, having multiple heat treatments, represented the actual heat treatment schedule of valves prior to service, whereas the SA specimens were expected to yield a better precipitate size distribution.

From the SA and SA+HT samples, TEM specimens were made using conventional grinding and electropolishing techniques. Images of  $\gamma'$  precipitates were acquired in either brightfield or centered darkfield ((001) $\gamma'$ ) modes (Fig. 1a). Precipitate boundaries, where the boundary could be noted with confidence, were manually masked in Photoshop (version 8) to produce corresponding binary images (Fig. 1b). Diameters of  $\gamma'$  precipitates were measured from the binary images using ImagePro Plus (version 4.5). These values were used to determine the temperature

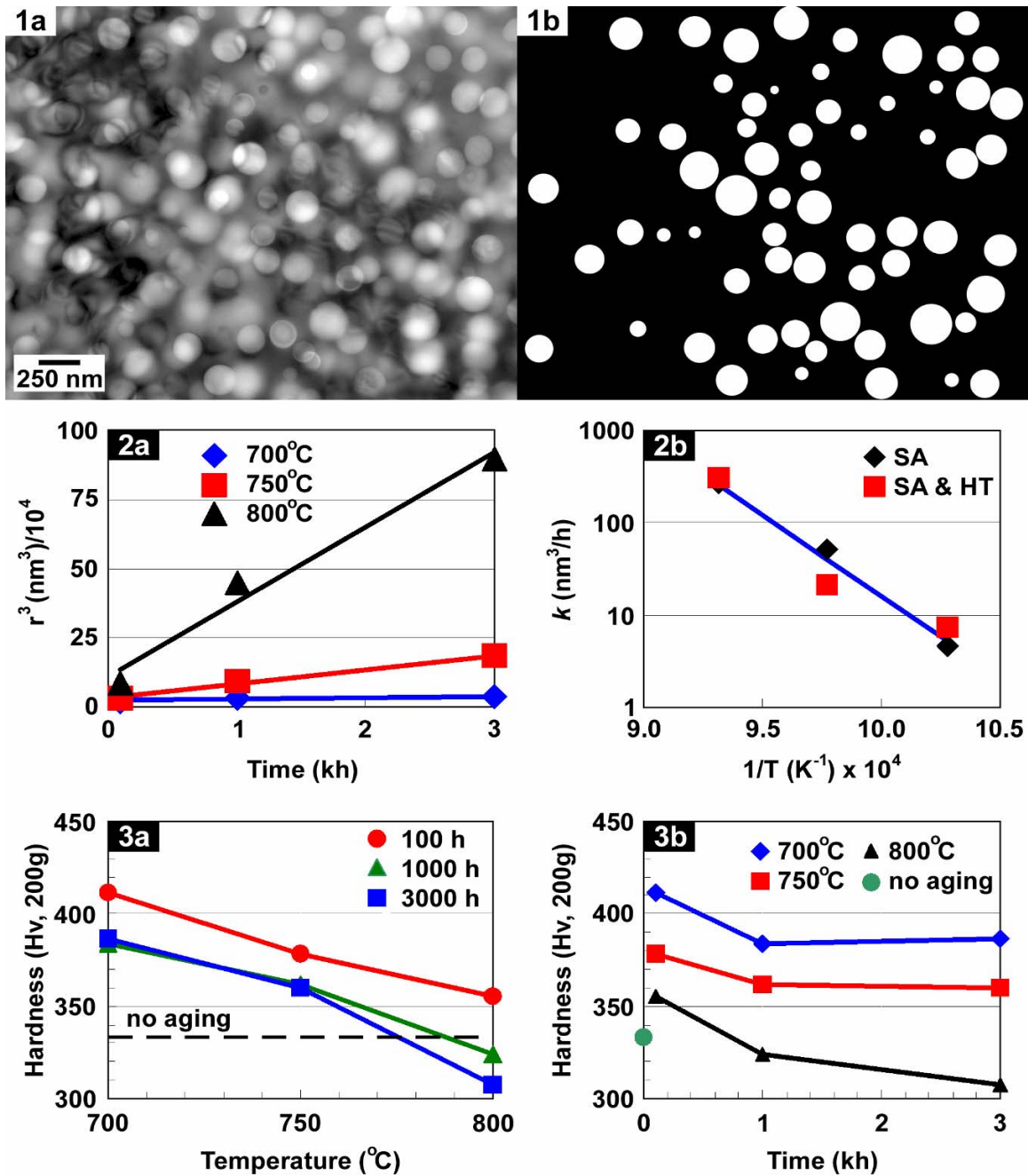
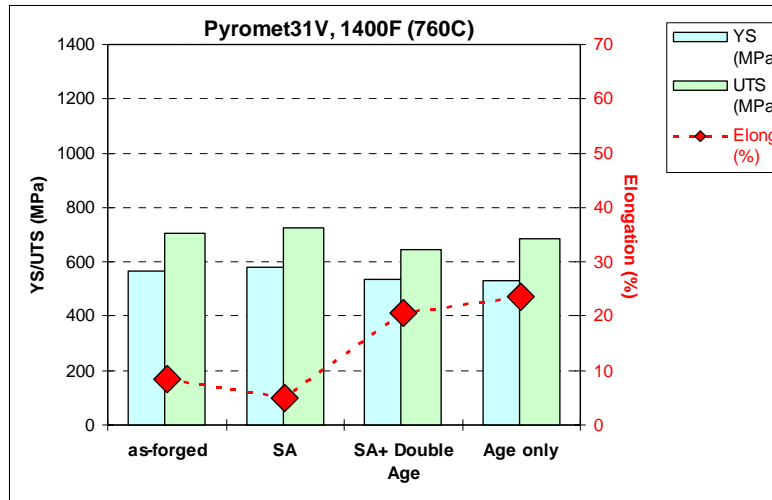


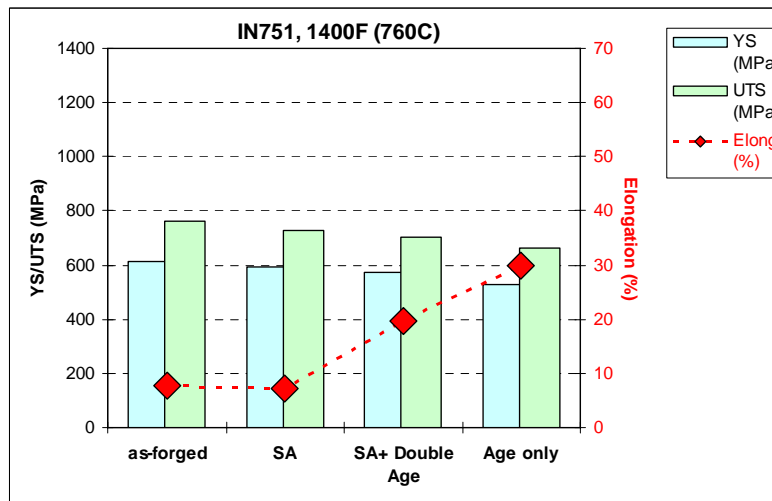
**Figure 1.** a.)  $\square'$  precipitates in aged Pyromet31V; b.) binary image constructed from image in a.)

**Figure 2.** a.) Temperature-dependent growth rates of  $\square'$  precipitates; b.) Activation energy for diffusion.

**Figure 3.** Hardness behavior of aged Pyromet 31V in SA+HT condition: (a.) Temperature; and (b.) time dependent hardness dependent rates of  $\square'$ -volume change (Fig 2a). These rates were used to calculate an activation energy for volume diffusion developed by Lifshitz and Slyozov and by Wagner (the LSW theory).[1,2] With this activation energy and service time known, the local operating temperature for components made from Pyromet 31V can now be estimated from measurement of  $\square'$  precipitate diameters. Additionally, Vickers Hardness measurements of SA and SA+HT samples were acquired, and provide useful insights into this alloy's response to aging (Fig. 3).



A



B

**Figure 4.** Mechanical properties of A) Pyromet 31V, and B) alloy 751, tested at 760°C in various processing conditions.

To further support this evaluation of valve alloy and temperature capability with TRW, mechanical properties specimens were also made from Pyromet 31V at various stages of processing, including the standard final valve condition (SA+double aged HT), and from alloy 751, which are both being used in newly designed valves by TRW for Waukesha, and which are candidates for coatings to improve resistance to moisture-enhanced oxidation. The preliminary mechanical testing of these alloys in

different processing conditions at room temperature and at 760°C (1400°F) was completed at the end of August, 2006. Properties at elevated temperature are shown in Figure 4. This comparison shows that both Pyromet 31V and 751 alloys show good yield and ultimate tensile strengths in the SA and aged only conditions at 760°C, relative to the standard SA+double aged condition, with reasonable ductility. These test results are consistent with

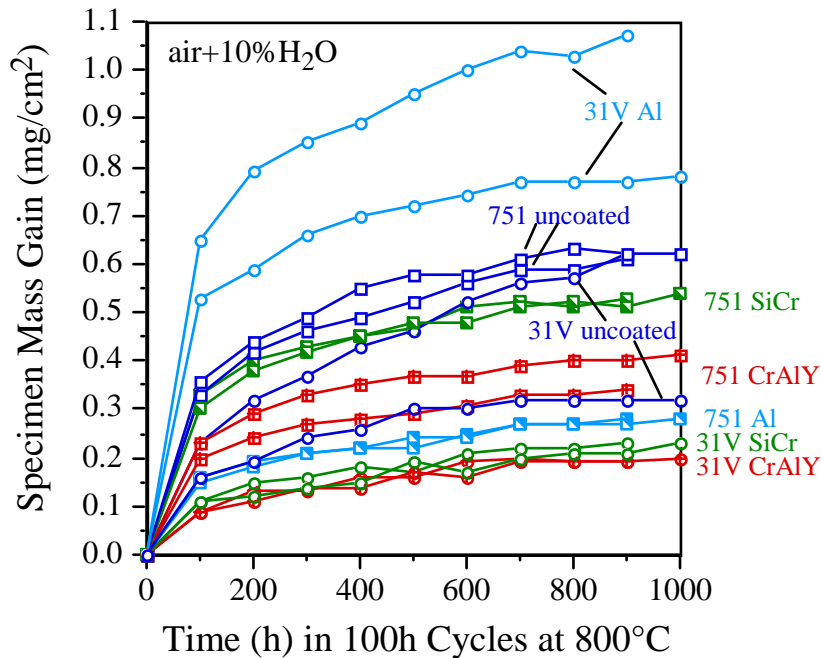


**Figure 5.** Cyclic oxidation (100h cycles) of various coated and uncoated discs of Pyromet 31V and alloy 751, tested at 800°C in air with 10% water vapor. Commercial coatings on superalloy discs were obtained by TRW and provided to ORNL for testing.

the hardness data, which indicate that strength drops off only at higher temperatures.

Finally, ORNL and TRW obtained commercial oxidation-resistant coatings based on Cr or Al to enhance the resistance to moisture-induced oxidation, which degrades mechanical strength and can lead to failure. ORNL is performing oxidation testing at 850°C in 10% water vapor and in air to assess the oxidation-resistance benefit of several different coatings relative to bare metal, for both the Pyromet 31V and 751 superalloys. Oxidation data for exposure to 1000h is shown in Fig. 5. Most of the coated specimens show better oxidation resistance than the bare metal specimens, with the exception of the first aluminized coatings on the Pyromet 31V. ORNL will provide microanalysis to determine coating behavior and compatibility with the valve alloys.

## Conclusion

The initial characterization phase of exhaust valves made from standard Pyromet 31V alloy is complete. ORNL and TRW defined a collaborative program to explore alternate processing and alternate alloys with more stable microstructures for upgraded performance relative to standard Pyromet 31V in 2005, and microstructural and mechanical properties screening began in 2006. In FY2006, commercial oxidation-resistant coatings were obtained on discs of Pyromet 31V and alloy 751, and testing at 800°C in 10% water vapor to about 1000h has shown most of these coatings to be effective for enhancing oxidation resistance. Together with valve design changes, the ultimate goal of this project is to provide exhaust valves with more temperature capability and reliability for engine-testing.



## References

- [1] M. Lifshitz and V.V. Slyozov, J. Phys. Chem. Solids, **19** (1961) 35.
- [2] C. Wagner, Z. Electrochem., **65** (1961) 581.
- [3] N.D. Evans, P.J. Maziasz, and J.J. Truhan, "Phase Transformations During Service Aging of Nickel Based Superalloy Pyromet 31V," pp. 809-816 in Proc. Solid-Solid Phase Transformations in Inorganic Materials 2005, vol. 1 – Diffusional Transformations, eds. J.M Howe, D.E. Laughlin, J.K. Lee, U. Dahmen, and W.A. Soffa, TMS, Warrendale, PA (2005).

## FY2006 Awards/Patents

None

## FY 2006 Publications/Presentations

- 1) N.D. Evans, Y. Yamamoto, P.J. Maziasz and J.P. Shingledecker, "Age Induced Gamma Prime Coarsening and Hardness Behavior in Pyromet 31V" in *Microscopy and Microanalysis* **12**(Supp 2) (2006) 1044-1045.

## Acronyms

WED – Waukesha Engine - Dresser

ORNL – Oak Ridge National Laboratory

TEM – transmission electron microscopy

SEM – scanning electron microscopy



## 2.3.2 Characterization and Development of Spark Plug Materials and Components

*H. T. Lin\** (primary contact), *M. P. Brady\**, *M.D. Kass\*\**, and *J.B. Tassitano\*\**

*\*Materials Science and Technology Division*

*\*\*Engineering Science & Technology Division*

*Oak Ridge National Laboratory, Oak Ridge, TN 37831-6068*

*Phone: (865) 576-8857; Fax: (865) 574-6098; E-mail: [linh@ornl.gov](mailto:linh@ornl.gov)*

*DOE Technology Program Manager: Ron Fiskum*

*Phone: (202) 586-9154; Fax: (202) 586-7114; E-mail: [Ronald.Fiskum@ee.doe.gov](mailto:Ronald.Fiskum@ee.doe.gov)*

*ORNL Technical Advisors: Tim Theiss and David Stinton*

*Phone: (865) 946-1348; Fax: (865) 946-1248; E-mail: [theisstj@ornl.gov](mailto:theisstj@ornl.gov)*

*Phone: (865) 574-4556; Fax: (865) 241-0411; E-mail: [stintondp@ornl.gov](mailto:stintondp@ornl.gov)*

---

### Objective

- Provide insight into the wear mechanisms of natural gas spark plug electrodes as a function of field exposure time and engine conditions.
- Increase the wear resistance of spark plug electrode materials to at least 1 year (or a 2X improvement) in advanced natural gas reciprocating engines designed to meet aggressive emission and efficiency goals.

### Approach

- Characterize engine tested spark plugs to identify key erosion mechanisms and limitations of existing materials.
- Develop, engine test, and optimize new electrode materials for improved erosion resistance based on findings from the characterization effort.

### Accomplishments

- Completed evaluation and characterization of a range of commercially available and developmental spark plug electrode alloys subjected to an accelerated testing protocol in a laboratory gasoline engine in collaboration with Federal Mogul. The alloys represented a wide range of oxidation resistance and thermophysical properties. A key finding was a stronger than anticipated correlation between alloy thermal conductivity and wear, which in many cases overwhelmed improvements in oxidation resistance.
- Completed two sets of natural gas engine tests at ORNL using a Caterpillar G3406 industrial natural gas engine. The first set of plugs was manufactured from model ferritic, austenitic, and Ni-base microstructures optimized for Cr<sub>2</sub>O<sub>3</sub> scale formation. A key finding was the apparent superior resistance to environment-driven cracking of Fe-base alloys, compared to more typically used Ni-base electrode alloys. A second set of spark plugs was manufactured from conventionally available electrode and precious metal insert pad alloys, selected for improved compatibility. Engine testing was completed and post-test analysis is underway.

### Future Directions

- Complete post-test characterization of latest engine tested spark plugs, and conduct additional engine testing for a final iteration of spark plugs manufactured from commercially available electrode alloys and precious metal insert materials.



- Complete initial development of novel, alternative spark plug electrode materials and deliver to collaborators for spark plug manufacture and engine testing.
- Complete transfer of technology via open literature publication relaying understanding gained over the course of this

### **Introduction**

Natural gas (NG) reciprocating engine manufacturers have identified ignition systems as one of the key technologies to achieve cost/performance/emission characteristic goals for lean and stoichiometric engines. Spark plug erosion and subsequent failure have been identified as a major issue in long-term durability of natural gas ignition system. Current spark plug lifetimes are on the order of only ~2-6 months, which results in loss of performance and necessitates frequent, costly downtime maintenance for the plug replacement. Desired spark plug lifetimes for NG engine end users are on the order of at least 1 year (or a 2-fold increase in the spark plug life). It has been recognized that as cylinder pressures, compression ratios, and ignition voltages are increased, and conditions further move towards leaner burning combustion, spark plug reliability and lifetime performance will become even more critical and could limit further advances in engine development. The goal of this effort is to identify the mechanisms of electrode wear and to design new electrode materials to improve the lifetime and reliability of NG spark plugs to meet the lifetime goal.

### **Approach**

Microstructural and spectroscopic analysis of end-of life J-type spark plugs from field-operated NG engines led to the identification of wear phenomena driven by oxidation and cracking of the electrode material during engine operation. The spark plugs typically consisted of a Ni-base electrode alloy with Pt-4W or Ir insert pads at the sparking surface. Extensive cracking and oxidation at the Ni-alloy/insert pad weld interface were observed, as were grain boundary attack and cracking of the insert pads themselves, particularly Pt-4W. The susceptibility of the Pt-W grain boundaries was traced to internal oxidation of W at these locations, followed by volatilization of the W-oxide that was formed. These findings were unexpected, as wear of spark

plug electrodes is typically primarily associated with loss of material due to sputtering, melting, ablation, and particle erosion phenomena during sparking. Efforts in FY2006 focused on engine testing of a range of model and commercially available electrode alloys and precious metal/platinum group inserts selected to systematically explore the effects of a range of thermal, mechanical, and chemical materials parameters on wear behavior. A conventional J-type spark plug arrangement was selected to allow relative comparison of materials effects, and comparison with fielded-tested commercial J-type plugs previously characterized. These spark plugs were manufactured via collaboration with Federal Mogul (FM). Two types of engine testing were pursued: an accelerated test criteria at FM using a laboratory-modified gasoline engine, and a Caterpillar G3406 industrial natural gas engine test bed at ORNL.

### **Results**

The accelerated laboratory gasoline engine tests at FM indicated a stronger than expected effect of alloy thermal conductivity on the rate of electrode wear. This was exacerbated by the use of solid center electrodes of the candidate alloys at this exploratory stage, rather than the Cu-cored approach used to improve thermal conductivity in commercial plugs, such that some plugs/electrode alloys likely ran significantly hotter than others. Note that Cu coring at the exploratory stage adds significant manufacturing complexity. These findings did reveal that the addition of elements such as Cr and Al to improve oxidation resistance could also significantly degrade thermal conductivity as well as moderately depress melting point, such that the benefits gained by improved oxidation resistance could be fully negated. In some instances, the highly alloyed, oxidation-resistant materials behaved far worse than less oxidation-resistant compositions. It should be noted that the aforementioned spark plug electrodes did not incorporate precious metal/Pt group insert pads. However, the insights

gained can be applied to plugs with insert pads, particularly regarding the observed oxidation/cracking behavior at the electrode alloy/insert pad interface in field-tested plugs.

Spark plug electrodes based on model  $\text{Cr}_2\text{O}_3$ -forming alloys with ferritic, austenitic, and Ni-base microstructures were run in a short-term NG engine test at ORNL for comparison with conventionally used 95% Ni base and Ni-15Cr base electrode alloys. These plugs were run for 67h to gain insight into the behavior of electrode alloys without precious metal/platinum group insert pads, for comparison with the accelerated laboratory gasoline engine tests at FM, and as baseline information for subsequent NG tests using alloys with insert pads. Representative microstructures of the solid center electrode alloys are shown in Figs. 1-3. A complex heterogeneous oxide surface was formed on the conventional 95% Ni base electrode alloy (Fig. 1), with regions of Ni-Mn-Ti-Si-Ca-P-O and Ni-Mn-Cr-O phases. Similar complex surface oxides containing base alloy additions, as well as P, S, etc species were observed on the surfaces of all electrodes examined. Cracking of the surface oxide was evident in the surface of the 95% Ni alloy, and confirmed in the cross-section. Even more extensive cracking was observed on the model Ni-base alloy, Ni-25Cr-0.4Si-0.15La wt.% alloy, whose composition was selected to optimize oxidation resistance (Fig. 2). However, cracking was not observed in an optimized Fe(Ni) base austenitic alloy, Fe-25Cr-20Ni-0.4Si-0.15La wt.% (Fig. 3), nor the corresponding model Fe-base ferritic alloy, Fe-25Cr-0.4Si-0.15La wt.% (microstructure not shown). These results suggest that Ni-base alloys are more susceptible to oxidation-cracking attack than Fe-base alloys. Although such alloys without precious metal insert pads are not candidate NG electrodes, such oxidation-cracking attack was observed in field-tested spark plugs at the Ni-base electrode alloy/insert pad interface. Reduction in these phenomena may lead to improved NG plug life via improved durability of the electrode alloy/insert pad interface.

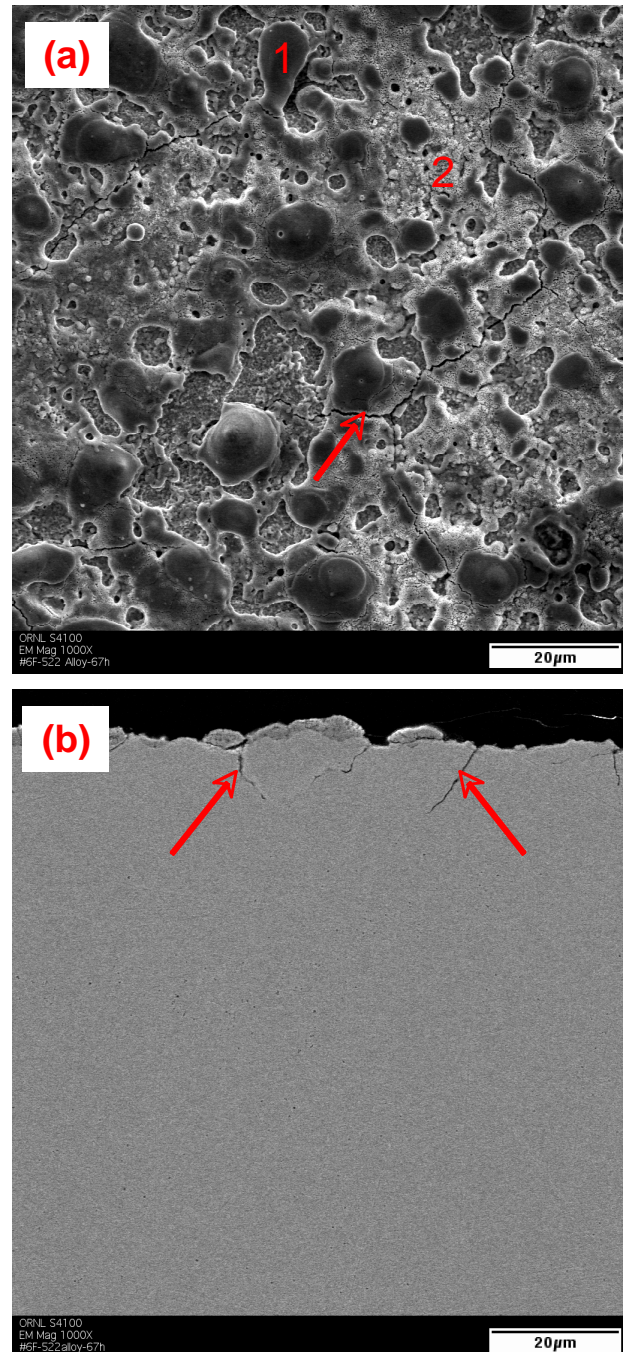


**Figure 1.** SEM micrographs of surface and polished cross section of conventional 95% Ni base electrode alloy after 67h test in Caterpillar G3406 nature gas engine. 1 and 2 denote the Ni-Mn-Ti-Si-Ca-P-O and Ni-Mn-Cr-O phases, respectively. The arrows indicate the crack formation after engine testing.

Attempts were also made to assess the extent of gap growth for the NG tested model and conventional electrode alloys. However, the

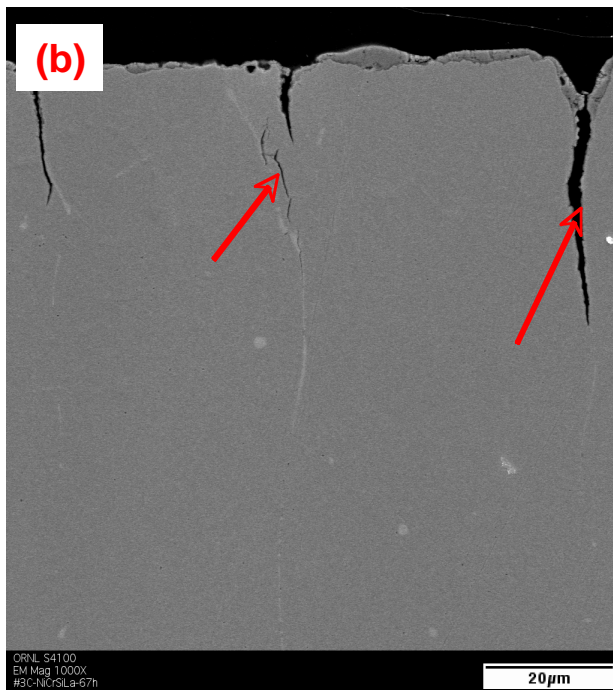
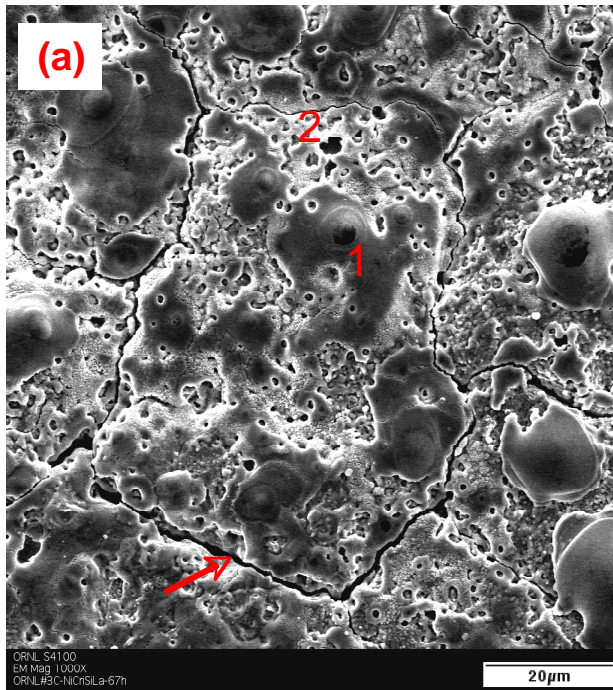


**Figure 2.** SEM micrographs of surface and polished cross section of model Ni-base alloy (Ni-25Cr-0.4Si-0.15La wt.%) alloy after 67h test in Caterpillar G3406 nature gas engine. 1 and 2 denote the Ni-Cr-Si-Ca-P-C-O and Ni-Cr-O phases, respectively. The arrows indicate the crack formation after engine testing.

measurements suggest possible movement of the center electrode during the test, such that reliable

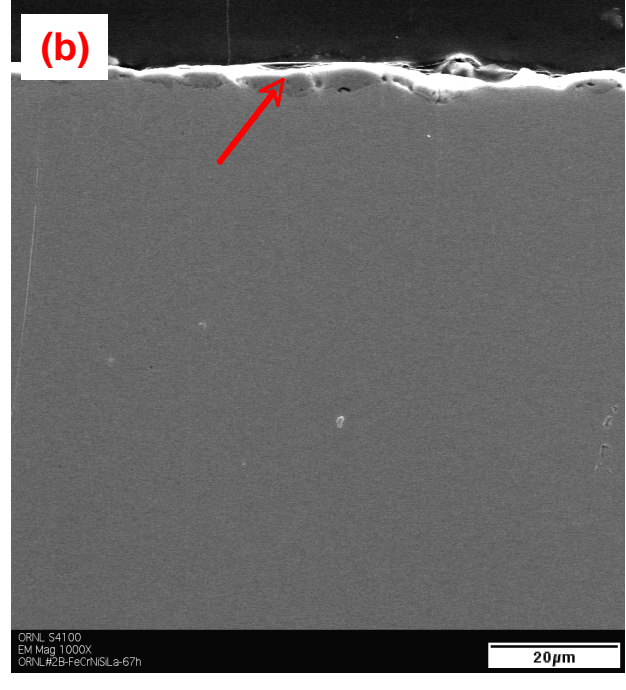
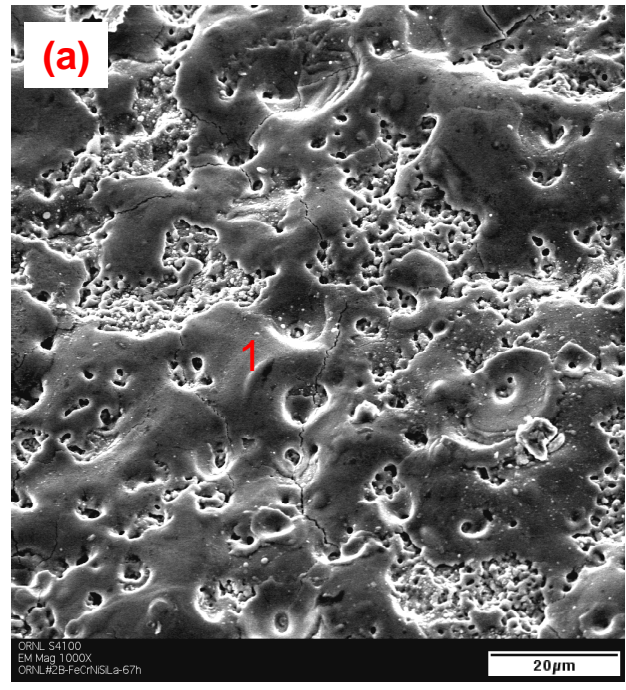


**Figure 3.** SEM micrographs of surface and polished cross section of optimized Fe(Ni) base austenitic alloy (Fe-25Cr-20Ni-0.4Si-0.15La wt.%) alloy after 67h test in Caterpillar G3406 nature gas engine. 1 denotes the Ni-Fe-Ni-Cr-Si-C-O phase. Arrow indicates the Fe-Ni-Cr-O oxide scale formed.



gap growth values could not be obtained. Qualitatively, the gap growth of these electrode alloys, with no precious metal/Pt group insert pads (estimated to be on the order of 10-50 microns), exceeded by at least a factor of two the potential material loss due solely to oxidation scaling processes, i.e. sputtering, melting, ablation, and particle erosion phenomena likely were the main sources of materials loss/gap growth for these alloys.

Based on these findings, and previous studies of field-tested conventional spark plugs, a series of plugs incorporating Pt group metal insert pads and Ni and Fe electrode alloys selected to improve materials compatibility between electrode alloy/insert pad and oxidation resistance was manufactured in collaboration with FM. These materials were selected from commercially available alloys. The electrode alloy was Ni-15Cr base for the improved oxidation resistance relative to the conventionally use 95% Ni base alloys, with a range of Ir and Ir-Pt insert pads. One set of spark plugs also used a commercially available, Fe-Cr base ferritic electrode alloy, due to the increased resistance to cracking observed for Fe-base materials, and the relatively high thermal conductivity of ferritic alloys. Conventionally used Pt-4W and Pt-10Ni insert pad alloys were specifically excluded due to previously observed oxidation-cracking driven materials loss from the selective oxidation of the W/Ni components in the Pt-alloy. The first set of test plugs accumulated approximately 250h of NG operation. Preliminary microstructural analysis revealed loss of the insert pad alloy in many cases, and evidence of significant interdiffusion and attack at the electrode alloy/insert pad interface. It is not yet clear whether this rather poor behavior was due to materials limitations in the engine environment or manufacturing issues with these prototype plugs. Detailed electronic microscopy analysis on both as-received and 250h-tested plugs to elucidate the observed degradations is in progress.

## Future Work

Additional NG engine testing and characterization of the spark plugs manufactured from commercially available electrode alloys and precious metal/Pt group inserts, selected for improved compatibility and oxidation-cracking resistance, will be completed. Efforts have also been devoted to identification and optimization of new alternative electrode alloys and insert pad materials for improved wear (a patent disclosure submitted in 2005). Some of these materials are currently in engine testing at FM and will be characterized and assessed in FY 2007. Additional alloys based on these findings will be optimized early in FY 2007 and delivered to FM and other collaborators for spark plug manufacture and engine testing. For example, discussions are ongoing with Woodward about collaborating on this spark plug work, but with a different emphasis than our collaborations with FM. During FY 2007, technology transfer efforts will include an open literature publication relaying understanding gained over the course of this program.



---

DE



## 3.2b – TAT Lab Performance and Analysis

Abdi Zaltash

Engineering, Science and Technology Division

Oak Ridge National Laboratory

(865)-574-4571; email: [zaltasha@ornl.gov](mailto:zaltasha@ornl.gov)

DOE Technology Development Managers: Patricia Hoffman, Debbie Haught

202-586-6074; email: [patricia.hoffman@hq.doe.gov](mailto:patricia.hoffman@hq.doe.gov)

202-586-2211; email: [debbie.haught@hq.doe.gov](mailto:debbie.haught@hq.doe.gov)

---

### Objective

- Oak Ridge National Laboratory (ORNL) investigates emerging technologies, identifies R&D opportunities and, in consultation with the Department of Energy (DOE) Program Manager, selects the technologies to be developed and conducts supporting in-house research.

Advanced designs for thermally activated technologies (TATs) will entail extensive research, development, manufacturing cost analysis, field-testing, and performance verification. Performance evaluation of advanced TAT designs can enhance existing applications such as heating, cooling, refrigeration, humidity control, and direct fuel-fired activities, as well as potential new applications. The objective is to develop “next generation” TAT equipments with better designs and materials that will lower the cost and improve the performance of heating, cooling, refrigeration, ventilation, and humidity control technologies.

### Highlights

Evaluation of an integrated packaged gas-fired heat pump (rooftop unit GEDAC #13) was conducted at the Thermally Activated Heat Pump (TAHP) Environmental Chambers. This evaluation resulted in the next packaged heat pump unit (GEDAC #16). Significance of ORNL work: (1) private industry partner did not have access to a suitable psychrometric chamber for the evaluation of performance and emissions and (2) ORNL has years of experience working with the chemical industry in developing and testing alternative refrigerants, modify the prototype at ORNL, and evaluate the modified prototype.

### Technical Progress

Thermally activated technologies (TATs) can be directly fired or operated using waste heat in

combined heat and power applications. TATs have a long history and have seen generations of service both in direct-fired systems (where fossil fuels are used directly) to produce chilled water for air conditioning or in refrigeration and dehumidification as well as in equipment using steam or hot water to provide these services. Further advances in efficiency, size, and cost will result in greater use of TATs and in progress toward national energy and environmental goals. This is particularly true in the development of TATs that are powered by recovered waste heat.

TATs represent a diverse portfolio of equipment that uses heat for heating, cooling, humidity control, thermal storage, or shaft/electrical power. TATs are the essential building blocks for integrated energy systems (IES) that can help maximize energy savings and economic return. Thermally activated systems also offer customers reduced seasonal peak electric demand and enable future electric and gas grids to operate with more level loads.

DOE’s TAT development activities in recent years have focused primarily on absorption technology and desiccant technology. Desiccant equipment has been successfully applied for many years in industrial applications or where humidity control is critical. New desiccant technology is being adapted to meet the emerging comfort and indoor environmental quality needs of commercial and institutional buildings. It is expected that, in the next 1-3 years, U.S. industries will begin

commercialization of a natural gas-fired small commercial absorption chiller and residential heat pump now under development as part of this program. DOE and ORNL are cooperating in a national partnership to support final product development and commercialization.

In Japan, many hundreds of thousands of small natural gas-driven heat pumps have been sold (typically 50,000 to 80,000 annually). Although very reliable and energy efficient, the Japanese products are not suited for normal U.S. commercial applications (Japanese equipment is split-system zoned refrigerant equipment that is not suitable for typical U.S. high temperature applications). This activity is to start with the basic technology used in the best Japanese gas-driven heat pumps (the engine) and develop gas-engine driven heat pumps suitable for U.S. drop-in commercial rooftop applications (by far the single largest product segment). Initial evaluations include:

- baseline (emissions, efficiency, and fuel consumption)
- development of several heat transfer components for U.S. applications (exhaust heat exchanger, engine coolant exchanger, and micro-channel outdoor coil)
- vibration and noise (minimize in design)
- engine intake and exhaust system (including catalyst)
- controls (fuel/engine management and complete heat pump system controls)
- parasitic load reduction (starting system and transformer)
- development of single packaged rooftop configurations.

## Results

Performance and emissions evaluation of an integrated 10-ton gas-driven heat pump unit (GEDAC #13 rooftop unit) were conducted in the ORNL TAHP Environmental Chambers. Previous results from the ORNL evaluation were used by industry partner in developing this “next generation” integrated packaged system. The packaged unit was installed in the larger room (outdoor chamber with 15 ft by 18 ft footprint) with supply/return air from the smaller room (indoor chamber with 15 ft by 12 ft footprint).

This unit was operated over a wide range of ambient conditions including the operating conditions for standard rating and performance tests [1]. Table 1 shows these operating conditions. It should be noted that the evaluations were conducted at high and low speed of the engine.

Fifty five cooling and heating tests were conducted. These included thermal imaging of the outdoor coil to verify the temperature distribution across this heat exchanger. Optimization of the heat exchangers with this novel technique to eliminate the potential maldistribution will result in cost effective and more compact outdoor coils for this system. These included cooling tests up to 125°F and heating tests down to 17°F. Heating run is conducted at high engine speed.

Cooling modes were conducted from 67 to 125°F at both high and intermediate engine speeds. At the high engine speed in cooling mode, the unit maintained a coefficient of performance (COP) above one at 95°F outdoor temperature. Unit capacity of 10, 9.5, 9.3 and 8.9 achieved at ambient temperatures of 95, 110, 115 and 120°F respectively (Figure 1). At the intermediate engine speed, the unit achieved cooling capacities of 8.5, 8.0, 7.6, 7.3 and 7.0 RT at ambient temperatures of 95, 110, 115, 120 and 125°F respectively (Figure 2).

Thermal image of the outdoor coil was taken at design cooling temperature 110°F to observe coil performance. As shown in Figure 3, the distribution is fairly uniform over the whole face of the coil. At the outlet of the coil a liquid temperature of 120° F with 10 to 15 degree sub-cooling observed.

Heating modes were conducted from 75 to 17°F. On the heating mode case, sixteen tests were conducted (Figure 4). GEDAC #13 achieved gas heating COP of 1.53 at 47°F outdoor design temperature. A total heating capacity of 161,425 Btu/h (47.3 kW) was achieved.



**Table 1.** Operating conditions for evaluation of commercial thermally activated heat pump

Test	INDOOR UNIT			OUTDOOR UNIT		
	Air Entering			Air Entering		
	DB (°F)	DP (°F)	WB (°F)	DB (°F)	DP (°F)	WB (°F)
<b>COOLING TESTS</b>						
Standard Rating Conditions “A” Cooling Steady State*	80	60.2	67	95	66.5	75**
“B” Cooling Steady State*	80	60.2	67	82	55	65**
“C” Cooling Steady State Dry Coil*	80	36.8	57***	82	55	65**
Low Temperature Operation Cooling*	67	49.8	57	67	49.8	57**
Maximum Operating Cooling Conditions*	80	60.2	67	115	55	75**
High Ambient Temperature	80	60.2	67	110	58.2	75**
“D” Cooling Cyclic Dry Coil*	80	36.8	57***	82	55	65**
Higher Ambient Temperature	80	60.2	67	120	51.3	75**
Highest Ambient Temperature	80	60.2	67	125	47.1	75**
<b>HEATING TESTS</b>						
Standard Rating Conditions High Temperature Heating Steady State*	70	53.5	60 (max)	47	38.7	43
High Temperature Heating Cyclic*	70	53.5	60 (max)	47	38.7	43
High Temperature Heating Steady State*	70	53.5	60 (max)	62	52.7	56.5
Low Temperature Heating Steady State*	70	53.5	60 (max)	17	9.4	15
Maximum Operating Conditions*	80			75	59.5	65

\* Operating Conditions for Standard Rating and Performance Tests [1].

\*\* Wet bulb temperature (WB) condition is not required

\*\*\* Wet bulb sufficiently low that no condensate forms on evaporator

Note: DB is the dry-bulb temperature and DP is the dew-point temperature.

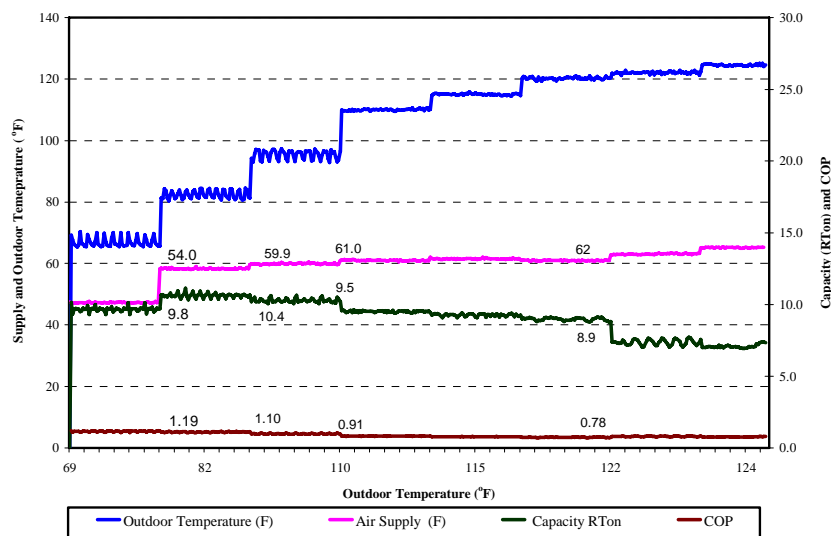


**Figure 1.** Cooling performance of GEDAC #13 at high speed

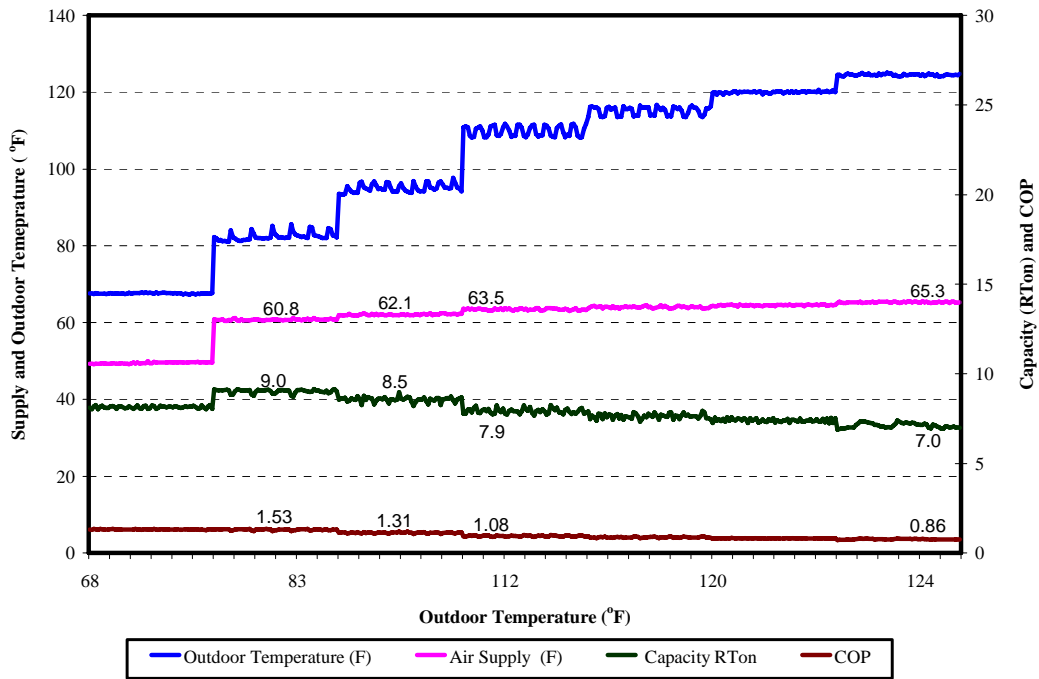


**Figure 2.** Cooling performance of GEDAC #13 at intermediate speed

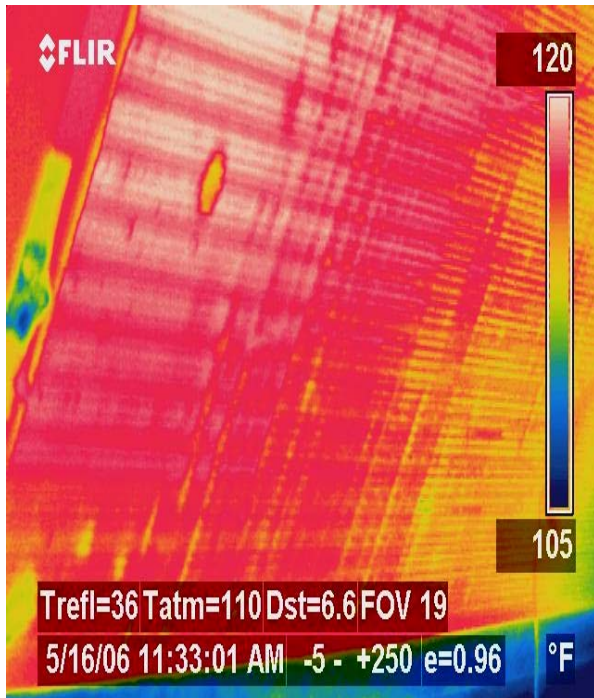


**Figure 3.** GEDAC #13 Outdoor coil thermal image at 110°F

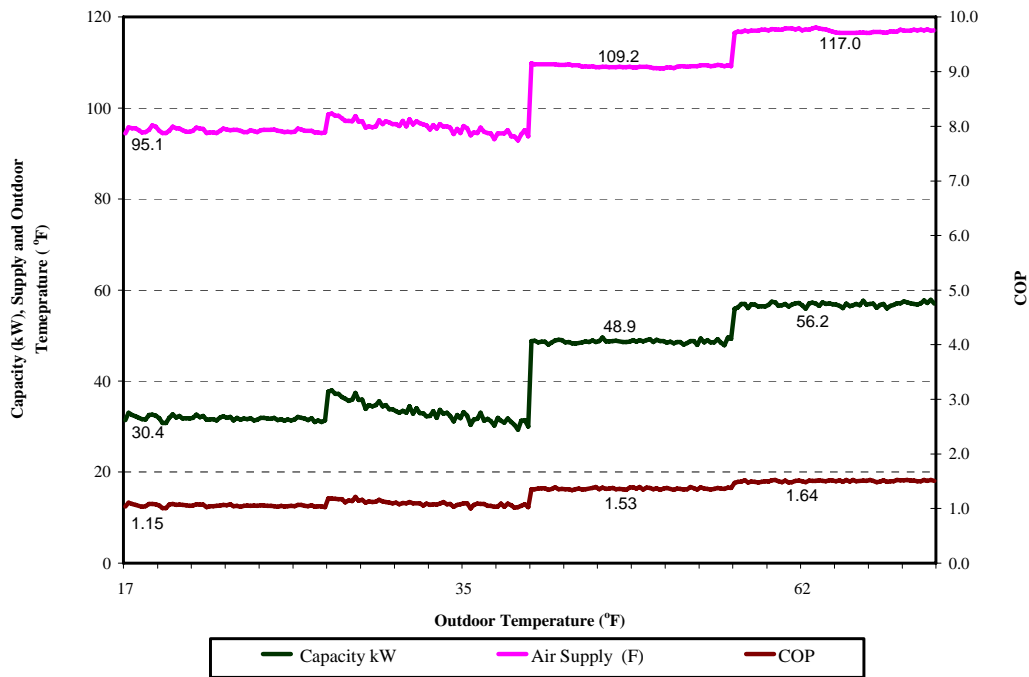


**Figure 4.** Heating performance of GEDAC #13

The next unit (GEDAC #16) has been modified based on the results of this study.

### Conclusions and Recommendations

Unit COP improved from previous split unit. Overall GEDAC #13 unit produced the desired result. The unit coefficient of performance (COP) at 47° F (design point) is 1.53. A total heating capacity of 161,425 Btu/h (47.3 kW) and supply air temperature of 110 ° F was achieved. The results showed that the performance of the unit significantly increased when the coolant was fully diverted to the indoor coil. The defrost cycle did not performed as designed. The next unit (GEDAC #16) has been modified based on the results of this study. These modifications include new defrost cycle, improving the capacity at low heating ambient conditions, re-designed indoor and outdoor coils. The performance of GEDAC #16 package unit will be evaluated in the TAHP Environmental Chambers.

### Status of Milestone(s)

All heating and cooling tests were completed as scheduled.

### Industry Interactions

Southwest Gas, Blue Mountain Energy, Team Consulting

### References

1. ANSI/ARI 210/240-94 Standard, "Unitary Air-Conditioning and Air-Source Heat Pump Equipment", 1998.
2. ANSI/ASHRAE Standard 40-2002, "Methods of Testing for Rating Heat-Operated Unitary Air-Conditioning and Heat Pump Equipment", 2002.
3. ANSI Z21.40.4a-1998 and CGA 2.94a-M98 Standard, "Performance Testing and Rating of Gas-Fired, Air-Conditioning and Heat Pump Appliances", 1998.



### 3.3 – Industry Partnership

*Patti Garland, Jim Sand*  
Engineering, Science and Technology Division  
Oak Ridge National Laboratory  
(202)-470-0292; email: [garlandpw@ornl.gov](mailto:garlandpw@ornl.gov)

DOE Technology Development Managers: *Patricia Hoffman, Debbie Haught*  
202-586-6074; email: [patricia.hoffman@hq.doe.gov](mailto:patricia.hoffman@hq.doe.gov)  
202-586-2211; email: [debbie.haught@hq.doe.gov](mailto:debbie.haught@hq.doe.gov)

---

#### Objective

Desiccant research at ORNL resulted in two commercially successful HVAC products, one with SEMCO and one with Trane, which are undergoing targeted field and verification studies. Market acceptance and widespread application of the energy saving and indoor environmental advantages of this technology are being fostered through demonstrations of advanced thermally activated technologies and activated desiccant systems as called for in the Strategic Goals listed in the DOE Thermally Activated Technologies Roadmap published in 2003.

A competitively procured subcontract with Trane was completed in FY2005. Work under the competitively procured subcontract with SEMCO will be completed in FY2007 with carryover funds remaining from FY2005. Two demonstration sites have been selected and are undergoing data collection and analysis: Carnegie-Mellon University's Intelligent Workplace in Pittsburgh, PA, and a Lowes Store in Spartanburg, South Carolina.

#### Highlights

Work within this project area has yielded an R&D 100 Award in 2005 and another R&D 100 Award in 2006:

[http://www.ornl.gov/info/press\\_releases/get\\_press\\_release.cfm?ReleaseNumber=mr20060705-00](http://www.ornl.gov/info/press_releases/get_press_release.cfm?ReleaseNumber=mr20060705-00)



**ORNL Project Manager Jim Sand with Trane CDQ –  
Winner of R&D 100 Award – 2006**

[http://www.ornl.gov/sci/engineering\\_science\\_technology/cooling\\_heating\\_power/current\\_news.htm#rd100](http://www.ornl.gov/sci/engineering_science_technology/cooling_heating_power/current_news.htm#rd100)



**ORNL Project (SEMCO Revolution) Wins an R&D 100 Award – 2005**

### Technical Progress

The SEMCO Subcontract Phase 5 Final Report, “Field Test Performance Verification: Integrated Active Desiccant Rooftop with Heat Pump Capability,” was issued as an ORNL TM: ORNL Sub-01-4000031065.

Lowe’s – The system has been performing well and the remote monitoring has been installed. This effort was significant since many security concerns raised by Lowe’s caused a more expensive approach to be applied. Data is being collected during this cooling season but data thus far has shown that the Revolution technology has the capability of significantly increasing the dehumidification capacity over that possible with the conventional units currently used. As a result, few tons of cooling is required to reach improved comfort for their customers. The system delivers very low dew point air. The Revolution provides 450% of the dehumidification provided by the RTU.



Carnegie-Mellon University - The pilot site at CMU has been performing exceptionally well. Previous to the installation of the system, numerous problems existing during the cooling season, specifically condensation on the radiant cooling panels and discomfort as a result of poor humidity control. The Revolution unit has been operated to deliver very dry, outdoor air throughout this cooling season.

Data has been archived and shows that the space humidity has been controlled as desired, despite a high percentage of outdoor air and the “all glass” structure. It has been reported that for the first time the radiant cooling technology can be utilized effectively without condensation. CMU staff has been closely monitoring the unit as well as the integral energy recovery module.



Margaret Morrison Building on Carnegie-Mellon Campus

The unit operates to deliver 2000 cfm of outdoor air at a 40 grain (low dewpoint) level using only 5 tons of cooling where a conventional system would use more than 15 tons.

**Status of Milestone(s)**

Draft report on subcontractor field installations of SEMCO IADR unit at Carnegie-Mellon University and Lowes completed on schedule.

**Industry Interactions**  
SEMCO, Incorporated



SEMCO Revolution on roof of Margaret Morrison Building



### 3.6a – Organic Rankine Cycle

Jim Sand, Ed Vineyard  
 Engineering, Science and Technology Division  
 Oak Ridge National Laboratory  
 (865)-574-0576; email: [vinyardea@ornl.gov](mailto:vinyardea@ornl.gov)

DOE Technology Development Managers: Patricia Hoffman, Debbie Haught  
 202-586-6074; email: [patricia.hoffman@hq.doe.gov](mailto:patricia.hoffman@hq.doe.gov)  
 202-586-2211; email: [debbie.haught@hq.doe.gov](mailto:debbie.haught@hq.doe.gov)

#### Objective

This work builds upon previous research to characterize reversible chemical reaction systems that can be used as new, safer active working fluids in this thermo-mechanical converter.

For FY 2006, ORNL will concentrate on designing the recuperator, heat input, and heat rejection heat exchangers, for a bench scale working system.

#### Highlights

The Cooling, Heating and Power (CHP) group at ORNL completed an interim report on selection of optimal working fluids or use in Organic Rankine Cycles (ORCs) The report indicates that the dismal thermal conversion efficiencies of 8 – 15% currently being obtained with conventional ORCs be improved to 20 -30% by using zeotropic mixtures as working fluids in these systems.

#### Technical Progress

As shown below in the Temperature (T) vs. Entropy (S) plots for pure and mixed Rankine cycle working fluids, essentially all of the opportunity to improve the efficiency of ORCs operating with low grade waste heat comes from internal recuperation of thermal energy from the working fluid after turbine expansion. Sharper focus on enhanced heat recovery and improved heat exchangers for ORCs and thermally activated technologies in general fits well with ORNL's current strategic program plans.

#### Status of Milestone(s)

Due to programmatic changes and retirement of principal investigator, project was delayed in FY 2006. Activities will be redirected in FY 2007.

#### Industry Interactions

United Technologies Research Center (UTRC), E. I. DuPont DeNemours Company – Fluorochemicals Division

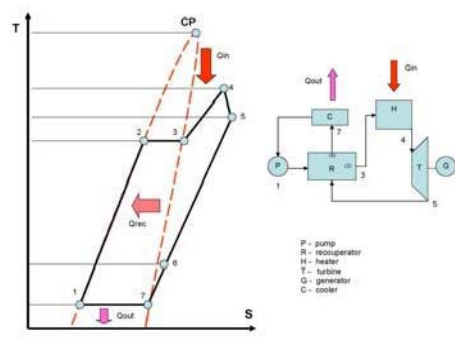


Fig 2a Organic Rankine Cycle for pure substances

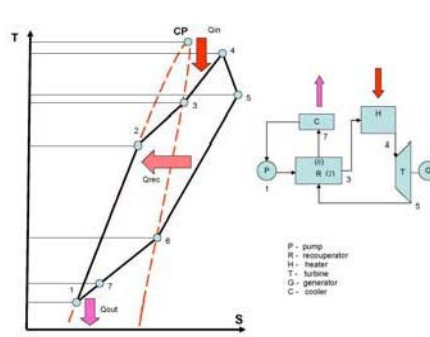


Fig 2b Organic Rankine Cycle for mixtures





### 3.7b Thermal Energy Performance Evaluation

*Jim Sand, Andrei Petrov, Abdi Zaltash, and Ed Vineyard*  
*Engineering Science & Technology Division*  
*Oak Ridge National Laboratory*  
*Oak Ridge, TN 37831-6070*  
*(865) 574-4571, E-mail: [zaltasha@ornl.gov](mailto:zaltasha@ornl.gov)*

*DOE Technology Development Manager: Patricia Hoffman*  
*(202) 586-6074, (202) 586-7114 (Fax), E-mail: [Patricia.Hoffman@hq.doe.gov](mailto:Patricia.Hoffman@hq.doe.gov)*

---

#### **Objective**

For FY 2006, ORNL will continue to independently benchmark and measure the relevant performance characteristics of thermally activated equipment regenerated with primary and/or waste heat sources in the laboratory. ORNL data and published results from these newer, commercially available systems will assure the accuracy and availability of important performance results required by the U.S. HVAC and IES/CHP engineering communities.

#### **Highlights**

- Comparative analysis of the performance data of the SEMCO unit in two operation modes for the desiccant wheel regeneration (NG-based and waste-heat) shows better fuel utilization with CHP system by optimum use of the available thermal energy for heating the regeneration air. The results of this study confirmed the feasibility of implementation of the CHP-based SEMCO air-conditioning system at Pepperell High School (Lindale, GA) commissioned in September 2006.
- Analysis of summertime and wintertime comfort in the CHP Lab building maintained by the SEMCO unit indicates that it provides comfortable climate conditions inside the building.
- Visualization of the frost/defrost cycle in combination with other SEMCO cycle parameters is a valuable background input towards CFD simulation of the frost/defrost cycle in order to optimize it. Extensive laboratory testing and system performance monitoring that resulted in system hardware modifications and selection of a heat pump defrost algorithm.
- Research plans were developed to test a “superhydrophobic” surface concept patented by ORNL as a means of improving the frost free and defrosting performance of heat pump equipment.
- The environmental test chamber has arrived and is in storage at ORNL. Work has begun on a mezzanine structure for the air handling units that will allow the chamber to be placed in the Heat Exchanger Advanced Technologies laboratory. The chamber is expected to be running by April 2007.

## Technical Progress

As described in **ORNL/SUB-01-4000010402** entitled “Desiccant Based Combined Systems: Integrated Active Desiccant Rooftop Hybrid System Development and Testing” the IADR product was developed to independently control both temperature and humidity delivered to an occupied space, during the cooling season, while accommodating up to 100% outdoor air. The system has the unique advantage of being able to process any percentage of outdoor air and adjusting to the load requirements of the space by varying the sensible heat ratio (SHR). The need for improved cooling season humidity control (dehumidification), especially when high outdoor air volumes are required, is essential for facilities located in hot and humid climates designed to meet the ventilation requirements set by ASHRAE 62 and the energy efficiency requirements set by ASHRAE 90.1.

During the heating season, the IADR system will often be required to act as a heating unit as well. This is especially true if the system is installed as a dedicated outdoor air system (DOAS), where it operates with all outdoor air. Traditionally this heating is accomplished through the use of either an indirect gas fired heat exchanger or electric resistance heat. Each method presents a performance disadvantage, especially when high outdoor air volumes are required.

Indirect gas fired options typically do not offer the modulation necessary to accommodate large outdoor air percentages. This presents two potential problems. One is the introduction of very warm air during moderate outdoor air conditions. Since minimum run times are required to protect the life of the heat exchanger, this can result in a wide fluctuation in space temperature. The other is that during the heating season design days, undesirably cold air can be “dumped” to the space when the heater is cycled off but the supply fan continues to run as required to deliver the necessary ventilation air. The use of electric resistance heat has the obvious disadvantage of extreme operating costs due to its very low operating efficiency. At traditional energy costs, a BTU of electric resistance heat will cost approximately 2.2 times the cost of the indirect fired gas approach assuming an 80% efficient heat

exchanger. Unless a high end electric heating control method is employed (i.e. SCR) to modulate the heating output, the electric resistance heating approach can result in the same dumping of cold air associated with the indirect gas approach.

Another important market driven factor is that since hot and humid climates have, by definition, relatively mild heating seasons, electrical utilities have been extremely successful convincing their customers to design around all electric facilities (i.e. use electric resistance heat) in exchange for favorable electric rates. Although the heating season is short, the heating cost per BTU is extremely high with this heating method so annual energy costs can be significant. This is supported by the research findings resulting from a DOE sponsored demonstration sites (discussed later). A major pharmacy located in south Florida and using electric resistance heat paid the same amount for electricity in February as it did in August.

To address the need for heating by the IADR and to accomplish a stated development objective of high operating energy efficiency, the necessary parts were combined with novel control capabilities to integrate a heat pump cycle into the refrigeration portion of the hybrid system. This option offers an excellent fit to the hot and humid climates most likely to employ the IADR since they inherently have moderate heating seasons, allowing the enhanced heat pump performance capable with this system to satisfy the entire heating season needs.

### *IADR Design for Dehumidification Benefits the Heat Pump Integration*

Since the IADR hybrid system includes an advanced vapor compression cooling section, only a few additional parts are required to complete the infrastructure for an effective air cooled heat pump system. A simplified heat pump piping schematic is provided as Figure 1 to show the major components required for heat pump operation.

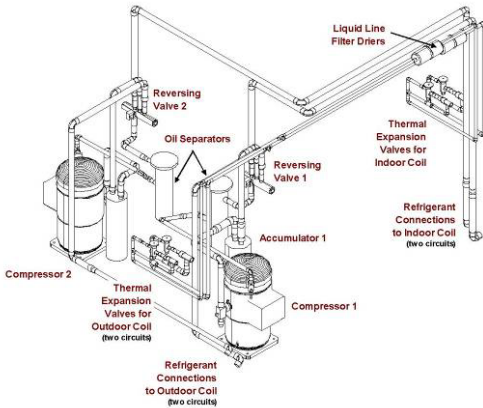


**Figure 1.** A schematic showing the major components required by the heat pump cycle integrated into the IADR hybrid system (outdoor and indoor coils are not shown)

To accommodate 100% outdoor air operation in the dehumidification/cooling mode, the cooling side components (coils, compressors, etc.) designed into the IADR have a much greater capacity per cubic foot per minute (cfm) of airflow processed than traditional packaged equipment. Traditional packaged systems are designed for approximately 400 cfm/ton of cooling output while the IADR is designed for approximately 175 cfm/ton. This design approach results in the size of the evaporator coil, condenser coil, condenser airflow and compressor capacity being large relative to the airflow delivered. This design approach is highly beneficial for heat pump operation.

### *Compressor Capacity*

In addition to the high ratio of compressor tons to airflow processed, a high heating output results from the fact that all of the energy output experienced when in the heat pump mode is translated into temperature increase. During the cooling mode, a portion of the energy produced is allocated to condensing moisture (latent load). This latent portion is significant (say 50%) if all outdoor air is being processed. This is not the case in the heat pump mode.

Another factor enhancing performance in the heat pump mode is the compressor heat. This heat degrades cooling capacity but increases the heat output provided during the heat pump mode.

### *Outdoor Coil and Airflow Capacity*

During the heat pump operation the outdoor air coil becomes the “cooling coil” while the indoor coil becomes the “heating coil”. Since the heating performance is directly impacted by the difference between the refrigerant temperature and the ambient air temperature, and since the ambient air temperature can be quite low during the heating season, it is advantageous to keep this temperature difference to a minimum. This is accomplished by maximizing the outdoor coil surface area and operating with the highest possible outdoor airflow. High outdoor coil area and low temperature differentials are also important to minimize the likelihood and duration of frost formation on the outdoor coil. When the outdoor ambient humidity content is above the dew point of the outdoor coil surface, and if this surface temperature is below freezing, frost can slowly accumulate on the coil surface. This frost is removed by reversing the refrigeration flow and temporarily reverting back to cooling so that the outdoor air coil heats up and melts the frost. Since cold air leaves the indoor coil when heating is actually needed, it is advantageous to minimize both the frequency and duration of this defrost cycle.

### *Installation Sites Used to Obtain Performance Verification*

Three separate IADR systems were investigated at different locations to benchmark the heating performance resulting from the integration of a heat pump option. The first system installed to condition the ORNL CHP laboratory located in Oak Ridge Tennessee provided an excellent opportunity to observe heating performance at high outdoor air percentages and in a relatively cold environment.

The second site selected was an existing pharmacy located in St. Petersburg Florida to provide data from a hot and humid climate during continuous actual operating conditions. The third system was installed within the SEMCO test laboratory located in Columbia, Missouri allowing a wide range of tests to be completed since airflows and indoor coil entering conditions could be modulated as desired. Basic details are provided for two of these installations.

### *Oak Ridge National Laboratory's CHP Test Lab*

An IADR system having a nominal cooling capacity of 12.5 tons was installed to condition the CHP Laboratory at ORNL located in Oak Ridge Tennessee. The system was operated to provide approximately 3,200 cfm of supply airflow which comprised of between 50 and 100% outdoor air depending upon the pressurization needs of the facility. A small fume hood exhausted approximately 1,000 cfm and the building envelope was not well sealed. This new system was installed during July of 2004 and it has been operated to handle the outdoor air sensible and latent cooling loads, all of the space latent load and most of the space sensible load. An existing split system and hot water space heaters supplement the capacity of the IADR when needed. The 99% heating design condition for this location is 19°F according to the 2001 ASHRAE Fundamentals.

Traditionally, heat pumps would not be successfully applied to facilities with this climate, especially of high outdoor air percentages were required.



**Figure 2.** Photos of the IADR installed at the ORNL CHP laboratory.

### *SEMCO Inc.'s Research and Development Test Laboratory*

An IADR system having a nominal cooling capacity of 12.5 tons was installed to help condition the SEMCO R&D Air Test Laboratory located in Columbia Missouri. The system is operated to provide approximately 3,000 cfm of supply airflow which is comprised of approximately 50% outdoor air.

This system has been operating since November of 2004 and it has provided an excellent opportunity to test a variety of operating conditions for the heat pump capability of the IADR system. The

99% heating design condition for Columbia Missouri is 5°F according to the 2001 ASHRAE Fundamentals. This provided the most extreme heating season operating conditions of the sites investigated. As shown by Figure 3, the IADR system located within the SEMCO test laboratory differed from the systems installed at the other two sites in that the system was built as a “split system” with the main system being located indoors but the condensing section being located outdoors.



**Figure 3.** Photos of the IADR system installed within (main unit) and outside (condensing portion) of the SEMCO R&D Test Lab in Columbia Missouri

The extreme outdoor air temperatures and consistent cold conditions that existed for this system due it location offered the most effective site for optimizing the defrost control algorithms and methods. The application of air side heat pump technology used to condition a high percentage of outdoor air, as was the case for this test site is highly unusual and provided an excellent challenge to the performance capabilities of the IADR heat pump integration.

### *Comparative analysis of the performance data of the SEMCO unit in two operation modes for the desiccant wheel regeneration (NG-based and waste-heating modes)*

The aim of this study was to compare the efficiency of the SEMCO operation in baseline mode, when the regeneration stream of the SEMCO unit is heated by the natural gas burner, and in CHP mode, when the regeneration stream is heated by the hot water circulating in hot water coil installed upstream of the desiccant wheel in the regeneration duct (Figure 4). The hot water is produced in the heat recovery unit (HRU) driven by exhaust gas from the microturbine (MTG).

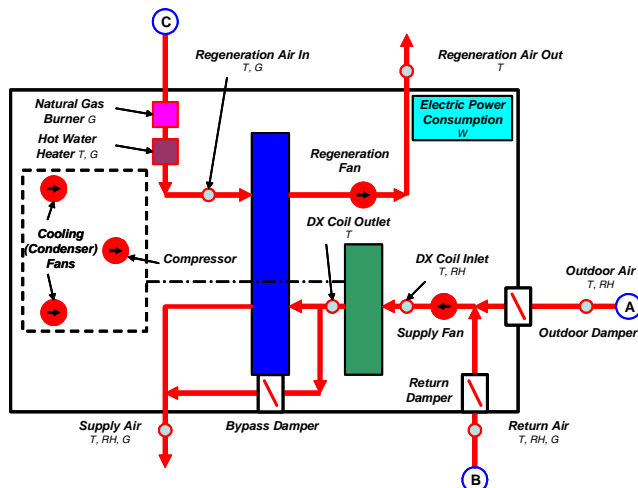


**Figure 4.** Schematic diagram of the SEMCO unit

The results show that while the system efficiency of the NG-based operation does not change with increasing number of IADR units, the efficiency of the waste-heat operation improves significantly with increasing number of IADR units (more efficient use of the available thermal energy). This efficiency was found to be 84.6% which exceeds the NG-based mode efficiency of 80.7% (Figure 5).

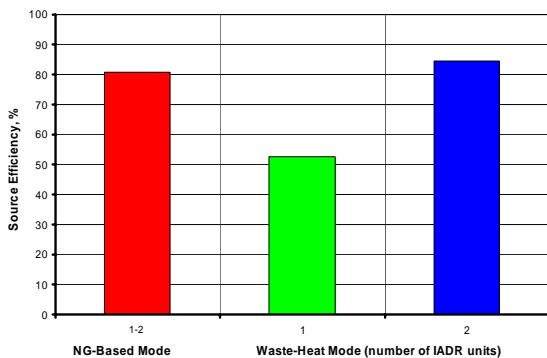


**Figure 5.** Comparison of NG-based and waste-heat efficiencies versus number of SEMCO units at MTG  $W_{el}$  12.2 kW

To study the effect of the improved electrical efficiency of the MTG, the next simulation case was with the MTG operating at higher electric power output of 20 kW (Figure 6). These data show that with two participating SEMCO units at MTG power output of 20 kW in the waste-heat mode, the source efficiency is lower than that of the NG-based mode by 14.3%, and with three

SEMCO units, when the use of thermal energy increases, the source efficiency in the waste-heat mode exceeds that of the NG-based mode by 9.3%. The importance of the maximum use of the available thermal energy for heating regeneration air is evident from Figure 8, when for similar arrangements with two SEMCO units, the efficiencies at MTG power output of 12.2 kW (with better use of the thermal energy) are higher than those at MTG power output of 20 kW (when the thermal energy is not fully used).

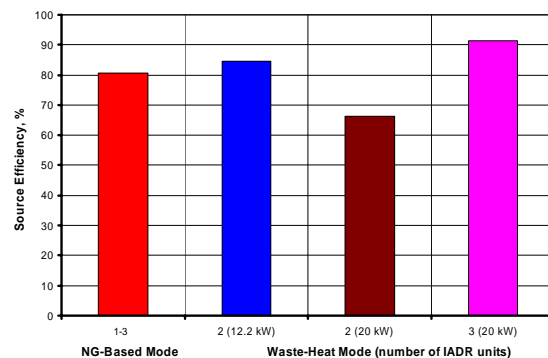


**Figure 6.** Comparison of NG-based and waste-heat efficiencies versus number of SEMCO units at MTG  $W_{el}$  12.2 kW and 20 kW

Comparative analysis of the performance data of the IADR unit in two operation modes: NG-based and waste-heat shows better fuel utilization with CHP system by optimum use of the available thermal energy for heating the regeneration air. It is very important to minimize all possible thermal losses on the hot water and the exhaust gas sides in a CHP system. Although existing CHP arrangement with one IADR unit did not show an improvement in efficiency compared to the NG-based mode of operation, the analysis shows that there is a great potential for improvement by maximizing the use of the available thermal heat with two or more IADR units. The results of this study confirmed the feasibility of implementation of the CHP-based SEMCO air-conditioning system at Pepperell High School (Lindale, GA) commissioned in September 2006.

*Summertime and Wintertime Comfort in the CHP Lab Building Maintained by the SEMCO Unit*

The aim of this research was to evaluate of the capability of the SEMCO unit to keep the building

environment within the comfort conditions set by the ANSI/ASHRAE Standard 55-2004. The 2,000 ft<sup>2</sup> building selected for climate control is a poorly-insulated metal structure with metal roof that can transfer large amounts of radiant heat during hot sunny days. In addition to numerous openings in the building, there is an exhaust hood fan in the chemistry laboratory, which removes approximately 1,000 cfm of air from the building. All the above-mentioned factors plus hot and humid summer days make the task of maintaining the comfort conditions inside this building extremely difficult.

The summertime comfort level results are shown in Figures 7 and 8. Figure 7 shows the data for the outdoor temperatures of 82-91°F and Figure 8 - for the outdoor temperatures of 92-97°F. Two curves for 80 and 90% acceptance of climate conditions inside the building are also given in these figures.

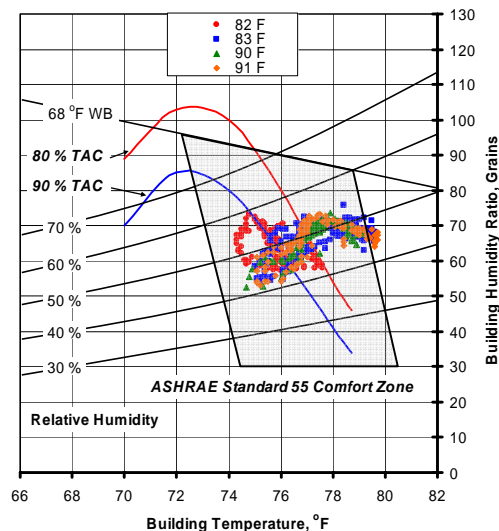


**Figure 7.** Summertime comfort data for outdoor temperature 82-91 °F

The summertime performance results show that the SEMCO unit is capable of maintaining the comfort conditions in accordance with the ANSI/ASHRAE Standard 55-2004. For lower outdoor temperatures, roughly 95% of all the data considered lay inside the ASHRAE-specified comfort zone, and more than 50% of those are within the 80% comfort line (Figure 1). For higher outdoor temperatures the percentage of the data

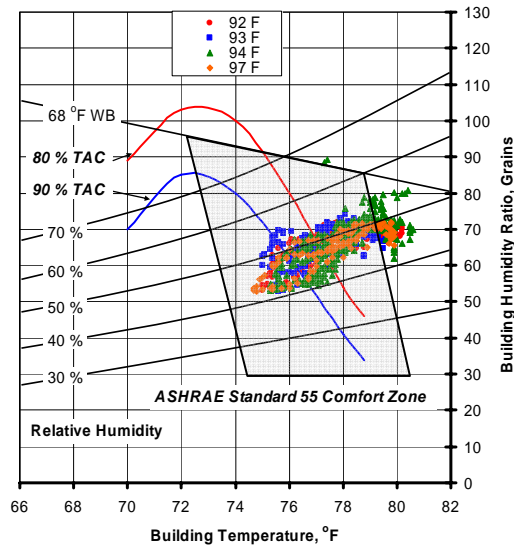


**Figure 8.** Summertime comfort data for outdoor temperature 92-97 °F

points outside the ASHRAE comfort zone is slightly higher, but it does not exceed 10% of all observed points. Roughly 50% of the data points are within the 80% comfort zone of the ANSI/ASHRAE Standard 55-2004.

The analysis of the comfort conditions during 2006 winter period was performed for the outdoor temperature range of 27-31°F with relative humidity values of 63-71%. The supply flowrate was approximately 2,200 cfm split between outdoor flowrate (approximately 1,900 cfm) and return flowrate (approximately 300 cfm). During this study, no other climate control unit was used in this building.

The results (Figure 9) indicate that, although the temperature inside the building is kept well within the standard [4], the humidity ratio is below the lower limit. This is due to obvious restriction on humidity ratio control inside the building during heating season – it cannot be higher than the humidity ratio of outdoor air. In fact, the building humidity ratio should be almost equal to the outdoor humidity ratio. This is true for this specific case.

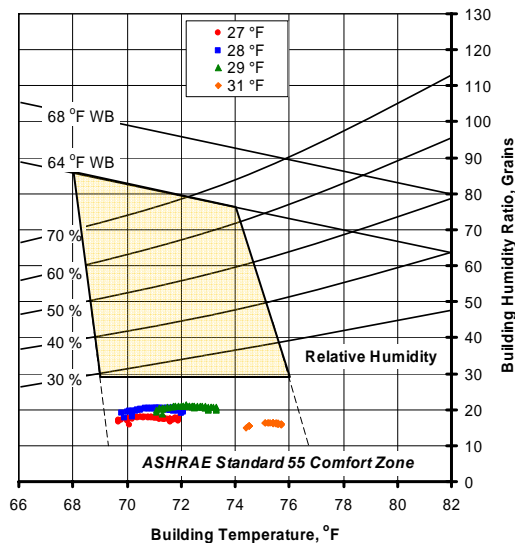


**Figure 9.** Wintertime comfort data for outdoor temperature 27-31 °F

The SEMCO unit did an excellent job in providing comfortable climate conditions inside the building during the summertime performance evaluations. During the wintertime, the temperature of the building was also controlled comfortably and well within the temperature limits set by the ANSI/ASHRAE Standard 55-2004. As expected, the space relative humidity levels observed were below the limit recommended by the Standard since the laboratory is not humidified.

### *Managing the Defrost Cycle*

One of the main barriers to heat pump use, especially where high outdoor air percentages are required is the need for defrost cycles. When operating in the heating mode, the heat pump essentially “flips” the normal cooling cycle so that the outdoor coil acts as the evaporator and the indoor coil becomes the condenser. As the outdoor coil cools the outdoor air, the coil surface temperature frequently drops below 32 °F. If the outdoor dew point is above the coil surface temperature, moisture in the outdoor air will be condensed and frost will begin to form. As the frost builds, airflow across the coil will slowly decrease while the frost begins to degrade the transfer characteristics of the coil. The net result is less heating capacity being available and the need for the compressor to work harder to meet the desired condition. Therefore, this frost formation

must be carefully managed and removed before a significant degradation in performance occurs (see Figure 10).



**Figure 10.** Photo of frosted outdoor coil of the SEMCO unit installed at the ORNL site

The elimination of this frost formation is easily done. By switching back to “cooling mode” through the activation of a “reversing valve” the outdoor coil once again becomes the condensing coil, heats up and quickly melts the frost that has formed. The problem during defrost occurs at the indoor coil. When in defrost mode, the indoor coil cools the supply air to very low temperatures which is problematic, especially if outdoor air is being delivered by the system. As a result, most heat pump systems currently rely on inefficient electric resistance heat to operated during the defrost cycle to isolate the occupied space from the cold air leaving the coil.

The IADR incorporates the capability of using the gas fired regeneration burner and the variable speed active desiccant wheel to provide an effective indirect gas fired heating source. A novel approach was devised to anticipate the need for a defrost cycle then bring on the indirect fired gas heat for a short duration to maintain an acceptable supply air temperature. As the first step of the defrost control algorithm optimization was to isolate the building space from the cold air leaving the indoor coil during the defrost mode.

The next step will be development of general defrost algorithm for the family of SEMCO units. To develop it, a better understanding of their operation in frost/defrost mode is required. As a first stage, the visualization of the frost/defrost process with conventional and thermal image

video recording devices and simultaneous recording of all thermodynamic data in the SEMCO unit has been performed. Images of outdoor coil at some operation conditions (just before the onset of the defrost mode, end of the defrost mode, and return to normal operation) are shown in Figure 11. These data will be used in development of the comprehensive CFD model of the SEMCO unit operation in the frost/defrost mode that would allow optimization of the defrost cycle in each specific case.

### **Conclusions and Recommended Future Work**

These research/demonstration installations involving the integrated vapor compression – active desiccant hybrid system (IADR) with heat pump integration were successful. All original objectives were met, the measured performance matched or exceeded the modeled expectations and all end users are very satisfied with the results. Attractive heating costs relative to either gas or electric resistance heating were documented as a result of high system operating efficiency.

Owners applying this technology could expect to reduce the cost associated with heating by approximately 40% and 71% compared to indirect gas and electric resistance heating respectively.

This design approach has been implemented as part of newly constructed high school CHP-based IADR air-conditioning system (Lindale, GA) commissioned in 2006. This project applies numerous SEMCO IADR systems which include the heat pump option. These systems are applied as both dedicated outdoor air systems and complete VAV systems. This opportunity allows the performance of the IADR and the integrated heat pump cycle to be further optimized since all

systems will be equipped with instrumentation and data trending. Four of the systems are also combined with on-site power generation to form an effective CHP site, using the heat of rejection from the engine to regenerate the active desiccant wheels. The feasibility of implementation of this approach has been confirmed in the current study. This heat will also be used for space heating with the heat pump being used for back-up heat as needed.

Future work will include further optimization of the defrost cycle of the SEMCO unit during heating mode operation with thermal visualization and CFD approach in order to develop generalized model of defrost optimization applicable to each specific case.

### **Status of Milestone(s)**

Final draft report on IADR laboratory results was issued in September 2006 entitled, “Comparative Performance Analysis of IADR Operating in Natural Gas-Fired and Waste Heat CHP Mode”.

### **Industry Interactions**

SEMCO, Incorporated, Advanced Heat Transfer, LLC.

### **References**

1. Petrov A.Y., Sand J.R., Zaltash A., Fischer J., Mitchell R., Comparative Performance Analysis of IADR Operating in Natural Gas-Fired and Waste-Heat CHP Mode, Proceedings of IMECDE-2006, Paper IMECE 2006-13201, November 5-10, 2006, Chicago, IL.
2. Petrov A.Y. and Sand J.R., Comfortable Level at ORNL CHP Test Laboratory Building with SEMCO Revolution

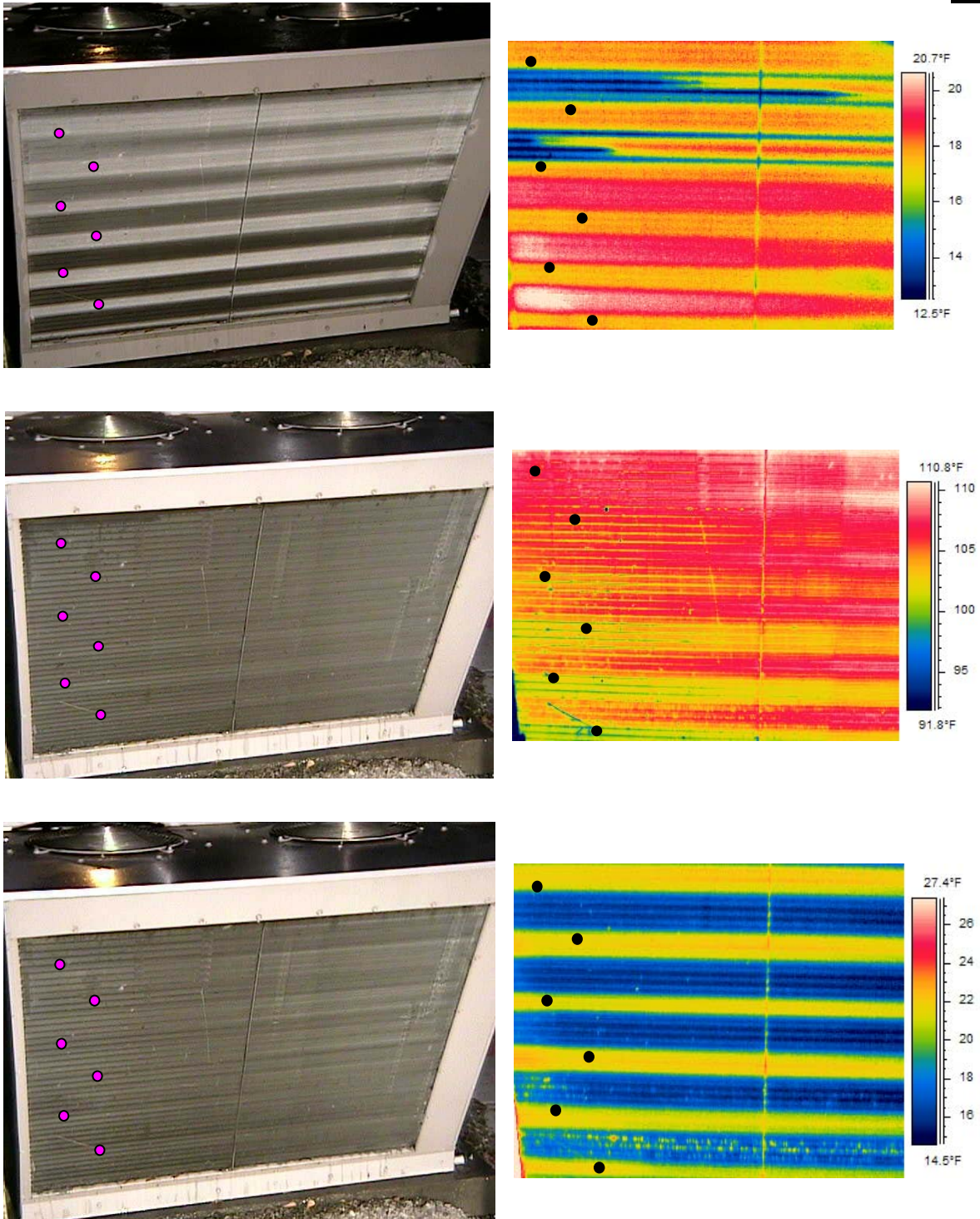


**Figure 11:** Images of outdoor coil at some operation conditions (just before the onset of the defrost mode, end of the defrost mode, and return to normal operation) of the SEMCO unit



3. Integrated Active Desiccant Rooftop Unit, ESTD Newsletter, 2006, 5.
4. Harriman L.,G., Brundrett G.W., and Kittler R., Humidity Control Design Guide for Commercial and Institutional Buildings, ASHRAE, Atlanta, GA, 2001.
5. Nevins R. et al, Effect of Changes in Ambient Temperature and Level of Humidity on Comfort and Thermal Sensations, ASHRAE Transactions, 1975, 81 (2).
6. Petrov A.Y., Sand J.R., Zaltash A., Fischer J., Mitchell R., and Wetherington G.R., Performance Analysis of Integrated Active Desiccant Rooftop Air-Conditioning System Operating in Heating Mode, Proceedings of IMECDE-2005, Paper IMECE 2005-79238, November 5-11, 2005, Orlando, FL.
7. ANSI/ASHRAE Standard 55-2004, Thermal Environmental Conditions for Human Occupancy, ASHRAE, Atlanta, GA, 2004.
8. Berglund L., Comfort and Humidity, ASHRAE Journal, 1998, 40(8), pp. 35-41



### 3.7c – Micro-Channel Heat Exchanger Development

*Ed Vineyard*

*Engineering, Science and Technology Division*

*Oak Ridge National Laboratory*

*(865)-574-0576; email: [vineyardea@ornl.gov](mailto:vineyardea@ornl.gov)*

*DOE Technology Development Managers: Patricia Hoffman, Debbie Haught*

*202-586-6074; email: [patricia.hoffman@hq.doe.gov](mailto:patricia.hoffman@hq.doe.gov)*

*202-586-2211; email: [debbie.haught@hq.doe.gov](mailto:debbie.haught@hq.doe.gov)*

---

#### **Objective**

Development work on micro-channel heat exchangers for TAT equipment will continue in FY 2006. Additional partners have been recruited to assist in development activities.

#### **Highlights**

ORNL has discussed the potential for using micro-channel or miniature heat exchangers for military cooling applications. There are presently problems with some types of equipment operating in extreme temperatures that are causing accelerated failures. Other government agencies are interested in collaborative efforts for absorption equipment and micro-channel heat exchangers.

#### **Technical Progress**

ORNL discussed plans with a utility company to develop a microchannel heat exchanger in their next-generation rooftop unit. The development efforts will most likely focus on the condenser since that is the heat exchanger with the greatest potential for reducing the size and weight of the unit. The condenser is the largest of the two heat exchangers and reducing its overall height could also help with reducing the overall height of the unit which is one of the goals to aid in meeting local code requirements.

We discussed the possibility of an outside vendor supplying a prototype heat exchanger for the unit. The vendor agreed in principle to furnish a heat exchanger and to aid in the design.

The decision was made to use one circuit instead of two for the rooftop unit. This will simplify the overall design and make it easier to service and improve overall reliability.

#### **Status of Milestone(s)**

The milestone for testing a prototype micro-channel heat exchanger has been delayed due to the disassembly of the test loop which is being moved to the Heat Exchanger Advanced Technologies laboratory. The decision was made to delay the milestone since the loop is being moved with Laboratory Maintenance funds, resulting in a program savings of over \$200,000.



### 3.7e – Woven Graphite Fiber Heat Exchanger

*Ed Vineyard, Randy Linkous*  
*Engineering, Science and Technology Division*  
*Oak Ridge National Laboratory*  
*(865)-574-0576; email: [vineyardea@ornl.gov](mailto:vineyardea@ornl.gov)*

*DOE Technology Development Managers: Patricia Hoffman, Debbie Haught*  
*202-586-6074; email: [patricia.hoffman@hq.doe.gov](mailto:patricia.hoffman@hq.doe.gov)*  
*202-586-2211; email: [debbie.haught@hq.doe.gov](mailto:debbie.haught@hq.doe.gov)*

---

#### **Objective**

Development work on woven graphite fiber heat exchangers for thermally activated equipment was initiated under a DOE Lab Call in FY 2005. Work in FY 2006 will involve testing a heat exchanger to validate heat exchanger models which predict a significant performance improvement for woven graphite fiber heat exchangers.

#### **Highlights**

ORNL has initiated tests in one of the new wind tunnels obtained last year. The heat exchanger is shown in Figure 1 installed in the wind tunnel. A test matrix consisting of approximately 90 test points was developed to enable a parametric analysis of the heat exchanger over a wide range of operating conditions.



**Figure 1.** Woven Graphite Fiber Heat Exchanger installed in wind tunnel.

#### **Technical Progress**

A visiting professor from Vanderbilt University working for ORNL has developed a model of the woven graphite heat exchanger to analyze the theoretical performance. The model is an equivalent resistance model that incorporates lateral conduction to describe the heat transfer between tubes in the fiber. Results suggest that high conductivity fibers can significantly improve

the heat transfer. However, for extremely large conductivities, performance will degrade due to parasitic heat losses. Furthermore, contact resistance between the fiber and tube govern the performance more than the fiber conductivity.



### **Status of Milestone(s)**

The milestone for initiating tests for a prototype woven graphite fiber heat exchanger was completed as scheduled in July 2006.

### **Industry Interactions**

- 3-TEX
- Office of Naval Research
- Foam Application Technologie

### 3.7g – CFD Modeling Analysis

*Ed Vineyard, Pat Geoghegan*  
*Engineering, Science and Technology Division*  
*Oak Ridge National Laboratory*  
*(865)-574-0576; email: [vineyardea@ornl.gov](mailto:vineyardea@ornl.gov)*

*DOE Technology Development Managers: Patricia Hoffman, Debbie Haught*  
*202-586-6074; email: [patricia.hoffman@hq.doe.gov](mailto:patricia.hoffman@hq.doe.gov)*  
*202-586-2211; email: [debbie.haught@hq.doe.gov](mailto:debbie.haught@hq.doe.gov)*

---

#### **Objective**

To employ computational fluid dynamics (CFD) modeling to provide an insight into the fluid mechanics and heat transfer mechanisms within complex heat exchange systems.

#### **Highlights**

Good collaboration with the engineers at a utility company developing a gas-fired heat pump has resulted in a prototype unit that has been heavily influenced by the CFD findings.

A presentation from the CHP group was made to the utility. The presentation included images from the CFD modeling and resulted in very positive feedback.

#### **Technical Progress**

CFD modeling of the unit focused on both the outdoor and indoor sections. Preliminary studies on the outdoor section highlighted the critical importance of heat exchanger selection and positioning in terms of balancing pressure losses. A low pressure loss coefficient in one heat exchanger results in a high flow bias that has adverse effects on the performance of the other heat exchangers making up the system.

CFD modeling also made it possible to investigate the performance of the outdoor section driven by two 24" axial fans as compared to a single 36" axial fan arrangement. It was found that the single fan approach yielded heat exchanger capacities that were approximately 5% lower than the two-fan approach. Temperature contours are shown below in figures 1a and 1b. The single fan did have the positive effect of pulling air through the centre of the unit and would provide significant cost savings. For these reasons the prototype was constructed to allow easy fan arrangement substitution.

The indoor section of the unit was also modeled using CFD. The position of the centrifugal fan relative to the evaporator was varied to achieve maximum exchanger performance. Again, the angular position of the exchanger was found to be critically important. Figure 2 shows the effect of the duct inlet position on the flow through the condenser. The inlet runs below the evaporator from the right-hand-side and creates a dead-space on that side. Such a set-up can significantly reduce the overall unit performance.

#### **Status of Milestone(s)**

CFD laboratory is completed and initial analysis results have been obtained for the prototype unit. April 2006 milestone was completed as scheduled.

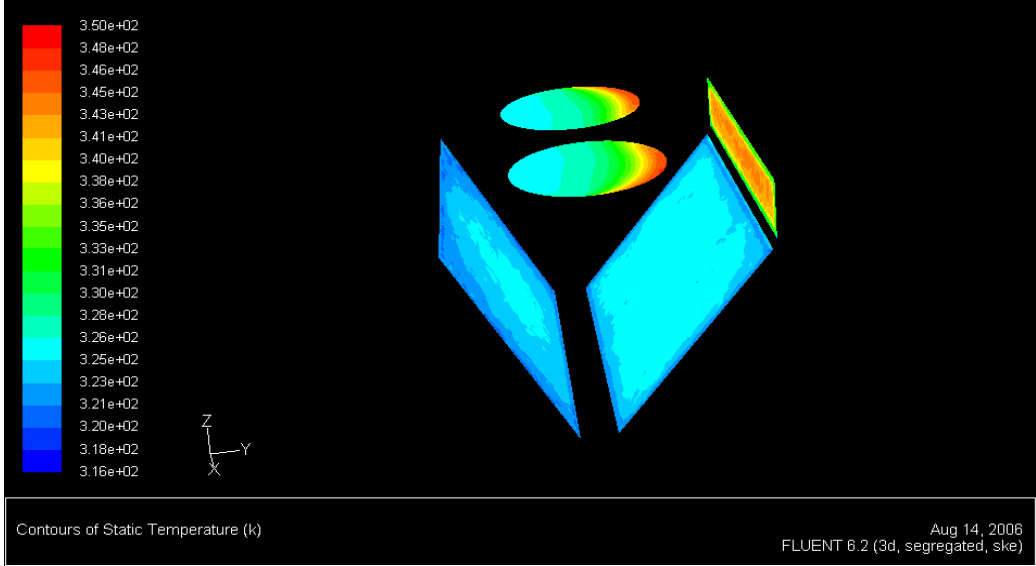


Figure 1a. Outdoor section heat exchanger temperature contours resulting from twin 24" axial fans.

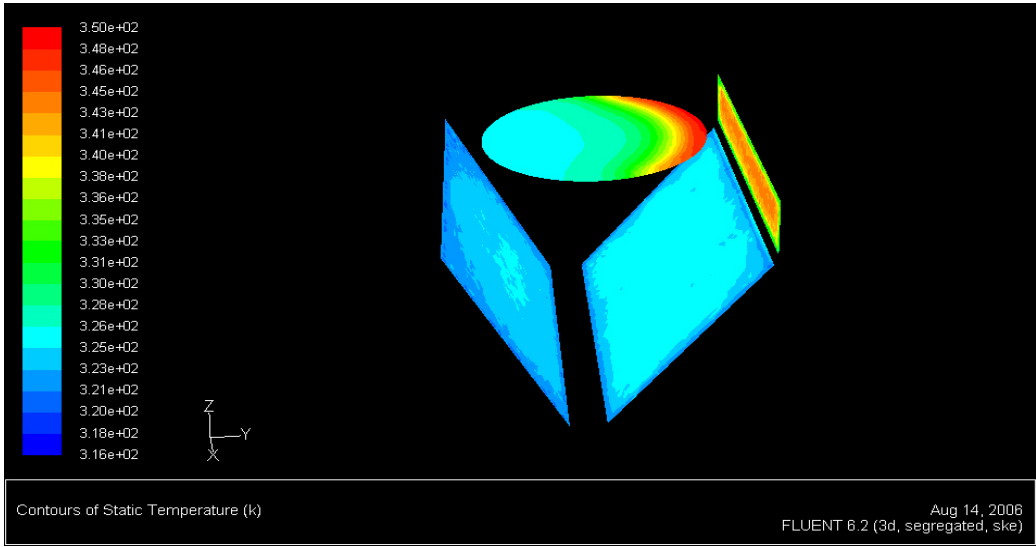
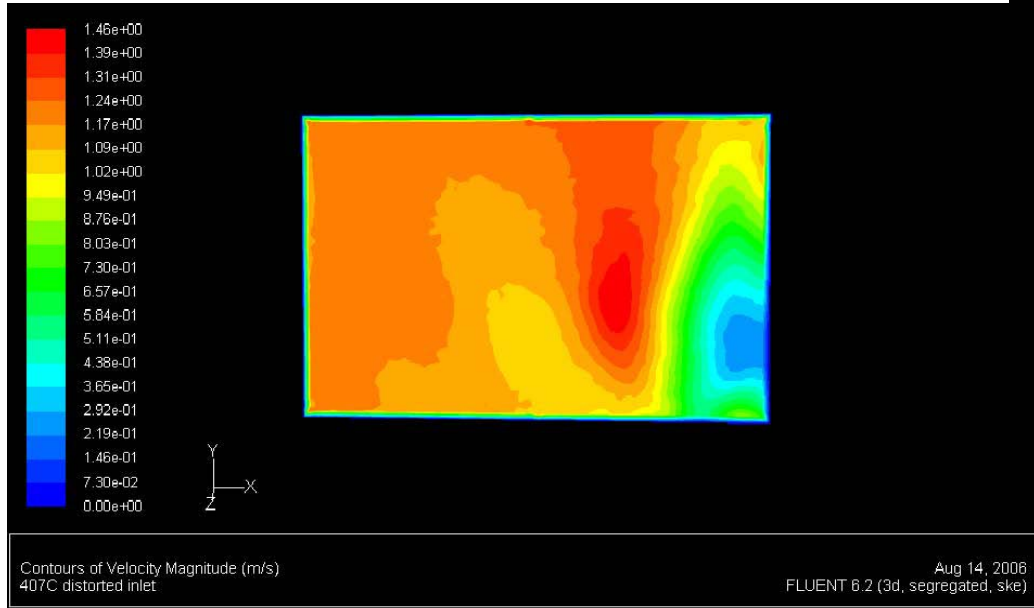


Figure 1b. Outdoor section heat exchanger temperature contours resulting from a single 36" axial fan.



**Figure 2.** Flow through the indoor evaporator when air is introduced from one side.



### 3.8 – Rotating Heat Exchanger

Abdi Zaltash, Andrei Petrov  
Engineering, Science and Technology Division  
Oak Ridge National Laboratory  
(865)-574-4571; email: [zaltasha@ornl.gov](mailto:zaltasha@ornl.gov)

DOE Technology Development Managers: Patricia Hoffman, Debbie Haught  
202-586-6074; email: [patricia.hoffman@hq.doe.gov](mailto:patricia.hoffman@hq.doe.gov)  
202-586-2211; email: [debbie.haught@hq.doe.gov](mailto:debbie.haught@hq.doe.gov)

---

#### Objective

This activity will investigate a commercially available rotary heat exchanger presently used in an absorption air conditioner. Performance of the heat exchanger will be measured by determining the heat transfer characteristics such as pressure drop and capacity and evaluating the suitability for other thermally activated applications. The biggest challenge will be to measure temperature gradients throughout the heat exchanger.

#### Highlights

Evaluation of the hot water-fired Rotartica lithium bromide/water air-cooled absorption unit (1.3-ton or 4.5 kW chiller) with rotating heat exchanger at the TAHP Environmental Chambers at various ambient conditions. The plans are to first document the performance improvement for rotating heat (and heat/mass) exchangers based on the Rotartica unit and then assess the technical potential for using rotating heat exchangers in other applications. Significance of ORNL work: (1) private industry partner did not have access to a suitable psychrometric chamber for the evaluation of performance and emissions of these units over a wide range of outdoor and indoor conditions (with temperature and humidity control) and (2) independent evaluation of these units with their respective indoor units to verify the ease of installation, reliability and durability of these units and their sub-components.

#### Technical Progress

The hot water-fired Rotartica lithium bromide/water air-cooled absorption unit) is an innovative absorption technology based on integrated rotating heat exchangers to enhance heat and mass transfer resulting in a potential reduction of size, cost, and weight of the “next generation” absorption units. Rotartica Absorption Chiller (RAC) unit is powered by hot water generated using the solar energy and/or waste heat from power generation equipment (for example from a reciprocating engine). Typically LiBr/water absorption chillers are water-cooled units which use a cooling tower to reject heat. Cooling towers require a large amount of space, increase start-up and maintenance costs. However, RAC is an air-cooled absorption chiller (no cooling tower). The purpose of this evaluation is to verify RAC performance by comparing the COP and the

cooling capacity results with those of the manufacturer.

The performance of the RAC was tested at Oak Ridge National Laboratory (ORNL) in a controlled environment at various hot and chilled water flow rates, air handler flow rates, and ambient temperatures (Figures 6-7). Evaluations were initially conducted at nominal flow rates of chilled and hot water (2,375 lb/h or 18 kg/min and 4,250 lb/h or 32 kg/min respectively); the hot water temperature was kept constant at 194°F (90°C). The chilled water temperature was varied by changing the air flow rate through AHU and the cooling water temperature was controlled by changing the air temperature inside the environmental chamber where the Rotartica unit is located. Automated Logic Control and Web Control have been used successfully for sharing performance evaluations with the manufacturer.

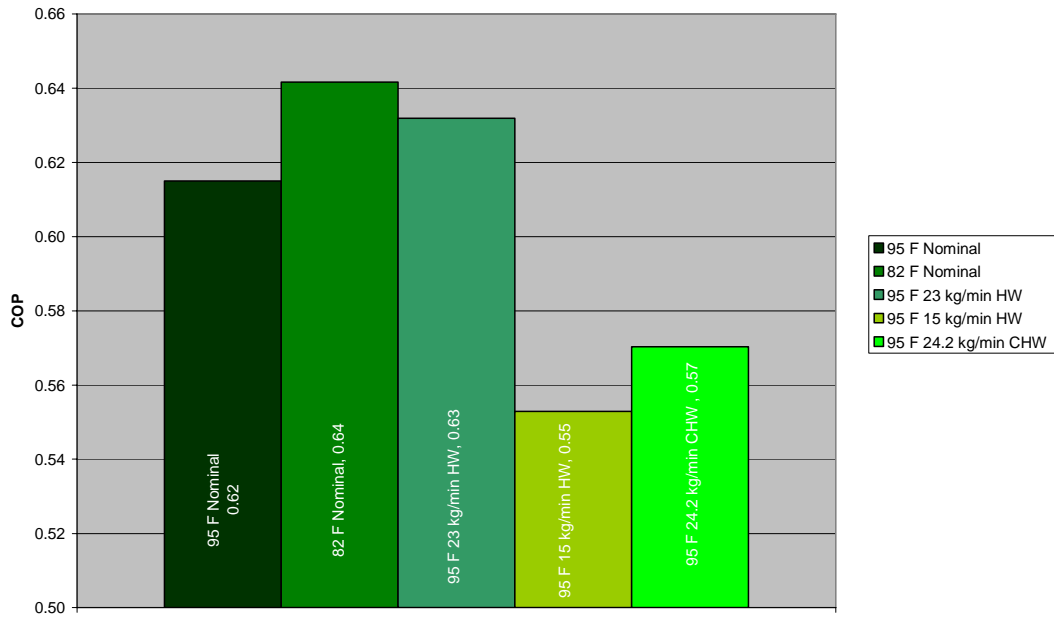


**Figure 6.** COP of Rotartica unit at various ambient temperatures, hot water and chilled water flow rates and air handler air flow rate of ~2200 scfm

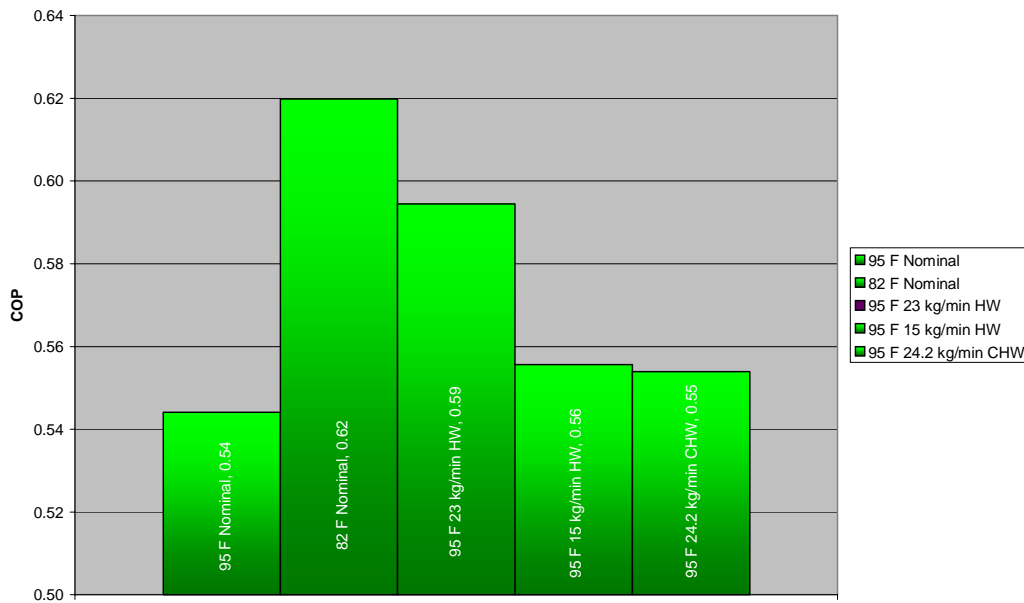


**Figure 7.** COP of Rotartica unit at various ambient temperatures, hot water and chilled water flow rates and air handler air flow rate of ~650 scfm

### Conclusions and Recommendations

Generally, these units operated well over a wide range of ambient conditions. This study resulted in

a complete performance map of the RAC, although additional tests should be run to test extremes and discover the limits of the RAC.



Evaluation showed that the experimental values were in good agreement with the manufacturer's values for the RAC. Additional testing as well as comparison to other absorption chillers without a rotating heat exchanger will show the added performance in the heat exchanger itself as well as the feasibility of future use of a rotating heat exchanger in other applications. Additional variables such as higher and lower ambient temperatures, hot water temperatures, flow rates, and variable RAC drum rotational speeds can be tested to discover limits of the RAC.

**Status of Milestone(s)**

Performance tests for the Rotartica unit were completed as scheduled.

**Industry Interactions**

Rotartica

**References**

4. ANSI/ASHRAE Standard 40-2002, "Methods of Testing for Rating Heat-Operated Unitary Air-Conditioning and Heat Pump Equipment", 2002.
5. ANSI Z21.40.4a-1998 and CGA 2.94a-M98 Standard, "Performance Testing and Rating of Gas-Fired, Air-Conditioning and Heat Pump Appliances", 1998.
6. ANSI/ARI Standard 560, "Absorption Water Chilling and Water Heating Packages", 2000.



**CHP**



## 4.1. Integrated Energy Systems (aka Cooling, Heating, And Power or CHP Systems)

*R. C. DeVault, P. W. Garland*

*Engineering Science and Technology Division*

*Oak Ridge National Laboratory, Oak Ridge, Tennessee*

*Phone: (865) 574-2020, E-mail: [devaultrc@ornl.gov](mailto:devaultrc@ornl.gov) or [garlandpw@ornl.gov](mailto:garlandpw@ornl.gov)*

---

### **Objective**

The objective of the proposed work is to develop and deploy highly efficient IES and include these as an essential element within the scope of the OE DE program. IES focuses on technologies that have broad utilization potential such as cooling, dehumidification, humidification, water heating, steam heating, drying, and shaft power from heat energy. Key program elements are packaged/modular IES development, DG thermal recovery research, IES field evaluations and end-use integration, and analytical tools/validation.

### **Approach**

ORNL issued a solicitation in FY 2001 for research development, integration, and testing of “first generation” packaged/modular IES-CHP systems for buildings. Availability of such systems will reduce the installed cost of DE/IES systems and improve overall system efficiency compared with current field-engineered IES installations. Awards were made in late FY 2001 and seven multi-year projects were initiated on a variety of DG/IES technologies, ranging from 30 kW microturbine-based packages to large megawatt (MW)-scale central plant modular systems. The NiSource, Capstone and Ingersoll-Rand projects were completed in FY05. The GTI and Honeywell projects were completed in FY06. The Burns & McDonnell project will continue into FY07 with FY06 money. The UTRC project will continue into FY07.

ORNL provides in-house research in support of the industrial subcontracts. ORNL also develops and maintains screening tools, provides analytical support, and provides technical guidance to our industrial partners. Subtask progress is noted below.

### **Accomplishments:**

- The final reports for the following projects were delivered to ORNL:
  - Testing and analysis of the Honeywell Integrated Energy System at Fort Bragg
  - GTI Integrated Energy System project
  - Testing and analysis of the Burns & McDonnell IES System at the Domain Site
- Held a ribbon-cutting for the Dell Children’s Hospital Energy Plant. Complete Joule Milestone on schedule.
- Completed initial testing of the new low-flow conditioner was completed at the University of Maryland Integration Test Center.
- In-house testing was started on the Interotex rotating heating pump.
- Phase I of the Historical Reports Database was completed containing over 300 reports.
- CHP credit was successfully included in the LEED calculation for new construction

### **Future Direction:**

- Continue data analysis and testing of the IES System at Dell Children’s Hospital.
- Complete design and prototyping of UTRC engine-PureComfort System.
- Complete closeout of the University of Maryland Integration Test Center

- Continue populating the historical reports database
- Continue in-house equipment testing in the CHP Environmental Chambers

### **Subtask 4.1.1 – Packaged/Modular IES Development**

**The following projects were ongoing in FY06.**

- Burns and McDonnell in Kansas City, Missouri, partnered with Solar Turbines Inc. and Broad USA, to design and construct a IES system that provides electricity from a Taurus 5,200 kW turbine generator, up to 3,000 refrigeration tons (RT) of free waste heat driven absorption cooling and up to 17,000 RT of additional supplemental gas-fired cooling. Data acquisition and analysis of the Domain Site in Austin, Texas continues was initiated in 2004. The final report was delivered to ORNL in 2006. A second test site, Dell Children’s Hospital in California was designed in 2005. The system was installed in 2006. **Data acquisition and analysis will continue into 2007 under 2006 carryover funds.** (PIC #504) [Patti Garland]
- Gas Technology Institute (GTI) in Des Plaines (Chicago), Illinois, partnered with Waukesha and Trane, to combine Waukesha engine generators with Trane absorption chillers. Engine sizes range from 290 kW to 770 kW (matched to several absorption chillers) producing a modular range of sizes to match a variety of building types/markets. **This project was completed in 2006.** (PIC #506) [Tim Theiss]
- Honeywell Laboratories in Minneapolis, Minnesota, developed and field-tested a large (5.2 MW) IES packaged system. The turbine generator will be combined with a 2,000 RT absorption chiller and a prototype was set up and tested at Fort Bragg, North Carolina. Test and verification of the packaged system continued into 2006. The final report was delivered to ORNL in 2006. **This project was completed in 2006.** (PIC #507) [Patti Garland]
- UTRC in East Hartford, Connecticut provided an IES system based on off-the-shelf components to make a packaged system within the project's first year; an additional optimized IES system also will be developed.

Early in FY 2003 (November 2002), United Technologies Power formed a strategic alliance with Capstone. UTRC’s systems will be based on the use of Capstone’s 60kW in multiple-unit IES packages coupled to Carrier absorption chillers. In FY 2005, test and verification of the UTRC PureComfort 240 was started at an A&P Supermarket. Data collection and analysis continued into 2006. Additionally, in FY 2006, UTRC focused on CHP technologies for improved value PureComfort systems. **UTRC will be performing work in 2007. We are awaiting the task description.** (PIC #510) [Bob DeVault]

### **Highlights**

- **Gas Technology Institute (GTI) – this project was completed in 2006**

The Gas Technology Institute (GTI) recently submitted their final report on the Waukesha engine-based Integrated Energy Systems (IES) project. Other project partners include: Trane, Ballard, and University of Illinois-Chicago. The team developed, built and tested an advanced 600-kW IES package that has an efficiency of over 70%. The two-module system requires only seven connections in the field, lowering installation costs and reducing total installed cost (including the absorption chiller) from nearly \$2,500 to less than \$2,000 per kW – a 25% reduction. The system included a Waukesha 615 kW engine-generator, GE switchgear, a Trane absorption chiller, and Cain heat recovery equipment. Ballard Engineering developed the control system. The IES design provides controls to vary engine jacket water outlet temperature. This feature provides for a 40% increase in the production of chilled water when called for. The report included design details at the component and system level, laboratory test results, an economic assessment of different markets (locations) and applications. Lesson learned from the project and additional recommendations are also detailed.

## Highlights

- **Honeywell – this project was completed in 2006**

The final report, *Modular Integrated Energy Systems, June 2006*, was delivered to ORNL. The report contains the following sections:

- Introduction
- Technology Development
  - IES Reference Designs
  - Exhaust-Driven Absorption Cooling Technology
  - IES Control Optimization
- IES Technology Field Demonstration
  - System Description
  - Site Description
  - Overview of Results
- Performance Monitoring
  - Field Monitoring Overview
  - Summary Performance Results
- Conclusions
  - Development of Reference Designs
  - Development of Exhaust-Driven Absorption Cooling Technology
  - Development of On-line Control Optimization Technology
  - IES Plant Operations

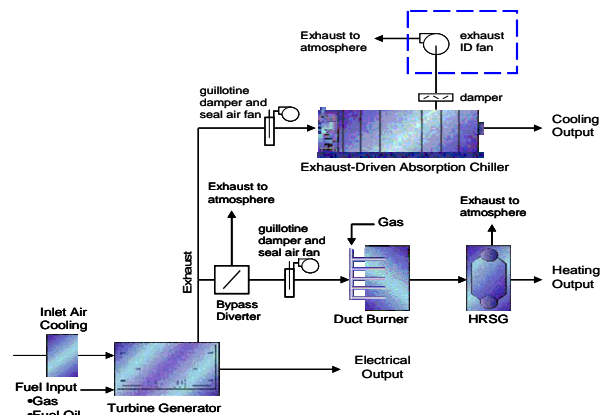
## IES System Measured Performance

System Performance: The Integrated Energy System operated throughout the year, providing electricity and heating (steam and hot water) to the buildings on the post. The absorption chiller (and other cooling equipment) provides seasonal cooling. Performance Data indicate that the Integrated Energy System fuel use efficiency is:

- >70% year-round
- Frequently >75% even in cooling-only operating mode

As an addendum to the final report, Honeywell provided a letter report discussing the investigation and resolution to a problem with the variable frequency drive (VFD) for the induced-draft (ID) fan that controls exhaust flow thru the CHP absorption chiller.

Background: The exhaust ID fan is shown in the CHP system figure below.



The VFD drive had failed due to what appeared to be overheating on two occasions in the past, and plant operators believed that a design problem existed. Simply replacing the VFD again was not the correct course of action. It was noted that the ID fan motor never operated at high load, with most periods of operation being at or below 50% of motor rating (so overloading of the motor was quickly ruled out as a cause of the problem).

The project team consulted with motor and drive experts to determine a potential cause for the problem. It was determined that the problem was that the motor and the VFD were not compatible. During construction of the CHP system, the motor and the VFD had been procured from two different suppliers. Due to an oversight, there was no requirement for the two vendors to coordinate on the equipment selection process. This resulted in the motor and VFD being incompatible with each other. A search of on-line databases showed that this type of compatibility issue had been fairly common during the 1990's. While this type of incompatibility is less common today, it can still be a problem. Apparently, most large AC induction motors are now generally designed to be suitable for "inverter duty". However, this is not always the case (as we learned here).

Problem Resolution: Following a number of discussions with motor and drive experts, the project team determined the proper solution was to replace both the motor and the VFD with units that are known to be compatible. The new VFD and



motor will be installed by the Honeywell Energy Services Team at Ft. Bragg, at no cost to the ORNL/DOE project. This work should be complete by mid-October. This new equipment will then be tested and placed into operation. If sufficient cooling demand exists at that point in the season, the plant operators will closely monitor the operation of the new equipment. Close monitoring will continue when the cooling season resumes in the spring of 2007.

*Key Deliverable II:*

The “Modular Integrated Energy systems, Task 5 Prototype Development Reference Design Document.” presents a set of Reference Designs for Modular Integrated Energy Systems (IES).

Development of standardized packaged IES modular systems will provide lower life-cycle costs, and will also speed the acceptance of this technology in the marketplace. Streamlining the upfront design process is needed to produce the greatest benefit from IES technology. The project team’s focus is on IES modular systems in the 1- to 5-MW size range, with 900 to 3000 tons of cooling. These systems are typically intended for central plant and district energy applications serving multiple buildings.

Because large IES systems’ (1 to 5MW in size) installation scenarios vary widely, packaging is dependent on modularity, namely, the ability to construct a system by choosing from a selection of compatible components with standardized interfaces. This is especially important for larger IES systems, where the physical size of the equipment prohibits the manufacture and shipment of the entire system in one enclosure. Designing these systems as a number of component modules with each corresponding to a piece of major equipment (i.e. gas turbine-generator, heat recovery steam generator, and absorption chiller or chiller-heater) simplify the design and installation process by reducing the amount of site-specific engineering and site preparation required. The benefits of applying a “reference” package design are:

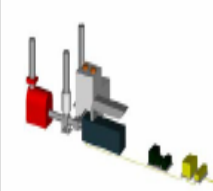
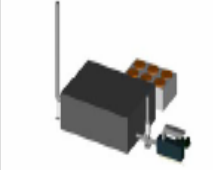
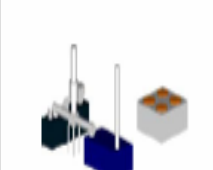
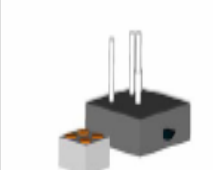
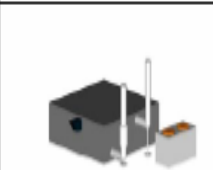
- The amount of custom design work for a given site application is greatly reduced. These modular Reference Designs provide

IES systems that are more cost-competitive through a reduction in installed cost and optimal matching of equipment to the energy loads.

- These improved economics can serve to validate applications that may have otherwise been difficult to justify (from a purely economic standpoint). For these applications, the other benefits provided by IES technology (e.g., reduced emissions, improved IAQ, and increased energy efficiency) are thus made available to the central plant/building owner and occupants.
- Readily available reference designs can serve to shorten the time required to perform the upfront analysis needed to quantify the economic and other benefits offered in each individual application. This will help speed the process of evaluating candidate IES applications.

The Reference Designs are built around a gas turbine as the prime mover, and an exhaust-driven absorption chiller (or chiller-heater). An overview of the designs is shown in the following table.

## Reference Design Overview

Title	Arrangement	Description
R-1		5.7-MW Turbine, 1,000-Ton Chiller, Outdoor Installation with HRSG and Inlet Air Cooler, New Chiller Building, Existing Plant Expansion
R-2		5.3-MW Turbine, 3,300-Ton Chiller-Heater, New Standalone Plant Building
R-4		4.6-MW Turbine, 1,300-Ton Chiller-Heater, Complete Outdoor Installation, Auxiliaries Installed in Existing Space
R-6		3.5-MW Turbine, 2,000-Ton Chiller-Heater, New Standalone Plant Building, Dual Chiller-Heaters
R-8		5.7-MW Turbine, 900-Ton Chiller-Heater, Existing Plant Expansion, All Contained in Existing Space

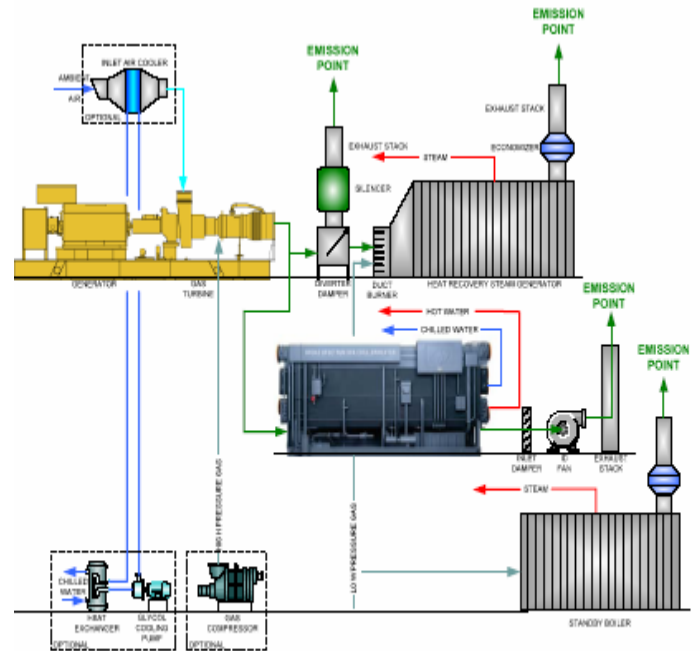


Figure 2-1. System Arrangement: Reference Design R-1

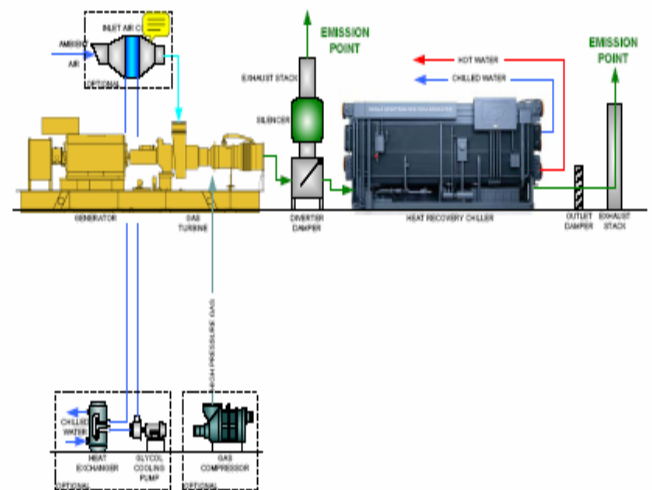


Figure 2-2. System Arrangement: Reference Design R-2, R-4, and R-8

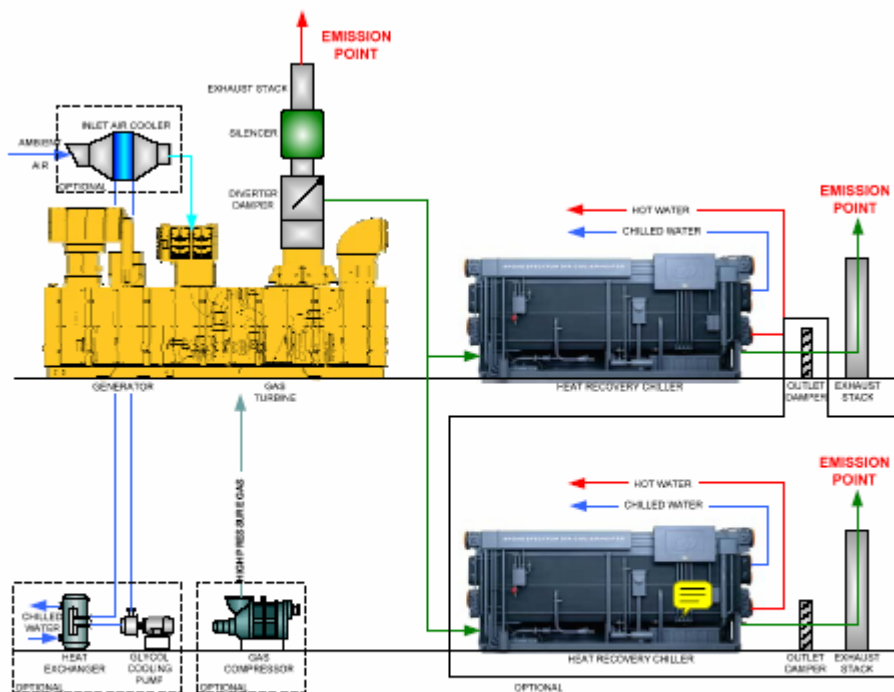


Figure 2-3. System Arrangement: Reference Design R-6

## Highlights

- **Burns & McDonnell – this project will continue into FY2007 under carryover funds** •

Burns & McDonnell General Progress:

- Tours of the Domain and the Dell sites were held on April 20, 2006, in conjunction with the Gulf Coast CHP Application Center, CHP Seminar, with over 40 participants.
- The following reports were submitted to ORNL: •

*CHP Modeling Report*, October 2006 - This report, the first in a series on modeling, deals with the original Burns & McDonnell CHP economic model and suggested improvements. The remaining modeling reports will address Dell specific economics and our evaluation of ORNL modeling tools.

*Draft Test Plan for the Dell Children's Medical Center CHP System*, October 2006.

*Data Mining Algorithms for Modeling Efficiency of a CHP System*, May 2006.

*Final Report of the Domain CHP Demonstration Project*, August 2006.

A Domain Turbine System Efficiency Optimization Tool in Excel Spreadsheet format and a User's Manual have been provided to ORNL.

A Dell IES project flyer has been prepared to be used at industry conferences, peer review meetings, website postings etc. This flyer will be updated periodically to include project progress and system performance information.

B&McD participated in a CHP panel at Electric Power 2006 (May 2 – 4, 2006) to present an overview of the Dell project design and anticipated performance.

## Domain Site System Performance

The official data collection period on the Domain site was from June 1, 2004 through October 31, 2005. Performance reports were reviewed by ORNL. The final report on the Domain CHP Project was submitted in June 2006, after much discussion and analysis by ORNL. The CHP system was primarily operated on an intermittent



basis during the work-week for an average of 8 hours per day. Austin Energy made a commercial decision to dispatch the plant in that manner when the site chilling loads were not growing as had been expected. Basically, they dispatch the plant when they can base load the absorption chiller and when it is most economical relative to their central generation. Over time as the site developer attracts more tenants resulting in additional chilled water load growth, they will likely be able to baseload the plant more often. [Austin Energy operated the system on a 24 hour period for short durations to support program testing objectives.]

a. The ambient temperature during the testing period varied from a low of 64°F during the heating season to a high of 98°F during the cooling season. b. Turbine inlet cooling was active throughout the test period, providing approximately 56°F inlet air to the combustion turbine. c. The combustion turbine was generally operated at full load providing an average electrical output of 4237 kW. d. [Part load testing was accomplished for brief periods to support testing objectives.] e. The average combustion turbine efficiency, operating at full load, was approximately 29%. f. The absorption chiller output varied from a low of 933 tons to a high of over 2600 tons and was highly dependent upon the Domain chilled water load. g. The CHP System gross efficiency varied from a low of 53% to a high of 91% and tracked closely with the absorption chiller output.

One performance problem worth noting is the apparent degradation of the absorption chiller during the intermittent operation. It was believed that the chiller performance was being influenced by the starting and stopping of the turbine each day. The engineering fix was to install an upgraded purge system on the chiller that would accommodate intermittent operating conditions. The work plan and drawings were completed in early-2006. Installation of the new purge system is being held up, pending contract negotiations between Austin Energy and Broad.

### *Dell Children's Hospital Site Progress*

The following Joule Milestone was completed on schedule:

Annual Metric: Develop one packaged CHP system which operates at 70+ % efficiency. ORNL's independent evaluation of the test data indicates an IES efficiency of 73% on HHV and 80% LHV. A Joule milestone completion report is forthcoming.

The following project design milestones are complete:

- Equipment Layout Development – Complete
- Major Mechanical Procurement Specifications – Complete
- Electrical and Miscellaneous Equipment Specifications – Complete
- Final Mechanical Shop Drawings – Complete
- Equipment Anchoring Design Package – Complete
- Mechanical Piping and HVAC Design Package – Complete
- Final Electrical Shop Drawings – Complete
- Final Controls Design Package – In progress
- As-built Design Package – In progress

### **Highlights**

#### **UTRC – this project will continue into FY2007**

In FY2006, UTC Power proudly introduced the PureComfort™ 330R cooling, heating and power solution; a reliable energy source with low emissions. This innovative system features a proven absorption chiller/heater that provides space cooling in the summer, space heating in the winter and continuous year-round thermal capacity, while a lean-burn reciprocating engine provides 334 kW of reliable power year-round. This results in a simultaneous heating and cooling system.

The thermal capacity can be used for domestic hot water, supplemental heating, reheat for HVAC systems and/or preheating for facilities systems. As a result, overall grid power consumption is significantly reduced throughout the year.

The PureComfort™ 330R solution includes a double-effect absorption chiller/heater from

Carrier Corporation. The chiller/heater is driven by the exhaust from the lean-burn engine. With the double-effect absorption chiller/heater, the PureComfort™ 330R solution can achieve an overall energy utilization of more than 80% which is far greater than the 33% typical of a central power plant.



The remote monitoring feature enables our service organization to monitor system performance round-the-clock, which means we can respond quickly if there's ever a need, minimizing downtime.

**Features**

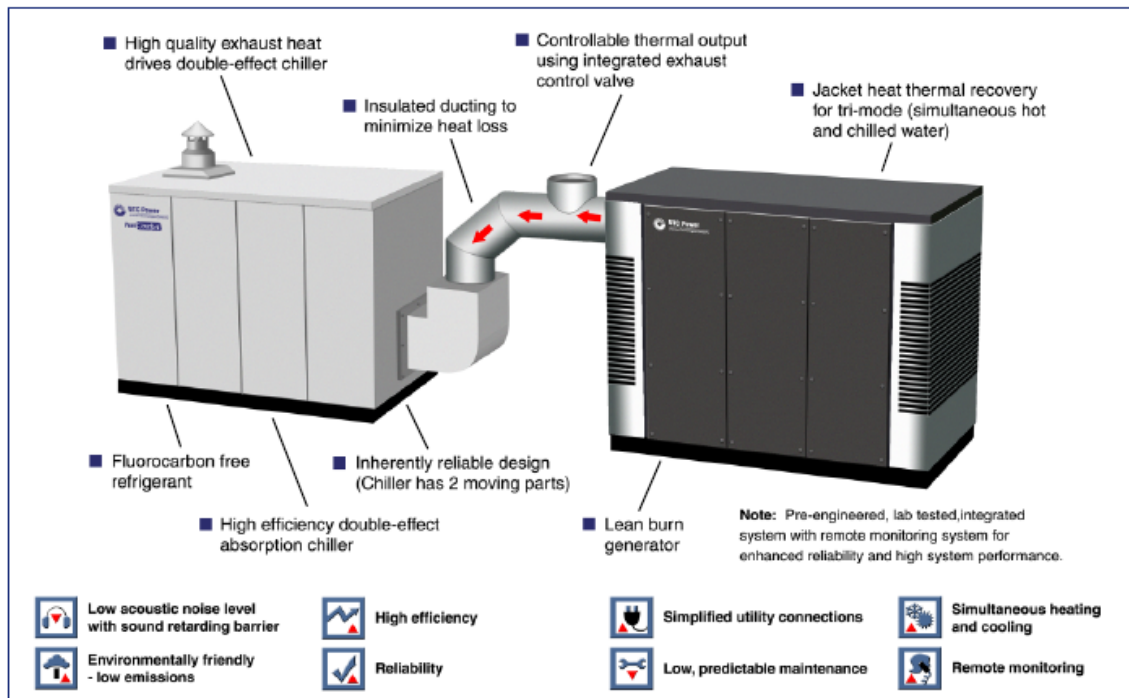
- High energy efficiency
- Low emissions
- Indoor/outdoor capable
- Scalable configuration
- Proven technology
- Operates both grid connect/independent

- High availability
- Continuous business operation

**Benefits**

- Lower electric bills
- Environmentally friendly
- Increased flexibility
- Maximizes energy savings

The PureComfort™ 330R CCHP has a lean-burn reciprocating engine prime mover. This system utilizes a 334 kWe reciprocating engine's exhaust to drive an absorption chiller. Additional thermal heat is available for simultaneous tri-generation capabilities. This system is available through out the U.S. but doesn't meet California CARB 2007 emissions levels.



### *System Performance*

As a summary, the recip engine/hybrid chiller system has demonstrated a cooling capacity of 115 RT at ARI rated conditions. Operation of the system in heating mode has demonstrated 450 kW capacity. Cooling water return temperatures have been varied from 61 °F to 105 °F. Chilled water return temperatures have been varied between 61 °F to 51 °F. Transient tests have been performed where the cooling water has been ramped from 85 °F to 68 °F in 23 minutes to determine if the chiller control system can maintain stable operation during this rapid thermal transient. Chiller operation has been verified from 25% to 100% of rated capacity.

The performance of the Cummins QSK19 engine has been verified at engine air inlet temperatures ranging from near 60 °F to 105 °F. The data collected has shown that engine outlet power and efficiency is not affected by the inlet air temperature in the range tested. In applications where the prime mover would be operating at high ambient temperatures, such as in tropical regions, the system performance would not be adversely affected.

### **Subtask 4.1.2c – DE Integration Lab Test and Evaluation- Abdi Zaltash**

Evaluation of the “next generation” 10-ton packaged heat pump unit (GEDAC unit) with R407C (interim alternate refrigerant) has been completed at various indoor and outdoor conditions in cooling and heating modes. These tests were conducted at ARI Standard 210/240 rating conditions. These include cooling tests up to 125°F and heating tests down to 17°F. The control scheme for heat recovery and defrost cycle during heating tests was also evaluated to achieve optimum performance. These tests have been reported to the manufacturer.

In addition, the installation of the hot water-fired Rotartica lithium bromide/water air-cooled absorption unit (1.3-ton or 4.5 kW chiller) with rotating heat exchanger was completed. Evaluations have been conducted at various ambient temperatures from 75 to 104°F. The measured COP is around 0.62 at 95°F ambient

temperature. Automated Logic Control and Web Control have been used successfully for sharing performance evaluations with the manufacturer. The plans are to document performance improvement for rotating heat (and heat/mass) exchangers based on the Rotartica unit and then assess the technical potential for using rotating heat exchangers in other applications. The web control could be accessed (external to ORNL) by the following instructions:

1. <https://buildingstech.ornl.gov>
2. Login page (USERNAME "ANONYMOUS" and PASSWORD "re5y4msh") then click "Login" [THIS IS NEW TO SATISFY COMPUTER SECURITY AT ORNL]
3. Move the mouse pointer to the left area of the screen - the Automated Logic navigation window will show up.
4. Click on the "+" sign located at the left of the ORNL block.
5. Click on the "+" sign located at the left of the 3144\_Annex block.
6. Click on the expression "Northwall\_Controller" and the front page Rotartica and ammonia/water chiller graphics will show up. From the graphics menu, select ROTARTICA. Here the table with current performance values is displayed.
7. If you want to see the logic diagram, click on "Logic".
8. If you want to see the trends for each particular parameter, click on red "T" associated with each parameter. Then click on "Trends". The trend graph will show up.
9. If you want to see the webcam image, click on black triangle located next to Graphics, and then click on the "webcam access" and type the user name "Guest" and password "vth9vo2u".
10. If you want to return back to Logic, click on "Logic", and to front page Rotartica - click on black triangle located next to Graphics, then click on "ROTARTICA". "F11" provides you with a full screen of data.

Please note that Webcam requires JAVA software (free copy) at the website:

[http://java.com/en/download/windows\\_xpi.jsp](http://java.com/en/download/windows_xpi.jsp)

Completed evaluations of the SEMCO unit in the CHP Integration Laboratory in which waste heat recovery from the exhaust of the microturbine-based CHP system was used for desiccant regeneration. Effective use of low grade waste heat generated is a key component for optimum utilization of fuel consumption and improved source efficiencies. This integrated system was then compared with the performance of the SEMCO unit when natural gas combustion was used as the thermal source for desiccant regeneration. Results of this study will be reported in a paper entitled “Comparative Performance Analysis of IADR Operating in Natural Gas-Fired and Waste-Heat CHP Modes,” which was submitted and accepted for publication in the proceedings of 2006 ASME IMECE conference (Paper #: IMECE2006-13201) to be held in Chicago, November 5-10, 2006.

#### **Subtask 4.1.2. DG Thermal Recovery and Integration Research/Collaboration with University of Maryland [Patti Garland]**

Work in FY2006 focused on testing of the low-flow conditioner within the liquid desiccant dehumidification unit on System 1 and commissioning of the new absorption chiller on System 2. Additionally, ORNL is working with the University of Maryland on a close-out plan for this project. Dennis Moran, the principle investigator at the University of Maryland, has left the university. His replacement, Dr. Joe Orlando started on July 1<sup>st</sup>. Two graduate students, Joy Bian and Sandeep Nayak, graduated in December 2005 with a Master of Science and PhD degrees in Mechanical Engineering respectively. Both went to work in industry. A new student, Shirley Luo, has been hired to continue tests. Shirley Luo attended the 1-week microturbine training class. ORNL assisted with development of the following 3 project-related presentations made at the DE Peer Review: Integrated Energy Systems/Cooling, Heating, and Power Systems for Buildings – Dennis Moran, University of Maryland; Neural Net Optimizing – Darrell Massie, US Army; Commercial Liquid Desiccant Technology – Andy Lowenstein, AIL Research.

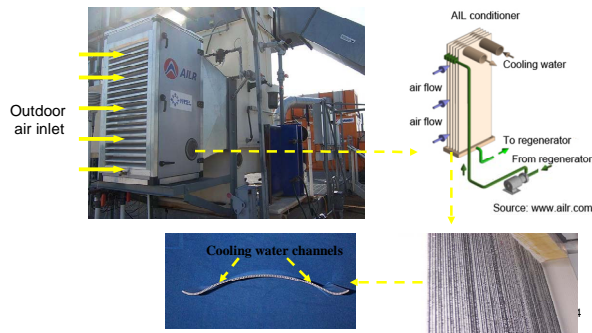
#### *System 1 Performance*

CHP System 1 – The Kathabar liquid desiccant cooling tower was drained for the winter months. Modifications to the system to include the low-flow absorber were completed. This work provided ORNL the opportunity to work in partnership with NREL, who co-developed the low-flow absorber with AIL Research.

DTE Technologies, the manufacturer of the system generator, announced they are terminating operations and selling off assets. They do not want the generator on-site returned, as it is a beta-unit, however they will no longer maintain the unit. The overheating problem of the DTE engine was solved by replacing a defective radiator cap. It also solved the overflow problem, which happened when the flow to the liquid desiccant system was closed off and glycol solution went to the dump radiator directly. The spark plugs and air filter were replaced on the engine. Even with the listed maintenance, the periodic engine periodic shutdown problems were not solved completely.

The Kathabar system commissioning was completed in early June. A desiccant foaming problem happened both for AIL conditioner and Kathabar conditioner. When it occurred, there was desiccant overflow and carry over from the AIL conditioner. Also the PH value for desiccant is much lower than natural. The desiccant filter with active carbon filters were changed twice to purify the desiccant solution. An active carbon filter bag was also installed inside the Kathabar conditioner. Anti foaming solution was added to the desiccant solution. The foaming phenomena is less, but still cannot be ignored. There are also some black ‘hairlines’ produced inside AIL conditioner when flushing it with high desiccant flow. [As the LiCl solution emerges from the air processor, it contains some kind of black ‘paint’ that looks like streamlines that are marked or visualized in black ink. A sample of desiccant and black hairlines were taken for testing by AIL Research.

• Introduction



g/kg to 13.1 g/kg. Outdoor air temperature is changing from 66.2°F to 82.5°F. For 75kW engine load test days, humidity ratio for outdoor air is changing from 12.9 g/kg to 18.5 g/kg. Outdoor air temperature is changing from 88.2°F to 92.9°F.

Generally speaking, under similar outdoor air conditions, the prototype AIL conditioner has comparable performance with the original Kathabar conditioner. The outdoor air humidity ratio has considerable effect on AIL conditioner performance. With 75kW engine load, when humidity ratio increases 25%, dehumidification level increases 30% and total cooling capacity increases by 12%. The effect of outdoor air temperature also could not be ignored. With a 50kW engine load, when humidity ratio decreases 4% and temperature increases 7.6 °F, dehumidification level increases 12% and total cooling capacity increases 40%.

The following are test results for system 1:

Fig.1 and Fig. 3 depict the dehumidification performance of AIL conditioner under different outdoor conditions with 50kW and 75kW engine load. Fig.2 and Fig.4 depicts the total cooling capacity of AIL conditioner under different outdoor conditions with 50kW and 75kW engine load. For 50 kW engine load test days, the humidity ratio for outdoor air is changing from 9.2

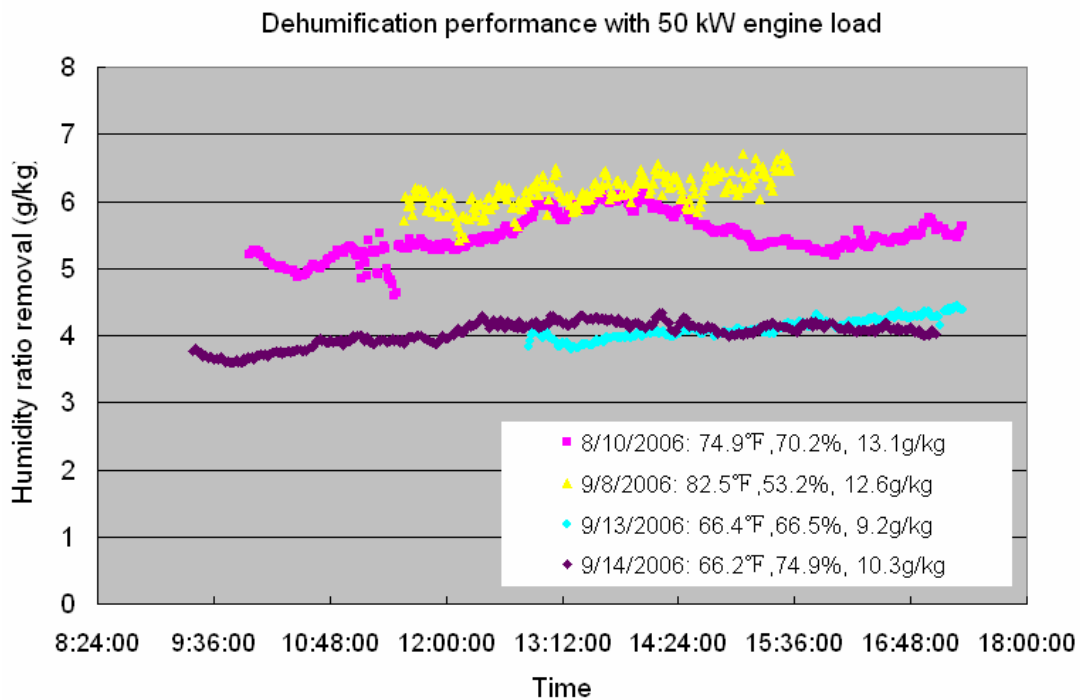


**Figure 1.** AIL conditioner performance with 50kW engine load

AIL conditioner total cooling capacity with 50 kW engine load

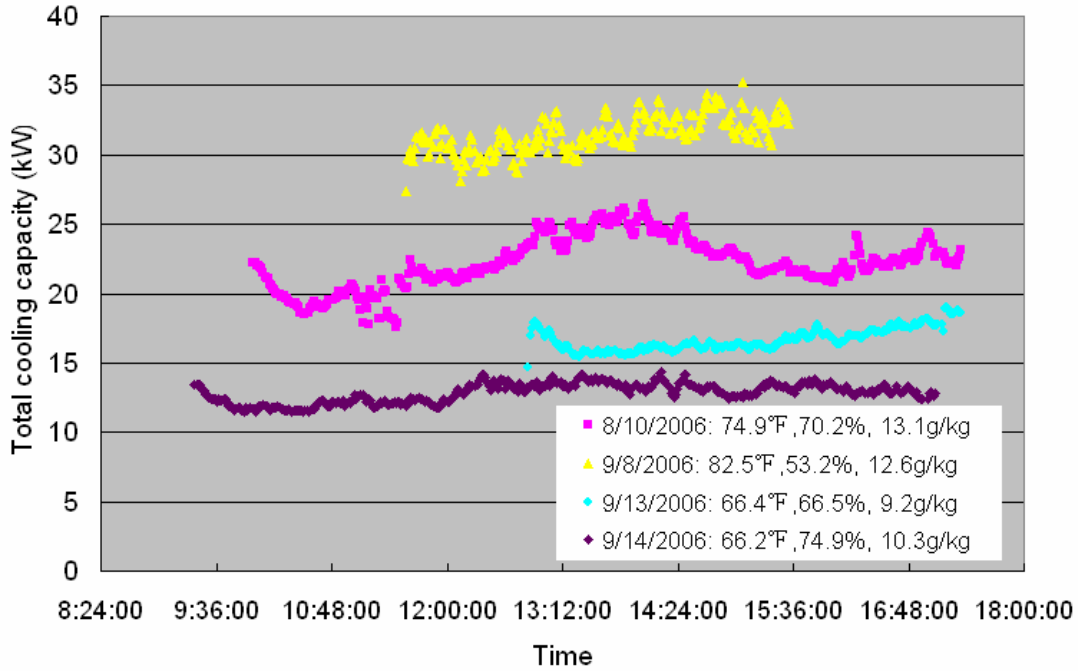


Figure 2. AIL conditioner total cooling capacity with 50kW engine load  
AIL conditioner dehumidification performance with 75 kW engine load

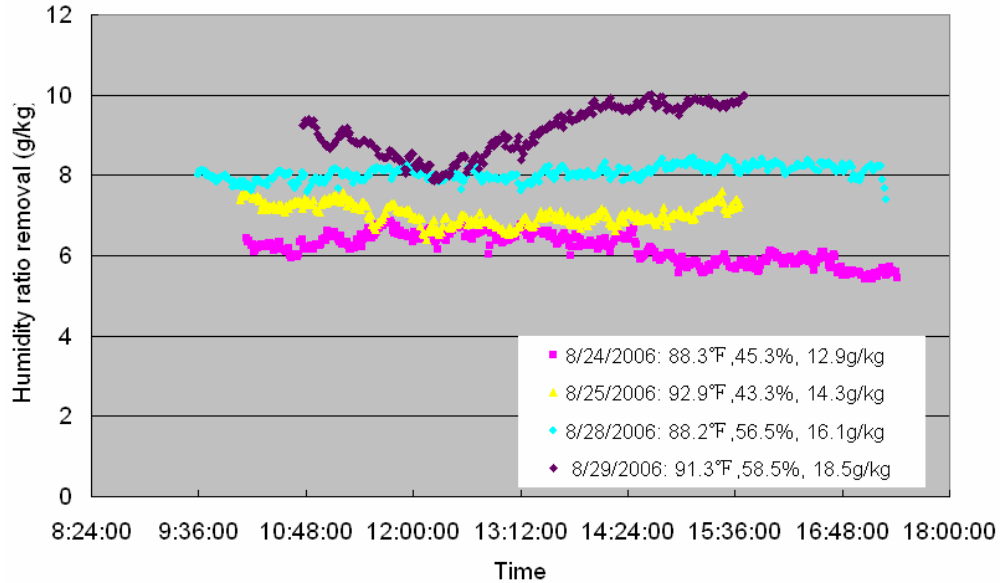
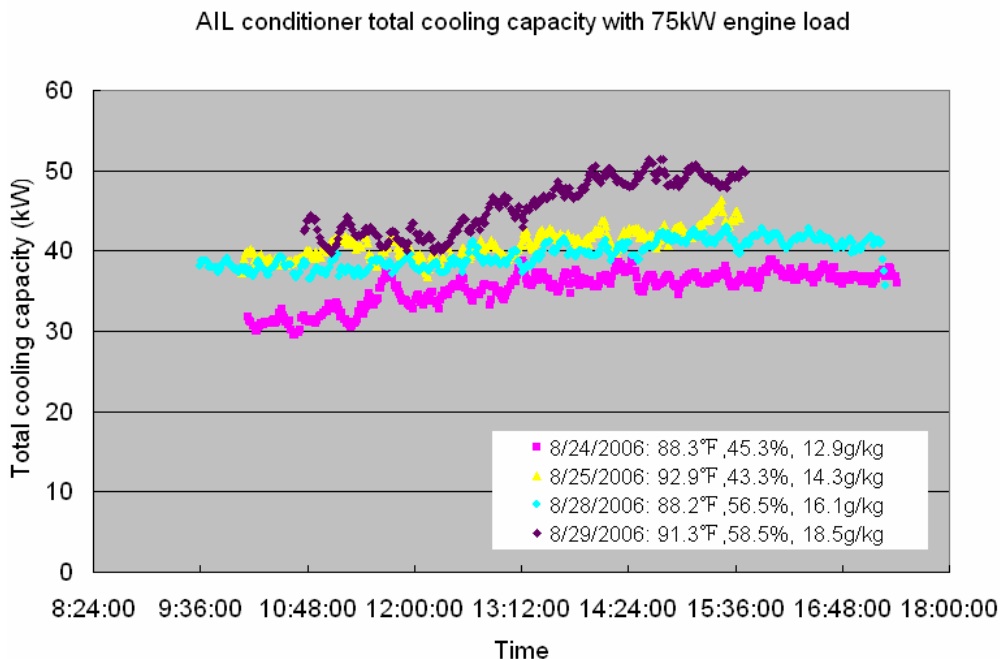


Figure 3. AIL conditioner performance with 75kW engine load



**Figure 4.** AIL conditioner total cooling capacity with 75kW engine load

#### System 2 Performance

The chilled water system was drained for the winter in October. The microturbine was operated at power levels ranging from 50 – 60 kW intermittently in January and February to collect data for investigating system performance to determine if core replacement in 2005 had affected operating characteristics. The work focused collecting data to characterize performance over a range of operating conditions. An overheating problem of the microturbine occurred in May. A replacement fan inverter board and LCM fan were ordered from Capstone and installed. The problem was partly resolved. Although the microturbine was operational, the temperature for the ECM board was still higher than LCM board on hot days. Capstone specifies the temperature difference between these two boards to be less than 10°F. Capstone updated the control software, and U of M purchased new control boards and new fans to control the boards.

There has been much difficulty in commissioning the Broad chiller for the summer. An “A/C WATER OFF” fault was on frequently. Subsequently, the chilled water pump would run for only 10 seconds before the fault automatically

shut it down. The cause of the fault was a bad flow sensor, which was replaced. Subsequently, the damper valve between the microturbine and Broad chiller did not respond to the chiller’s control and opened when the chiller was not running on August 8. The hot waste gas coming from the microturbine passed through chiller’s generator, however there was no water circulating there. This caused the crystallization inside chiller generator. Broad engineers assisted with the problem. The leaking cooling water pipe was welded. Also the flexible pipe after the cooling water pump was tightened to avoid leakage. The cooling water loop leakage problem was solved. However, the chilled water flange they repaired in July completely popped out again because of the high pressure there. The control problem of the damper valve is being resolved. A new control board has been shipped from the Broad factory in China and will be installed before the next cooling season. In the mean time, a manual switch was installed to open the damper valve temporarily.



#### **Subtask 4.1.2e. Integrated Energy Systems Technology Update [Bob DeVault]**

The final report on the IEA Heat Pump Conference was revised to include information regarding the CHP session and lessons learned.

Several key first generation packaged systems of engines, CTs and microturbines and thermal devices have been installed and commissioned during 2005 and significant lessons learned have been recorded that will lead to more effective and cost competitive second generation solutions. For example, adaptation of thermal components to recycle wasted energy to cool, heat, and dehumidify is achieving first order success. Projects like A&P Mt. Kisco is showing the need to better match the thermal cooling load to increase the chiller utilization. A similar situation is emerging at the Ritz Carlton (to a lesser extent).

Austin Energy's district cooling facility has seen the need to cycle their 2,500 RT absorber due to slower than projected load growth. This latter site caused operating problems with the chiller as it was not designed to cycle and thus could not initially remove internally generated non-condensable. Getting to the right amount of packaging from a single lift module to an erector set have been employed with varying success. These lessons have been documented and presented to the industry in several venues. Finally, during the rising cost of natural gas in 2005, it became clear that a near term strategy for CHP is two fold: 1) migrate to opportunity fuels, 2) work where electric constraints are severe (New York, parts of New England and California, of 3) replace low efficient boilers with CHP where you are displacing natural gas in the boiler and displacing "gas on the margin" electricity as a byproduct of boiler heating.

These lessons have been documented and presented to the industry in several venues. Finally, during the rising cost of natural gas in 2005, it became clear that a near term strategy for CHP is two fold: 1) migrate to opportunity fuels, 2) work where electric constraints are severe (New York, parts of New England and California, of 3) replace low efficient boilers with CHP where you are displacing natural gas in the boiler and displacing "gas on the margin" electricity as a byproduct of boiler heating.

#### **Subtask 4.1.3. CHP Economics/Modeling [S. K. Fischer]**

ORNL worked with staff at the Gulf States Regional Application Center and the ORNL FEMP program to resolve problems with the BCHP Screening Tool and with the RateScriptEditor used to compute monthly energy costs in the BCHP Screening Tool calculations. Utility rate data files were produced for landfill gas for a proposed project selling heat and power

to the U.S. Army installation at Fort Campbell, Kentucky and for "simulated" energy costs in Hawaii (artificially priced natural gas was used as a surrogate for diesel fuel and propane). Technical problems concerning transfer of data between the BCHP Screening Tool and the RateScriptEditor were corrected. Problems persist with performing desiccant calculations using the BCHP Screening Tool. There have been serious difficulties in obtaining detailed energy results for desiccant operation from the DOE2 "kernel" of the BCHP Screening Tool and also deep-rooted problems (or even errors) in the desiccant implementation performed by the initial subcontract developer for the BCHP Screening Tool.

S. Fischer provided one-on-one training on use of the BCHP Screening Tool to staff at the Gulf States Regional Application Center in December. This interaction with end-users identified several program modifications that would aid individuals using the BCHP Screening Tool without requiring significant effort in modifying the source code. These included (1) incorporation of alternative equipment depreciation schedules (GARD had "hard-wired" factors for 7 year declining balance depreciation into the code), (2) user specification of escalation factors for energy and labor costs, and (3) cash flow calculations for the duration of a proposed project. Effort was also directed toward a significant update of program documentation to aid end users.

The University of Illinois at Chicago is utilizing the BCHP screening tool to support their final project as part of the Introduction to CHP Mechanical Engineering course. There are 4 groups of students working on 4 separate buildings and CHP applications. This is the first time the BCHP Screening Tool by the University. In the past, they used the Building Energy Analyzer developed by GTI.

#### **Subtask 4.1.11. Research Survey, History of DOE Programs [S. K. Fischer]**

Material was accumulated on approximately 500 publications from the EERE Program and the organizations that preceded it at the Department of Energy. Publications that were received in "hard copy" were categorized and filed; those that were



received in an electronic format were "processed" for later use. Publications were received on CD's in both "PDF" and "TIFF" formats; in every case the files were not sorted as to subject area and "cryptic" file names were employed (e.g. "ANASSE~1.PDF" "CALOR~1.TIF" "PRD1A2~1.PDF"). The PDF files were (1) copied, (2) renamed to reflect the sponsoring national laboratory and the publication name, and (3) a Microsoft Access database was created to keep track of all of the electronic files associated with putting the reports on-line (approximately three separate files will be required for each publication placed on-line). Subsequent effort was directed toward dividing the publications into meaningful categories and constructing the HTML instructions associated with the web-pages for each publication.

Web pages have been created for approximately 350 individual publications. These can be viewed at <http://www.ornl.gov/~fis/>. Report covers and publication cover pages were "cleaned up" to remove evidence of wear and tear from 20 to 30 years of use by covering over undesired creases, stamps, and handwritten notes with clean patches. Abstracts from the publications were copied into the HTML code to be displayed alongside the picture of the cover, and links were created to other useful pages. Additional publications available only in hard copy are being scanned and added to the on-line reports database as time allows. ORNL has been working to anticipate and sidestep any copyright issues that may arise in making PDF files available for papers published in technical journals and conference proceedings. Although this is a DOE DE-funded project, this work has been of interest to DOE BTP personnel. Project review meetings were held at DOE HQ in September for DE personnel and for BTP personnel.

Space was obtained for the historical "database" of publications on one of the public internet servers at ORNL and work was initiated on creating web pages for viewing or downloading PDF files for publications. Significant effort was directed toward creating an organization or "structure" for the database. There are three computer files associated with each of the reports in the database; one containing HTML instructions that tell

internet browsers (e.g. Internet Explorer, Netscape) how to display the web page, one containing a JPG image of the report cover, and a third with the PDF file itself.

A key-word index that can be used to search for specific terms or phrases has been developed. This is not the same as the website search feature that has been suggested, but it avoids problems associated with users having JavaScript enabled in their Internet Explorer or Netscape installation and also computer security problems with running JavaScript on some versions of Windows. The key word index is available from:

[\\www1\home\http\ornl\sci\engineering\\_science\\_technology\eere\\_research\\_reports\key\\_word\\_index.html](http://www1/home/http/ornl/sci/engineering_science_technology/eere_research_reports/key_word_index.html)

Each of the publication web pages contains one or more lines on the order of: "**Keywords:** absorption cycle, absorption modeling, falling film, ammonia/water" I wrote a program that reads all of the site web pages and creates an alphabetized list of the key words contained in these HTML instructions and the corresponding URL of the webpage. These are automatically assembled into the key word index whenever the code is executed.

Introductory paragraphs were written for most of the "organizational" pages, which SHOULD increase our site's visibility in Google style searches -- that's kind of a wait and see process and it may or may not be sufficient.

#### **Subtask 4.1.12. Ground-Coupled/Geothermal Absorption Systems Calculation [V. C. Mei]**

This activity is to evaluate the engineering and economic potential for ground-coupled absorption systems as an alternative to using cooling towers. Using existing ground-coupling engineering models (developed previously in DOE's electric ground-coupled heat pump program), ground-coupling potential will be evaluated for replacing cooling towers for absorption chiller applications (both stand-alone absorption chillers and absorption chillers incorporated in Integrated Energy Systems (cooling, heating and power).



A technical report, “Cost Comparison of Ground Coupled and Cooling Tower Absorption Systems,” was prepared for the DOE sponsor. In the report, the cost to own and operate a ground coil coupled and a cooling tower system were analyzed. The study reported that the initial ground coil is much higher than a cooling tower system with the same cooling tonnage. However, after adding the operating and maintenance costs, the life cycle costs for both systems are actually quite close.

The project has been completed. A letter report, “Cost Comparison of Ground Coupled and Cooling Tower Absorption Systems,” was sent to the DOE sponsor in January, 2006.

#### **Subtask 4.1.13. ORNL District System Evaluation [J. B. Berry]**

ORNL is upgrading the site infrastructure and adding capacity for the on-site chilled water system. ORNL management is interested in evaluating whether an advanced CHP packaged system could be installed to upgrade the chilled water system while also improving on-site energy security and will provide staff to provide information for this assessment. These extensive system modifications offer an opportunity to install advanced, energy efficient technology in an ORNL District CHP System.

A report entitled, “Combined Heat and Power at Oak Ridge National Laboratory” was completed. The executive summary follows: ORNL site infrastructure needs and facilities were matched with IES system designs to determine the best candidate for further evaluation. The IES reference design that was selected is the Solar Mercury 50 (4.6 MW) gas combustion turbine/generator integrated with Broad BE-400 (2600 ton) two-stage absorption chiller. Turbine exhaust would be used to produce 25 MMBtu/hr of chilled and hot water simultaneously. ORNL’s Central Chilled Water Plant would provide space for a stand-alone building to house the turbine, chillers, balance of plant equipment, and switchgear. The Mercury-based IES also offers ORNL research opportunities in advanced IES application, control, and power electronics.

Both quantitative economic factors and qualitative benefits were evaluated. The economic evaluation concluded that annual operating costs would break even if electricity energy prices nearly doubled to \$0.046/kWh while gas prices stayed constant at \$7.50/MMBtu. Therefore, a decision was made not to pursue system installation with current operating cost.

Reconsideration of an ORNL IES is recommended when the DOE-Oak Ridge-Tennessee Valley Authority (TVA) electric contract is renegotiated. Contract negotiations are scheduled for completion in early in FY06.

A report entitled, “CHP at ORNL” documented evaluation of a Mercury turbine installation at ORNL to meet electric and cooling loads. The economic evaluation concluded that annual operating costs would break even if electricity energy prices nearly doubled to \$0.046/kWh while gas prices stayed constant at \$7.50/MMBtu. A contract between DOE-Oak Ridge Operations (ORO) and Tennessee Valley Authority (TVA) has not been negotiated, but it is expected that this contract will not result in a large enough increase in electricity demand charges to justify an on-site CHP system.

## 4.2 Distributed Energy Systems Applications Integration

*C. Randy Hudson*

*Engineering Science and Technology Division*

*Oak Ridge National Laboratory*

*Oak Ridge, TN 37830-6070*

*(865) 574-0578 email: hudsoncrii@ornl.gov*

*DOE Technology Development Manager: Debbie Haught*

*(202) 586-2211 email: debbie.haught@ee.doe.gov*

---

### **Objective**

One of the missions of the Distributed Energy Program was to lead a national effort to integrate DE technologies at end-user sites and to document and disseminate the findings of those efforts. Strategies to accomplish that mission included:

- Investment in a diverse portfolio of RD&D projects across complementary technologies: prime movers, thermally activated technologies, and CHP systems,
- Performance of systems integration, implementation, and outreach activities aimed at addressing infrastructure, institutional, and regulatory needs, and
- The establishment of collaborative technology transfer partnerships, including cost-shared RD&D projects.

### **Approach**

Three cost-shared solicitations have been conducted in the industrial, high-tech, and institutional market sectors. In FY 2004, the institutional market sector solicitation was issued for cost-shared projects that would utilize integrated (packaged) distributed energy systems in the specific markets of healthcare, education, hospitality, and grocery/supermarkets. All accepted projects had to have a minimum vendor cost share of 50% and had to have the potential for further replication in the marketplace without federal assistance. Out of 46 vendor proposals, eight vendors were selected for award. Five projects from that solicitation are currently active.

### **Accomplishments**

Five projects started initial operations in FY 2006. One remaining project (RealEnergy) is on hold due to host site facility expansion design and construction.

### **Future Activities**

In FY 2007, remaining projects that are operational will collect operating experience data and prepare and disseminate final documentation on the overall project experience.

## Introduction

A large portion of the existing distributed generation and the potential for future distributed generation installations is found in the industrial and commercial sectors. As a result, the foci of this effort has been to identify and assess promising applications for integrated distributed energy (DE) systems and to conduct projects that validate and demonstrate the benefits of DE technologies in targeted sectors.

This activity is intended to encourage the expanded use of distributed energy technologies in applications where there is a suitable combination and coincidence of electrical and thermal demand. Demonstration projects, begun in FY04, are underway to encourage the utilization of integrated packaged systems in the healthcare, education, hotel, and grocery sectors. Descriptions of the active projects are provided below.

### *Eastern Maine Medical Center–Jan Berry/Randy Hudson*

ORNL integrated a team that includes Eastern Maine Medical Center (EMMC), in Bangor, Maine, Vanderweil Engineering, and Cianbro. The team designed and installed a Solar Turbines gas turbine to generate 4.4 MW of electricity, 24,000 lb/hour of steam, and drive a 500 ton absorption chiller for the hospital. The new CHP system will respond to the following concerns: high energy costs, fuel use diversity, the need for additional chilled water capacity, the need to deliver services under any climatic condition, utility reliability, diverse thermal heating load profile, and emissions compliance. It is estimated that the system will save the hospital approximately \$700,000/year in energy costs. The project completed construction and was undergoing initial start-up testing at the end of FY06.

### *Butler Hospital–Jan Berry/Randy Hudson*

Butler Hospital, a 380,000-ft<sup>2</sup> hospital complex located in Providence, Rhode Island, installed a United Technology Corporation (UTC) PureComfort System, which packages four Capstone microturbines to generate 240 kilowatts of electricity and 110 tons of chilled

water using a Carrier exhaust fired absorption chiller. Although hospitals have backup power generation for critical functions in case of blackouts, integrated systems, like the one at Butler, enable greater flexibility for system operators to provide a range of services in case of grid failure. Of particular interest is how Butler has replaced steam use with hot water using the same room-by-room terminal heaters/chillers. Butler now runs hot water through the units during the winter, and cold water through the same units in the summer. In addition, handling, storage and heating of No. 6 fuel oil is eliminated, both reducing cost and eliminating the need for an air emissions permit. The project demonstrates the cost and energy savings of this pre-engineered, packaged integrated energy system that can be easily replicated throughout the healthcare sector of the economy while acquiring data on system performance in this high-profile setting. Butler Hospital projects an annual savings of \$92,000 in utility costs from the IES installation.

The system started operation in December 2005. In the nine month period from December 2005 through August 2006, the system operated at an 87.3 percent capacity factor, generating nearly 1.4 million kWh of electricity.



UTC PureComfort System installation at Butler Hospital

### *Verizon–Randy Hudson*

The telecommunications industry requires reliable high-quality power and facility cooling for critical central office switch operations. To meet these needs, Verizon Communications, Inc., under a DOE/ORNL cost-shared competitive procurement, has installed the largest fuel-cell based CHP system

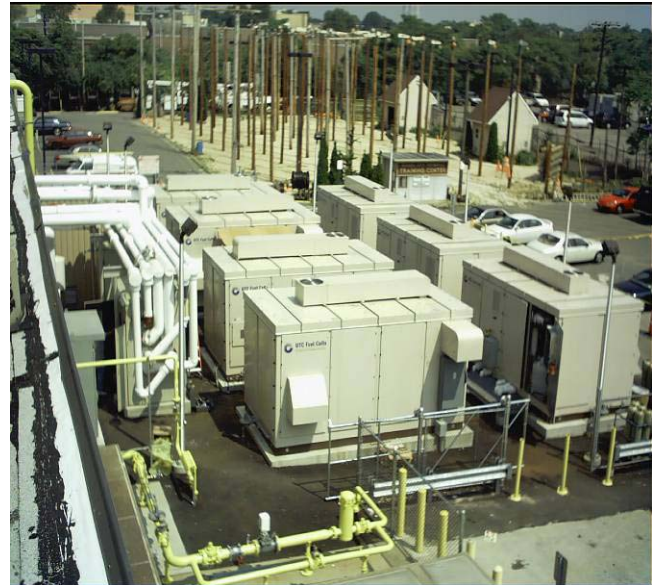
in the United States into a 300,000 sq. ft. Central Office on Long Island in New York. The CHP system is a topping cycle with base-load electrical power provided to the building by seven UTC PureCell 200 kW fuel cells and a dual-fuel (natural gas and diesel) engine. The fuel cell/engine combination generates up to 2.6 MW of electricity, providing essentially all the electrical needs of the large facility. Supplemental/backup power comes from the Long Island Power Authority (LIPA) grid and two standby diesel engines. Waste thermal energy from the fuel cells drives two 70-ton Thermax lithium bromide (LiBr) absorption chillers for cooling in the summer and an unfired heat recovery steam generator (HRSG) for space heating in the winter.

The fuel cells and the engine are typically paralleled to the grid, but can run in isolation should the grid become unavailable. The system became operational in June 2005. Annually, the facility is expected to produce approximately 11,100 MWh of electrical energy and 16,000 million BTU (MMBTU) of useful thermal energy. The fuel cell, engine, chiller and HRSG CHP system were designed to enhance the reliability of Verizon's telecommunications facility while providing an essentially free source of heating and cooling.

The system operated successfully during FY06 producing an annual cost savings of over \$650,000. A final report on the project will be completed in FY07.

*RealEnergy*—Randy Hudson

The project calls for installation of two 300 kW recip engine generators, a heat recovery unit, and absorption chiller at a community hospital in central California (Madera Community Hospital). Due to hospital facility expansion (independent of the CHP system), the CHP plant construction has been postponed for at least 12 months. It is not clear at this time when, or if, the project will be completed.



Fuel cells and absorption chillers outside Verizon central office facility

*Pepperell High School*—Jim Sand/Randy Hudson

The Pepperell High School CHP/active-desiccant field demonstration, field performance verification project in Lindale, Georgia is a unique integration of islanded IC engine power generation with thermally activated, desiccant, building ventilation and humidity control. Participants collaborating in the project are DOE, ORNL, SEMCO Corporation, Deutz Corporation, CM Engineering, and Floyd County Schools. The IES concept of this project is to use the electrical and thermal power provided by a 215 kW<sub>e</sub> Deutz, packaged, IC-engine cogeneration system to operate four SEMCO Revolution™ active-desiccant/vapor compression rooftops as grid independent, dedicated, outdoor air systems supplying up to 18,000 cfm of fresh ventilation air to this new 1500 student high school. The system installation and startup was completed in September 2006.

*Ritz Carlton Hotel*—Randy Hudson

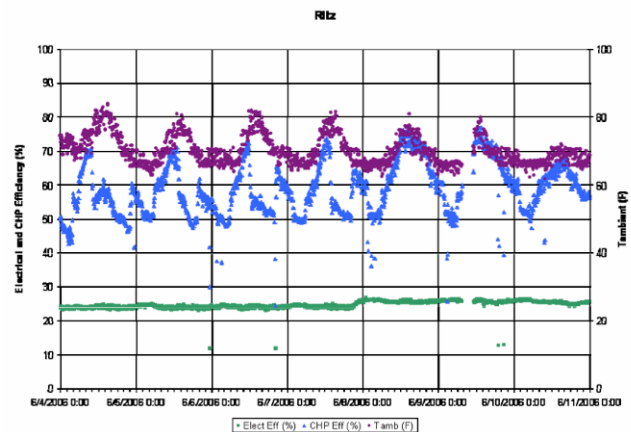
This project installed and is monitoring the performance of a United Technology Corporation (UTC) PureComfort System, which packages four Capstone microturbines to generate 240 kilowatts of electricity and 110 tons of chilled water using a Carrier exhaust fired absorption chiller, at the Ritz Carlton Hotel, San Francisco, CA. The results from this project will be used to provide the traditionally risk-adverse hotel building design community with

confidence that integrated CHP systems are technically and commercially viable alternatives to traditional power and HVAC products. In addition, the knowledge gained from this hotel installation will be directly invested in further integration of future PureComfort systems and will serve as a basis for the development of next generation integrated CHP systems. The system was commissioned in December 2005. Performance data has been informative and was used to diagnose a deteriorating natural gas compressor component.



UTC PureComfort System at the Ritz Carlton Hotel

The figure below shows the PureComfort™ system efficiencies for the first week of June; ambient temperature is also included. Generally, the electrical efficiency was nearly constant at about 25%, with wide variations in CHP efficiency because of the varying chilling demand by the hotel (which correlates with ambient temperature). Typically, the CHP efficiency varied between 50% and 70%; on two instances the efficiency approached 80%. For the month of June, the composite CHP efficiency was 60%.



Ritz Carlton CHP System Efficiency Week of June 4, 2006

*Utica College*—Theresa Stovall

This project was focused on an IES system at Utica College to provide CHP and to be used for the engineering curriculum. However, due to funding constraints, this project was cancelled. A set of design documents was prepared that may prove useful for future projects.

*Wingate Hotel*—Theresa Stovall

This project was intended to demonstrate a packaged, ultra-low emission state-of-the art integrated system, thus opening a channel for replication throughout the Wingate system as well as other hotel chains. However, due to funding constraints, this project was cancelled. A set of design documents was prepared that may prove useful for future projects.

*Basin Electric*—Theresa Stovall

The goal of this project is to verify the technical and economic feasibility of capturing thermal energy from a 30 MW gas turbine driving a natural gas pipeline compressor with an Organic Rankine Cycle (ORC) machine producing 4

MW of emission-free (no fuel and virtually no emissions) electricity in the summer and 6 MW in the winter. The site selected supports an electric coop that requires power and voltage support for the grid, which includes an Indian Nation with an important hospital load. This project integrates the ORC generator assembly into an ownership structure involving a partnership between the utility, Ormat, and the pipeline. The pipeline owner sells the resource (waste heat) to Ormat, which uses that resource to produce electricity and delivers the power to the utility. The utility then integrates that resource into the grid, firming the power supply and interconnecting the project to the consumers. The resulting overall system uses natural gas as a fuel to cogenerate mechanical power (for the compressor) and electrical power (for the grid) at a remote site. The installation was completed and operation started in the summer of

2006. Data collection and performance evaluation will continue into 2007.

*Industrial End-Use Activities with Project Partner Energy Solutions Center*

This project addresses CHP systems and how to integrate DG equipment within manufacturing processes with the greatest opportunity to use waste heat. This program focuses on innovative packaged CHP systems for specific applications that are highly replicable and can be integrated with industrial process energy needs. In FY2006, system operation and data collection continued at Higgins Brick [Chino Hills, California] and Arrow Linen [Brooklyn, New York]. Data collection and final reporting will be completed in FY2007, under carryover funding.

*Higgins Brick–Patti Garland*

The goal of this project is to verify the technical and economic feasibility of a combined heat and power system at a brick making facility. An innovative Combined Heat and Power (CHP) plant was installed at the site that uses three 80 kW Bowman microturbines to provide power and waste heat for preheating the combustion air of a large brick kiln. The twelve-month evaluation period was initiated effective May 1, 2005. A Connected Energy website allows the project team to remotely monitor and collect data on the operation of the CHP system.

During the months of October, the CHP system was not in operation. The owner has requested that the system be shut down during the current period of high natural gas prices. A meeting held November 3 at the Simmax offices in Santa Anna, California followed by a site visit to the Higgins plant in Chino Hills, CA to discuss the owners concerns.

The system was not operational in the months of November, December, 2005 and January, February 2006 for the winter break. The kiln is normally shut down in the winter months to avoid the high winter natural gas rates, allow any necessary repairs to the plant equipment, and to build up orders for the coming year.

During the winter shutdown, data from June, July, August, and September was analyzed. The data suggest the CHP system has a very positive impact on the efficiency of the kiln as currently configured. Projected costs for delivering electricity over the next year were an average of 7.5 cents/kWh. This is expected to be several cents below the summer rates by the local electric utility. The CHP power cost consists of 6 cents/kWh for the Simmax tolling charge and an additional 1.5cents/kWh for a fuel cost allowance. This calculated CHP power cost is based on \$7 million BTU gas and an allowance for kiln efficiency increases.

The brick kiln was returned to operation on March 17 after the winter break. During the initial heat-up period, one microturbine was operated to assist with the kiln heat up process. The microturbine was then shut down on March 31 due to uncertainty with the energy service contract between Simmax and Higgins.

During the month of April [while the system was shut down], equipment and instrument modifications were completed that will both improve the operation of the CHP system and provide more reliable data acquisition.

Operation of the microturbines was resumed on May 4 after a strategy meeting between Higgins and Simmax Energy that set the terms of the energy service contract for the year. In addition, given the power requirements at the plant, it was decided to operate two turbines, keeping one turbine as a back-up.

Except for some minor downtime the CHP systems performed very well for the month of May with an estimate of the effective cost of electricity at about 8.5 cents/kWh which is well below the grid charge of 11 cents/kwh.

Operation for the month of June and July was very intermittent. The turbines were tripping and it was thought that most of the incidents were due to power quality problems originating from the grid. SoCal Edison has promised to look into the problem.

Operation for the month of August mirrors July and once again was very intermittent. These outages are also causing damage to microturbine components primarily due to overheating. Therefore, most of the time, Simmax was struggling to keep just one turbine in operation.

Despite the significant period of downtime during the months of operation in 2006, the CHP system typically saved around \$3000 and achieved a system efficiency over 60%.

See Figure 1 for an example month of August, with a calculated savings of \$2,571 for the month. Had the plant been able to avoid the downtime, it is estimated that the plant could have saved \$6.011 in power charges for the month of August.

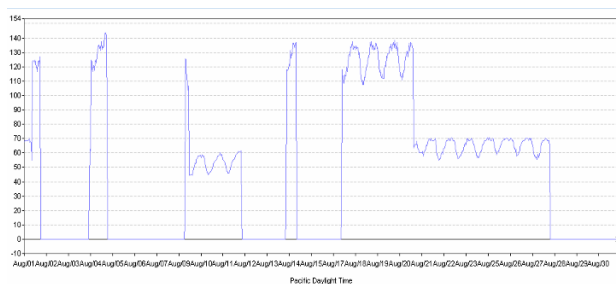


**Figure 1** – Higgins Brick’s Microturbine Power Generation for the Month of August

*Arrow Linen*–Patti Garland

The goal of this project is to evaluate a CHP system at Arrow Linen in Brooklyn, NY. The project, in coordination with KeySpan and NYSERDA will also evaluate the ASERTTI long term testing protocol. The CHP system is comprised of two 150 kW Coast Intelligen packaged systems using MAN engines. Two heat exchangers recover heat from both the jacket and the exhaust of the engines to provide process hot water for use in the laundry operation and to preheat boiler make-up water for production of 115 psig steam that is used throughout the plant.

Data acquisition was initiated at the Arrow Linen site in Brooklyn on October 1. Except for a short duration outage in October by one of the two Coast Intelligen engine-generator sets, the plant provided power and process heat to the laundry facility. Initial data analysis included some discrepancies in the data reported by the

Connected Energy data acquisition system and the operating log provided by the plant. These discrepancies were resolved.

During the remainder of the year, the two Coast Intelligen engine-generator sets using MAN engines continued to provide remarkably reliable power service and process heat to the laundry facility for the two shift, six days per week operation. The CHP System efficiency averaged above 60%, with energy savings of about \$4, month.

The plant did experience interruptions for a couple of days in July due to a brown-out on the grid for this section of Brooklyn.

For July the CHP efficiency averaged 62.2 %, somewhat lower than the value for June. This was primarily caused by the higher ambient temperatures during the month of July. Preliminary data analysis continues to indicate that Arrow Linen could avoid paying high electric demand charges, thus potentially saving well over \$4,000 in some months on their utility bills.

Figure 2 provides a snapshot of the daily and weekly typical power production of the CHP system during the month of August. The engines are automatically started up each day and ran six days a week providing most of the power consumed in the plant. Table 1 provides the CHP plant statistics for August. It can be seen that the CHP system efficiency averaged 66.5%, the favorable result driven mostly by the lower ambient temperatures experienced in August as compared to the month of July.

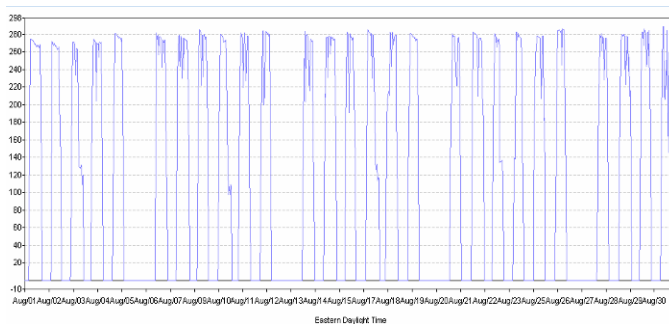


**Figure 2.** CHP Power Production during August 2006



**Table 1. August Operating Results**

Total Power Consumed on Site (kWh):	117,227
Gross Power Generated (kWh):	82,744
Estimate Parasitic Load (KWh):	6,074
<b>Net Power Generated (kWh):</b>	<b>76,670</b>
<b>Fuel Consumed (MBtu):</b>	<b>1,180,477</b>
Useful Thermal Energy (MBtu):	523,705
<b>Boiler Fuel Avoided (MBtu):</b>	<b>654,631</b>
System Efficiency:	<b>66.5%</b>

The following are the FY2007 deliverables.

1. Protocol Summary Report: Complete mid-November 2006

2. Draft -Arrow Linen Case History & Applications Manual Insert. Complete end of November 2006
3. Draft - Higgins Case History & Applications Manual Insert Complete end of December 2006
4. Issue Final Arrow Linen Case History Report. Complete end of January 2007
5. Issue Final Higgins Case History Report. Complete end of February 2007



## 4.3 – Cooling, Heating, and Power

*Patti Garland*

*Engineering, Science and Technology Division*

*Oak Ridge National Laboratory*

*(202)479-0292; email: garlandpw@ornl.gov*

*DOE Technology Development Manager: Merrill Smith*

*202-586-3646; email: merrill.smith@hq.doe.gov*

---

### Objective

The objective of this activity is to promote CHP installations into the public and private sectors by focusing on the issues of CHP awareness, regulatory and institutional barriers, and CHP economic feasibility. In regards to CHP awareness, there is a tremendous need to educate citizens, business executives, and public policy makers on the merits of clean, efficient energy generation using CHP. In regards to regulatory and institutional barriers, there are CHP systems that are commercially viable today but that developers have trouble getting installed because of roadblocks in siting, permitting, and interconnecting. This work complements ORNL Projects under Integrated Energy Systems and End-Use Systems Integration.

### Approach

ORNL issued a solicitation at the end of FY 2002 for CHP-related projects. The objective of the solicitation was to support activities that facilitate and encourage the use of CHP technology in the U.S. The statement of work for the solicitation was developed in response to the “Consensus Action Items from the CHP Roadmap Process” issued in June 2001, which supports the National Energy Plan. ORNL is synthesizing the data and tools developed under these contracts and is disseminating the information to the CHP application centers and stakeholders.

### Accomplishments:

- In the 4 year period of this effort, over 20 reports were issued. Other products include databases, tools, calculators, presentations, workshops, case studies, and briefings.
- Completed the 2006 CHP Action Agenda: Positioning CHP Value: Solutions for National, Regional and Local Energy Issues
- Presented the results of this program area at the December 2005 DE Peer Review Meeting. The results of the DE Peer Review indicate that this project presentation, entitled: *CHP Outreach, Education and Markets* scored highest of all 17 projects scored by the End-Use Integration Panel #1. The reviewers recommended increasing out-year funding to this project.
- Continued biannual face-to-face meetings and quarterly conference calls with the RACs.
- Developed a model to calculate CHP credit to support the US Green Building Council’s LEED certification process for new construction. The methodology ensures that appropriate credit is assigned for innovative on-site cooling, heating and power systems.
- Completed one-on-one training on the BChP screening tool with Rohini Brahme, a staff member at the Gulf Coast CHP RAC. Responded to questions regarding the BChP screening tool from the Midwest and Northeast RACs.

### **Future Direction:**

- ORNL will continue to provide technical support to the CHP Regional Application Centers through screening, analyses, modeling, and coordination of activities.
- ORNL will continue to provide technical support to HUD.
- ORNL will provide a consolidated list of all products developed under this program.

### **Introduction**

The National CHP Roadmap set the course for achieving 92 GW of CHP capacity in the U.S. This goal is expected to result in estimated energy savings of 2.4 quadrillion Btu per year and a reduction of 276 million tons of CO<sub>2</sub> per year compared to separate electricity and thermal energy generation. The National CHP Roadmap was the culmination of a wide array of industry-led activities including meetings, workshops, and public forums. The origin of these activities was a conference held in Alexandria, Virginia, on December 1, 1998, where the “CHP Challenge” was initiated by the DOE and the U.S. Environmental Protection Agency (EPA) with the goal of doubling the amount of CHP capacity in the U.S. from 46 GW to 92 GW by 2010. The purpose of the roadmapping effort was to organize all the ideas into a plan for action. Eighteen CHP workshops were held at locations across the country to convene stakeholders and discuss problems and solutions. These workshops involved almost 1000 individuals, representing equipment manufacturers, electric and gas utilities, architect and engineering firms, project developers, federal and state agencies, universities, national laboratories, and public interest groups.

The culminating event was the National CHP Roadmap Workshop held October 12-13, 2000, in Baltimore, Maryland. This workshop brought together representatives from the previous workshops to discuss progress made and to chart the next steps. As a result, the Roadmap consists of a series of specific actions for raising CHP awareness, eliminating regulatory and institutional barriers, and developing markets and

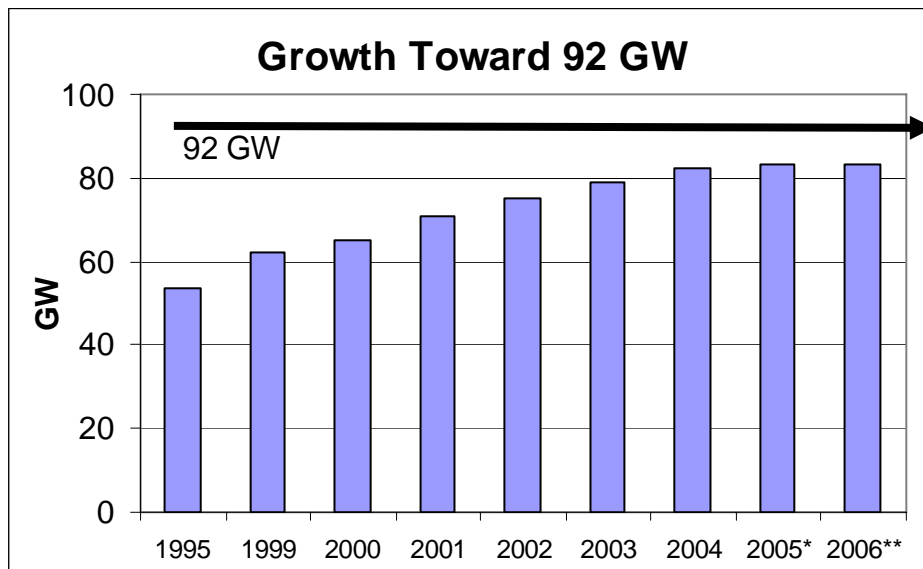
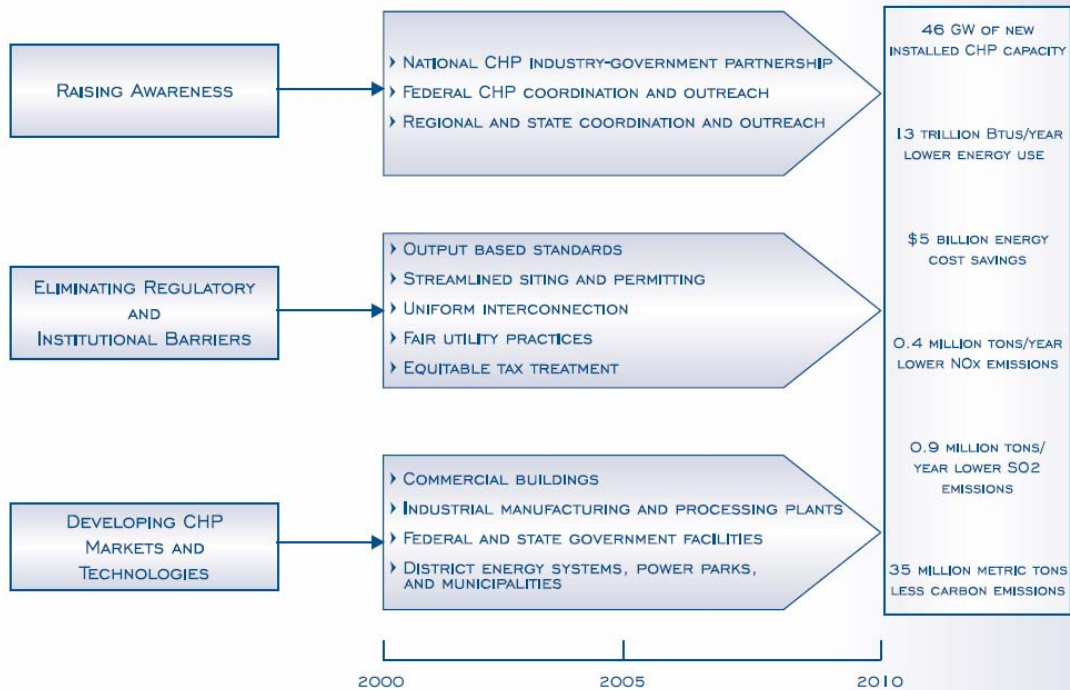
technologies, all aimed at achieving the CHP Challenge goal of doubling CHP by 2010.

ORNL, in support of the National CHP Roadmap is interested in substantial improvements in the number of applications of combined CHP systems. The vision of this project is to maximize the use of affordable combined heat and power systems powered by distributed energy resources in order to make the U.S. energy system cleaner, more efficient, and more reliable. The results, successes, and experiences from the tasks in this project will be posted to the DOE DE website and distributed to the Regional CHP Application Centers and industry partners through webcasts, conferences, workshops, training, teleconferences, and face-to-face meetings.

### **Accomplishments and Progress**

ORNL has been working with EEA in the development of a CHP Installation Database, which has been the primary source for tracking progress to the 92 GW goal. The database has 3,179 operating sites representing over 83.3 GW of capacity. Figure 4.3.1 highlights the growth of CHP in the U.S. from 1999 to 2005. Since the development of the Roadmap, the most significant growth period was in the 2000-2003 timeframe. The past two years have seen a relatively low growth rate in CHP capacity.

## National CHP Roadmap



Source: “*EEA CHP Installation Database Progress Report – July 2006*”, Energy and Environmental Analysis, Inc, preliminary report to Oak Ridge National Laboratory.

\* Updated 2005 data

\*\* Partial year 2006 data

**Figure 4.3.1: Progress to 92 GW of CHP Capacity**



Between 2000 and 2005<sup>1</sup>, 805 sites representing 22.6 GW were actually installed. During the same timeframe 203 sites representing 1.46 GW were retired, leaving a net addition to the database of 602 sites and 21.2 GW. Figures 4.3.2 and 4.3.3 illustrate growth in the 2000-2005 timeframe by commercial, industrial, and other applications by both site and capacity additions. The “other” applications pertain primarily to

agricultural and mining applications (non-manufacturing and non-commercial market sectors). Annual CHP site additions increased from 2001 to 2003 and then have decreased in 2004 and 2005. There has been a decrease in CHP capacity additions every year since 2001. While commercial applications make up the majority of new CHP sites, capacity (MW) additions are dominated by industrial applications.

---

<sup>1</sup> Only trends through 2005 are detailed; 2006 data is incomplete at this time. Partial 2006 data includes an incremental six sites and approximately 50 MW of capacity.

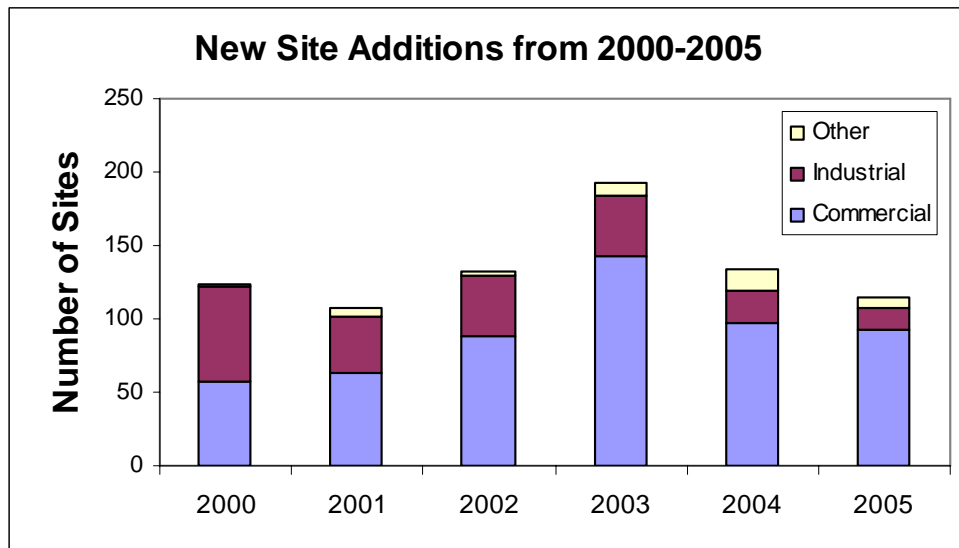


*Figure 4.3.2: New CHP Site Additions 2000-2005*

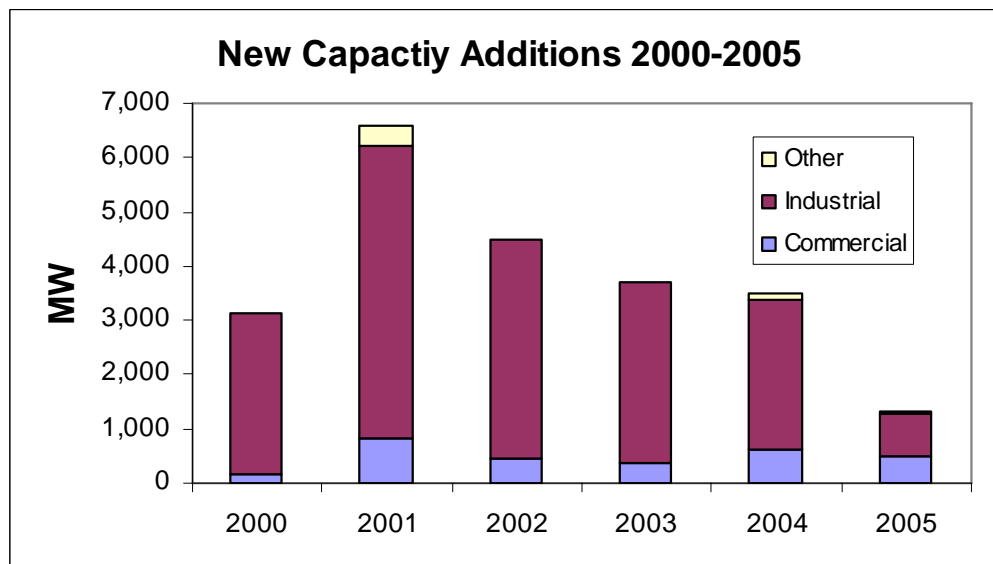


*Figure 4.3.3: New CHP Capacity Additions 2000-2005*

The majority of site additions in the 2000-2005 timeframe have been natural gas-fired reciprocating engines less than 1 MW. Figures 4.3.4 and 4.3.5 show the breakdown of new 2000-2005 CHP sites by prime mover,

fuel and size. The updated 2005 data contains an increase of 27 biomass sites and approximately 90 MW of increased biomass capacity.

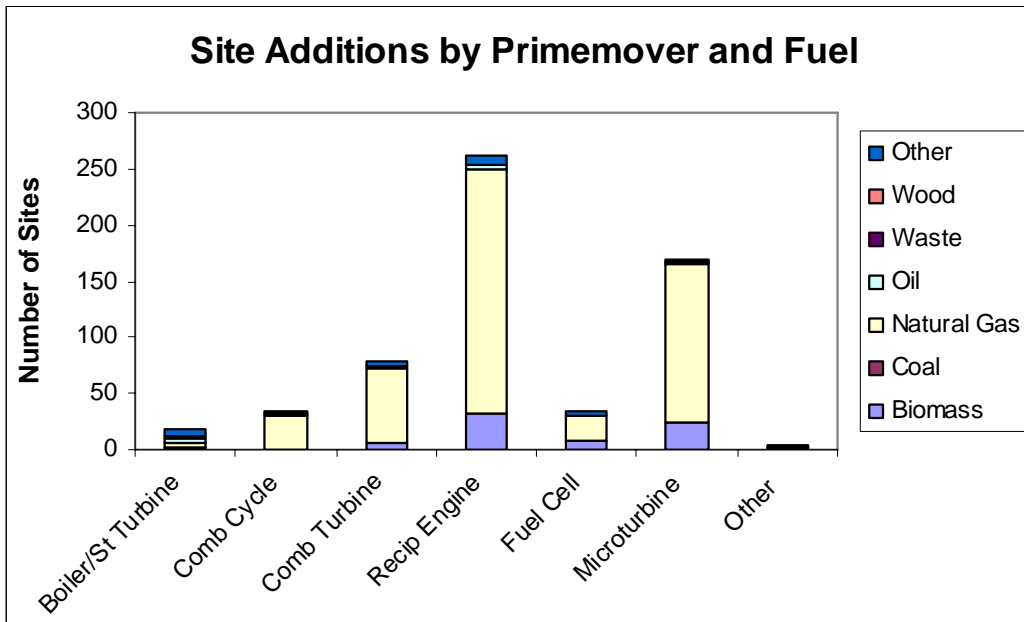


*Figure 4.3.4: New CHP Site Additions 2000-2005 by Prime Mover and Fuel*

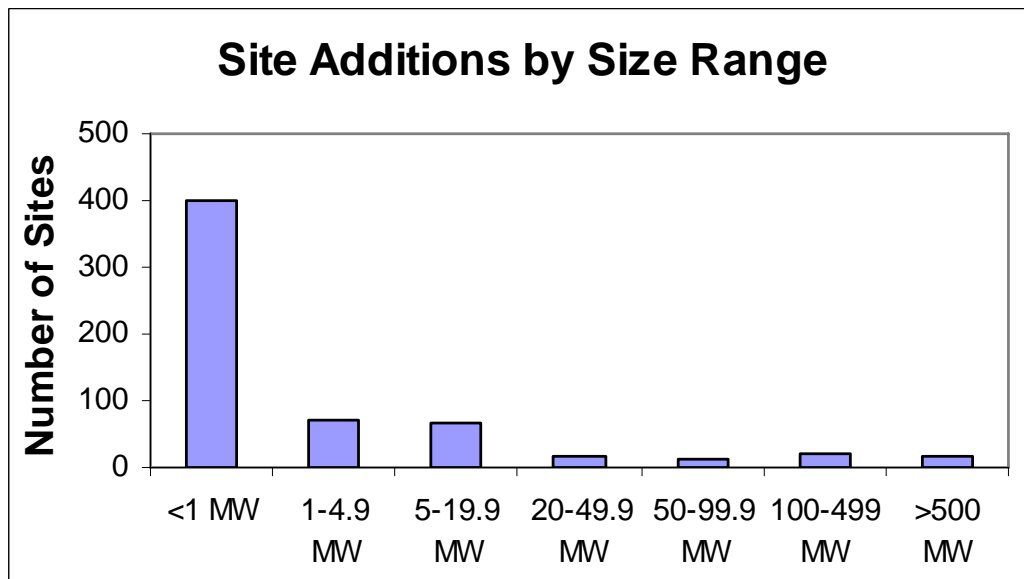


*Figure 4.3.5: New CHP Site Additions 2000-2005 by Size Range*

Figure 4.3.6 illustrates the breakdown on new site additions by market sector for both commercial and industrial applications.

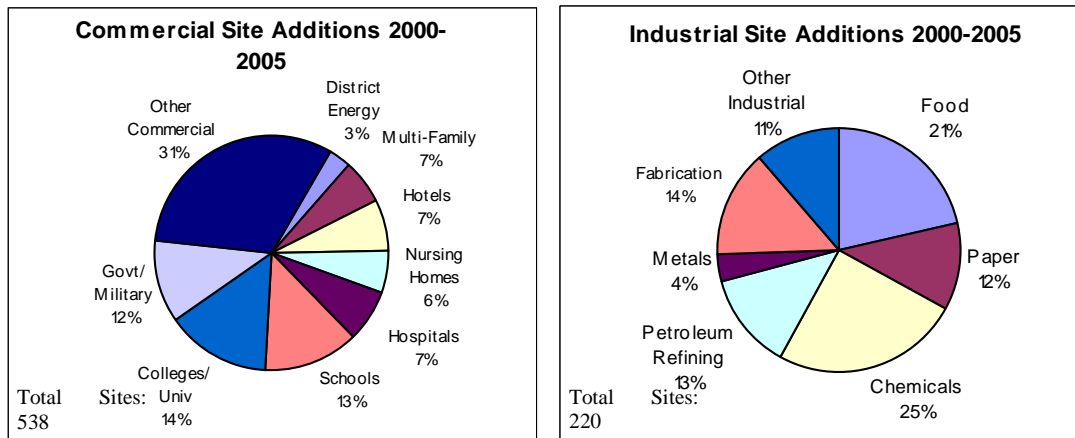


**Figure 4.3.6: New CHP Commercial and Industrial Site Additions 2000-2005 by Market Sector**

With regard to geographical trends in new CHP, growth tends to be concentrated in the Northeast, Midwest, Gulf Coast, and West Coast. Figure 4.3.7 illustrates states with growth in CHP. Favorable spark spreads and incentives for CHP have facilitated growth in California and New York. Pennsylvania has been added to states identified in last year’s report.

**FY2006 Progress Update on Subtasks**

4.3.1 Facilitate CHP working group; review environmental models and utility interconnection and tariff practices with project partner ACEEE. This projects tasks are: 1) identify individual interconnection and tariff practices on a state-by-state basis, 2) conduct a review of existing emissions models to produce some basic rules of thumb for regulators, policy makers, and CHP system developers to estimate the general local environmental impact of a CHP system, and 3) facilitate the CHP Analysis Working Group. The project tasks are complete. In 2006, ACEEE held two CHP Analysis Working Group meetings and issued the following reports:

- *Combined Heat and Power: Connecting the Gap between Markets and Utility Interconnection and Tariff Practices (Part I), and*
- *Combined Heat and Power: Connecting the Gap between Markets and Utility Interconnection and Tariff Practices (Part II).*

These reports describe: The adoption of combined heat and power (CHP) systems by American industries has made substantial strides in the last few years. Viewed on many levels, this progress is most certainly a win for all involved—the industry, the utilities, the consumer, and the environment. Many states have programs in place financially endorsing the adoption of CHP, easing the economic transition, and many utilities are now working with those states in that regard. Some utility companies have begun to optimistically acknowledge the market potential for CHP on their own. But to say that substantial strides have been made is not a convincing reason to ignore that much work is yet to be accomplished. The increased adoption of CHP nationwide still faces major hurdles: stiff barriers to entry from a sluggish utility core; technological, economic, and safety inhibitors; and an industry information gap in regard to varied state and utility policies. In order to expose and explore these issues more broadly, ACEEE embarked on an initial state review of utility company policies and practices focused on distributed energy resources (DER), and CHP more specifically. The results were both heartening and emblematic. The purpose of the reports are threefold: one, to expose still existent barriers to entry for proposed CHP facilities; secondarily, to highlight the need for a national interconnect standard; and lastly, to show the hierarchy that currently exists in regard to the progressivism of CHP policies nationwide on a state-by-state and regional basis. Although the main focus of Part II is on

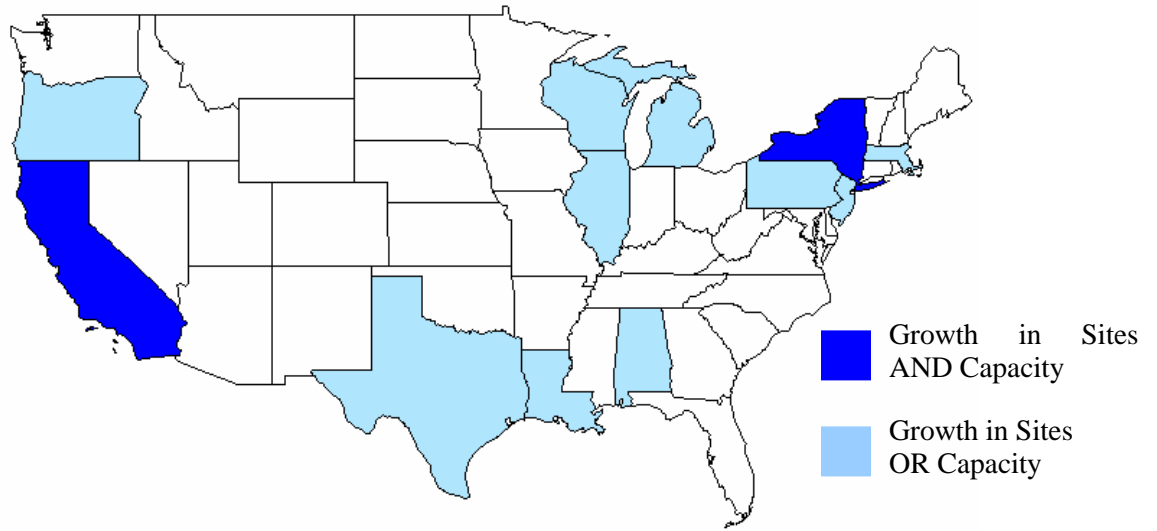


*Figure 4.3.7: 2000-2005 CHP Growth by State*

states not included in Part I, it is also meant to provide national and regional perspectives.

4.3.2 Prepare market segment reports, trade show booth materials, conduct workshops with project partner AGF. The project tasks are: 1) natural gas and energy price volatility study, and 2) market analysis of CHP potential in national account sectors. This project tasks are complete: 1) Prepared a 2-part report that presents a summary of an in-depth study of the issue of energy price volatility and the impact of volatility on consumers, industry participants, and the penetration of new technologies, and 2) in conjunction with AGF's National Accounts Energy Alliance, completed a report on market potential for advanced thermally activated BHP in Five National Accounts Sectors.

4.3.3 Prepare database of CHP installations with turbine inlet cooling and/or thermal energy storage with project partner Cool Solutions. This project is complete. A final summary report and database have been published and can be found on the DOE DE website. Many combined heat and power (CHP) systems can and do incorporate thermal energy storage (TES) and/or turbine inlet cooling (TIC) systems to improve the overall system economics. 56 CHP installations have been identified and entered into the database, each incorporating either TES or TIC, or both. 53 of these installations are in the U.S. The rated capacities of all combustion turbines are based on the standard ambient air conditions of 59 °F and 14.7 psia at sea level, as selected by the International Standards Organization (ISO).

4.3.4 Preparation of CHP issue papers with project partner DUA. The purpose of this project is to provide California Edison decision makers with input on policy and market opportunities to DER integration where it brings value to the customers and the grid. In 2006, the final report was issued: *The Value of Distributed Generation and Combined Heat and Power Resources in Wholesale Power Markets*. This report evaluates DG/CHP as wholesale power resources, installed on the utility side of the customer meter. The

basic elements of utility resource planning are applied to DG/CHP projects the way a utility would evaluate conventional system resources. The intent of the report is to show utility planners and DG/CHP resource developers how these resources can be used to the advantage of the electric power system by lowering the cost of providing service to customers. Applications that have maximum value to the power system should provide the greatest return on investment to developers. The report also includes brief discussions of how DG/CHP resources might be exploited in evolving deregulated markets.

4.3.5 Coordination of CHP meetings and stakeholder outreach with project partner Energetics. The project tasks are: 1) plan and coordinate the CHP Roadmap meeting, 2) Coordinate the CHP Team meetings, and 3) Coordinate education and outreach materials. Status of Tasks: 1) The 2005 workshop was held in New York City in October, 2005. A summary report on the 2005 workshop is included at the end of Section 4.3. The 2006 workshop was held in Seattle, Washington, September 2006. The final report for this workshop will be completed in FY2007. 2) Meetings are held on a quarterly basis in Washington DC. Stakeholder partners, including USCHPA, IDEA, HUD, EPA, VA, and industry partners participate in these meetings, and 3) Coordinated development and implementation of the IES Webcast held in September 2005. Approximately 581 persons viewed the webcast as individuals or in 29 viewing groups set up by CHP Regional Application Centers.

4.3.6a Analysis of Environmental Regulatory Barriers and Incentives for CHP with Project Partner Energy and Environmental Analysis. This project tasks are: 1) Air quality permitting barriers to CHP, 2) CHP Emissions/Credit Calculator, 3) CHP Permitting and Regulatory Requirements Database, and 4) Environmental Regulatory Analysis on CHP/DG issues white papers. Status of tasks: 1) The final report is being completed to include reviewer comments. 2) The CHP Emissions Calculator (EC) was completed in FY2005. In FY2006, EPA provided funding for EEA to further develop the calculator. The enhanced calculator can be found at the following

website:

[http://www.epa.gov/chp/project\\_resources/calculator.htm](http://www.epa.gov/chp/project_resources/calculator.htm)

3) The regulatory requirements database for small electric generators can be found at:

<http://www.eea-inc.com/rrdb/DGRegProject/index.html>

4.3.6b CHP Applications and Analytical Support with Project Partner Energy and Environmental Analysis. Project tasks include: 1) Development of a CHP installation database, 2) installation cost analysis for small CHP, 3) DG/CHP financing options, and 4) electric rate primer. Status of tasks: 1) The CHP installation database is complete and is posted at: <http://www.eea-inc.com/chpdata/index.html>. A sort of the CHP installations have been made by state and then grouped into Regions consistent with the CHP Regional Application Centers. The RACs reviewed for accuracy the sites in the database and added sites that were not in the database. Reports against the CHP Goal of 92 GW are taken from this database. This database will be updated to include 2006 data. 2) Two reports, *Financing Issues for Small Scale DG/CHP, Part I-Financing Options*, and *Part II-Is Financing a Constraint for Small Scale DG/CHP*, have been drafted and are undergoing review. 3) Two reports, *DG Financing Options* and *Industry Feedback on Financing Issues*, are being finalized to include reviewer comments, and 4) The final report, *Impact of Electric Rate Structures on CHP Economics*, is being prepared based on reviewer comments.

4.3.6c Analysis of Industrial and Commercial CHP Markets with project partner Energy and Environmental Analysis. Project tasks include: 1) Inventory of existing industrial/commercial boiler population, 2) evolution in the demand for steam, 3) changing CHP applications, 4) forecast of new and conventional industrial CHP. This project is complete. The following reports were issued: *Characterization of the U.S. Industrial/Commercial Boiler Population*, *Evolution of the U.S. Industrial Boiler Sector*, and *Forecast of Industrial CHP*.

4.3.6d DG Operational Reliability and Availability Database with project partner Energy and Environmental Analysis. The increased deployment of Distributed Generation (DG)/Combined Heat and Power (CHP) has been identified as a means to enhance both individual customer reliability and electric transmission and distribution system reliability. DG/CHP reliability and availability performance relates to several significant issues affecting market development. The reliability/availability profiles for DG/CHP systems can affect electric standby charges and backup rates, the value of ancillary services offered to Independent Transmission System Operators (ISO), local grid stability and reliability, customer power delivery system reliability, and customer economics. Interest in power reliability has heightened in recent years in light of highprofile system. This project represents the first attempt to establish baseline operating and reliability data for DG/CHP systems in more than a decade. This project is complete with publication of two documents: 1) *Executive Summary Report: Distributed Generation Operational Reliability and Availability Database* that can be found at: [http://www.eea-inc.com/dgchp\\_reports/DGRELExecSummaryReport.pdf](http://www.eea-inc.com/dgchp_reports/DGRELExecSummaryReport.pdf), and 2) the final report, *Distributed Generation Operational Reliability and Availability Database*, can be found at the following url: [http://www.eea-inc.com/dgchp\\_reports/FinalReportORNLDGREL.pdf](http://www.eea-inc.com/dgchp_reports/FinalReportORNLDGREL.pdf).

4.3.7 Facilitation of CHP in the Northwest with project partner Energy International [now Energy and Environmental Analysis]. Project tasks include: 1) Market assessment of the opportunities for combined heat and power (CHP) in the Pacific Northwest, specifically in the states of Washington, Oregon, Idaho, and Alaska, including developing a baseline of existing CHP in each state, estimating the technical and economic market potential for CHP in each state, and providing a comprehensive review of market, regulatory and institutional impediments to CHP development in the Northwest, 2) case studies and a brochure for regulators and policy makers. 3) Adding Arizona and Nevada to the market

assessment developed in task 1, and 4) Western States Summary Evaluation including a consolidated summary report of the CHP market potential in the eight states that represent the market focus of the DOE-WRO (Alaska, Hawaii, Idaho, Oregon, Washington, California, Arizona, and Nevada.). This project is complete. The final report summary titled: “CHP Market Potential in the Western States,” can be found on the Pacific CHP Regional Application Centers website: [www.chpcenterpr.org](http://www.chpcenterpr.org). The following case studies were completed and provided to the Pacific RAC for posting on their website:

- 525 kW Wind/Diesel Hybrid CHP Plant in Alaska
- 130 MW Gas Turbine Combined Cycle Power Plant at SP Newsprint Company
- Lewis and Clark College 30 kW microturbine CHP in Portland, Oregon
- Kimberly Clark 52 MW Wood-Chip Fired Steam-Turbine Generator in Washington
- Columbia Boulevard Wastewater Treatment 320 kW Fuel Cell and Microturbine Plant in Portland, Oregon
- Kenai Fjords National Park 5 kW solid oxide fuel cell in Seward, Alaska

4.3.8 Development of guide on sustainable metropolitan energy planning with project partner Gas Technology Institute. This project is complete. The guide was submitted as the official U.S. entry to the International Competition for Sustainable Urban System Design, the San Diego/Tijuana region was the subject for creation of an integrated energy, environmental, land-use, and transportation design for the year 2103. In addition, the entry included an information resources guide for all American cities that will describe innovative approaches to sustainable energy planning, derived from the seven finalist cities in the U.S. competition. The guide will provide information on clean power generation, distribution and use technologies, alternative transportation fuels/fleets, energy efficiency programs and practices, financing for municipal sustainability, and emerging technologies. Two documents were published: 1) *Model for Sustainable Urban Design*, and 2) *Blueprint for*

*Urban Sustainability: Integrating Sustainable Energy Practices into Metropolitan Planning.*

For copies of these documents, please see:

[http://www.gastechnology.org/webroot/app/xn/xd.aspx?it=enweb&xd=1researchcap\1\\_6distenergy\1\\_6\\_1\\_researchcapabilities\energyandenvironmentalhomepage.xml](http://www.gastechnology.org/webroot/app/xn/xd.aspx?it=enweb&xd=1researchcap\1_6distenergy\1_6_1_researchcapabilities\energyandenvironmentalhomepage.xml)

4.3.9 Development of environmental permit screening tool with project partner I.C. Thomasson. The tool developed under this project will assist facilities that desire to install cogeneration plants to determine the air permitting process that would be required to meet applicable environmental regulations and standards. This Environmental Permitting and Screening Tool is applicable to facilities interested in installing a gas turbine between one and five megawatts and located in the EPA’s Region IV located in the Southeastern United States [Mississippi, South Carolina, North Carolina, Tennessee, Georgia, Alabama, and Florida. The tool provides a brief overview of gas turbines, emissions produced by a cogeneration plant and how gas turbines are regulated, the applicable Code of Federal Regulations, and how to determine the type of permit required. The final report was completed: *Air Permitting Screening Tool: For ~5 MW Gas Turbine Combined Cycle Equipment in EPA Region IV.*

4.3.10 Screening and ranking of potential college and university campus sites for CHP with project partner IDEA. This project is complete. The final report is provided in powerpoint format and can be found on the DOE DE website. A presentation on consensus survey and lessons learned was provided by IDEA Executive Director Rob Thornton at IDEA’s 15<sup>th</sup> College and University Conference held in 2002. For that presentation, see:

[http://www.eere.energy.gov/de/pdfs/chp\\_idea\\_survey.pdf](http://www.eere.energy.gov/de/pdfs/chp_idea_survey.pdf)

4.3.11 Coordination of regional initiatives and stakeholder activities with project partner NEMW Institute. The project tasks are complete: 1) Education and Outreach Briefings, 2)



Manufacturing Sector Initiatives, and 3) CHP/DE Regional Initiatives. The following capital hill briefings were held:

- On April 25, 2006, *A Perfect Storm*, explored the perfect power system. Reliable and affordable electricity continues to be a key factor that will determine the future of the U.S. economy. Unfortunately, today's electricity grid and generators are antiquated, vulnerable to disruption, and inadequate to power future needs reliably. The briefing provided an overview of how we got to where we are, the options we face, and the consequences of the choices we make. Speakers included: Richard Munson, executive director of the Northeast-Midwest Institute and author of *From Edison to Enron: The Business of Power and What It Means for the Future of Electricity*, and Kurt Yeager, director of the Galvin Electricity Initiative.
- On October 3, 2005, *Distributed Energy and the Energy Bill*, which addressed legislative solutions needed, even after the recent energy bill, to overcome the policy barriers to distributed electricity generation. Discussing those barriers and the benefits of distributed generation were representatives of the U.S. Combined Heat and Power Association, International District Energy Association, American Council for Energy-Efficient Economy, and Calpine Corporation.
- On December 14, 2005, *Recycled Energy and Regional CHP Application Centers*, highlighted the network of Regional CHP (combined heat and power) Application Centers. RACs, part of the Department of Energy's Office of Distributed Energy, seek to address the numerous barriers to the introduction of innovative and efficient energy systems. The following personnel made presentations: Suzanne Watson, Watson Strategy Group; Sandy Glatt, U.S. Department of Energy, Erin Russell Story, Northeast CHP Initiative, Louay Chamra, Mississippi State University, and Ted Bronson, Power Equipment Associates.

The following guide was issued and can be found on the NEMW website: *Combined Heat and Power Education and Outreach Guide to State and Federal Government*, issued October 2005. Quarterly teleconferences for the CHP Regional Initiatives were held throughout 2006. Coordination of the industry-led CHP Regional Initiatives will be funded by EPA in 2007.

#### 4.3.12a A review of distributed generation siting procedures with project partner Resource Dynamics.

This project is complete. The final report was issued and is posted on the DOE DE website. The final report includes recommendations for state and local regulators to improve DG siting:

- Reducing permitting and interconnection times
- Mandating statewide utility business terms
- Standardizing and streamlining the interconnection process; consistent with IEEE 1547
- Considering the value of CHP thermal output and the DG state of the art in state air emissions requirements
- Providing incentive programs that give an early push towards market adoption of new DG technologies and energy efficient technologies such as CHP

The report also includes four siting principles to guide DG developers and customers in reducing siting costs and time:

- Careful up-front planning will avoid unnecessary risks
- Developers should budget for interconnection uncertainty, and try to get resolution on these issues as soon as possible
- To reduce costs, developers should consider DG equipment that has been pre-certified in states where that applies.
- Make use of existing government and utility providing siting tools.

#### 4.3.12b Market potential of opportunity fuels in DER/CHP applications with project partner Resource Dynamics. Phase I of this project

included 3 tasks and is complete: 1) collect and evaluate opportunity fuel information, 2) explore DER/CHP technology options, and 3) develop potential market estimates and make recommendations. This work has been of much interest to the CHP community, as evidenced by the webcast request and the many invited presentations. The final report can be found on the DOE DE website. Phase II of this project will be complete in FY07. In the Phase II effort, a state-by-state analysis of the impact of state level renewable portfolio standards will be performed, using state target dates and impacts as well as emerging values of renewable energy certificates (RECs). This analysis builds off of the completed Task 3 opportunity fuel assessment. It will analyze the potential capacity from opportunity fuels that would satisfy the state renewable portfolio standards, based on availability of fuel, economics of opportunity fueled CHP, and prospects for wind and solar renewables.

4.3.13 Assessment of target markets (healthcare, education, data processing) with project partner University of Illinois, Chicago. This project is complete. The final report has been published and can be found on the DOE DE website. This report defines the opportunity for CHP in three specific commercial building market segments

- Smaller Educational Facilities,
- Smaller Healthcare Facilities, and
- Data Centers/Server Farms/Telecom Switching Centers

Major issues affecting each of these markets are explored in the report in detail to provide guidance on the best manner to present the CHP concept to meet individual market concerns and needs.

4.3.14 Information dissemination, awareness campaigns, stakeholder meetings with project partner USCHPA. This work is complete. It consisted of three tasks: 1) select and profile industrial market sectors with high potential for CHP utilization, 2) evaluate CHP technologies and applications, and 3) exchange information with stakeholder groups to promote the awareness and deployment of CHP. The work under this contract was completed in 2005.

4.3.16 Coordination of Regional CHP Application Centers with project partner Power Equipment Associates. This project consists of multiple tasks including: 1) attend kickoff meetings of each Regional Application Center to provide: Input / guidance to application center approach, provide sources / clarification of existing application center processes and activities, provide guidance on startup or leveraging of industry coalitions and provide summary of strengths from other regions, 2) Develop Regional Application Center Steering Committee/Working Group, 3) plan and conduct quarterly application center working group conference calls, 4) issue annual regional application center coordination reports and presentations, and 5) complete a CHP Tool Box, a resource guide for CHP Application Centers.

The following are highlights of the FY2006 accomplishments:

- Coordinated development of the 8 RAC poster presentations for use at the DE Peer Review
- Held RAC face-to-face meeting in conjunction with the October 2005 CHP Roadmap meeting held in New York.
- Coordinated a RAC overview session as presented to the 2005 Roadmap meeting audience.
- The RAC end-of-year report [in presentation format] was completed on December 31, 2005 and submitted to ORNL.
- The Tool Kit was provided to the RACs at the October 2005 Roadmap meeting held in New York.
- The following focus areas have been established by the RACs:
  - Midwest – Hospitals, Ethanol, Farms, A/Es, Municipal Utilities, Regulatory
  - Intermountain – Waste Water Treatment and Landfills, Regulatory
  - Mid-Atlantic – Government facilities, opportunity fuels
  - Northeast – Commercial Office Buildings, HUD, Grid Congestion Relief, Wood Products, Hospitals, A/Es

- Northwest – Farms, Waste Heat to Power, District Energy
- Pacific – Ultra Clean Technologies, Waste Heat to Power
- Gulf Coast – Hurricane Recovery Efforts, Cooling and Dehumidification Technologies, Hospitals
- Southeast – Hurricane Recovery Efforts, Cooling and Dehumidification Technologies, Agriculture
- The state energy partnerships solicitations for DOE buildings and DOE ITP have been provided to the RACs.
- The agenda for the May 2<sup>nd</sup> RAC face-to-face meeting included the following items:
  - RAC Task Order
  - Coordination Efforts: EPA, HUD, VA, and FEMP
  - New Tools for CHP: CHP Toolkit, CHP Capacity Optimizer, BCHP Screening Tool, ASERTTI DG Database, Website Effectiveness, EPA Emissions Calculator
  - *What's Working and What's Not?* Policy Issues, Targeted Market Workshops Results and Plans, Project Support, How Should We Measure Success
- A face-to-face coordination meeting of the DOE CHP Regional Application Centers (RAC) was held on May 2<sup>nd</sup>, 2006. The purpose of the May RAC face-to-face meeting was to 1) share information on emerging issues and actions among the regions that can help each RAC and Initiative optimize its performance through leveraging other actions of the group, 2) Learn about emerging US DOE DER projects, and those of other government partners that can have a regional impact, and 3) Provide a feedback mechanism to US DOE as to what is working and what's not with respect to CHP Installations.

- A RAC face-to-face meeting was held in conjunction with the September CHP Roadmap Workshop held in Seattle.
- The quarterly calls of the Regional Application Centers continue.

#### 4.3.20 Technical support to HUD.

Under a work-for-others agreement with HUD in support of the HUD Energy Action Plan, ORNL is providing technical assistance in the area of CHP for multi-family housing.

ORNL developed screening software for evaluating CHP potential in multi-family housing. This stand-alone program is based on an appendix attachment in the FY2005 *HUD CHP Guide #2 Feasibility Screening for Combined Heat and Power in Multi-Family Housing*, whose audience is apartment building owners and managers. The program is being adapted to include CHP systems incorporating uses of recovered heat for space cooling in addition to space heating and hot water heating. ORNL is providing technical assistance on an as-needed basis to the eight DOE Regional CHP technical assistance centers who have been enlisted to reach and advise owners of apartment buildings on the opportunities for using CHP. A copy of the ORNL developed program can be downloaded from the following website: [http://www.ornl.gov/sci/engineering\\_science\\_technology/cooling\\_heating\\_power/success\\_analysis\\_HUD.htm](http://www.ornl.gov/sci/engineering_science_technology/cooling_heating_power/success_analysis_HUD.htm)

#### 4.3.21 Technical support to LEED.

This task is complete. The CHP Calculation Methodology for LEED-NC v2.2.EA Credit 1, *Guidance on Combined Heat and Power Systems Supplying Electricity or Recovered Thermal Energy to LEED Applicant Buildings*, was issued by the U.S. Green Buildings Council on March 28, 2006.

In FY2006, ORNL worked with a U.S. Green Building Council's Leadership in Energy and Environmental Design (LEED) committee to foster market transformation for cooling heating and power (CHP) technology. This advanced technology supplies on-site electricity and recycles thermal energy to increase fuel use efficiency from 33% to over 75%. LEED is transforming the



market for energy-efficient technology by recognizing the use of advanced technology in a formalized certification process--building owners proudly displace their LEED certification status.

ORNL was an active participant on the LEED CHP subcommittee [hosted by the U.S. Green Buildings Council], which ensured that appropriate LEED credit is awarded for on-site power generation CHP. Objectives of ORNL are to participate in reviews, and model and evaluate CHP applications for incorporation into guidance issued by LEED. In addition, ORNL participation is encouraging development of LEED 3.0 to more fully incorporate benefits of CHP such as reduced air emissions and improved efficiency of fossil fuels. ORNL developed a model and analyzed example cases for how the calculation methodology, developed by the committee, would be applied. This model had been reviewed and approved by the full Technical Advisory Group (TAG) for LEED Environment and Atmosphere credit 1 for incorporation in guidance provided with LEED 2.2. The TAG has approved all 4 proposed cases for deploying CHP system. LEED credit available for the fourth case, third-party ownership of a district CHP system, was finally approved by the TAG after continued prompting by ORNL's Jan Berry.

### **CHP Project Reports:**

A description of reports published under this project are included within the above tasks along with the appropriate urls.

### **CHP Project Databases:**

A description of databases developed under this project are included within the above tasks along with the appropriate urls.

### **Results of the October 2005 Roadmap Workshop**

2005 marked the sixth year that a national workshop on combined heat and power had been sponsored by the Department of Energy, the Environmental Protection Agency, the U.S. Combined Heat and Power Association, and

numerous national, state, regional, and local government organizations, private companies, research institutions, and non-profit associations. Each year since the first CHP workshop – the CHP Summit in 1999, at which the CHP Challenge was established – CHP stakeholders have gathered to discuss both the progress of CHP development in the country as well as the barriers that remain.

In 2005, this annual meeting was combined with the 6<sup>th</sup> Annual World Conference on Decentralized Energy and CHP, sponsored by the World Alliance for Decentralized Energy (WADE). Combining the two meetings provided an opportunity for attendees to learn about the world market for CHP, technical advances in CHP and DE technology and systems, and policy, regulatory, economic, and environmental issues that still need to be addressed throughout the US and the world for a robust CHP market.

Two-hundred and fifty-six (256) delegates and speakers attended the International DE and CHP Conference; approximately 165 of them stayed to participate in the 6<sup>th</sup> Annual Roadmap Workshop. Delegates from outside the United States hailed from:

- Brazil
- Scotland
- Canada
- Portugal
- Turkey
- Australia
- The Netherlands
- France
- Finland
- Japan
- China
- Korea
- Belgium
- Sweden
- India
- New Zealand
- Czech Republic
- Nigeria
- Lithuania

The 2005 National CHP Roadmap Workshop focused on the market for CHP today in the US, and on the opportunities and actions needed to

improve that market during 2006. A “situation analysis” was presented to Roadmap Workshop participants in the form of a CHP Action Agenda, in which the strides made since 1999 were described and the changes in technology, market development, policies, regulations, and education and outreach activities were outlined. All eight Regional CHP Application Centers (RACs) provided short updates on their activities, illustrating the breadth and depth of CHP activities in regions throughout the country. Delegates to the workshop then contributed their thoughts about activities undertaken in their communities and/or organizations during the last year.

The workshop then continued with the first-ever CHP Café. This facilitated series of conversations on CHP was designed to engage participants in small group discussions on CHP issues that they thought would have the most impact on their organizations’ successes; on what and where the best opportunity for deployment of CHP was; and what might be needed to improve or expand those opportunities. This Café process resulted in conversations on the following topics:

- Target markets for CHP
- Target audiences for CHP
- Utility inter-relationships
- Economics of CHP – Monetizing CHP
- Strategic issues, such as climate change, grid connections, and environmental externalities
- Regulatory environment
- Technology development

The conversations were captured on “butcher-block” paper, which is now being recorded, categorized in the above-noted topic areas, and analyzed into activities and actions that might be addressed by national, state, regional, and local CHP stakeholders and advocates. Among the preliminary issues of concern and the best opportunities for deployment of CHP are the following:

Target Markets for CHP - Targeted region-specific markets include New York City, Southwest Connecticut, and the Midwest. Target vertical markets include hospitals; supermarkets; hotels;

wastewater treatment plants; nursing homes; federal government buildings; agricultural environments where waste heat can be capture; high-end residential buildings; and critical infrastructure facilities that operate 24/7.

Target Audiences for CHP - CHP can meet most needs in a wide variety of industrial, commercial, and institutional buildings. Among the best market opportunities are energy security facilities, including hospitals, police, and fire station, and municipal buildings. The major messages for these markets include valuable energy efficiency resulting from installation; reliability; and economic benefits.

Utility Inter-Relationships – Key issues include convincing utilities of the use of CHP as a customer retention strategy; addressing utility opposition to microgrids because they are seen as competitive to the utility business; and analysis of the utility requirement to “serve all customers” which leads to large back-up capacity requirements and fees for distributed generation. A major topic includes the need to “incentivize” utilities to adopt CHP, simplifying our message; and allowing utilities to make money on DG, rather than purely through-put.

Economics of CHP – Key issues include local electric rates (spark spread is poor in some geographic locations); high first costs, which in turn lead to subsidies; high gas prices; financing constrains; the need to value reliability; and the need for packaged systems to reduce installation costs.

Strategic Issues – Energy has become a national issue – a major topic of conversation. Among the key issues are grid reliability and stability, vis a vis combined heat and power and distributed energy; inclusion of CHP in renewable portfolio standards; valuing and accounting for externalities; monetizing the environmental and energy efficiency benefits of CHP; selling CHP projects and framing the risk of not investing in CHP and DE; and acting on “pain”, e.g., using national disasters to our advantage by underscoring the value of CHP and DE in these situations.

Regulatory Environment – The regulatory environment for CHP continues to be uneven across the country. Key issues for action include involvement with FERC and standard interconnection proceedings both nationally and at the state level; and educating regulators about the benefits of DE and CHP, particularly when the power grid is being re-built or expanded.

Technology Development – The primary need is development of reliable packaged systems, using off-the-shelf products and systems that can be assembled off-site and installed as a package, or modular, system on site.



## 5.1 Ancillary Services Offered by Distributed Energy (DE) Systems

*John Kueck , Tom Rizey, Leon Tolbert, Burak Ozpineci*

*Engineering Science and Technology Division*

*Oak Ridge National Laboratory*

*Oak Ridge, TN 37932-6070*

*(865) 574-5178, email: [kueckjd@ornl.gov](mailto:kueckjd@ornl.gov)*

*(865) 574-5203, email: [rizydt@ornl.gov](mailto:rizydt@ornl.gov)*

*Debbie Haught, DOE Program Manager*

*(202) 586-2211, email: [debbie.haught@ee.doe.gov](mailto:debbie.haught@ee.doe.gov)*

---

### Objectives

- Develop methods for autonomous control of local voltage regulation from DE utilizing programmable inverters in several different sizes (62, 125, and 250 kVA) and a 300kVar synchronous condenser connected to ORNL's distribution system.
- Evaluate the economic and engineering feasibility of supplying reactive power locally from DE to regulate local voltage and control power factor to improve the efficiency and reliability of the utility distribution system.
- Determine if reactive power can be supplied from local DE sources with independent voltage control so that an expensive hierarchical control and communications system is not required.
- Address key barriers to the local supply of reactive power so that it may be supplied without requiring the local utility to either modify the existing distribution system or perform engineering analysis of the circuit.
- Develop "Rules of Thumb" implementation guidelines for utilities to reduce the need for detailed engineering studies for the installation of DE.
- Evaluate the incremental costs and potential benefits of DE as a source of reactive power in the electric transmission & distribution power grid. Evaluate economically viable ancillary services from DER.

### Approach

- Establish a DE reactive power producing laboratory with both generator and inverter-based DE technologies to test individual and multiple reactive power producing DE.
- Use the ORNL campus distribution system to demonstrate that several reactive power producing DE devices can operate in close electrical proximity to regulate voltage or net power factor without extensive communications and control.
- Use a mathematical programming platform (Matlab/Simulink) and real-time controller (dSpace) to implement various algorithms and strategies for feedback control.
- Use power system and simulation software (SKM and Matlab SimPower) to model the performance of the DE in controlling voltage and net power factor and evaluate local control methods.
- Demonstrate that DE inverter designs with local control can be developed and packaged to economically supply adequate reactive power levels to satisfy utility and user needs.
- Conduct an economic assessment of DE as a source of reactive power and a limited number of case studies with specific utility information. Identify potential market value based on available information.

### Accomplishments

- A unique and first-of-its kind R&D laboratory for evaluating reactive power from DE has been established at ORNL. The Distributed Energy Communications & Controls (DECC) Laboratory is capable of testing both rotating- (generators, motors) and power electronic-based (inverters) reactive power producing DE.
- A 300kVar Synchronous Condenser or SC (large synchronous motor unloaded and overexcited) is operational for evaluating the local control of rotating-based DE with an actual distribution system. The SC interfaces with 2.4kV distribution circuit #4 of the 3000 substation through a 480V/1000A power panel.
- The capability of testing 3-phase inverters for producing reactive power from DE has been established at the laboratory. The lab has the capability to test 75A (62kVar), 150A (125kVar) and 300A (250kVar)

inverters either off the grid using load banks or on the grid interfaced with the ORNL distribution system through a 480V/600A power panel.

- A Matlab/Simulink Software Platform and dSpace Real-Time Control Hardware and Software provides a versatile programming environment for developing and testing various control algorithms and schemes for the reactive power producing DE in the laboratory.
- An assessment study of the viability of using DE systems to provide different ancillary services has been completed along with a study on the potential economic viability of incorporating reactive power into DE.
- All milestones for the year have been met ahead of time. Last year on April 27, 2005, we met the FY05 milestone of operating the 300 kVar SC for the first time to inject reactive power into circuit #4. On February 23<sup>rd</sup> of this year, the milestone of operating the inverter on circuit #2 to demonstrate its ability to compensate for fundamental reactive power, harmonics, and unbalanced load conditions was achieved. On September 6, 2006, we met our final FY06 milestone of operating the SC and inverter simultaneously and in parallel.
- A 125kVar Power Inverter was operated on the 2.4kV distribution circuit #2 of the ORNL distribution system through a 480V power panel. The operation of the power inverter met a milestone of injecting reactive power into the distribution system in February 2006. The power inverter regulated the line voltage and net power factor of the local circuit by varying its reactive power output. *AOP Milestone 4.4.1*
- A commercial mathematical simulation software model of the power inverter and SC connected in parallel to the ORNL distribution system was developed to model the interaction between the two DE devices as they controlled their local voltage independently with the injection of reactive power. The model results confirmed the validity of the control algorithms for regulating voltage with either device prior to testing.
- On September 6th, the final FY06 milestone for the reactive power producing DE effort was met more than three-weeks ahead of schedule with the simultaneous operation of the 150A inverter and the 300kVar SC. Both the inverter and SC were controlled by the dSpace real-time controller using our control algorithms to regulate line voltage locally at their respective 480V power panels. Each device regulated their local voltage independent of the other. *AOP Milestone 4.4.1*

#### **Future Direction**

- Determine how to better model the voltage, current and power changes due to reactive power producing DE at the circuit and substation levels. These include expanding the model capabilities to cover unbalanced loading, voltage sensitive loads, and real-time loading changes.
- Develop a cost goal for the local supply of reactive power from DE so that the inverter and synchronous generator/condenser based DE can be evaluated to determine at what cost level it would be competitive with conventional reactive power compensation, such as feeder-level shunt capacitor based regulation.
- Continue testing of multiple DE in parallel and in series to enhance our controls and fully evaluate interaction with multiple devices and develop engineering guidelines for DE application in providing voltage regulation and net power factor regulation.
- Only a portion, perhaps 30%, of total distribution system reactive resources would need to be dynamic. A determination must be made for the optimum level of dynamic reactive support for various distribution system models.
- When dynamic reactive support from DE is controlling local voltage levels, conventional voltage droop control schemes will no longer function. Conventional schemes rely on the voltage characteristic of load; with local dynamic support, voltage will not droop as power flows increase. An “artificial” power flow – voltage curve may be needed to simulate a natural voltage droop characteristic. Computational methods are needed for the simple and quick development of this curve for various distribution system models.
- Move the concept of reactive power producing DE from the laboratory to the field environment by working with our partners, such as Southern California Edison and their distribution circuit of the future, to implement the concept to a much larger extent (provide a large part up to all of the local dynamic reactive power) on a utility distribution circuit or circuits.

## Abstract

The Distributed Energy Communications & Controls (DECC) Laboratory is a unique first-of-its kind R&D facility for testing reactive power producing distributed energy resources (DER). Reactive power doesn't perform work like real power, but it is necessary for energizing inductive and capacitive loads and for supporting voltage and preventing voltage collapse. Reactive power occurs when reactive loads (capacitors or inductors) are present and voltage and current are out of phase. When reactive power is present, current either lags (when reactive power is being consumed) or leads (when reactive power is being produced) the voltage. Real (or active) power, which does work, is only present when voltage and current are in phase. However, when voltage and current are out of phase, greater overall power capacity (due to the vector sum of real and reactive power) is needed to get the same level of real power and do the same level of work.

When capacitors are used to supply reactive power, they create a significant problem in that the level of reactive power they produce decreases with the square of the local voltage. That is, when the voltage is 80% of nominal, capacitors are only producing 64% of their rated reactive power. Thus capacitors lose their impact when they are needed the most! Reactive power supplied from DER is called dynamic reactive power. Dynamic reactive power does not decrease with decreasing voltage, and it can be raised or lowered very quickly in just the needed amounts.

The laboratory is exploring the use of both rotating (generators, motors) and static-based (inverters) Distributed Energy (DER) technologies for producing dynamic reactive power for supporting voltage and correcting power factor both locally and on the campus distribution system.

The goal of the laboratory is to work with the power industry, manufacturers, and universities in developing local control for producing reactive power from reciprocating engines, microturbines and fuel cells using synchronous generators and inverters. The laboratory is fully operational with an area for testing and operation of a 300kVar synchronous condenser (250hp synchronous motor operated unloaded and overexcited) and an

inverter testing area. The inverter testing area is capable of testing an inverter either off the grid using resistive and reactive load banks or on the grid by interfacing with the ORNL distribution system via a 480V/600A distribution panel to a 750kVA transformer connected to a circuit from the 3000 substation. Three different ratings of three-phase programmable inverters, 75A (62kVA), 150A (125kVA) and 300A (250kVA) are available for testing and will have already run tests with the two lower rated inverters.

## Introduction

The additional current flow associated with reactive power can cause increased losses, excessive voltage sags, and increased power capacity requirements. Transmission system operators have to ensure that reactive reserves are available to handle system contingencies such as the loss of a generator or transmission line because increased current flows after the occurrence of these types of contingencies can produce greatly increased reactive power absorption in transmission lines. Some transmission system operators are now considering new rules for distribution systems which require a minimum allowable power factor. These minimum power factors, if guaranteed by a sufficient level of dynamic reactive reserves, could reduce the amount of reactive reserves that the system operator would have to provide. Distributed Energy Resources (DER) could be ideally suited for providing dynamic reactive reserves in the distribution system.

DER, includes such resources as microturbines, reciprocating engine generators, and fuel cells. DER is often installed at or near electrical loads for local power and to take advantage of CHP (cooling, heating and power) benefits that come from waste heat recovery of DER by thermally-activated technologies. With the right control scheme and algorithms, DER could be controlled to supply local dynamic reactive power and to regulate local voltage. Some DER devices utilize synchronous generators, which can be directly connected to the local power system, and some, such as fuel cells or microturbines, must be interfaced to the local power system through an inverter because they produce DC or high-frequency AC that must be converted to 60Hz AC.

Similar to a synchronous generator, the inverter can also be designed and controlled to “inject” dynamic reactive power locally and regulate voltage. Thus, a DE with a synchronous condenser or inverter could supply dynamic reactive power reserves.

The Oak Ridge National Laboratory (ORNL) has established the Distributed Energy Communications & Control (DECC) Laboratory which is a new and unique first-of-its kind laboratory for studying reactive power supplied from DE. ORNL is unique in that it owns and operates its own electric distribution utility for the laboratory campus, and can configure the distribution system to provide opportunities for testing of reactive power injection effects from the laboratory. The ORNL distribution system is directly fed by the TVA 161kV backbone transmission system. The laboratory and project are also unique in that the tests are designed by representatives from the electric utility industry and DE manufacturers to address the actual challenges faced by DE and utilities currently and in the future.

The DECC project has the overall goal of developing methods of incorporating distributed energy (DE) that can produce reactive power locally and for injecting into the distribution system. The objective for this new type of DE is to be able to provide voltage regulation and dynamic reactive power reserves without the use of extensive communication and control systems.

### DECC Laboratory

The DECC Laboratory has been established for studying reactive power supplied from both rotating and power electronic-based DE. The electrical design and layout of the Reactive Power Laboratory is shown in Figures 1 and 2. Figure 1 shows the laboratory’s interface with the ORNL distribution system while figure 2 shows the layout at the laboratory itself. The laboratory is located at the north end of the Oak Ridge National Laboratory campus at building 3114. The test areas of the laboratory are in the building while the transformers and load banks are just to the east of the building. The laboratory equipment interfaces to the ORNL distribution system through two different distribution circuits (#4 and

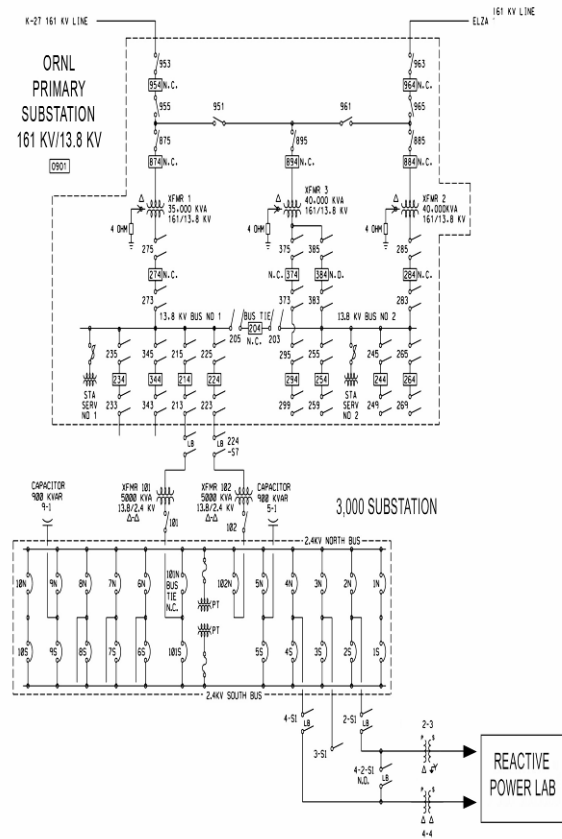


Figure 1. DECC Laboratory Interface with the ORNL Distribution System.

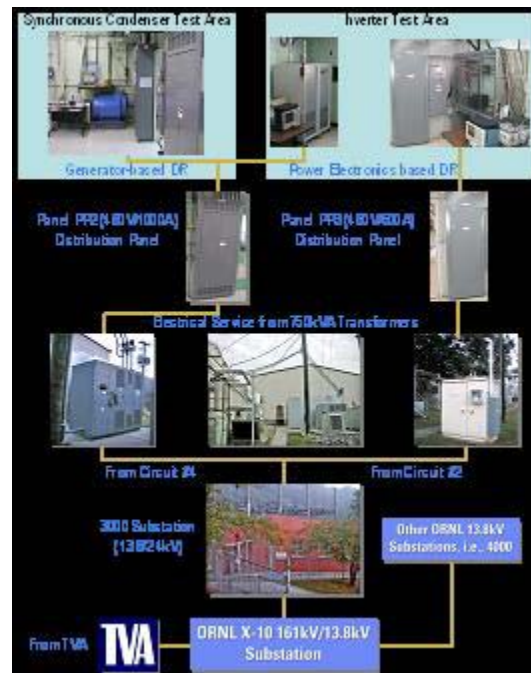


Figure 2. Reactive Power Laboratory Layout

#2 fed from ORNL's 13.8/2.4kV Distribution Substation 3000). The rotating-based DE of the laboratory consists of a 300kVar synchronous condenser (1250hp synchronous motor unloaded and overexcited) which is fed from circuit #4. The power electronic-based DE of the laboratory consists of an inverter test area which is fed from circuit #2. The test area currently has a 150A inverter for testing and previously tested a 75A inverter. Both areas of the laboratory are fully functional as of February 2006.

The laboratory includes the following equipment:

- 250hp synchronous motor for use as a synchronous condenser
- 75A, 150A, and 300A programmable inverters
- Two 750kVA 2.4kV/480V pad-mount transformers for interfacing to circuits #4 and circuit #2 of the ORNL 13.8/2.4kV distribution network at the 3000 Substation
- 480V/900A three-phase electrical panel configuration for the 250HP synchronous condenser interface (via a 450A motor starter) to the ORNL 2.4kV distribution circuit #4
- 480V/600A three-phase electrical panel configuration for the inverter interface to ORNL 2.4kV distribution circuit #2
- Dranetz/BMI PowerGuide 4400 Meters; one located at the motor/starter and the second at the electrical panel.
- Yokogawa WT3000 Digital Power Meter
- Danfysik Ultrastab 866 Current Transducer Systems, one for measuring the synchronous condenser output currents, a second for measuring the inverter output currents and a third for measuring the load bank currents.
- Matlab/Simulink and Real-Time Workshop software for design voltage regulation and power correction control algorithms for the synchronous condenser and inverters
- dSpace real-time control hardware and software for implementing autonomous feedback control for the synchronous condenser and inverter
- 150kW dc power supply for the providing DC voltage to the programmable inverters
- 6.6kW dc power supply for providing excitation to the synchronous condenser

- Resistive (0 to 500kW in 1kW steps) and Reactive (0 to 300kVar in 3.75kVar steps) load banks with remote control
- Portable resistive load bank (0 to 100kW in 1kW steps) for use on either power panel
- 75HP Induction Motor for use as a dynamic load

Important capabilities of the laboratory include:

Testing Areas: The laboratory provides testing capability of rotating (generator or motor) and power electronic or static (inverter) based DE. Also, the laboratory has the capability to test vendor provided reactive power producing DE, such as a microturbine or reciprocating engine.

Distribution Interface: The laboratory interfaces at two different electrical locations on the ORNL distribution system. This provides the capability to test single or multiple reactive power producing DE and also their interaction. The DE devices can be connected in parallel (by using both power panels) or in series (by using only one power panel).

Substation: The reactive power compensation at the substation can be relaxed to provide a more severe testing scenario for the laboratory. Shunt capacitor banks at the substation provide power factor correction for the ORNL distribution system. The reactive power compensation can be relaxed by switching out some of these capacitor banks. Presently, the substation has 900kVar of reactive power compensation in capacitor banks in units of 150kVar.

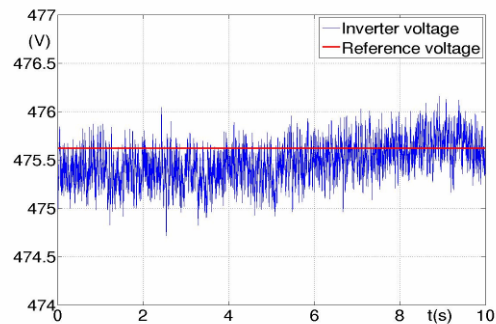
Distribution and Power System: The laboratory interfaces with the TVA grid through the ORNL distribution system. The TVA transmission lines provide power to ORNL at 161kV and it is stepped down to 13.8kV at ORNL's substation. Secondary substations, such as the 3000 substation, which provides the electrical interface for the laboratory, steps it down further to 2.4kV. Our ownership of the distribution system allows the capability to vary loading and reconfigure the distribution feeder circuits for testing different operating scenarios at the DECC Laboratory.

### Test Results - Simultaneous Operation

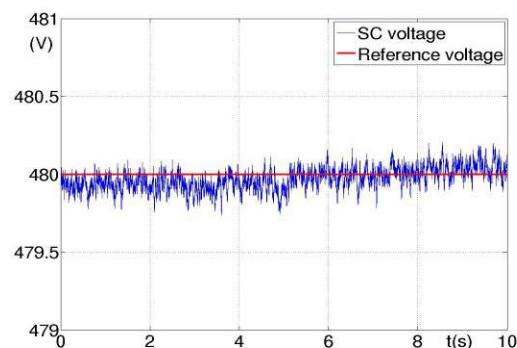
On Wednesday, September 6th 2006, the final FY06 milestone for the reactive power producing Distributed Resources (DR) effort was met more than three-weeks ahead of schedule with the simultaneous operation of the 150A (125kVar) PowerEx Inverter and 300kVar Synchronous Condenser (a large synchronous motor operating unloaded and overexcited). Both the Inverter and Synchronous Condenser (SC) were controlled by the dSpace real-time control hardware and software system to regulate line voltage locally at their respective power panels. Each device regulated their local voltage independent of the other. The real-time controller used control algorithms that ORNL designed using the Matlab/Simulink environment.

The successful parallel operation of the two dynamic reactive power producing DE devices in our testing is an important first step towards using multiple DEs to provide dynamic voltage regulation. The operation of multiple DEs under local control for dynamic voltage regulation on the same distribution system/circuit is vital for its use on distribution circuits of the future. These future circuits will depend on DE devices to provide most if not all of the dynamic reactive power needs of a circuit. The DR devices must operate so that they don't interfere with each other or with the current protection practices and hardware of the distribution system. Our testing is laying the groundwork for "Rules of Thumb" for this new DE paradigm which gives DEs another added value both in utility system support and cost benefit.

The voltage regulation results are shown in Figure 3. During the simultaneous operation, the inverter was operated at a reactive power output level of around 36.5kVar while the SC was operated at an output level of around 45kVar as shown in Table 1. Both devices were set to regulate their local line voltage, and they did this independent of the other. The inverter was set to regulate its average ac line voltage (average of the three phase-to-phase voltages,  $V_{ab}$ ,  $V_{bc}$  and  $V_{ca}$ ) at 475.6 or 2 volts above the unregulated line voltage as shown in Figure 1a and indicated in Table 1. The synchronous condenser was set to regulate its average ac line voltage at 480V or



(a) Voltage regulation by the inverter at power panel PP3 of the laboratory.



(b) Voltage regulation by the SC at power panel PP2 of the laboratory.

**Figure 3.** Local voltage regulation by the inverter and SC on September 6<sup>th</sup>.

approximately 2 volts above the unregulated line voltage as shown in Figure 3b and indicated in Table 1. In the case of the inverter, regulation was achieved by setting the inverter's DC voltage to 790Vdc via the 144kW power supply and then using our feedback control to regulate the output of the inverter to increase/decrease voltage to maintain the reference set point of 475.6V. The inverter was operating at 12.5kHz and so could respond in microseconds to any voltage changes. In the case of the synchronous condenser, our feedback control increased/decreased DC from the 6.6kW power supply to adjust the SC's excitation appropriately to regulate the SC's output to maintain the reference set-point voltage of 480V. The SC is obviously much slower than the inverter due to its large inertia but could respond in milliseconds to voltage changes.

**Table 1. Key parameters for the simultaneous DE operation on September 6th.**

Parameter	Inverter (125kVar)	Synchronous Condenser (300kVar)
AC Distribution System Interface	ORNL Circuit #2 Power Panel PP3	ORNL Circuit #4 Power Panel PP2
Voltage without regulation (V) <sup>1</sup>	473.7	478.2
Voltage with regulation (V) <sup>1</sup>	475.6	480.0
Current Output (A) <sup>2</sup>	44.5	54.0
Reactive power output (kVar)	36.5	45.0
% of Device Rating <sup>3</sup>	29.2	15.0
Losses (kW) <sup>4</sup>	3.0 <sup>5</sup>	5.5 <sup>5</sup>
% losses <sup>6</sup>	8.2	12.1

<sup>1</sup>Average of the three phase-to-phase RMS (root-mean-square) voltages before and after the inverter and SC are controlled to regulate their local voltage.

<sup>2</sup>Average of the three line RMS currents from the device.

<sup>3</sup>kVar output divided by the device's rated kVar in percentage. The 150A rated inverter ideally could provide around 125kVar if all of its thermal cooling (for the IGBTs) is satisfied. From previous testing, the SC (synchronous motor overexcited and unloaded) was found to be capable of producing just over 300kVar.

<sup>4</sup>The DR's losses for producing the needed reactive power output. The losses include the DC power needed by either inverter or SC along with the active power consumed from the ac distribution system.

<sup>5</sup>The inverter consumes 5 kW of active power from the DC power supply while injecting 2 kW to the distribution system. The SC consumes 1 kW from the DC power supply and 4.5 kW of active power from the ac distribution system.

<sup>6</sup>Ratio of losses divided by the kVA (square root of kW squared plus kVar squared) in percentage. The % losses for the SC fall to around 6% when the unit is operating at 36% or higher output. The losses for the inverter should fall as well and reach lower than 5% when the unit is operating above 50% of rating and lower than 3% when the unit is operating above 75% of rating.

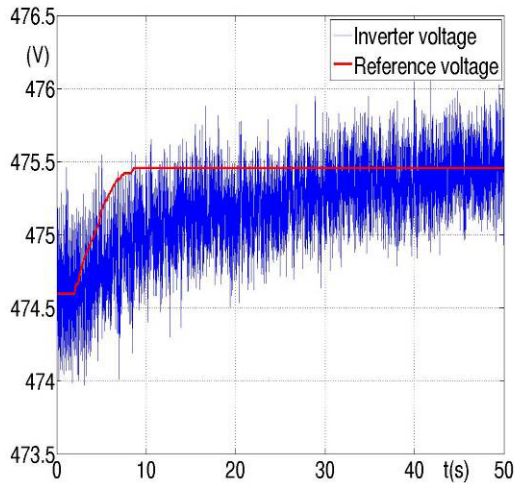
The dynamic response of the inverter and SC to a step change in the voltage reference during the parallel operation was also tested. Figure 4 shows the inverter's response to a 1-volt increase and then a 1-volt decrease from the original reference point. Figure 5 shows the SC's response to a 2-volt increase and a 5 volt decrease. Even though, the response is for a voltage step change, a similar response would be expected for a step change in

load requiring the SC or inverter to increase/decrease their output in similar fashion.

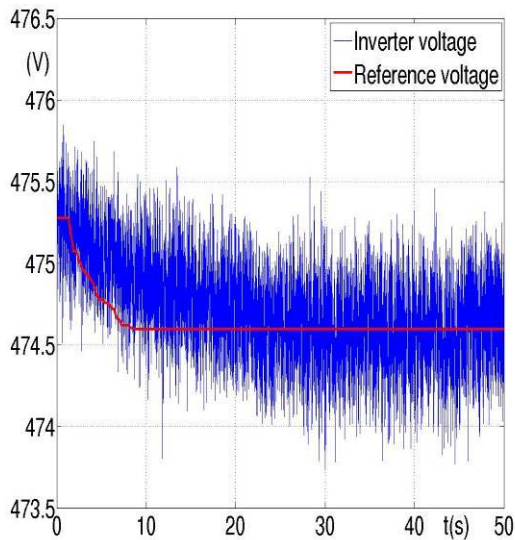
The control variables are the gains of the PID (proportional, integral, differential) feedback controller for the two devices. The objective is for the two devices to dynamically output reactive power to regulate voltage to closely match the reference voltage. The tradeoff is that the gains of the controller need to be adjusted to achieve a fast response but with minimal over/under-shoot of the inverter/SC voltage regulation when the reference voltage changes (either due to load changes or because of a change in regulation setting). The feedback control that was used for the simultaneous operation of the inverter and SC on September 6th used a PI controller and the gains were adjusted as indicated earlier. As shown in Figures 4a and 4b, it took about 30s for the inverter voltage to reach a steady operating point around the reference setting after a 1 volt step change with the gains that were used for the inverter controller. As shown in Figures 5a and 5b, it took longer, around 40 to 60s, for the SC voltage to reach a steady operating point around the reference setting after a 2 to 5 volt step change with the gains that we used for the SC controller. The gains could be set higher to shorten the response time of either the inverter or SC however the tradeoff is an increase in the over/under-shoot of the controls.

## References

1. S. D. Henry, D. T. Rizy, P. A. Boheme & J. D. Kueck, Reactive Power Laboratory: Synchronous Condenser Testing & Modeling Results, Interim Report, Oak Ridge National Laboratory, ORNL/TM-2005/174, August 22, 2005.
2. J. D. Kueck, B. J. Kirby, L. M. Tolbert, D. T. Rizy, "Voltage Regulation: Tapping Distributed Energy Resources," Public Utilities Fortnightly, vol. 142, no. 9, September 2004, pp. 47-51, <http://www.pur.com/puftocs/sep04.cfm>.
3. L. M. Tolbert et. al., Power Electronics for Distributed Energy Systems and Transmission and Distribution Applications, Oak Ridge National Laboratory, ORNL/TM-2005/230, December 2005.



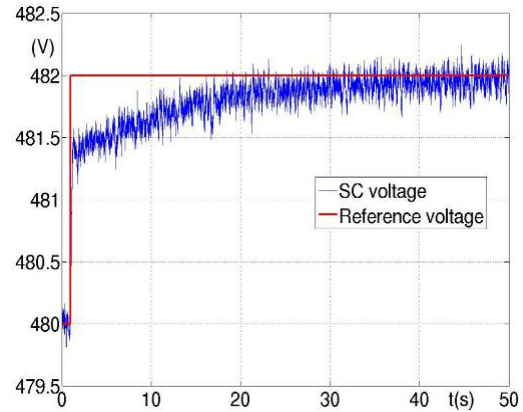
(a) Dynamic response of inverter to a 1V increase in voltage reference setting.



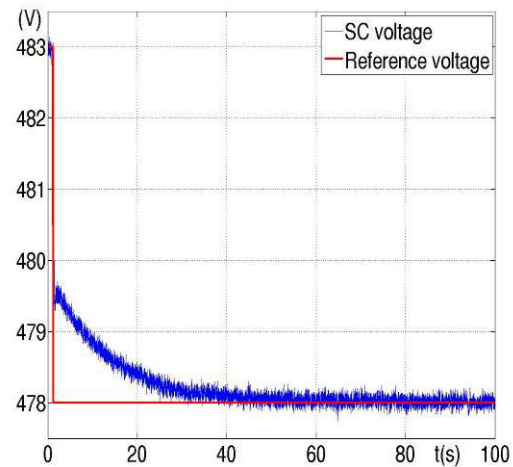
(b) Dynamic response of inverter to a 1V decrease in voltage reference setting.

**Figure 4.** Dynamic response of inverter to a step change in the voltage reference.

4. J. B. Campbell et. al., Ancillary Services Provided From DER, Oak Ridge National Laboratory, ORNL/TM-2005/263, December 2005.
5. F. Fran Li, John Kueck, Tom Rizy & Tom King, A Preliminary Analysis of the Economics of Using Distributed Energy as a Source of Reactive Power Supply, Oak Ridge



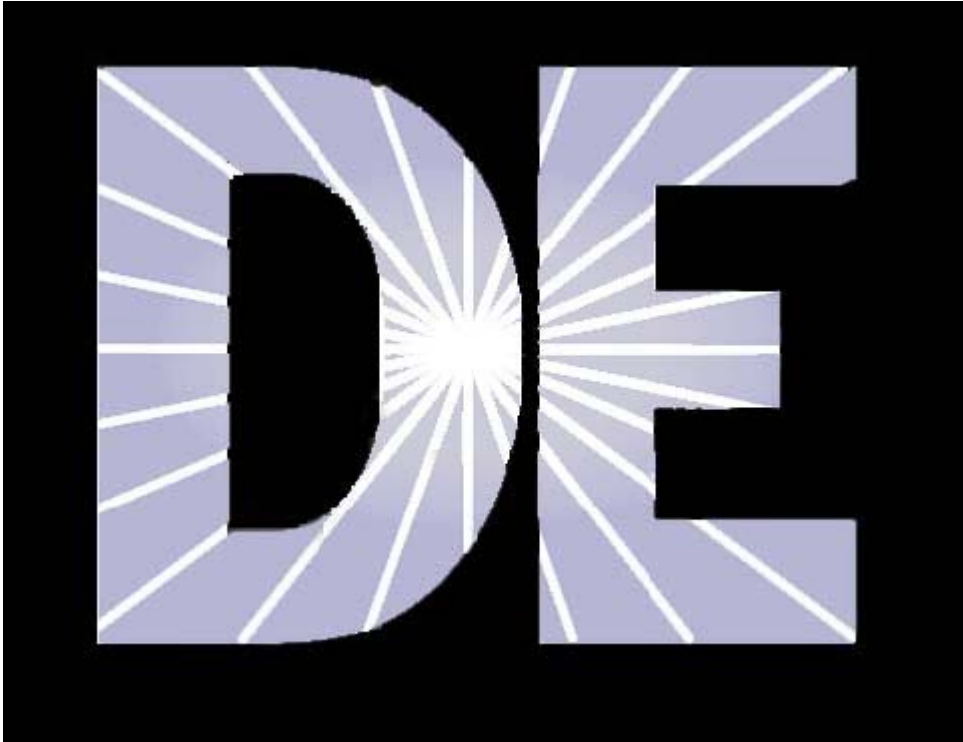
(a) Dynamic response of SC to a 2V increase in voltage reference setting.



(b) Dynamic response of SC to a 5V decrease in voltage reference setting

**Figure 5.** Dynamic response of the SC to a step change in the voltage reference.

6. National Laboratory and Energetics Incorporated, final publication pending, May 2006.
7. F. Li, W. Zhang, L. M. Tolbert, J. D. Kueck and D. T. Rizy, "Assessment of the Economic Benefits from Reactive Power Compensation," 2006 Power System Conference and Exposition, October 2006.
8. S. D. Henry, J. D. Kueck, D. T. Rizy, T. Baldwin, F. Li and Y. Xu, "The Use of Dynamic Voltage Regulating Distributed Energy Resources to Extend the Margin to Voltage Collapse", submitted to the IEEE Transactions on Power Systems, October 2006.
9. 2006.







## 6.1 DE Crosscutting, Systems Integration, and Analysis

*Therese Stovall*  
*Engineering, Science and Technology Division*  
*Oak Ridge National Laboratory*  
*(865)574-0329; email: [stovalltk@ornl.gov](mailto:stovalltk@ornl.gov)*

*DOE Manager: Patricia Hoffman*  
*(202) 586-6074; email: [patricia.hoffman@ee.doe.gov](mailto:patricia.hoffman@ee.doe.gov)*

---

### **Objective**

- Provide the foundation for informed program management decisions, including the definition of program priorities, direction, effectiveness, and strategy.
- Facilitate the deployment of advanced technologies developed under the program mantle by conveying the full extent of potential benefits and the role of DE in the energy market.
- Support cooperation and partnership with other DOE offices and other government agencies, such as the EPA, FERC, and IRS. This cooperation will meet their needs, as well as facilitating the DE program's efforts to remove deployment barriers under the control of these agencies.

### **Approach**

- Consider Distributed Energy benefits analyses on a national, regional and local basis. A broad national analysis will provide potential market penetration of DE. However, due to regionalized market and regulatory drivers, it is important to understand impacts within local and regional areas. Several SCE feeders were selected for a localized analysis.
- Analyze the expansion potential of DER in the customer-owned utility market.
- Quantify the value of DER in ancillary electricity markets such as reserves and reactive power. Coordinate DOE efforts with the Mid-Atlantic Distributed Resources Initiative (MADRI), with particular emphasis on advanced metering and improving the DE business case.

### **Accomplishments:**

- ORNL contributed significant content to the draft DOE report on DE benefits required by Section 1817 of the National Energy Policy Act.
- An ORNL report describing the potential for DG in the customer-owned utility market was published.
- The final report describing the detailed SCE feeder study was published.
- Supported the National Research Council review of the End Use portion of the DE program.
- Approval of a Mid-Atlantic regional model interconnection procedure, support and funding for an LMP benefits study, increased participation and collaboration from key utility stakeholders, and regional stakeholder agreement to consider and act on a MADRI-developed DER Action Plan.

### **Future Direction:**

- Examine DE benefits associated with full grid integration, including an evaluation of diversified DE reliability and power quality effects.
- Support revisions to the broad benefits study mandated by the 2005 Energy Policy Act.
- Evaluate DE case studies regarding grid-integrated DE in the Consolidated Edison service area.
- Coordinate the MADRI examination of the business case and advanced metering areas.

## Introduction

A large number of studies have been performed over the last 30 years that describe and quantify the benefits of Distributed Energy (DE) to system owners. These benefits typically include reduced utility expenses and the provision of back-up power. However, the establishment of a broader DE program at the Department of Energy (DOE) led to a number of questions regarding the benefits of DE to society in general, as well as to other stakeholders. These broader benefits are often poorly understood and difficult to quantify. In fact, the earliest analyses focused simply on listing possible benefits and their recipients. For example, total air emission reductions benefit society at large while voltage support may benefit only electric customers located in close proximity to the DE. The question becomes more complex as you try to assign monetary values to the benefits, and to address the issue that benefits to one group of stakeholders may involve added costs to other stakeholders. Over the past five years ORNL has studied the benefits of Distributed Energy Resources (DER) in several different areas. Case studies, quantification of market benefits to different stakeholders, an analysis of competing power sources, and a preliminary examination of DE benefits for customer-owned utilities were conducted, with reports and summary articles published for the broader industry. We have learned that broad national estimates must be supplemented with more localized studies and that defining a DE business case that is attractive to utilities can be most challenging. The most recent projects have examined the role of DE for municipal utilities and the ability of DE to defer T&D investment on specific circuits.

## Accomplishments and Progress

The assessments reported here share a common starting point, namely that energy cost savings for customers who operate DE often represent revenue reductions for the utility that serves that customer. Utilities have addressed this situation in a number of ways, few of which are conducive to the increased use of DE. These assessments are focused on finding mutually beneficial situations for the DE owner and the utility via: (1) examining utility market conditions unique to customer-owned utilities,

(2) examining the DE potential to displace or defer T&D expansion investments, and (3) examining multiple business case models for DE

Stan Hadley, Therese Stovall, and Jim Van Dyke examined the customer-owned utility (COU) market, especially the municipal utility market, from the perspective of its Distributed Energy (DE) application potential. This study reviewed the overall municipal utility industry as compared to the electric industry as a whole and described the possible ways that DE may be used in a customer-owned utility setting. Few, if any, analyses of the benefits of DE have focused on the benefits specific to the size, structure, and responsibilities of customer-owned utilities. Based on this assessment, there are many customer-owned utilities (see Fig. 2) with the resources and experience base necessary to add economically-beneficial DE to their generation portfolio. The data also show that this market may not have been explored to the same extent as the private utility market. Considering the many beneficial factors that may uniquely apply for municipal utilities, this sector would seem to be an appropriate target for a more detailed market analysis and for DE educational efforts.

Another project examined whether DE could offer enough load relief to practically defer distribution system expansion costs, thereby reducing utility costs by an amount greater than the reduction in sales revenue associated with a DE installation. Two southern California feeders were selected, one in a suburban area and one in a rural area, as shown in Figure 3. The assessment sought to determine whether sufficient DE, at a price attractive to customers, could be installed to avoid the planned capacity expansion for these two circuits. With currently available California DE incentive payments, sufficient DE market penetration may indeed occur. A careful examination of the load profiles for the individual customers and for the circuit as a whole showed that the peak load could be reduced to a level that would eliminate the need to build additional distribution capacity. The assessment tool developed in this project could be used to define the minimum distribution expansion cost at which DE installations would be the preferred alternative.

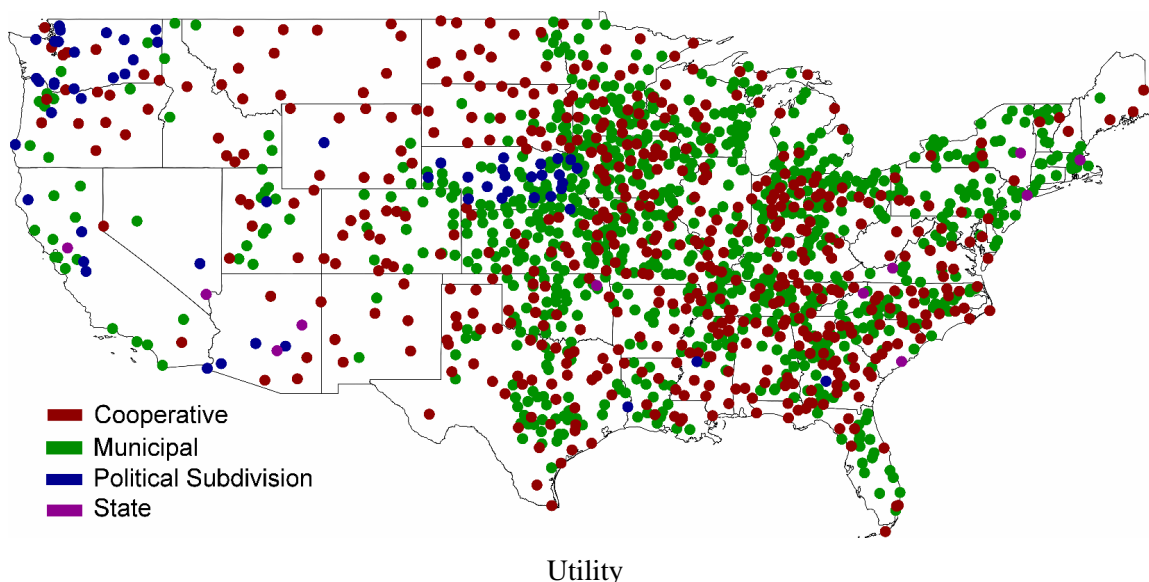


**Figure 2.** Customer-Owned Utilities In Contiguous US

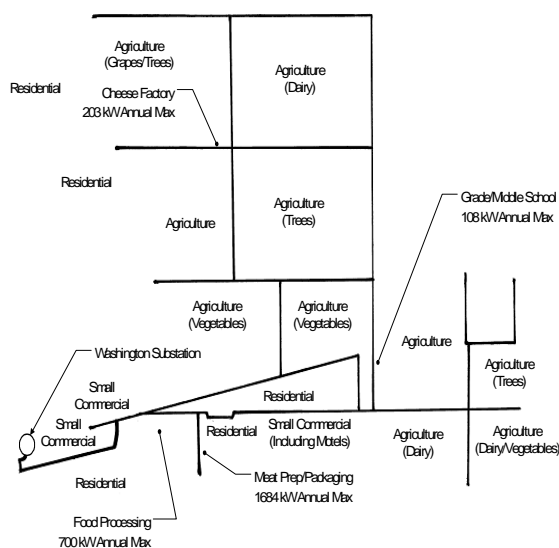


**Figure 3.** Circuit map for one of two feeders examined in study of the use of DE to defer T&D investments

from both the utility and customer perspective on any given circuit.

Working with a team assembled by Pat Hoffman to produce the DE Benefits evaluation called for in the Energy Policy Act, section 1817, ORNL produced five draft chapters, one each on the technical aspects of peak reduction, reduced transmission losses, the use of DG to provide

ancillary services, the impact of DG on grid reliability, and the impact of DG on power quality. ORNL also provided reviews and comments to chapters describing the use of DG for emergency power, the impact of rates and market rules on DG, and the report glossary. This task involved close coordination with persons from multiple laboratories and consulting firms.

The Mid-Atlantic Distributed Resources Initiative (MADRI) seeks to identify and remedy retail barriers to the deployment of distributed generation, demand response and energy efficiency in the Mid-Atlantic region. MADRI was established in 2004 by the public utility commissions of Delaware, District of Columbia, Maryland, New Jersey and Pennsylvania, along with the U.S. Department of Energy (DOE), U.S. Environmental Protection Agency (EPA), Federal Energy Regulatory Commission (FERC) and PJM Interconnection. The collaborative process also includes electric distribution companies, distributed generation developers and owners, demand response companies, and other interested stakeholders. This year MADRI published the MADRI Model Small Generator Interconnection Procedures MADRI's Steering Committee approved this document as a resource for commissions developing

interconnection procedures for small generators. The steering committee also noted that while consensus was not achieved in all areas, the document produced by the subgroup did break new ground in several new areas: (1) Developing procedures for connecting to area networks, (2) Defining the “certification” requirements required to receive expedited project review, and (3) Developing a procedure for expedited evaluation of proposed 10 kVA to 2 MVA facilities that do not export power. The effort involved in producing the MADRI Interconnection Model Procedures was an opportunity to foster consistency in small generator interconnection rules and practices among the five MADRI jurisdictions. This document has already been used by the Pennsylvania PUC as the basis for a rule-making process.

### **Project Publications**

(including those not covered in previous annual progress reports):

1. S. W. Hadley, T. K. Stovall, J.W. Van Dyke, Customer-Owned Utilities and Distributed Generation: Potentials and Benefits, ORNL/TM-2005/257, February 2006
2. Tim Kingston and Therese Stovall , “Exploring Distributed Energy Alternatives to Electrical Distribution Grid Expansion in Southern California Edison Service Territory,” December 2005, ORNL/TM-2005-109
3. MADRI Model Small Generator Interconnection Procedures, November 22, 2005  
([http://www.energetics.com/madri/pdfs/inter\\_models\\_smallgen.pdf](http://www.energetics.com/madri/pdfs/inter_models_smallgen.pdf))

### **Presentations**

(including those not covered in previous annual progress reports):

1. Blueprint for a DER Action Plan to Be Considered by Mid-Atlantic PUCs, Brad Johnson.
2. MADRI State Briefing: Facilitating DR with Advanced Metering Infrastructure by Brad Johnson.
6. Brad Johnson, , Key Summary Points and Action Items, MADRI Interconnection Sub Group Meeting, Philadelphia, PA.
7. Brad Johnson, “MADRI DR Business Case Task,” MADRI Business Models Sub Group Meeting, Philadelphia, PA.
8. Brad Johnson, PAKey Summary Points and Action Items, MADRI Interconnection Sub Group Meeting, Philadelphia, PA.
9. Brad Johnson, “MADRI Interconnection Sub-Group Status Report,” MADRI Working Group Meeting #7, Trenton, NJ.
10. Brad Johnson, Joe Kerecman, “MADRI Role in Developing Regional Interconnection Requirements,” MADRI Steering Committee Meeting, Washington, DC.
11. Brad Johnson, Interconnection Discussion, MADRI Working Group Meeting #4, Newark, NJ.